Development of Photolysis Enhanced Oxidation Technologies for the Removal of Polycyclic

Aromatic Hydrocarbons from Offshore Produced Water

by

© Jing Ping

A Thesis submitted to the

School of Graduate Studies

in partial fulfillment of the requirements for the degree of

Doctorate of Philosophy

Faculty of Engineering and Applied Science

Memorial University of Newfoundland

October 2016

St. John's   Newfoundland and Labrador

Abstract

Offshore Produced Water (OPW) represents the largest volume waste stream from offshore oil and gas (OOG) production activities. It poses major environmental and operational challenges to offshore petroleum industries for requiring more efficient and environmental friendly on-site management. This is true particularly under growing regulatory and economic pressure to reduce the impact of waste discharges. Conventional on-site OPW monitoring and treatment is mainly focused on the oil and grease portion for meeting the regulatory standards, while limited efforts have been given to dissolved compounds especially including Polycyclic Aromatic Hydrocarbons (PAHs). PAHs are proved as one of the most significant contributors to the ecological hazard posed by OPW discharges because of their toxicity, persistency, and potential for bioaccumulation even at a trace level. As a result, effective measurement of PAHs in OPW is imperative, and advanced on-site treatment of the effluent is desired to improve the conventional systems.

This dissertation research focused on the development of new analytical testing methods and photolysis and its enhanced oxidation technologies for treating PAHs in OPW. They are composed of the key tasks including: a) refining of solid-phase extraction (SPE) and liquid-phase microextraction (LPME) pretreatment systems to extract PAHs from OPW; b) enhancement of gas chromotography-mass spectrometry (GC-MS) analytical methods for background and residual PAHs analysis; c) design and fabrication of photochemical

ii

oxidation reactors for batch- and bench-scale experiments; d) systematic one-factor-at-a-time (OFAT) analysis of key parameters and factors in the course of direct photolysis and photocatalysis; e) investigation of efficacy, parameters/factors interactions, kinetics and mechanisms of the enhanced hybrid oxidation systems by integrating photolysis and ozonation (O_3) and/or hydrogen peroxide (H_2O_2); and f) development of central composite design (CCD) based response surface modeling (RSM) models for process simulation and optimization.

The major contribution of this research is the development of compact, efficient, and eco-friendly technologies for on-site OPW testing and treatment. The developed technologies are proved technically sound by lab experiments with high efficiency in detection and removal of PAHs. The research outcomes bring significant environmental, economic and social benefits to industry, government and academia by providing not only effective but also environmentally benign methods for treating OPW generated from OOG production.

Acknowledgements

I would like to thank my supervisor Dr. Bing Chen for giving me the opportunity to work in his research group (the Northern Region Persistent Organic Pollution Control (NRPOP) Laboratory) and for his continuous guidance. Dr. Chen offered me valuable direction in my academic and professional endeavors and gave me the freedom to explore new ideas related to my research project. I gratefully acknowledge Dr. Chen whose academic, professional, and personal support throughout my PhD study, without which this work would not have been possible.

I would like to acknowledge and thank Drs. Tahir Husain and Kenneth Lee for serving in the supervisory committee and spending time on reviewing my work. I thank Dr. Baiyu Zhang for her assistance and helpful suggestions throughout my research project. I would also wish to express my sincere appreciation to several current and former research group members: Zhenyan Li, Jisi Zheng, Bo Liu, Dr. Pu Li, Dr. Liang Jing, Dr. Hongjing Wu, Ling Xiao, Yuan Chen, Qinghong Cai, Weiyun Lin and Zhiwen Zhu for their valuable collaboration, assistance, and discussion. I would also like to thank the other faculty and staff members of the Faculty of Engineering and Applied Science at the Memorial University of Newfoundland for their kindness and professionalism, which have supported my study significantly. I am grateful to thank the School of Graduate Studies of Memorial University of Newfoundland, and my supervisor for financial support. In

iv

Special thanks go to my husband Dr. Ping Lu for his love and support, and my parents-in-law Jiacheng Lu and Hongying Li for their support and encouragement. And to Louie Lu, my son, who has been the light of my life and who has given me the extra strength and motivation to get things done.

Finally I would like to dedicate this work to my father Donglin Ping and my mother Zhilin Zou, for the countless years of love.

Table of Contents

ix

x

List of Tables

xii

List of Figures

List of Symbols, Nomenclature or Abbreviations

ACE   Acenaphthene

ACY   Acenaphthylene

ANOVA   Analysis of variance

ANT   Anthracene

AOP   Advanced oxidation process

BaA   Benzo[a]anthracene

BaP   Benzo[a]pyrene

BbF   Benzo[b]fluoranthene

BghiP   Benzo[g,h,i]perylene

BkF   Benzo[k]fluoranthene

CAPP   Canadian Association of Petroleum Producers

CCD   Central composite design

CHR   Chrysene

COD   Chemical oxygen demand

COOGER   Centre for Offshore Oil, Gas and Energy Research

CTRL   Experimental control

DahA   Dibenzo[a,h]anthracene

DCM   Dichloromethane

DNA   Deoxyribonucleic acid

DOE   Design of experiment

EI	Electron impact
EPA	Environmental Protection Agency
FID	Flame ionization detection
FLA	Fluoranthene
FLO	Fluorene
FPSO	Floating production storage and offloading
FR	Fluorescence
GC	Gas chromatography
HF	Hollow fiber
HPLC	High performance liquid chromatography
HRMS	High-resolution mass spectrometry
IcdP	Indeno[1,2,3-cd]pyrene
ID	Internal diameter
IS	Internal standard
LLE	Liquid-liquid extraction
LPME	Liquid phase micro extraction
LRMS	Low-resolution mass spectrometry
MDL	Method detection limit
MPPE	Macro porous polymer extraction
MS	Mass spectrometry
MW	Molecular weight

NAP	Naphthalene
OFAT	One factor at a time
OPW	Offshore produced water
OSPAR	Oil Spill Prevention, Administration and Response Fund/ The Oslo Paris Convention
PAH	Poly aromatic hydrocarbon
PB	Process blank
PERD	Program of Energy Research and Development
PHE	Phenanthrene
PWRI	Produced water re-injection
PYR	Pyrene
QA/QC	Quality assuarance/quality control
RR	Recovery rate
RSD	Relative standard deviation
RSM	Response surface methodology
SBSE	Stir bar sorptive extraction
SIM	Selective ion monitoring
SP	Sample parallel
SPE	Solid-phase extraction
SPME	Solid phase micro extraction
SS	Stainless steel

TDS	Total dissolved solids
TOF	Time of flight
USAEME	Ultrasound-assisted emulsification
UV	Ultra Violet

Chapter 1 Introduction

Energy plays a pivotal role in our daily lives. It is becoming increasingly difficult to meet the demand for energy worldwide. The International Energy Agency (2008) stated that oil and gas would continue to be an important part of our energy supply in the foreseeable future. In order to find additional supply, oil and gas producers have been looking at more remote and difficult locations such as offshore area that contains large deposits of petroleum and natural gas. Both oil and gas account for 58% of the global commercial energy supply while 45% of this resource is produced in offshore (Salter and Ford, 2000). Figure 1-1 locates the major oil and gas activities in the Atlantic offshore. Since the first offshore well (Figure 1-1**: 2**) was drilled off the coast of Prince Edward Island (PEI) in Atlantic Canada in 1943, subsequent exploration activity has condensed on the continental shelf offshore from Nova Scotia (NS) (Figure 1-1**: 3** and **4**) and from Newfoundland and Labrador (NL) (Figure 1-1**: 1**). The offshore oil and gas (OOG) industry has contributed significantly to the economy of Atlantic Canada (OAG, 2012), however, it may come at a cost to the natural environment. Rapid expansion of oil and gas production in the offshore areas has provoked increasing attention to environmental issues associated with OOG operations. There is a growing recognition that the impacts associated with offshore produced water (OPW) discharge, the largest volume waste stream from OOG production activities (Veil, 2009; Neff et al., 2010), can be cumulative and longstanding (O'Hara and Morandin, 2010). OPW poses major environmental and operational challenges to offshore petroleum industries for requiring more efficient and

1

cost-effective treatment and disposal, particularly under ongoing regulatory and economic

pressure to reduce the impact of waste discharges.

Figure 1-1 Major Oil and Gas Fields in the Atlantic Offshore

1. Hybernia, Terra Nova, White Rose (North methyst), and Hebron;
2. Old Harry;
3. Sable Offshore Energy Project;
4. Deep Panuke.

(Adapted from Viking Marine, 2015 and OAG, 2012)

1.1 What is Offshore Produced Water (OPW)?

1.1.1 Sources

In subsurface formations, naturally occurring rocks are generally permeated with fluids such as water, oil, or gas (or their combinations). It is believed that the rock in most hydrocarbon-bearing formations was completely saturated with water prior to the invasion and trapping of petroleum (oil, natural gas, and/or gas liquids) (Amyx, Bass, and Whiting, 1960). The less dense hydrocarbons migrated to trap locations, displacing some of the water from the formation in becoming hydrocarbon reservoirs (Collins, 1975). Thus, reservoir rocks normally contain both petroleum hydrocarbons and water. Sources of this water may include flow from above or below the hydrocarbon zone, flow from within the hydrocarbon zone, or flow from injected fluids and additives resulting from production activities (Neff, Lee, and Deblois, 2010). This water, which occurs naturally in the reservoir, is commonly known as "formation water (FW)" and becomes "produced water (PW)" when the reservoir is produced and these fluids are brought to the surface (Veil et al., 2004). PW is then termed "offshore produced water (OPW)" for offshore production. Practically all stages and operations of OOG production are accompanied by undesirable discharges of liquid, solid, and gaseous wastes, while the discharges of OPW considerably dominate over other wastes. As shown in Figure 1-2, OPW treatment is the key link in the process of OOG production, which may significantly contribute to the success of the offshore production facility.

4
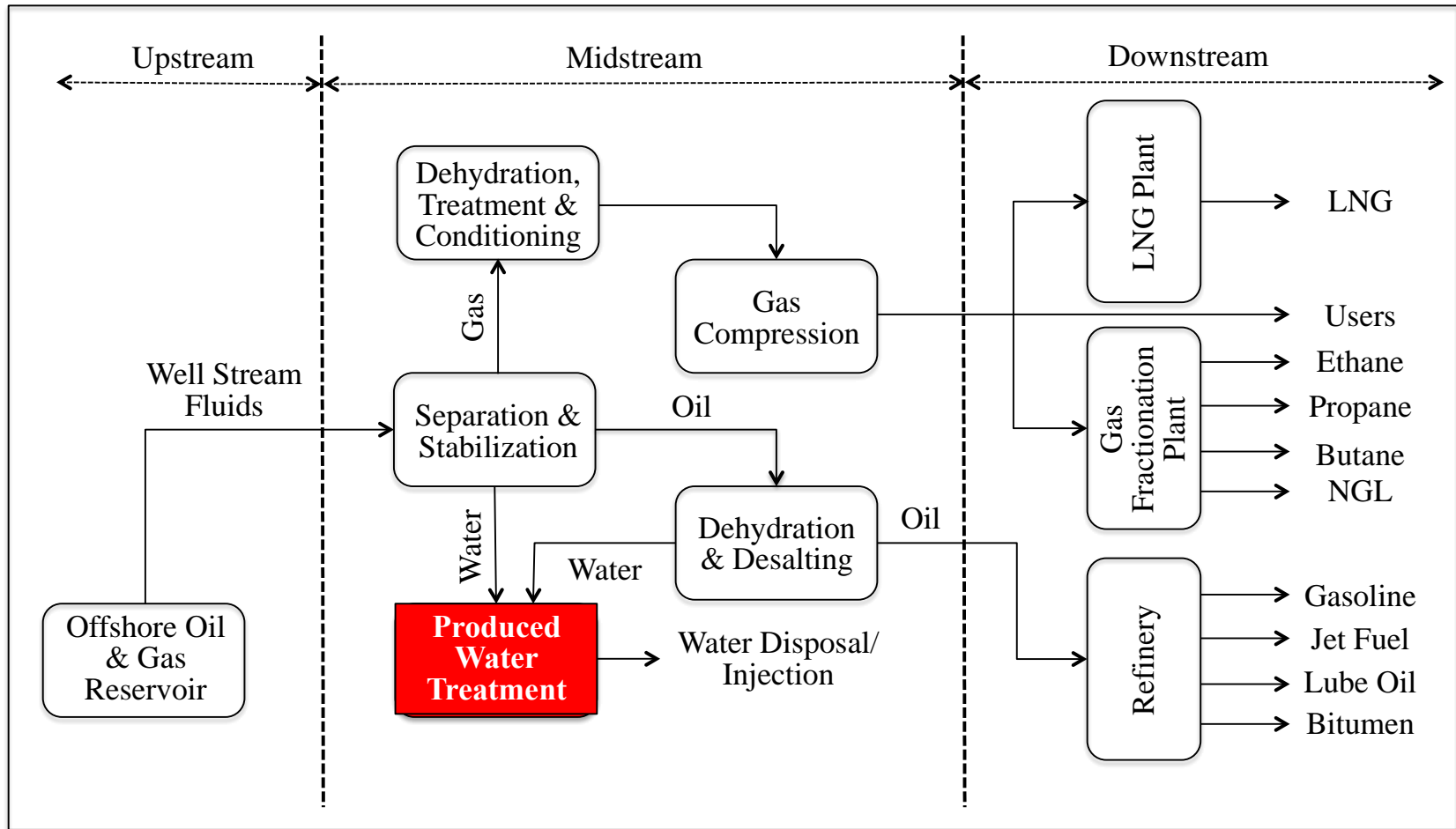
Figure 1-2 Schematic of Typical Offshore Oil and Gas (OOG) Production

(Adapted from Piping Engineering, 2015)

4

1.1.2 Volumes

The OOG industry generates hundreds of thousands of liters of OPW daily, most of which is discharged into the ocean and represents most of the waste discharged from offshore oil extraction production facilities. In 2014, an estimated 85 million bbls/d of OPW were discharged offshore throughout the world, with a corresponding oil production of 77 million bbls/d (Zheng et al., 2016). In 2015, OPW discharges for four projects in offshore Newfoundland (i.e., Hibernia, Terra Nova, White Rose, and North Amethyst Field) ranged from 13 to 39 million bbls/d, typically the largest volumes of OPW are associated with oil production. OPW volumes associated with gas production are usually significantly smaller (C-NLOPB, 2016). For example, in 2009, the Venture gas field on the Canadian Scotia Shelf was discharging 800 to 5,000 bbls/d of OPW (Neff et al., 2010). The well water cuts (or the ratio of PW to oil/gas equivalents (WOR/WGR)) will normally increase throughout the whole oil and gas field lifetime, such that when the hydrocarbon production from the field is shut down, the hydrocarbon content can be as low as a couple of percent with 98 percent water (Gomes et al., 2009; Neff et al., 2010).

1.1.3 Characteristics

OPW is a complex mixture of dissolved and particulate inorganic and organic chemicals. The physical and chemical properties of OPW vary considerably depending on the geographic location of the field, the geological contact of the water in the past, and the type of hydrocarbon product being produced (oil or gas) (Alley et al., 2011). As field production is initiated, OPW composition from the production wells may be continuously

transformed due to injection of seawater, reinjection of OPW, reservoir stimulation, bacterial activity, introduction of production chemicals and more (Veil et al., 2004; Veil et al., 2005; Gomes, 2009). **Table 1-1** demonstrates an example comparing some typical components in OPWs across the world. Obviously, it is practically impossible to articulate some average parameters of this composition, as no two OPWs are alike and even within the same well over time. Basically, petroleum hydrocarbons in the form of dispersed oil, dissolved or soluble organics are always present in OPWs, especially when the latter are mixed with other technological waters and solutions. They depend not only on the specific technological situation but on the fractional composition of the oil and the effectiveness of the oil/water separation methods as well, which brings another challenge in their effective post-treatment. Another characteristic of the chemical composition of most produced waters is their very high mineralization. It is usually higher than the seawater's salinity reaching up to 400 g/l (Gomes, 2009). Such mineralization is caused by the presence of dissolved ions of sodium, potassium, magnesium, chloride, and sulfate in OPW. Besides, OPW often have elevated levels of some heavy metals. OPW may also include chemical additives (e.g., corrosion/scale inhibitors, oxygen scavengers, biocides, emulsion breakers, coagulant and flocculants) used in drilling and producing operations and in the oil/water separation process, as well as miscellaneous produced solids (sand or silt), scales, and bacteria. The components in OPW can affect the oil/water partition coefficient, toxicity, bioavailability, and biodegradability (Li, Chen and Ping, 2014). Recent studies have furthermore revealed that OPW frequently contain naturally occurring radioactive material (NORM) and their daughter products, such as radium-226

6

and radium-228. They are leached from the reservoir by formation waters and are carried to the surface with OPW, oil, and gas, with the radioactive risk to the marine environment.
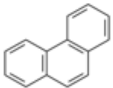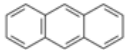
1.2 Polycyclic Aromatic Hydrocarbons (PAHs) in OPW
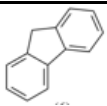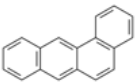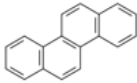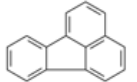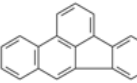
Polycyclic Aromatic Hydrocarbons (PAHs: also called polynuclear aromatic hydrocarbons) are the petroleum hydrocarbons that count for up to 10-35% organic compounds in light crude oil and 14-40% in heavy crude oil (Fingas, 2011). **Table 1-2** lists the United States Environmental Protection Agency (USEPA) identified 16 priority PAHs and their formula and key properties. Among all the contaminants in OPW, PAHs are of greatest environmental concern due to their extreme toxicity to marine biota, high resistance towards biodegradation in the marine environment, and possible carcinogenicity and mutagenicity (Neff et al., 2006; Neff et al., 2010; Harman et al., 2011). Even though their solubility is relative low, they can be absorbed and accumulated by biota with very conservative degradation trends (Vinas et al., 2009), which lead to the high toxicity and pose a risk of causing adverse effects to the ecosystem and human health. Nevertheless, the adverse impact of PAHs in OPW to the ocean could be even worse under the vulnerable arctic marine environment typically with cold climate, sea ice, migration and aggregation, seasonal effects, short food chain, etc. (AMAP, 2002; 2007) (**Table** 1-3)

7

Table 1-1 Comparison of Selected Contaminants in Offshore Produced Water (OPW) Across the World

(Neff, 2002 & 2010)

		Gulf of Mexico	North Sea	Scotia Shelf	Grand Banks	Indonesian
Petroleum Hydrocarbons	BTEX	0.96-5.33	na	na	na	0.33-3.64
(mg/l)	PAHs	0.04-0.6	0.419-1.559	2.148	0.845	na
Metals	Lead	<0.1-28	0.4-10.2	<0.1-45	0.09-0.62	na
(μg/l)	Mercury	<0.01-0.2	0.017-2.74	<10	NA	na
	Arsenic	0.5-31	0.96-1.0	90	<10	na
Radioisotopes	Radium-226	91.2-1,494	44.8	1.2	33.0	na
(pCi/l)	Radium-228	162-600	105	9.2	229.7	na

8

Table 1-2 General Characteristics and Structure of the16 USEPA Priority PAHs

(IPCS, 1998; Mackay et al., 2006; Singh, 2012)

Name	Abbreviation	Molecular Formula	Structure	Molecular Weight (MW)	Melting Point (^{o}C)	Vapor Pressure (Pa at 25 ^{o}C)	Solubility (mg/l)
Naphthalene	NAP	$C_{10}H_8$		128	81	10.4	32
Acenaphthylene	ACY	$C_{12}H_8$		152	92	0.9	3.93
Acenaphthene	ACE	$C_{12}H_{10}$		154	93	0.3	3.40
Fluorene	FLO	$C_{13}H_{10}$		166	115	0.09	1.9
Phenanthrene	PHE	$C_{14}H_{10}$		178	99	0.02	1.3

Name	Abbreviation	Molecular Formula	Structure	Molecular Weight (MW)	Melting Point (^{o}C)	Vapor Pressure (Pa at 25 ^{o}C)	Solubility (mg/l)
Anthracene	ANT	$C_{14}H_{10}$		178	216	0.001	0.07
Fluoranthene	FLA	$C_{16}H_{10}$		202	151	0.0006	0.265
Pyrene	PYR	$C_{16}H_{10}$		202	110	0.00123	0.132
Benz[a]anthracene	BaA	$C_{18}H_{12}$		228	256	5.70×10^{-7}	0.014
Chrysene	CHR	$C_{18}H_{12}$		228	161	2.8×10^{-5}	0.002
Benzo[b]fluoranthene	BbF	$C_{20}H_{12}$		252	168	5.0×10^{-7}	0.0012
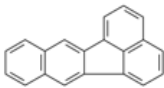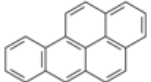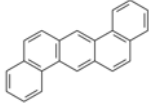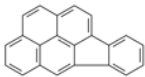
10

Name	Abbreviation	Molecular Formula	Structure	Molecular Weight (MW)	Melting Point (^{o}C)	Vapor Pressure (Pa at 25 ^{o}C)	Solubility (mg/l)
Benzo[k]fluoranthene	BkF	$C_{20}H_{12}$		252	217	5.2×10^{-8}	0.0005
Benzo[a]pyrene	BaP	$C_{20}H_{12}$		252	181	7×10^{-7}	0.11
Dibenz[a,h]anthracene	DahA	$C_{22}H_{14}$		278	268	1.33×10^{-8}	0.005
Benzo[ghi]perylene	BghiP	$C_{22}H_{12}$		276	278	1.4×10^{-8}	0.0026
Indeno[1,2,3-cd]pyrene	IcdP	$C_{22}H_{12}$		276	162	1.33×10^{-7}	0.00019

Table 1-3 Unique Features of the North Atlantic/Arctic Ocean and Implications on Broaden Scopes of the Impacts from OPW Discharge

Features	Impacts
Cold	- Difficult work conditions, especially in winter
	- Slow weathering of oil compounds due to reduced dilution, biodegradation and vaporization
Sea ice	- Difficult access, difficult to respond to spills
	- Intensified local impacts from ice trapping and concentrating of contaminants
Seasonal effects	- Low photochemical degradation rate of 2- and 3- ring PAHs as a result of extended periods of darkness, cold, and snow in winter
Migration and aggregations of animals	- Effects from localized OPW discharge in the North and Arctic impacts other parts of the world
	- Increased exposure time for animals to contaminants, typically in their sensitive periods (e.g., breeding, spawning, and popping)
Intact habitats	- Landscapes and wide-ranging species susceptible to major developments and to

Features	Impacts
	incremental growth
Short food chain and variety of species	- Disruption to key species can have major impacts to many other species

1.2.1 Environmental Fate of PAHs

OPW usually dilutes rapidly upon discharge to well-mixed marine waters (e.g., North Atlantic Ocean). Factors that affect the rate of dilution of OPW include discharge rate and height above or below the sea surface, ambient current speed, turbulent mixing regime, water column stratification, water depth, and difference in density (as determined by temperature (T) and total dissolved solids (TDS) concentration) and chemical composition between the OPW and ambient seawater (Nedwed et al., 2004). Dispersion modeling studies and field measurements of the fate of OPW differ in specific details, but most predict a rapid initial dilution of the discharges by 100- to 1000-fold within the first 50-100 meters downstream from the discharge point, which is followed by a slower rate of dilution at greater distances (Brandsma and Smith, 1996; Smith et al., 2004). The PAHs with lower molecular weight (MW) are more hydrophilic with the log K_{ow} values ranged from 3.37 to 4.46 (CCME, 1999) and were commonly found in the water phase of OPW. The higher MW PAHs are less water-soluble with the log Kow values ranged from 5.32 to 6.04 and are expected to be associated with particulates and oil droplets in OPW (Johnsen et al., 2004). As the discharge plume for most fields will rise towards the surface after discharge (principally due to its temperature), these compounds will follow the plume, settle down and accumulate in sediments, or be retained at certain depths of the water column depending upon the buoyancy of the supporting particulate matter. PAHs span the whole range from readily to poorly biodegradable, depending on the nature of the actual compound (Frost et al., 1998; Vinas et al., 2009). Biodegradation half-lives ranging from less than a day up to several months are described in the literature (Johnsen

14

et al., 2000), with the lower MW compounds being more degradable (but more abundant) (Neff, 2010).

1.2.2 Impacts of PAHs

The quantity of PAHs released to the ocean by oil and gas activities may be small; however, the associated local impacts are of the most concern especially when more development activities are expected in the near future. Most of the 16 USEPA priority PAHs have been identified in OPW. PAHs are considered the most significant contributors to the ecological hazard posed by OPW discharges because of their potential for bioaccumulation and toxicity (CAPP, 2001; Tsapakis et al., 2010). AMAP (2004) included PAHs in their assessment of Persistent Organic Pollutants (POPs). The key characteristics of POPs are their toxicity/carcinogenicity, persistence, and long-range transport capacity. Cold climates support this persistence. Moreover, lipid storage of animals as energy source leads to increasingly vulnerable food webs in the north Atlantic and Arctic region. It has been clearly demonstrated in the literature that PAHs do not have one single type of toxin action. Different toxicity mechanisms play a role depending on the compounds, the exposure (acute or chronic), the organism and the environment compartment. A number of toxicity mechanisms have been linked to PAHs, including non-polar narcosis, photo toxicity, and biochemical activation that, in turn, may result in mutagenicity, carcinogenicity and teratogenicity. Some PAHs may also have influence on hormone regulation, also referred to as endocrine disruption. Under short-term toxicity studies, non-polar narcosis is the most likely mechanism of toxicity to be observed

15

(Thomas et al., 2004; Casini et al., 2006). Effects due to more specific toxicity mechanisms, such as biochemical activation and subsequent mutagenic and carcinogenic effects, and disturbance of hormone regulation, may occur in the environment as a result of prolonged exposure to relatively low concentrations of PAHs (Johnsen et al, 2000; Frost et al, 2001; Lee et al., 2011). In general, lower MW PAHs are less toxic to aquatic organisms than higher MW PAHs. This is largely due to bioaccumulation potential. But compounds with more than 6 aromatic rings tend to be less toxic as the molecules are too big to transport through cell membranes. The higher toxic, less soluble PAHs are among those removed in substantial amounts with the dispersed oil. However, it has been found from recent studies that dissolved PAHs are contaminants of the most concern in terms of acute and chronic toxicity of OPW. According to Neff (2002; 2005; 2010), the two- and three-ring PAHs are identified as the main contributors to the ecological risk of PAHs in OPW discharge due to their elevated concentration levels in OPW and bioavailability to the water-column organisms, especially the sensitive marine species. Further treatment is therefore desirable after oil-water separation to reduce the emission of PAHs.

1.3 Statement of Problem

While OPW has generally been presumed that impacts would be negligible due to natural dispersion in the large volume of dilution capacity of ocean, there is emerging evidence from North Sea studies that suggested OPW discharges impacted biota (invertebrates, fish and larva) at greater distances from operational platforms than originally envisioned (Casini et al., 2006). Laboratory studies conducted in Norway also provided evidence of

16

endocrine (reproductive) effects on cod continuously exposed to low concentrations of OPW (Thomas et al., 2004). A study of the Program of Energy Research and Development (PERD) of Canada on the east coast oil and gas operations discovered that OPW contaminants may be transported to and concentrated within the benthic environment and the surface micro-layer as a result of chemical reactions following its discharge (Azetsu-Scott et al., 2007). Lee et al. (2011) recently reported that the accumulation of PAHs could cause severe oxidative DNA damage and therefore lead to tumors and cancer. Based on the condition that the volume of OPW generated from production process is massive and keep increasing, there are growing concerns about the long-term negative effects on the marine environment from OPW discharge and there is a potential that more stringent standards would be implement in near future especially for the regions with vulnerable biota. As an example, 'zero discharge' is required for oil and gas operations in the Arctic waters as per the Arctic Waters Pollution Prevention Act (Pollestad, 2005; OSPAR, 2008). In Canada, the Arctic Waters Pollution Prevention Act (AWPPA) (2012) stating that 'no person or ship shall deposit or permit the deposit of waste of any type in the Arctic waters' is a 'zero discharge' act to prevent pollution in Canadian Arctic waters.

To determine how "safe" OPW is to the environment and to assign limitations in terms of discharge volume to the sea, or to evaluate the efficacy of the treatment systems, water quality testing is of paramount important to properly characterize the chemical composition of OPW with particular attention addressed to the toxic components (Correa

17

et al., 2010). As mentioned above, even though the solubility of PAHs is generally low and usually decreases with increasing molecular weight, their hazard potential even in trace amounts can be relatively high, thus making their presence in the water cycle an acute as well as chronic risk to the environmental quality and human health. As a result, effective on-site measurements of PAHs especially for those in trace level in OPW is imperative. To achieve this, rapid, simple, precise and accurate analytical methods are desired by offshore industry and regulators for the identification and determination of PAHs in OPW.

On the other hand, as a result of emerging evidence of adverse environmental impacts of OPW discharge and increasingly stringent regulations of OPW discharge in some regions already in place, the secondary treatment before the disposal of OPW is one of the major environmental and operational issues from the perspectives of both industry and government. Existing on-site approaches may be constrained by limited space, shock-loading conditions, and/or requirements of low maintenance and high cost efficiency, and the harsh offshore environment (e.g., cold and high motion) makes the application even more challenging. Therefore, there is always a need to develop more robust, efficient, eco-friendly, and cost effective technologies for on-site treatment of OPW effluents from the primary treatment process. Thus, research into the improvement of OPW treatment prior to its discharges particularly in the Arctic and North Atlantic regions is required to assure the protection of ocean environment and sustainable utilization of our marine resources.

1.4 Objectives

Therefore, the objective of this research is to address the need and knowledge gaps of the offshore industry and government, targeting the contaminants that of the most environmental concern in OPW, PAHs, to develop compact, efficient, and environmental friendly technologies for removing PAHs from OPW.

The key tasks will include: 1) refining of solid-phase extraction (SPE) and liquid-phase micro extraction (LPME) pretreatment systems to extract PAHs from OPW; 2) enhancement of gas chromotography-mass spectrometry (GC-MS) analytical methods for background/residual PAHs analysis; 3) design and fabrication of photochemical oxidation reactors for bench- and batch-scale experiments; 4) systematic one-factor-at-a-time (OFAT) analysis of process variables in the course of direct photolysis and photocatalysis; 5) investigation of efficacy, parameters interactions, kinetics and mechanisms of the enhanced hybrid oxidation systems by integrating photolysis and ozonation (O_3) and/or hydrogen peroxide (H_2O_2); and 6) development of central composite design (CCD) based response surface modeling (RSM) models for process simulation and optimization.

1.5 Structure of the Thesis

The roadmap of this dissertation is shown in **Figure 1-3**. This dissertation is structured as follows. **Chapter 2** provides a comprehensive literature review of the recent developments of technologies in testing and treating PAHs in OPW; **Chapter 3** highlights

19

the development of a simple, low-cost, time efficient, highly selective and sensitive methods based on SPE, LPME and GC-MS for offshore real-time PAHs testing in OPW; **Chapter 4** develops direct photolysis and photocatalysis systems to remove PAHs from OPW. Phased OFAT experimental design has been applied for the analysis of significant environment parameters during the direct photolysis and photocatalysis processes; **Chapter 5** further develops hybrid photolysis enhanced oxidation systems by integrating the effects from ozonation and hydroperoxide (H_2O_2). CCD based RSM has been applied in simulating and evaluating the hybrid systems for developing system models and optimization; finally, conclusions of this dissertation research and the projected future work are drawn towards the end in **Chapter 6**.
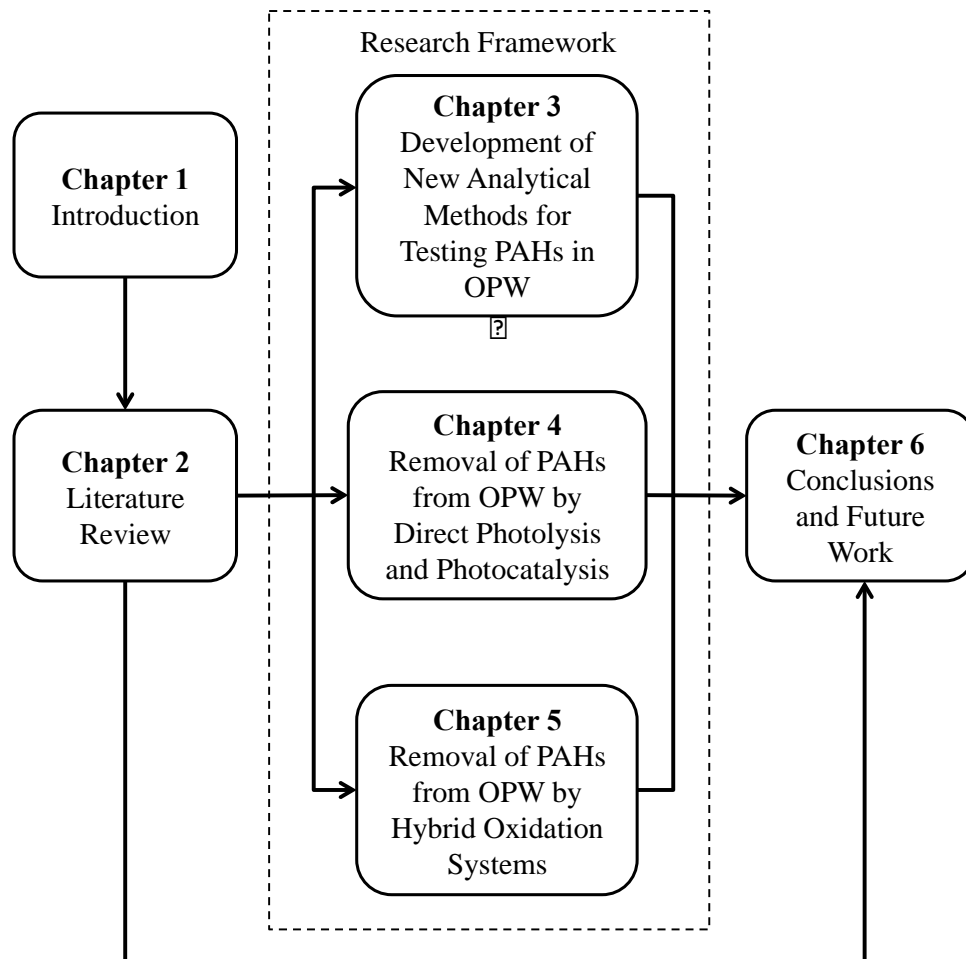
Figure 1-3 Roadmap of the Dissertation Research

Chapter 2 Literature Review

2.1 PAHs Analysis in OPW

Due to its hazardous characteristics, identification and determination of PAHs in OPW is a critical analytical issue. The main challenge with PAHs testing for OPW is their very low concentration and complexity of OPW matrices. Therefore, an appropriate extraction or a pre-concentration step combined with a suitable chromatographic technique is necessary to achieve the required sensitivity and selectivity. Nevertheless, since the real-time data are very important for the offshore decision makers, the quest for more simple, fast and efficient analytical methods for the on-site real-time testing of PAHs in OPW has never ceased.

2.1.1 Pre-treatment Methods

For trace levels of PAHs in aqueous samples, liquid-liquid extraction (LLE) is one of the most widely used extraction methods (Tor et al., 2003; Aydin et al., 2004). However, LLE has been regarded as a time consuming, tedious, labor-intensive method (Psillakis and Kalogerakis, 2003; Titato and Lan ças, 2006) and requires relatively large volumes of toxic organic solvents (Stege et al., 2009). In addition, emulsions developed during the LLE process can adversely affect the proper extraction of the target components in the suspended form (Kayali-Sayadi et al., 1998; Wolska et al., 2005). LLE was also reported to be less efficient in the extraction of low MW PAHs (Titato et al., 2005).

22

Solid-phase extraction (SPE) has been used as an alternative method to LLE for the extraction of PAHs from water samples because of its advantages over LLE (Marce′ and Borrull, 2000 ; D́rea et al., 2007). In comparison with LLE, SPE for pre-treating samples is relatively simple and speedy, and most importantly, minimizes solvent usage and sample demand. Another advantage of SPE is the low matrices interference. A recent study by Werres et al. (2009) claimed that the application of SPE in the analysis of PAHs in aqueous samples with high-suspended particulate matter content showed a much higher recovery rate and better precision than traditional LLE.

More recently, solid-phase microextraction (SPME) method has been developed based on SPE but without solvent consumption (Arthur and Pawliszyn 1990). However, it is expensive with the risk of fiber breakage and suffers the problem of sample carry-over, which leads to low sample recovery rates (Psillakis and Kalogerakis, 2003; King et al., 2004). In addition, SPME cannot be combined with commonly used auto-samplers on chromatographic instruments and require manual injection after pre-treatment, which should be avoided in real-time testing to reduce labor and errors (Zheng et al., 2012). In this case, SPE is more favored than SPME. But it should be noted that the reduced processing time and less sample volume requirement of SPE still may not satisfy intensive sample pretreatments (Aydin et al., 2004) for continuous real-time testing required for OPW monitoring unless such technology is properly enhanced to meet the offshore requirements.

23

Recent efforts have also been placed on miniaturizing the LLE procedure by greatly reducing the solvent (acceptor) to aqueous (donor) phase ratio, leading to the development of liquid-phase microextraction (LPME) such as single drop microextraction (SDME), hollow fibre liquid-phase microextraction (HF-LPME) and solvent bar microextraction (SBME), which have been widely used for sample pre-treatment (Charalabaki et al., 2005; Popp et al., 2001). LPME overcomes the drawbacks inherent to the conventional LLE method. These techniques have good sensitivity and consume less solvent (Wu et al., 2008; Sarafraz-Yazdi and Amiri, 2010). LPME combines extraction, concentration and sample introduction in one step, eliminating the disadvantages of conventional extraction methods, such as time consuming, operation and using expensive equipment (Zhao et al., 2006). LPME features no sample carry-over, wide selection of available solvents, low cost, minimal solvent use, short pre-concentration time, requiring no conditioning, no need for instrument modification, etc. (Hou et al., 2002). However, some drawbacks, such as instability and relative low recovery rate, especially in pretreatment of industry wastewater with complex matrices, were reported for LPME method (Charalabaki et al., 2005; Xu et al., 2007). The complex instrumentation and procedure as well as the high requirements for the lab skill lead to the difficulties on operation and automated injection with commercial auto-samplers. The feasibility and efficacy by using an enhanced LPME addressing its limitations should be further investigated and evaluated.

Rezaee et al. (2006) developed a more rapid and low-cost method named as dispersive

liquid-liquid microextraction (DLLME). Since the on-site monitoring usually can hardly provide the same experiment conditions for safety as in a certificated lab, the high consumption of toxic extraction and dispersion solvents may lead to a higher experimental risk. Ultrasound energy was then introduced to extract PAHs and other compounds to reduce the usage of solvents (Song et al., 2011; Donthuan et al., 2014). Ozcan et al. (2010) carried out a study using ultrasound assisted dispersive liquid-liquid microextraction (UA-DLLME) followed by gas chromatography-mass spectrometry (GC-MS) analysis. This improvement provided a more simple and efficient DLLME method with less solvent usage for detection of 16 PAHs in environmental samples including wastewater. However, the transmission of ultrasound energy in the samples can potentially cause degradation of analytes during the extraction, leading to the reduction of accuracy (Psillakis et al., 2004; Luquedecastro and Priegocapote, 2007; Sanchez-Prado et al., 2008).

In addition, only the manually injection was adopted in previous studies. For intensive detection in offshore platforms, the automated injection using auto-samplers of the analytical instrument is preferred. Nevertheless, although a number of studies have been conducted to analyze 16 PAHs by applying different analytical techniques in various water sample matrices (Delgado et al., 2004; Dórea et al., 2007; Pino et al., 2002; Saraji and Boroujeni, 2014), rare studies were focusing on PAHs in samples that have both high salinity and high organic content (e.g., OPW).

2.1.2 Detection Methods

Traditionally, after pre-treatment, PAHs detections have applied various chromatographic technologies, which can generally be divided into two groups: 1) high performance liquid chromatography (HPLC) based detection; and 2) gas chromatography (GC) based detection. HPLC based technologies typically include HPLC-fluorescence (FR), HPLC-ultraviolet (UV), and HPLC-mass spectrometry (MS) analysis; while the commonly used GC based approaches are GC-flame ionization detection (FID) and GC-MS analysis (DeVoogt et al., 1996).

HPLC-FR instruments have good sensitivity but a restricted linear range (Patrick et al., 2001). HPLC-UV and GC-FID instruments are rugged but have limited sensitivity (Michor et al., 1997). MS detection is more popular with reduced background interference particularly when applying the selective ion-monitoring (SIM) mode (Zheng et al., 2012, 2013). When comparing HPLC with GC, HPLC normally suffers from high intensity of background noise especially with complicated sample matrix, which results in low method detection limits (MDLs). Besides, in HPLC analysis, large volumes of solvent clusters must be used as the mobile phase (e.g., Acetonitrile), while the GC system uses carrier gas (i.e., helium or hydrogen) as the mobile phase. It should also be noted that, to support injury assessment using toxicity threshold, the MDLs should be in the ppb range for individual PAHs (COOGER, 2007). Previous MDLs in the ppb range have been achieved by extensive, time-consuming sample preparation and costly dioxin-like high-resolution mass spectrometry (HRMS) analysis (Patrick et al., 2001).

26

Nevertheless, some promising results have been reported by Pyle et al. (1997) and Ping et al. (2012, 2013), showing that with appropriate enhancements, combining GC with certain low-resolution mass spectrometry (LRMS) (i.e., ion trap mass spectrometer or quadruple mas spectrometer) allows the LRMS instruments to compete with expensive HRMS instruments.

Based on the literature, the refined coupling of SPE/LPME pretreatments with GC-MS detection has high potential for on-site real-time PAHs testing in OPW. Further research into the technology enhancement/redevelopment is highly in demand for investigating and evaluating the associated feasibility and efficiency.

2.2 PAHs Treatment in OPW

The treatment and disposal of OPW is one of the major environmental and operational issues particularly with increasing environmental awareness and under growing regulatory and economic pressure to reduce emissions of wastes. Currently, OOG operators treat OPW via one or more of the options provided in **Table 2-1**. The most widely used management practice for OPW is the ocean discharge option (Fakhru'l-Razi et al., 2009). On-board treatment of OPW is desirable due to the low shipping/handling cost as well as reduced health, safety and environment issues. OPW treatment can be challenging because floating, production, storage and offloading units (FPSOs) do not have abundant space or weight capacity for treatment equipment. In addition, since offshore environments are remote and typically harsh, equipment and processes that

27

operate there must be designed for those environments. **Table 2-2** summarized the conventional and recent development of technologies for OPW treatment.

2.2.1 Conventional Treatment Technologies

Many authors have described programs for OPW treatment at offshore facilities (Favret and Doucet, 1999; Tyrie, 2000; Caudle, 2000; Robinson, 2003; Greenwood, 2003; Ebenezer and Chen, 2012). The most widely used treatment techniques focus on removing dispersed oil to meet the regulated oil and grease concentration (Jelmert, 1999; Ayers and Parker, 2001; Plebon et al., 2006). Gravity based separation techniques have been the most extensive method for treating OPW.

Generally, OPW is firstly pretreated by skimmers or other basic separation equipment (e.g., API) to remove oil droplets greater than 100 microns in size (Veil, 2004). Some enhancement may be added including heat, electromagnetic, or baffles (CAPP, 2001). Sufficient retention time for separation is needed. The skim tank or API separator can double as a retention tank providing constant inflow rates to downstream equipment, alleviating the flow rate variation problem (Hawboldt, 2012).

Table 2-1 Offshore Produced Water (OPW) Management Options

Options	Description	Limitations
Water Minimization (Al-Muntasheri et al., 2010; Dong et al., 2011; Amini et al., 2012; Chen et al., 2014; Zheng et al., 2016)	Keeping water from the wells by mechanical blocking devices or water shut-off chemicals; keeping water from getting to the surface by dual completion wells, downhole oil/water separators, or subsea separation	- Not always technically Possible - High capital/operational expenses;
Geological Disposal (i.e., Produced water re-injection (PWRI)) (Veil et al., 2004; Bader, 2007; Clark and Veil, 2009; Maersk OIL, 2011; Zheng et al., 2016)	Water be re-injected back to its formation or into other formations	- Suitable injection zone needed; - Energy intensive; - High capital/operational expenses; - Treatment ability
Reuse/Recycle	Minimally treated produced water may be used	- Limited capacity;

Options	Description	Limitations
(Veil et al., 2004)	for drilling and work over operations within the petroleum industry	- Should be cost efficient
Treatment Followed by Discharge	Produced water may be discharged to the ocean as long as it meets offshore discharge regulations	- May involve significant treatment due to environmental concerns

Table 2-2 Offshore Produced Water (OPW) Treatment Options

	Efficiency/reduction		Pros	Cons
	PAHs in dispersed oil	PAHs dissolved in OPW		
Conventional Technologies				
Air floating (Cline, 2000; CAPP, 2001; Ekins et al., 2005; NETL, 2010; Zheng et al., 2016)	Yes	No	High feasibility; can be easily integrated with other technology; easy operation, robust and durable	Influenced by high-temperature; disposal of sludge
Hydrocyclone (CAPP, 2001; NETL, 2002; OGP, 2002; Jain Irrigation Systems Ltd, 2010; Zheng et al., 2016)	Yes	No	Compact modules satisfying all offshore applications; no chemical usage; reduction of TDS, dispersed oil and salts	Fouling; unstable flow rate caused by harsh/Arctic environment might reduce the efficiency
Recent Developments				

	Efficiency/reduction		Pros	Cons
	PAHs in dispersed oil	PAHs dissolved in OPW		
Centrifuge (Nature, 2013; Zheng et al., 2016)	Yes	No	Higher efficiency than hydrocyclone; can remove smaller oil droplets in OPW	High maintenance and operational cost; unstable flow rate caused by harsh/Arctic environment might reduce the efficiency
EPCON compact floatation units (CFU) (Ekins et al. (2005; Saad et al., 2006; Walsh, 2012)	Yes	No	Smaller volume and shorter retention time than traditional flotation units	Feed water streams with high clay and silt fines content can be a problem; not react well to flow surges

	Efficiency/reduction		Pros	Cons
	PAHs in dispersed oil	PAHs dissolved in OPW		
Coalescence (Grini, 2002; OGP, 2002; Tulloch, 2003; Ekins et al., 2005; Owens and Lee, 2008; Nature, 2013)	Yes	No	High feasibility; can improve efficiency of floatation, filtration and other physical separation processes	Possible chemical usage; pre-coalescers are generally sensitive to suspended solids and paraffinic crudes
Supercritical solvent extraction (C-Tour) (OSPAR, 2002; Grini et al., 2003; Knudsen et al., 2004; Offshore Magazine, 2006)	Yes	Yes	Potentially could be used in high volume applications Can achieve up to 95% removal rate for both dispersed and dissolved PAHs; compact modules	Sensitive to the available condensate quality; high-pressure re-circulation equipment is required; increase of BTEX concentration in the

	Efficiency/reduction		Pros	Cons
	PAHs in dispersed oil	PAHs dissolved in OPW		
				discharged OPW
MPPE (Meijer and Kuijvenhoven, 2002; OGP, 2002; Grini et al., 2003; Ekins et al., 2005; NETL, 2014)	Yes	Yes	Removal of the majority of aromatics including all PAHs	Incapability of treating high volume of oil field PW; energy intensive, with high cost and maintenance
Membranes (Nicolaisen and Lien, 2003; Brock et al., 2003Ekins et al., 2005; Natures, 2010; Hawboldt et al., 2012)	Yes	Yes	Can remove oil droplets with size up to 0.01 microns as well as dissolved hydrocarbons at the molecular level	Costly in capital and maintenance; weight and space

34

	Efficiency/reduction		Pros	Cons
	PAHs in dispersed oil	PAHs dissolved in OPW		
Steam Stripping (OGP, 2002)	Yes	Partially	Compact and picks the most volatile components in the liquid stream	Energy intensive; only for low volume, high contaminant loading applications; vulnerable to process disturbances; post treatment is necessary
Biodegradation (OGP, 2002; Van et al., 2003; Tchobanoglous et al., 2003; Haritash and Kaushik, 2009; Ping et al., 2011)	Yes	Yes	Environmental friendly	Weigh and space; only suitable offshore for low volume applications

	Efficiency/reduction		Pros	Cons
	PAHs in dispersed oil	PAHs dissolved in OPW		
Photo Oxidation based Processes				
Direct photolysis, UV/TiO$_2$, UV/O$_3$, UV/H$_2$O$_2$, UV/Fenton (Bares et al., 2006; Tarek et al., 2011; Han et al., 2012; Ma and Chen, 2012; Ping et al., 2011; 2013; Li, Ping, and Chen, 2013; 2014; Zheng et al., 2013; 2014; Liu et al., 2014; Jing et al., 2014; 2015)	Yes	Yes	Complete mineralization of organic pollutants at mild pressure and temperature; economically efficient; no chemical addition; compact; easy operation; no feed water quality requirement; disinfection	Process monitoring and optimization are demanded; efficiency could be low with OPW's chemical species

Increasing density difference between oil and water can also increase the rising velocity. This can be achieved by incorporating techniques such as air flotation (i.e., dissolved gas floatation (DGF), and induced gas floatation (IGF)) to lower density of oil droplets (Cline, 2000). The principle of flotation is to create fine air/gas bubbles that rise through the water to the top of the tank filled with OPW and carry small oil droplets and suspended particulates to the surface of the tank where they can be skimmed off as froth. IGF systems are far more common than DGF since they require far less space and are lighter, and IGF can remove oil droplets as small as 25 microns (CAPP, 2001; Ekins et al., 2005; NETL, 2010; Zheng et al., 2016).

The oil droplet rising velocity is also proportional to gravitational acceleration and mechanical methods, such as hydrocyclone, which can be used to increase gravitational acceleration to speed up the separation process (Faucher and Sellman, 1998; Frankiewicz, 2001; NELT, 2012). Hydroclones induce centrifugal motion to oily water by using tangential entrance and tapering designed cylindrical chamber. Due to the density difference, oil droplets aggregates around the core of the chamber while water moves and gathers on the outer wall. Typical range of minimum oil droplet sizes that can be removed by hydrocyclones is 10-15 microns (Colorado School of Mines, 2009; Jain Irrigation Systems Ltd, 2010). Hydrocyclone is the most commonly installed equipment on offshore platforms across the world (Hayes, 2004; sinker, 2007). This is due largely to its compact weight, small footprint, short residence, low energy consumption, and low maintenance (CAPP, 2001; NETL, 2002; OGP, 2002; Zheng et al., 2016).

37

As a result of the removal of the dispersed oil droplets, an associated reduction in the PAHs concentration is to be expected especially for the less water-soluble portion. However, while the oil portion can be mostly removed by conventional technologies, the dissolved organic compounds would remain unaffected. What is evidence is that the conventional technologies are ineffective in removing dissolved fractions of PAHs (e.g., Naphthalene (NAP) and Fluorene (FLO)), which are the most abundant PAHs in OPW and contribute most to its toxicity (Neff 2002; 2005; 2010). Besides, as temperature decreases, water viscosity increases leading to reduced rising velocity (CAPP, 2001). This means that in cold offshore environments, treatments based on gravity separation may not be efficient. Driven by environmental concerns about the long-term impacts on the ambient marine ecosystems from OPW discharge and increasingly stringent wastewater treatment guidelines (e.g., zero discharge), more research and development for new technologies that can remove dissolved PAHs are in increasing demand.

2.2.2 Recent Development for Treating PAHs

As discharge regulations are becoming more stringent and increasing awareness of the impacts of dissolved components in OPW, technologies that are capable of removing dissolved organics are emerging. There are a couple of currently developed treatment options, which can further reduce and/or remove PAHs from the OPW such as centrifuges, EPCON compact floatation units (CFU), coalescence (e.g., Mare's Tail; PECT-F; TORR), supercritical solvent extraction (e.g., C-Tour), absorbents (e.g., Macro Porous Polymer

38

Extraction (MPPE)), membranes, steam stripping, and biodegradation.

In comparison with hydrocyclones, centrifuges allows for separation of smaller oil droplets although the energy consumption and maintenance requirements are higher (Nature, 2013; Zheng et al., 2016). Oil-water separation in a centrifuge is based on centrifugal forces and the difference in specific gravity of oil and water. OPW has the gases removed from it and is injected into the centrifuge, where it is rotated at speed. Water will collect at the outside of the centrifuge; oil will collect in an inner layer. Oil and water are removed separately, under controlled conditions. An oil-water interface needs to be maintained. Oil is pumped back into the process and water is discharged. Centrifuges are usually applied as a polishing step when a performance standard (e.g. a discharge limit) cannot be achieved. On oil producing installations the use of centrifuges may be useful to clean skimming from degassers and IGF units, thereby avoiding buildup of sludge.

The Epcon CFU technology enhances standard, well-established gas flotation design principles by integrating them with confined swirling flow theory, producing a compact, high-performance OPW polishing system. The unit usually consists of a vertical chamber acting as a 3-phase separator where centrifuge and gas flotation techniques are used. OPW enters the EPCON CFU vessel in a horizontal, tangential direction. Facilitated by internal devices and air flotation effect caused by the release of residual gas from the water, added gas, or both, oil droplets agglomerate and coalesce, and eventually creating

a continuous oil or emulsion layer at the upper liquid level of the flotation chamber. The gas-rich stream is removed in a continuous process via an inserted pipe at the top of the vessel. Treated water exits through the bottom outlet for ocean discharge. The unit also degasses the water (Saad et al., 2006). In addition, the CFU has a smaller volume and shorter retention time than traditional flotation units currently in use offshore. From evaluation performance by Ekins et al. (2005), The EPCON CFU technology can decrease the oil content to below 5 ppm. On the other hand, there still exist a couple of key drawbacks of this system. For instance, vertical gas flotation units require continuous injection of suitable water clarifier/flotation aid polymer chemicals to achieve high water treatment specifications. In addition, feed water streams with high clay and silt fines content can be a problem if they settle inside the gas flotation vessel as the sediment can reduce residence time and cause misdistribution of gas. Moreover, this type of design does not react well to flow surges. Performance tends to deteriorate rapidly under these conditions (Walsh, 2012).

Based on Stoke's Law (CAPP, 2001), larger oil droplets are easier and faster to remove as larger droplets float to the surface faster than smaller ones and can be removed from the water phase; therefore, devices to promote coalescence of small oil droplets into larger droplets may be used, such as mechanical coalescing systems (e.g., Performance enhancing coalescence technology (PECT-F/PECT-U); Mare's Tail; Total Oil Remediation and Recovery (TORR)), and chemical flocculation and coagulation systems (e.g., G-Floc and CodeFlo) (Grini, 2002; OGP, 2002; Tulloch, 2003; Ekins et al., 2005;

Nature, 2013). One of the technology disadvantages could be the possible chemical input. And the other concern on this technology is that the pre-coalescers are generally sensitive to suspended solids and paraffinic crudes which tend to solidify and form blockages in the media (Owens and Lee, 2008), thus adding further complexity to the system maintenance.

The C-Tour process could be an enhancement to existing hydrocyclone technology, and thus potentially could be used in high volume applications (Grini et al., 2003). The process utilizes liquid condensate (NGL) from the gas scrubbers and injects it into the OPW upstream of the hydrocyclones. The dispersed and dissolved hydrocarbons, which have higher solubility in the condensate, go into the condensate phase and are separated in the hydrocyclones. This technology has been widely tested on both pilot and full scale on the Norwegian continental shelf (Grini et al., 2002; 2003; NETL, 2010; Ekins et al., 2005; Torvik et al., 2005). It can achieve up to 95% removal rate for both dispersed and dissolved PAHs (Offshore Magazine, 2006). However, it also has certain limitations, for example, the process is very sensitive to the available condensate quality, thus only a specific grade of gas condensate will suffice as the solvent, and this limits platform selection; in addition, high-pressure re-circulation equipment is required to guarantee the pressure in OPW (>10 bar) to keep the condensate in liquid form during the extraction process (OSPAR, 2002). Moreover, a shortcoming was discovered by Knudsen et al. (2004) who estimated an increase of 40% in BTEX concentration in the discharged OPW from C-Tour process.

41

MPPE is a LLE technology where the extraction solvent is immobilized in the macro porous polymer particles. In the MPPE unit, OPW is passed through a column packed with MPPE particles containing specific extraction solvent, which removes hydrocarbons from OPW (NETL, 2014). In-situ generation of extraction solvent is accomplished by periodically stripping the extracted hydrocarbons with low-pressure steam (Lee et al., 2002). Stripped hydrocarbons can be condensed and separated from feed water by gravity, and product water is either discharged or reused. MPPE technology has been successfully evaluated and installed by offshore operators in Norway for the removal of the majority of aromatics including all PAHs (Meijer and Kuijvenhoven, 2002; OGP, 2002; Grini et al., 2003). This technology is essentially used to reduce the toxic content of OPW and can withstand OPW with complex matrix. A study carried out by Statoil to compare the effect of different treatment technologies of oilfield-produced water on environmental impact factor (EIF) found that the MPPE technology had the highest EIF reduction of 84% (Grini, 2002; Buller, Johnson, and Frost, 2003). Pre-treatment through hydrocyclones or other flotation methods is however necessary before letting PW from oilfields flow into the MPPE unit (Meijer, 2004). The ability to incorporate this technology into offshore operations would be severely limited due to its incapability of treating high volume of oil field PW (more suitable for gas facilities) (Ekins et al., 2005). And it is also energy intensive, with high cost and maintenance (e.g., replacement of degenerated MPPE particles) (OGP, 2002, Ekins et al., 2005).

Membrane filtration can remove oil droplets with size up to 0.01 microns as well as

42

dissolved hydrocarbons at the molecular level (Nicolaisen and Lien, 2003; Brock et al., 2003; Hawboldt et al., 2012). They have been used more widely in onshore oil fields to remove salts. Low-pressure water is guided along a number of ceramic or synthetic filter elements, which contain pores of 0.1 - 0.2 microns (Ekins et al., 2005). Buildup of filter cake is avoided by a cross flow and a turbulent flow along the membrane surface. Part of the OPW passing through the membrane is directed to the pressure-pulse system for cleaning of the membranes, while the remaining part is discharged. The components that remain in the membrane after the pressure pulses need to be removed with chemicals periodically. The main part of aliphatic and aromatic hydrocarbons and solids remain in the concentrate, which is directed to a settling tank, where the oil can be separated easily in view of the high concentrations. Membrane processes can be categorized based on pore size ranges into microfiltration (MF), ultrafiltration (UF), nanofiltration (NF), and reverse osmosis (RO) (Xu and Drewes, 2006; NETL, 2012). This technology is relatively costly in capital and maintenance because smaller pore sizes require more care to operate and have more tendency of membrane fouling to occur (Ekins et al., 2005). That is why membrane filtration often requires multi–stage operations and pre-treatment is usually required to remove larger substances. Besides, membranes with a low molecular cut-off often have a low flux rate (Natures, 2010). Therefore, additional capacity is required for sustaining long-term use where weight and space then become a problem.

Steam stripping technology is based on vapor-liquid equilibrium. OPW components with boiling points lower than the boiling point for water, such as BTEX and other light

hydrocarbons, can normally be separated using a simple stripper configuration. In a typical stripper column a vapor stream enters at the bottom while the OPW enters the top. The vapor stream, which could be steam, air or another gas, will then pick the most volatile components in the liquid stream (known as stripping). Steam and hydrocarbon vapors are condensed and separated easily because of the high hydrocarbon content. Hydrocarbons that have been separated by steam can be directed to the condensate treatment system; and the water can then be discharged. Generally speaking, this process is energy intensive due to the need of steam. This system also has high space and weight requirement and is therefore suitable only for low volume, high contaminant loading applications (OGP, 2002). In addition, since the process is vulnerable to process disturbances, pretreatment of the OPW is preferable, for example, by using hydrocyclones (OGP, 2002). Moreover, post treatment is necessary as the air/hydrocarbon mixture must be treated before release or the mixture must be flared.

Biodegradation using microbiological organisms to break down and remove oil and aromatics from PW is a proven technology onshore for the treatment of PW prior to discharge to rivers (OGP, 2002; Van et al., 2003). But due to the large water hold-up volume and culture contact time (or residence time), these systems are very large and heavy, and therefore only suitable offshore for low volume applications (Tchobanoglous et al., 2003; Haritash and Kaushik, 2009; Ping et al., 2011).

In general, there are currently few widely recognized and highly efficient on board

44

treatment technologies available for PAHs removal from OPW in offshore platforms/FPSOs where current approaches are constrained by limited space, upset/shock loading conditions, and/or requirements of low maintenance and high cost efficiency. As such, the ability to incorporate these technologies into oil and gas operations in particular would be severely limited. Other promising technologies particularly those targeting dissolved PAHs need to be further investigated.

2.2.3 Challenges in Northern and Harsh Environments

As discussed in **Chapter 1**, the cold North Atlantic and Arctic Oceans have more vulnerable ecosystems and shorter food chains than those in the low-latitude regions (Cangelosi et al., 2007). Discharge of less treated OPW could cause much more severe effects on the local environment and aquatic lives and pose higher risks to the ecosystems and even human beings (Jing, 2012; Igunnu and Chen, 2012). The recent 'zero discharge' policy in Arctic (AWPPA, 2012; TWMA, 2014) poses even higher pressure on the OOG industry for requiring more efficient and eco-friendly treatment and disposal. As compared with the equatorial offshore sites, oil residuals discharged with OPW take much longer to decompose or be cleaned due to low ambient temperature and lead to long-term environmental impacts (considering the oil spill in the Gulf of Mexico in 2010). Additionally, the OPW carrying petroleum and chemical products may contain many toxic and carcinogenic contaminants with persistent and long-range transportation abilities.

45

Warmer water and air temperature due to the global climate change can help the decomposition and degradation processes; however, the semi-volatile and volatile organic compounds, such as PAHs (e.g., NAP) are readily reemitted to the atmosphere from contaminated water column at a higher temperature, and redeposit at high-latitude sites where vulnerable ecosystems and human communities exist (Jing et al., 2012). Furthermore, the global climatic changes are expected to alter the patterns of precipitation, evaporation, and ocean current and eventually cause more extreme weather conditions in the north, such as heavy storms, blizzards, and hurricanes. These unpredictable weather conditions together with the harsh environments will compromise the applicability and effectiveness of OPW treatment practices due to technical and safety concerns.

For example, in cold climate, the rising velocity of oil droplets decreases as water viscosity increases and the smallest range of oil droplets that the treatment unit usually can remove may not be removed. This effect may be reduced by the fact that temperature of water produced from a formation is usually high. At low temperature OPW components tend to have reduced water solubility, thus staying in dispersed oil phase. This may be beneficial in treatment point of view because dispersed oil can be removed by conventional treatment systems. However, as mentioned previously, compounds that may have volatized in warmer climates may stay in the dissolved phase, and therefore not be removed prior to discharge. These compounds such as NAP typically have high toxicity, leading to adverse effects on the marine ecosystems if without effective treatment. Some promising technologies such as catalytic photo oxidation to enhance the

46

traditional ones have emerged but still need more research.

Oil removal efficiency in most of OPW treatment units is reduced when they experience high fluxes in influent, especially those with short retention time. Rough sea may even cause significant damage to the treatment facilities due to the increased water pressure and air bubbles. In the harsh offshore environments, wave motions can cause inconsistent flow rates particularly for FPSO facilities. Motion or vibration may also result in mechanical problems in systems with moving parts or systems that rely on smooth water surface. This limits applications of some traditional treatment technologies. For example, floatation method utilizes skimming paddles to skim off oil foam from the water surface. Without stable water surface, desired oil removal efficiency may not be achieved. Furthermore, it has been suggested that the use of chemicals could also be compromised by the accidental spills during severe sea conditions (Satir 2008).

In extreme climates where manned operational controls are limited, highly reliable technologies, e.g., insensitive to motion, low maintenance, high automation, low chemicals and energy consumptions, are required. Because of the lower level of controls and discharge monitoring, low downtime equipment is needed. This would be very true given the extending exploration and development activities in the North Atlantic and Arctic Ocean.

47

2.2.4 Photolysis Enhanced Oxidation Technologies

Recent developments in the domain of chemical wastewater treatment have led to an improvement in oxidative degradation procedures for organic compounds dissolved or dispersed in aquatic media, in applying photocatalytic and photochemical methods, which are generally referred to as advanced oxidation processes (AOPs) (Munter, 2001; Gogate and Pandit, 2004; Kwom et al., 2009; Gilmour, 2012). The photolysis enhanced oxidation technologies are attractive alternatives to traditional non-destructive treatment processes since they can mineralize contaminants as opposed merely transporting them from one phase to another (Kishimoto and Nakamura, 2011; Estrada, Li and Wang, 2012). These technologies are commonly used in large-scale water and wastewater treatment plants because of its efficiency in destroying dissolved, volatile and non-volatile organic compounds as well as organic biocides as it can completely degrade the organic pollutants into harmless inorganic substances such as CO_2 and H_2O without generating additional waste streams or increase the bioavailability of recalcitrant organic pollutants (Stepnowski et al., 2002; Guieysse et al., 2004; Lin and Lin, 2007). The photo-activated chemical reactions are characterized by a free radical mechanism initiated by the interaction of photons at sufficient energy levels with the molecules of chemical species present in the solution, with or without the presence of the catalyst. The radicals can be produced using the photocatalytic mechanism occurring at the surface of semiconductors (i.e., titanium dioxide (TiO_2)), which substantially enhances the rate of generation of free radicals and hence the rates of degradation. An alternative way to obtain free radicals is using ultraviolet (UV) radiation by the homogeneous photochemical degradation of

48

oxidizing compounds such as hydrogen peroxide (H_2O_2) and ozone (O_3).

Many previous studies have explored the degradation of organic contaminants in wastewater by using UV based processes. Sugihara (2010) examined the aqueous photocatalytic treatment of diatrizoate using nanophase TiO_2. Experiments demonstrated that diatrizoate was degraded in aqueous TiO_2 suspensions illuminated with ultraviolet-A (UVA) light under both oxic and anoxic conditions. Lodha et al. (2011) has reported the direct photocatalytic degradation of rhodamine B (RB). The rate determining parameters including pH, dye concentration, H_2O_2 dose, and light intensity on the degradation process were studied in detail. The rate of photocatalytic degradation of the dye was observed to follow pseudo-first-order kinetics. Zapata et al. (2010) discovered that the photo-Fenton treatment at pilot plant scale was able to increase the biodegradability of a wastewater polluted with commercial pesticides from 50% to 95% as well as to reduce its toxicity from 96% to 50% of inhibition. The efficiency of the combined photo-Fenton/ biological system in terms of mineralization was 94%. Taralkar et al. (2013) designed a photocatalytic reactor and the reactor performance was analyzed by photocatalytic degradation of phenol in the presence of UV and TiO_2. The role of main factors that affecting the process has also been examined. Mohammad et al. (2014) investigated the optimum operating conditions, which yield the best performance of the photocatalysis process for the degradation of the synthetic dye in wastewater. Various operating parameters such as initial dye concentration, catalyst dose, suspension flow rate, pH, and H_2O_2 concentration were studied and optimized to inspect the behavior of the designed

49

reactor and to give higher efficiency to the reactor performance. Krzemińska (2015) claimed that photocatalytic process constitutes a promising technology for the treatment of food industry wastewaters such as winery and distillery wastewater, olive mile wastewater, dairy industry wastewater, molasses wastewater, candy and sugar industry wastewater, fresh-cut vegetable industry wastewater, containing difficult to biodegradable organic contaminants.

In oil spill research literature, photo oxidation is found one of the most important factors involved in the transformation of petroleum products that are released into the marine environment (Garrett et al., 1998; Dutta and Harayama, 2000; Prince et al., 2003; Jing et al., 2013). In photo oxidation, while saturated compounds are resistant, the aromatic compounds (e.g., PAHs) are particularly sensitive to photo oxidation (Garrett et al., 1998). Greater size and increasing alkyl substitution increase the sensitivity for aromatic compounds to photo-oxidation. Research has also demonstrated that while natural microbial populations in seawater partially biodegraded oil when sufficient nutrients were supplied, pre-treatment with photo oxidation increased the amount of crude–oil components susceptible to biodegradation, leading to significantly increased biodegradation of PAHs (Dutta and Harayama, 2000; Stepnowski et al., 2002).

Many studies have particularly investigated the degradation of PAHs in water and wastewater by using UV irradiation or its combination with other oxidants, such as O_3 and H_2O_2 (Sanches et al., 2011; Liu et al., 2014; Jing et al., 2014a). Woo et al. (2009)

characterized the photocatalytic degradation efficiency and pathways of five major PAHs in aqueous solution. Kwon et al. (2009) reported an inverse relationship between the reaction constant and the number of molecules for the UV-induced degradation of phenanthrene and pyrene. Włodarczyk-Makuła (2011) claimed that the removal efficiency of PAHs using UV was proportional to the duration and intensity of irradiation. Salihoglu et al. (2012) discovered that increasing temperature would have a direct positive effect on the destruction of PAHs. Tehrani-Bagha et al. (2012) applied UV-enhanced ozonation processes to destruct two organic surfactants and confirmed that the synergistic effects of O_3 and UV were more effective than the individual processes.

Comparing with other wastewater, OPW has its unique property with complex matrix containing elevated levels of minerals, hydrocarbons, heavy metals, suspended oil (non-polar), solids (sand and silt), production chemicals, etc. Among the AOPs, photocatalytic or photochemical degradation processes have been recently gaining significant attention and regarded as promising alternatives for OPW treatment (Qu, 2006). The major advantages of the photo oxidation based processes for removing PAHs from OPW include the complete mineralization of organic pollutants with operation at mild conditions of temperature and pressure, and the possibility to effectively use natural resources (i.e., sunlight or near UV light) for irradiation, which should result in considerable economic savings especially for large-scale operations (Tarek et al., 2011; Han et al., 2012; Ping et al., 2013). The UV equipment is reasonably compact with small footprint and fairly robust to on-site generation/operation and can handle upset or high-

51

loading conditions (Bares et al., 2006). It is fast, effective, efficient, low cost and environment friendly (Ping et al., 2013; Jing et al., 2015). It is also a relatively safe method since no chemicals are involved and there are no known taints or harmful by-products generated by the process. These features make the photolysis enhanced oxidation technologies well suited for applications in remote offshore oil production platforms or vessels where transportation, space, safety and cost are key concerns (Jing, 2015). Very recent research found that enhanced oxidation by photolysis could lead to positive results particularly in PAH removal from OPW. The Northern Region Persistent Organic Pollution Control Laboratory (NRPOP) at Memorial University where the author has been working is leading the research in the field (Ma and Chen, 2012; Ping et al., 2011; 2013; Li, Ping, and Chen, 2013; 2014; Zheng et al., 2013; 2014; Liu et al., 2014; Jing et al., 2014; 2015). For example, Ping et al. (2011) presented a preliminary study by conducting the bench-scale lab tests to explore the effect of UV irradiation on natural degradation of PAHs in PW generated from OOG production. The results demonstrated the capacity of UV irradiation in enhancing degradation of most of the PAHs in OPW. In some cases (e.g., Fluorene) the removal rate could reach up to 94.87%. Liu et al. (2014) tested the removal efficiency of NAP using UV irradiation with both suspended and immobilized TiO_2 catalysts. The results showed that the immobilized catalyst has a better enhancement to photo-oxidation. The turbidity was significantly reduced compared with suspended system. Jing et al. (2014) studied the photodegradation kinetics of NAP in natural seawater through a full factorial design of experiments (DOE). Results disclosed that fluence rate, temperature, and the interaction between temperature and initial

52

concentration are the most influential factors. An increase in fluence rate could linearly promote the photodegradation process. Salinity was reported to increasingly impede the removal NAP because of the existence of free-radical scavengers and photon competitors. Zheng et al. (2014) examined the removal efficiency of 16 US EPA priority PAHs by UV irradiation through a set of bench- and batch-scale tests. The removal efficiency of PAHs in 12 hours reached up to 93%. The results also indicated that the photolysis followed first-order reactions. The impacts of UV wavelengths on removal efficiency were quantified showing the better performance of UVC and the agreement with UV absorption spectrum of the target PAHs. The competitive interactions between different PAHs and their roles in influencing degradation rates were further investigated.

However, the studies have been limited in reporting on UV application to treating OPW and feasibility/advantages in combining with other advanced oxidation methods (e.g., UV/TiO_2, UV/O_3, UV/H_2O_2) (Qu, 2006; Correa et al., 2010; Ma, 2012; Li, 2014) for on-site treatment of OPW. In addition, some aspects of the photolysis enhanced oxidation process related to reactivity, kinetics and how changing environmental conditions can influence the efficiency still remain unclear, and questions regarding if the process is fundamentally different from the individual process alone remain unanswered.

2.3 Summary

The recent developments of technologies in testing and treating PAHs in OPW are presented and discussed in this chapter.

53

On one hand, it is of paramount importance to properly qualify and quantify PAHs in OPW in time due to the increasing concerns of their behaviors in the environment, which lead to the high toxicity and pose a risk of causing adverse effects to the ecosystem and human health. Four sample pretreatment methods (i.e., LLE, SPE, SPME, and LPME) and five detection methods (i.e., HPLC-fluorescence, HPLC-UV, HPLC-MS, GC-FID, and GC-MS) have been reviewed. The pros and cons of each have been thoroughly discussed with regard to the feasibility for on-site in-time OPW monitoring. It was found that the coupling of enhanced SPE or LPME pretreatment with optimized GC-MS detection could be good candidates for offshore real-time PAHs monitoring in OPW. Further research into the technology development is highly in demand for investigating and evaluating the associated feasibility and efficiency.

On the other hand, conventional on-site OPW treatment is mainly dependent on physical separation of the bulk of oil from the water to meet the regulatory standards, which has low efficiency in the removal of dissolved fraction of PAHs, which are highly toxic and persistent. Although there are technologies available with a clear potential for a significantly reduction of the concentration of PAHs in the discharged OPW, they all invariably have significant weight, space, load, maintenance, pre/post-treatment and cost limitations to be considered as on-site treatment technologies for installation on the platforms and the harsh offshore environment (e.g., cold and high motion) makes the application even more challenging. The photocatalytic or photochemical degradation

54

processes has been gaining significant attention and regarded as a promising solution because of its relatively small footprint, low cost and risk, high efficiency as well as its chemical-free nature. Based on the current understanding of the physical and chemical composition of OPW, the photolysis enhanced oxidation technologies has been put aware since they have great potential to be enhanced into compact, robust, fast, efficient, and environmental friendly systems which are relatively safe methods in treating PAHs with no added chemicals and harmful by-products. It deserves further exploration to address the shortcomings of existing technologies by optimizing the proposed system and to investigate the treatment efficiency.

Chapter 3 Development of New Analytical Methods for Testing PAHs in OPW[1]

3.1 Standards, Reagents and Materials Preparation

USEPA's 16 priority Polycyclic Aromatics Hydrocarbon (PAHs) compounds were chosen to represent PAHs in OPW in this research. The 16-PAH mixed standard, including NAP, ACY, ACE, FLO, PHE, ANT, FLA, PYR, BaA, CHR, BbF, BkF, BaP, DahA, IcdP, BghiP, was supplied by Agilent Technologies Inc. Mississauga, Ontario (p/n 8500-6035). The PAH stock solution had a nominal concentration of 500 μg/ml. The labeled PAHs with high purity were used as surrogates: NAP-d_8 (99%) and PHE-d_{10} (99%), obtained from Cambridge Isotopes Labs (St. Leonard, Quebec, Canada) and C/D/N Isotopes Inc. (Pointe-Claire, Quebec, Canada), respectively. P-Terphenyl-d_{14} (2,000 μg/ml) purchased from VWR International (Mississauga, Ontario, Canada) was used as internal standards (IS). Sodium chloride (NaCl) was also obtained from VWR International (Mississauga, Ont., Canada). The solvents, including ultra-high purity water, dichloromethane (DCM) and acetone of reagent grade or equivalent quality purchased from VWR International (Mississauga, Ontario, Canada) and Fisher Scientific (Ottawa, Ontario, Canada). The SPE apparatus and 6 ml/500 mg ENVI^{TM}-18 C_{18} polypropylene SPE cartridges were purchased from Supelco (Oakville, Ontario, Canada). GC supplies, including deactivated single tapered glass inlet liners and J&W Scientific DB-5MS UI fused silica capillary columns, were obtained from Agilent Technologies Inc. (Mississauga, Ontario, Canada).

56

[1] Research work described in this chapter is fulfilled by team work, the author's contributions include: method co-development, consumables purchase, lab coordination, experimental co-design, experiments set up, lab recording, data compilation and analysis, as well as papers drafting, from which some results in this chapter were extracted (i.e., Ping et al., 2010; 2011a; 2011b; 2013; Liu et al., 2011; 2012; Zheng et al., 2012; 2013; 2014; 2015; Li et al., 2013; 2014).

PAH stock: 0.05 ml 16-PAH mixture standards (Agilent, 500 μg/ml), 0.025 ml NAP-d_8 and PHE-d_{10} (1,000 μg/ml) were mixed together and diluted with DCM (Fisher, 99.99%) in 25 ml volumetric flask to give a stock solution of 1 μg/ml 16-PAH and 2 surrogates for further preparation of the calibration series and spiked water samples.

Calibration series: The PAH stock solution was further diluted with DCM to obtain 20 ng/ml, 10 ng/ml, 5 ng/ml, 2 ng/ml, 1 ng/ml, 0.5 ng/ml, 0.2 ng/ml and 0.1 ng/ml PAH mixture solution series for GC-MS calibration.

Working stocks for surrogates and internal standard: The 5 μg/ml NAP-d_8 and 0.5 μg/ml PHE-d_{10} solutions were prepared as the surrogate working stocks by diluting 0.05 ml and 0.005 ml standards (1,000 μg/ml) to 10 ml respectively. The 4 μg/ml IS working stock was made by diluting 0.02 ml standard solution (2,000 μg/ml) to 10 ml. The surrogate

57

working stocks were added to the water sample to examine method performance for each sample, while the internal standard was added to the sample concentrate to compensate variances in final extract volume, injection volume and instrument sensitivity.

Spiked distilled water samples: The spiked distilled water samples for SPE were obtained through diluting 400 μl PAHs stock to 2 L by distilled water. For LPME, 0.1 ml PAHs stock was diluted with distilled water in 500 ml volumetric flask. The concentration of each PAH in the water samples was 0.2 μg/l. Replicate samples were prepared for evaluating performance of the developed SPE-GC-MS and LPME-GC-MS system and were stored at 4 ^{0}C in the chromatography fridge before analysis.

Produced water samples: The produced water samples from an offshore platform were collected after the standard platform treatment with water quality characterized and summarized in **Table 3-1**. The collected produced water samples have high salinity and organic loading. When entering the lab, the produced water samples were placed at a 4 ℃ fridge and the darkness condition inside fridge was adopted to avoid light radiation to the samples. The OPW samples were used to validate the newly developed SPE-GC-MS and LPME-GC-MS analytical methods and to test their detection limits in the OPW matrix. Since the 16 PAHs expect NAP were all below the limits of detection (LODs) of the method so the samples were also spiked to test the recovery of the method.

3.2 Measurements of PAHs in OPW

3.2.1 Establishment of SPE Pre-Treatment

Each SPE cartridge was conditioned by sequentially aspirating 6 ml aliquots of selected solvent, 6 ml methanol and 6 ml distilled water (flow rate of ~2 ml/min), while preventing them from drying out between additions of solvents and the sample water. The 200 ml sample water with surrogate addition (i.e., NAP-d_8 and PHE-d_{10}) was loaded onto the SPE cartridges (flow rate of ~10 ml/min). Each cartridge was then air-dried for 10 mins and the PAHs were eluted twice with 1 ml selected solvent. The internal standard (0.5 ng of P-Terphenyl-d_{14}) was added to each sample extract before the GC-MS analysis. The blank (200 ml of distilled water) and samples were then analyzed by the GC-MS system. In this step, the traditional SPE pre-treatment has been enhanced through screening of conditioning/elution solvents including Acetone, Acetonitrile, DCM, Hexane, Methanol, Toluene, Acetonitrile+Toluene (v/v: 3/1), and Methanol+Toluene (v/v: 10/1). And the experimental runs were carried out with pH at low value (<3) and also unadjusted (~7).

Table 3-1 Water Quality Characterization of the OPW Samples (n = 2)

Parameters	pH	Conductivity (Ms/CM)	Turbidity (NTU)	Salinity (PSS)	DO/DO% (mg/l)	COD (ppm)
OPW	6.88	63.6	55.8	41.94	7.91/98.4	3154
Seawater[*]	~7.5	50	N/A	~35	N/A	2.71~5.71[*]

Note:

[*] - Faragallah et al., 2009

3.2.1.1 Selection of solvent

Figure 3-1 shows the chromatograph peaks of the targeting PAHs eluted by various solvents. Such outputs were gained through Single Ion Monitoring (SIM) mode. By comparing the shapes of peaks, the DCM, hexane and acetone were found to perform better with narrower peaks than the others with the DB-5MS UI fused silica capillary column. Since the intensity value of the PAHs obtained through DCM elution was ~25% higher than those of acetone and hexane, DCM was chosen as the extraction solvent in order to achieve the best extraction efficiency and instrumental performance.

3.2.1.2 Selection of pH

Low pH normally can help improve the extraction efficiency for the ENVI^{TM}-18 SPE absorbent (Supelco, 2010; USEPA method 525.2) due to the enhanced ionization of the targeting compounds in the water solution (Cranford, 2010). Therefore, the performance of SPE with low pH (<3) and unadjusted pH (~7) were compared (**Figure 3-2**) with regard to the PAHs extraction efficiency and recoveries. For this purpose, samples with both pH values were prepared and loaded to the solid phase. The PAHs in the sample water retained in the solid phase had then been eluted three times by 1 ml DCM at each pH scenario. The results showed that although the lowered pH was theoretically assumed to help achieve higher PAH extraction rate (i.e., from water to solid phase), it made the final elution (i.e., from solid phase to solvent) more difficult especially for the PAHs with low molecular weights. As can be seen from **Figure 3-2** (d), in the case of lower pH setting, there still exist significant residue amount of the eight early eluting PAHs (i.e.,

61

NAP, ACY, ACE, FLO, PHE, ANT, FLA, PYR) even after the third 1 ml DCM elution. It indicated that more than 3 ml solvent volume per sample was required in the elution step, leading to the reduced concentration rate. The possible reason could be that even though acidification can increase extraction efficiency, the strong binding between solid phase and compounds reduced the elution efficiency, leading more solvent consumption and final volume of the extract. Other extract concentration methods, for example, nitrogen blow down can help increase the concentration rate (USEPA Method 3535), however it is time consuming and increases the complexity of the whole process (Kemmochi et al., 2001).

Therefore, in the 6 ml/500 mg C_{18} (17% carbon loading) SPE cartridge, sequentially conditioned with 6 mL DCM, 6 mL methanol and 6 ml distilled water, loaded by sample water with unadjusted pH, and eluted twice with 1 ml DCM, provided the best results and was further applied throughout the research where SPE were needed.
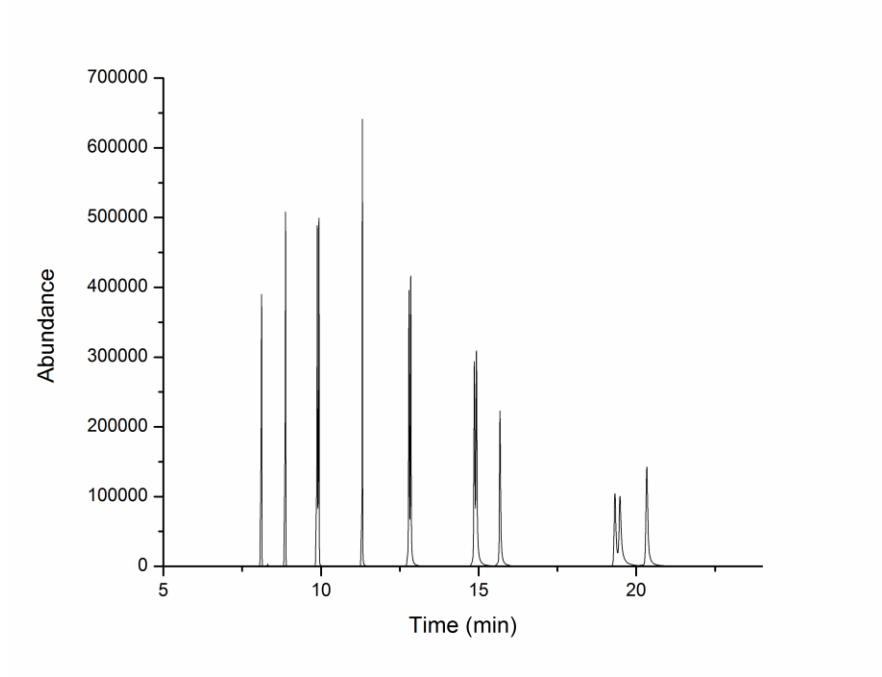
(a) Acetone

(b) Acetonitrile

63

(c) DCM

(d) Hexane

64
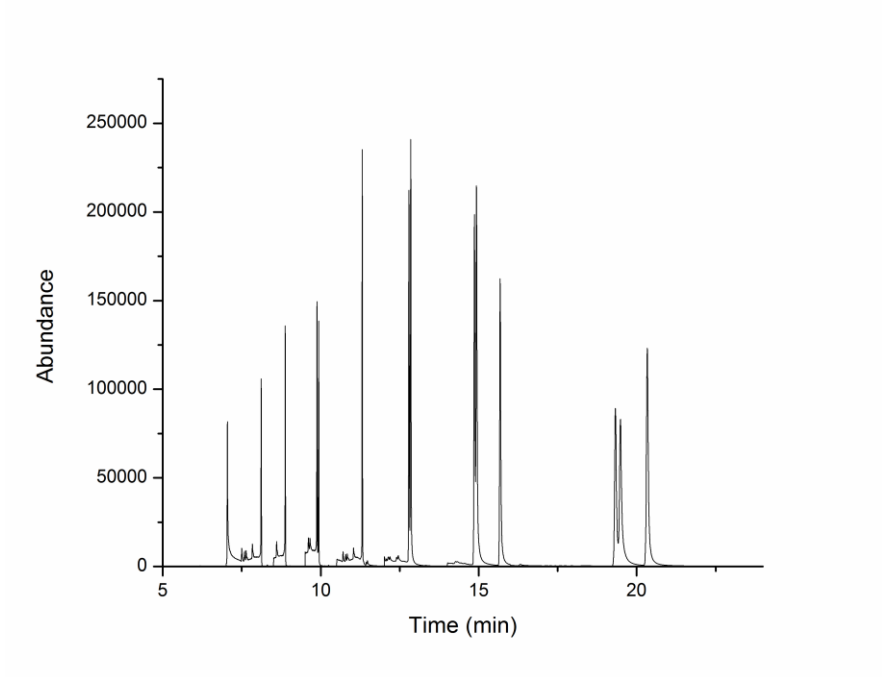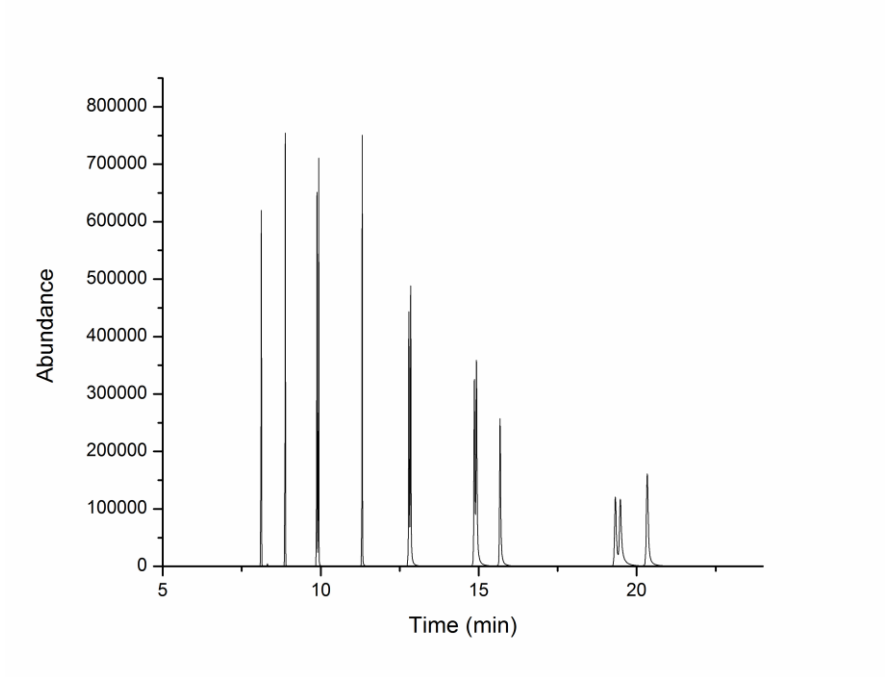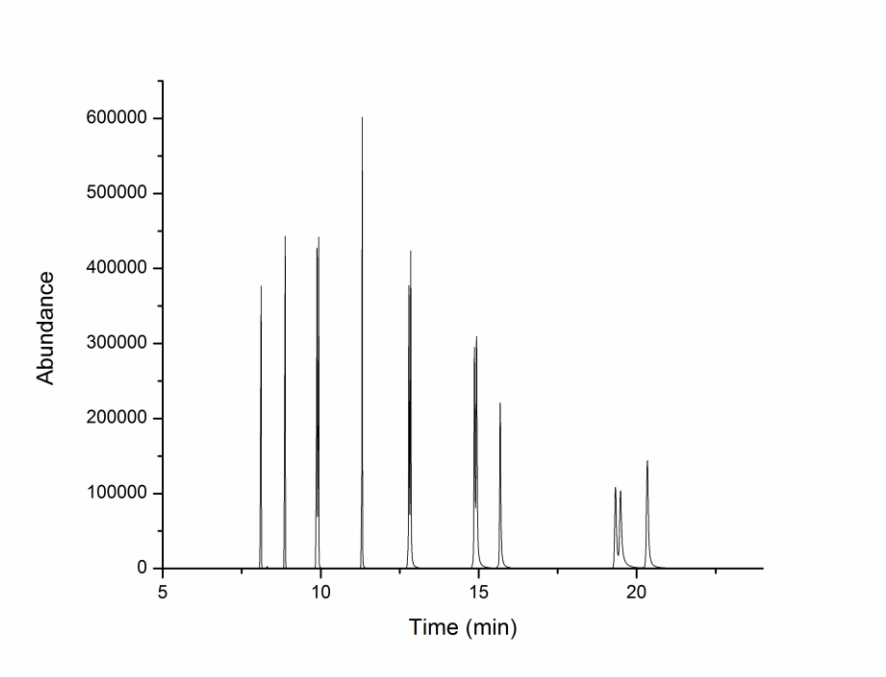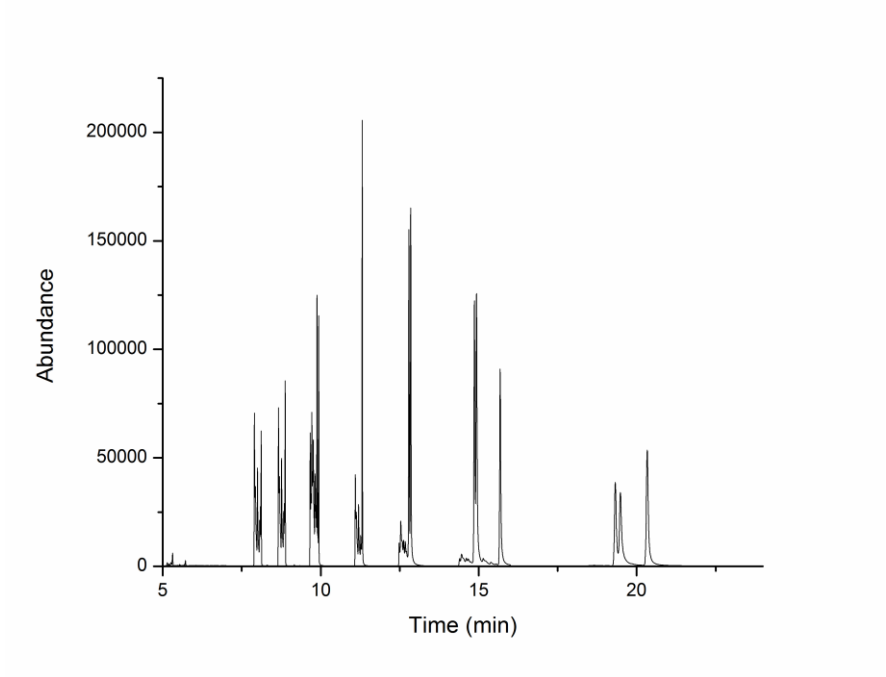
(e) Methanol

(f) Toluene

65
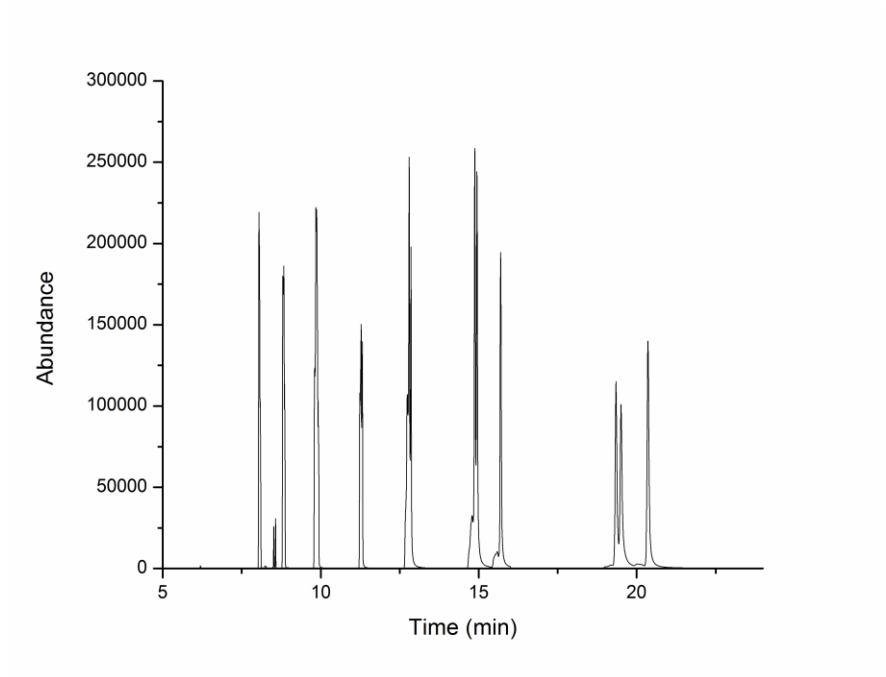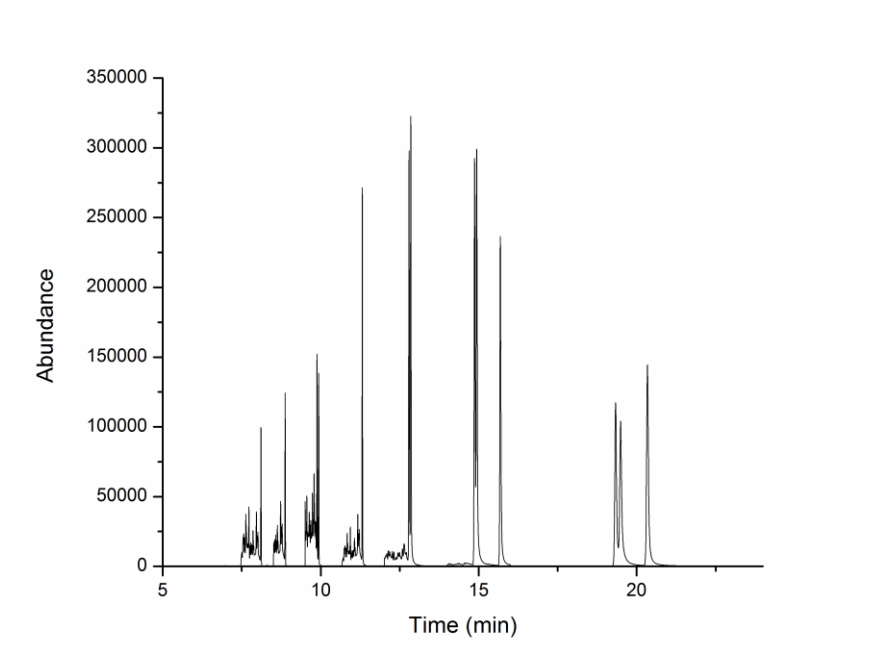
(g) Acetonitrile + Toluene (v/v: 3/1)
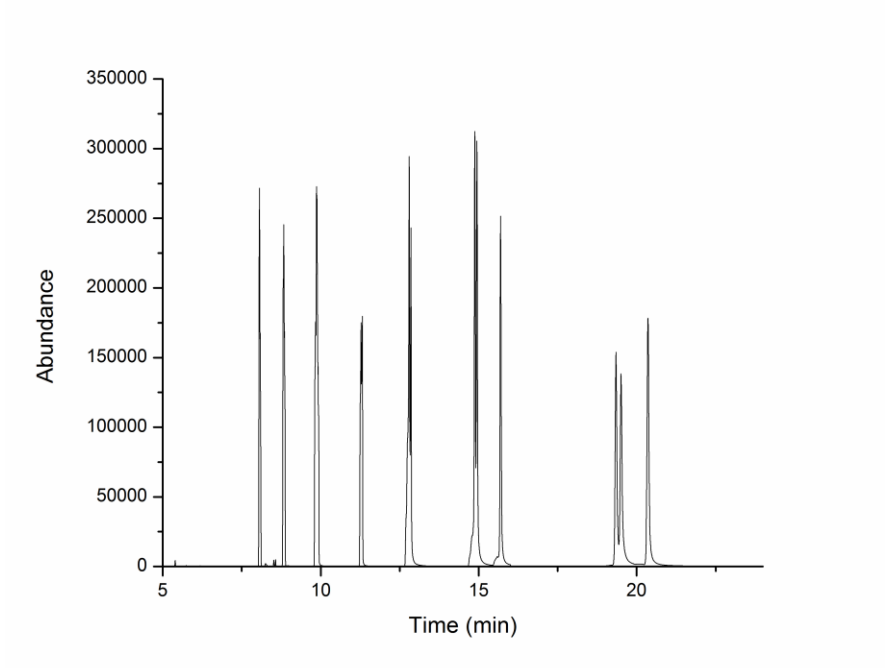
(h) Methanol + Toluene (v/v: 1/10)

Figure 3-1 PAHs Chromatograph Peaks with Varied Solvents Selections
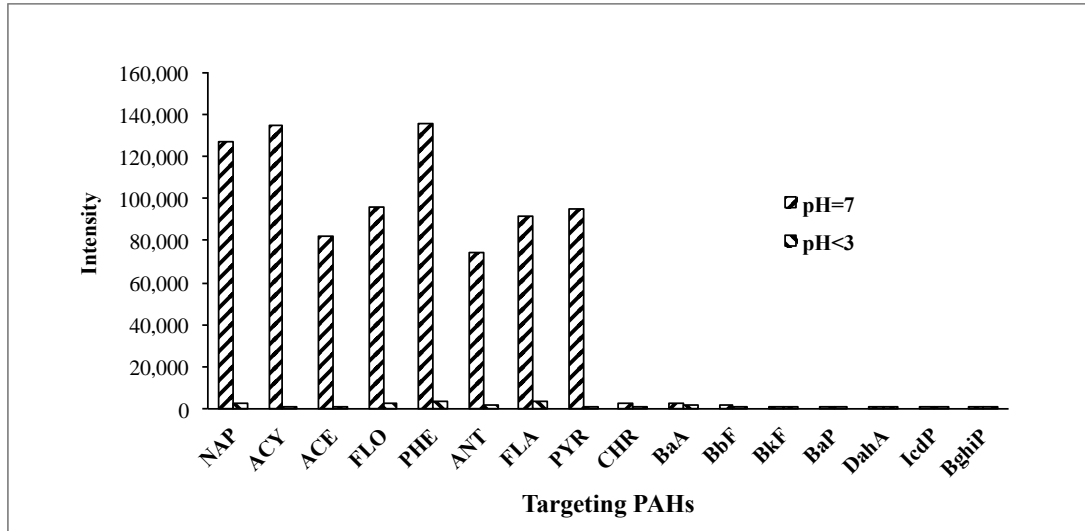
(a) First time elution by 1ml DCM
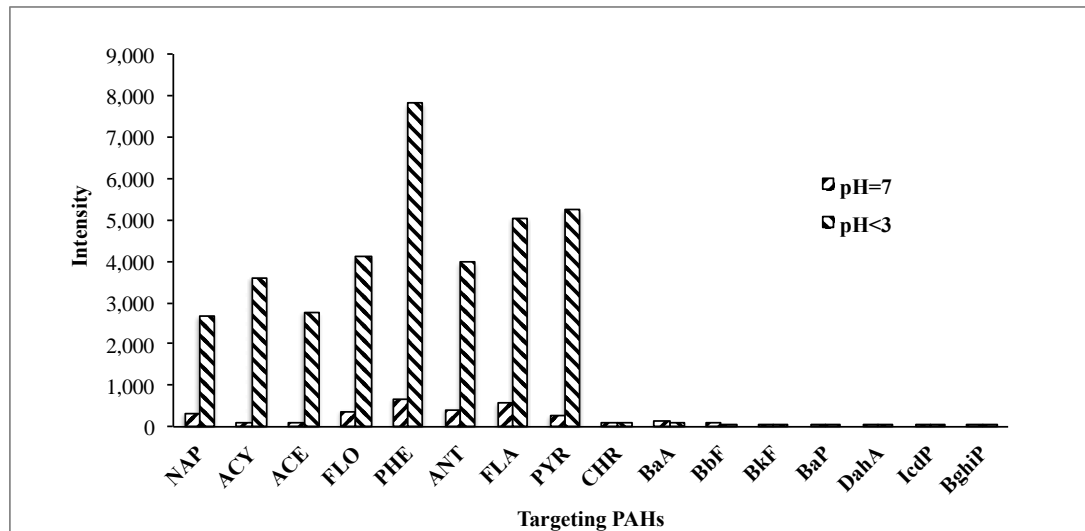
(b) Second time elution by 1ml DCM
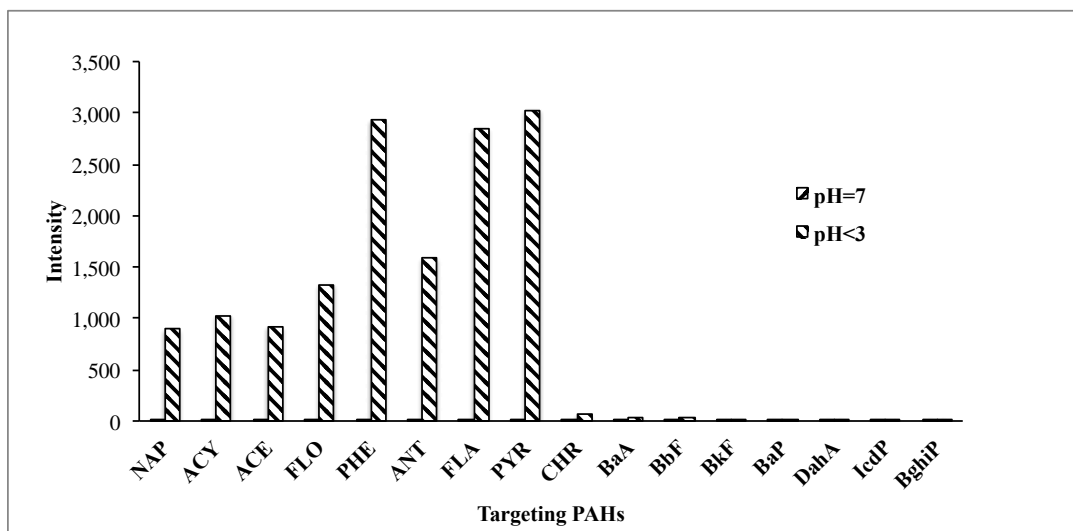
(c) Third time elution by 1ml DCM
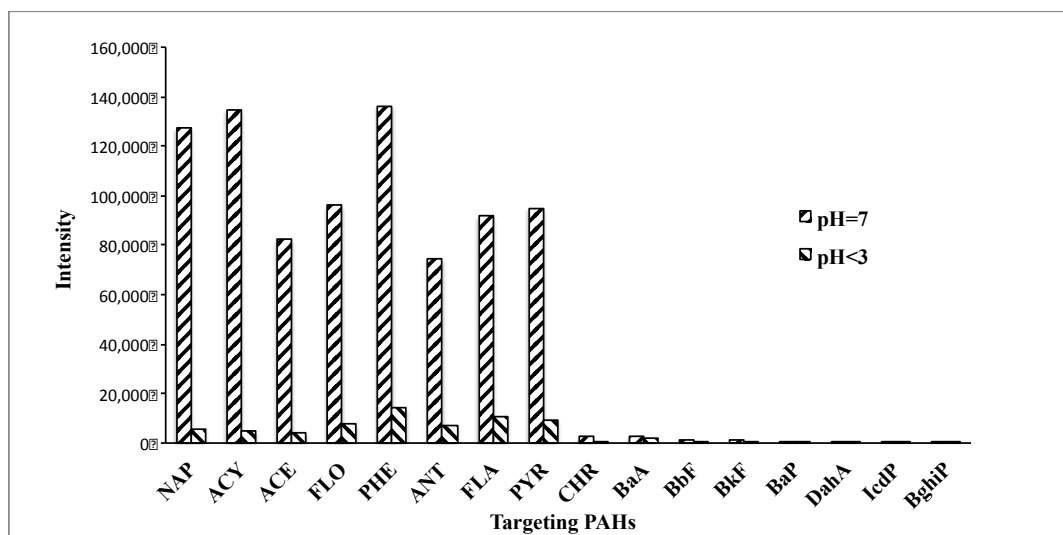
(d) Recoveries at both pH settings after 3 ml DCM elution

Figure 3-2 pH Impacts on PAHs Extraction Efficiency

3.2.2 Establishment of LPME Pre-Treatment

10 ml water sample with surrogates (NAP-D$_8$ and PHE-D$_{10}$) was transferred into a 10 ml glass-centrifuge tube. As an extraction solvent, DCM (0.25 ml) was added into the water sample. The glass-centrifuge tube containing the mixture was then placed on a mini incubating shaker (VWR International, Mississauga, Ont., Canada) operating at 1,000 rpm for 15 min at ambient temperature. During the shaking and mixing process, the solution became turbid due to the dispersion of fine DCM droplets into the aqueous bulk. The emulsification phenomenon favored the mass-transfer process of PAHs from the aqueous bulk to the organic phase. The emulsion was next centrifuged with a VWR Clinical 200 Large Capacity Centrifuge (VWR International, Mississauga, Ont., Canada) at 1,000 rpm for 5 min to achieve the phase separation. After centrifugation, DCM (50 μl) was removed from bottom of the tube by using a 100 μl Agilent syringe (Agilent Technologies Inc. Mississauga, Ontario) and transferred into a 150 μl micro vial (Agilent Technologies Inc. Mississauga, Ontario). After 0.5 ng of internal standard (P-Terphenyl-d$_{14}$, 5 μl of 0.1 ng/μl solution) was added into the micro vial, GC-MS analysis was performed. Sample results were not corrected for surrogate recovery. Method blanks (10 ml of distilled water) were processed along with the analysis of samples.

In this process, several parameters affecting extraction efficiencies, such as selection of organic solvent, solvent volume, agitation rate, extraction time, salt addition and centrifuge speed were optimized. To obtain the optimized extraction conditions, the ratio of relative peak area of analyte to that of internal standard has been used as the GC

69

response (relative peak area) to evaluate the extraction efficiency under different conditions.

3.2.2.1 Selection of organic solvent

LPME is a process dependent on equilibrium rather than on exhaustive extraction (Psillakis, 2001). When the partition equilibrium is reached, the amount of extracted analyte can be expressed as follows: (Zhao, 2004)

$$n = \frac{K_{odw}V_dV_s}{K_{odw}V_d + V_s}C_0 \qquad (3\text{-}1)$$

Where,

n = amount of analyte extracted by solvent when partition equilibrium is attained

K_{odw} = organic solvent-water distribution constant

C_0 = initial concentration of the analyte in the sample matrix

V_d = volumes of solvent, ml

V_s = volumes of sample, ml

As indicated by **Equation (3-1)** it is essential to select an appropriate organic acceptor phase for the establishment of LPME method, which is dependent on the chemical nature of the target analytes. The extraction solvent must meet four requirements: 1) it is convenient that the extraction solvent remain at the bottom of the centrifuge tube after phase separation. Hence, the extraction solvent should be denser than water and water

immiscible (Fontana, 2009); 2) the chosen organic solvent must have good affinity for target compounds to extract analytes well; 3) it should have excellent gas chromatographic behavior to be separated from the analyte peak in the chromatogram (Tankeviciute, 2001); 4) the organic solvent should have relative low health risk to the operator. Considering these factors, various solvents were examined in the preliminary experiments. 10 ml aliquots of distilled water fortified with 0.2 μg/l of each PAH were extracted by using 250 μL of each solvent in a shaker for 10 min with 1,000 rpm stirring rate. The emulsion was centrifuged at 1,000 rpm for 5 min to achieve the phase separation. Trials data indicated that DCM gave satisfying extraction efficiency. This is in accordance with USEPA Method 622. Therefore, in the following work, DCM was chosen as the extraction solvent.

3.2.2.2 Selection of solvent volume

From **(3-1)**, it can be seen that organic solvent drop volume is another important factor affecting LPME efficiency. The volume of solvent can significantly affect the extraction performance. Generally, lower solvent volume leads to the increase of the enrichment factor (EF) by decreasing the ratio between organic/aqueous phases (Saraji and Boroujeni, 2014). To increase the sensitivity of the LPME procedure, the volume of DCM were optimized. For this purpose, different volumes of DCM in the range of 100-250 μl were examined to extract spiked water samples (10 ml at the level of 0.2 μg/l), in triplicate, under the same experimental conditions as described above. A DCM volume of 100 μl was completely dissolved in the aqueous bulk. A DCM volume of 200 μl showed

71

significant solvent loss during extraction while the application of 250 µl showed acceptable residual volume. Based on previous literatures (Charalabaki et al., 2005; Zhao et al., 2004; Ozcan et al., 2010), increasing the organic solvent volume resulted in a decrease of detector response (i.e. decreased peak area) for all PAHs attributed to dilution effect. Based on the above consideration, in the following investigations the solvent volume was fixed at 250 µl. After extraction with 250 µl of DCM, recovered volume of DCM was (110±3 µl for spiked distilled water sample; 100±3 µl for produced water sample). This result also corroborated that collection of DCM was reproducible.

3.2.2.3 Selection of agitation rate

The effects of sample agitation on extraction efficiency need to be investigated. Based on the penetration theory of mass transfer of solute, the aqueous phase mass-transfer coefficient β_{aq} can be calculated by **Equation (3-2)** (Jeannot and Cantwell, 2001):

$$\beta_{aq} = 2\left[\left(\frac{D_{aq}}{\pi t_e}\right)\right]^{\frac{1}{2}} \tag{3-2}$$

Where,

D_{aq} = diffusion coefficient in the aqueous phase

t_e = exposure time of a small fluid volume element of one phase momentarily in contact with the other phase, min

72

According to the theory, β_{aq} increases with increasing stirring rate because at a faster stirring rate the value of t_e is smaller. As a result, agitation enhances extraction efficiency. Although higher stirring rates (> 1,000 rpm) result in greater extraction efficiency, they also gave rise to instability of the mini-shaker. Therefore, stirring rate of 1,000 rpm was used for subsequent experiments.

3.2.2.4 Selection of extraction time

As elaborated in the above, LPME is a process dependent on equilibrium. The amount of analyte extracted at a given time is dependent on the mass transfer of analyte from aqueous samples to the organic solvent drop. This procedure requires a period of time for equilibrium. Extraction yields should increase with increase sampling times. Nonetheless, for quantitative analysis it is not necessary to attain equilibrium if constant extracting conditions are maintained. Since the constant extracting condition is unknown by using the mini-shaker, it should be further investigated to find out an appropriate shaking time that can achieve well mixing and matching the chromatography run time and maximizing sample throughput.

3.2.2.5 Selection of ionic strength

The effect of ionic strength of the aqueous solution may have several effects upon extraction. Usually, depending on the solubility of the target analytes, adding salt (i.e., NaCl) to the sample can increase the ionic strength of the solutions, which enhances extraction of the analytes since it can decrease the solubility of analytes in the aqueous

73

sample and enhance their partitioning into the organic phase (Eisert and Pawliszyn, 1997).

However, the addition of NaCl may increase the instability of the organic solvent. It was

suspected that addition of salt increases the density of the solution so that the flotage of

organic solvent increases according to the following principle of Archimedes flotage:

$$rF_d = \rho_{aq}gV_d \qquad\qquad (3\text{-}3)$$

Where,

F_d = flotage of organic drop in the aqueous samples

ρ_{aq} = density of aqueous phase, ppm

g = gravity, m/s^2

V_d = volume of the organic drop, ml

Moreover, the addition of NaCl may even decrease the extraction efficiency during

sample pre-treatment by LPME (Casas et al. 2006; Gioti et al. 2005; Hou and Lee 2004).

As a result, the instability of organic phase also increases with the increasing amount of

NaCl. So, for the purpose of this study, the effect of ionic strength in this experiment need

to be further assessed.

3.2.2.6 Factorial design

Design of Experiments (DOE) has portrayed a major contribution in science and

technology since the time Sir Ronald Aylmer Fisher introduced this concept in the 1940s

74

(Belavendram, 2011). Factorial experimental design is one of the major approaches in DOE, which is commonly used to determine the influence of different factors in a system or procedure, and is satisfactory to estimate the linear models with a very low number of experimental run, thus reduces the time needed for the optimization of an investigated procedure and overall costs (Ozcan et al., 2009; Plesu et al., 2009). Besides, such approach would also lead the processes to obtain better performance and achieve greater reliability. Therefore, after selection of the most suitable extraction solvent (i.e., DCM) and its volume (i.e., 250 μl), the most appropriate agitation rate (i.e., 1,000 rpm) for analytes extraction, the other factors affecting the efficiency of the LPME, including the shaking time (denoted as X_1), ionic strength of the sample (denoted as X_2), and the centrifugation speed (an important parameter for the phase separation, denoted as X_3) have been optimized by a full factorial experimental design at two levels (2^3). For this purpose, a series of 10 ml aqueous samples spiked at 0.2 μg/l of each target analyte were extracted with 0.25 ml DCM with sample solution being agitated in a mini-shaker operating at the rate of 1,000 rpm. The lower and higher level for each factor was signed as "−" and "+", respectively. The corresponding levels (low and high level) for factors X_1-X_3 were 5 and 15 min, 0.5 and 1.0 g/ml, and 1,000 and 3,000 rpm, respectively. It should be noted that the low level of X_2 is relatively high because of the high salinity of produced water. The experimental design matrix is constituted as shown in **Table 3-2**. A full 2^3 design would have required eight experiments, which were triplicated in order to calculate the residual error. The experiments were performed in a randomized order to avoid any systematic error.

75

After processing the data by analysis of variance (ANOVA) using Design Expert 7.1 ®, the ANOVA tables were constructed to test the significance of the effect of each factor on the extraction efficiency. At significance level of 5%, the factor with F-value over critical F-value (5.318) has a significant effect on the extraction efficiency. It was found that the shaking time (X_1) has positive effect on the extraction of all PAHs. In other words, the LPME for 15 min gave better result than 5 min. Therefore, 15 min was chosen as extraction time for further studies; the centrifugation speed (X_2) posed negative effect on the extraction of all PAHs. Namely, centrifugation at 1,000 rpm achieved better phase separation. Therefore, 1,000 rpm was selected as centrifugation speed; the ionic strength of the sample (X_3) poses negative effect on the extraction of all PAHs. In this study, increasing NaCl concentration in the water sample from 0.5 to 1.0 g/mL decreased the extraction recovery of all PAHs. The obtained result was in agreement with relevant references (Regueiro et al., 2009; Fontana et al., 2009; Ozcann et al., 2010), which explained the effect of ionic strength of an aqueous sample on the emulsification phenomenon. Therefore, further experiments were performed without addition of NaCl into the samples.

As a result, the optimum conditions for LPME of PAHs from water were as follows: DCM as an extraction solvent, solvent volume: 250 μl; shaking time: 15 min at 25 ^{0}C with no addition of NaCl and centrifugation speed: 1,000 rpm. The enhanced LPME treatment was further applied throughout the research where LPME were needed.

76

Table 3-2 Factorial Design Matrix for LPME Optimization and Relative Standards Deviation (RSD) of PAHs Tests

Experiment No.	Codified parameters			RSD (%)
	X_1 (min)	X_2 (g/mL)	X_3 (rpm)	
1	-	+	-	5.003
2	-	-	+	5.319
3	-	+	+	4.635
4	+	+	-	4.477
5	+	-	-	4.405
6	+	+	+	4.213
7	+	-	+	5.101
8	-	-	-	4.388

3.2.3 Establishment of Gas Chromatography-Mass Spectrometry (GC-MS) Detection

An Agilent 7890A/5975C GC-MS equipped with an Agilent 7693 autosampler was used in this study. Data acquisition, processing and evaluation were carried out using Agilent ChemStation® software Version 2.01. The PAHs were identified by mass spectrum using the NIST/EPA/NIH Mass Spectro Library® Version 2.0f. The analytes were separated on a 30 m × 0.25 mm ID × 0.25 μm DB-5MS UI fused silica capillary column. An electronic pressure control was utilized to maintain a constant carrier gas (Helium of ultra-high purity) flow of 1.5 ml/min throughout the oven programs. Sample injections (2 μl) were performed using a split/splitless injector (single tapered inlet liner) in splitless mode with the injector set at 280 ℃. The transfer line temperature from the GC to the ion source was 300 ℃. PAH analyses were performed in the electron impact ionization mode (EI) using electron energy of 70 eV. The scan mode data were used for identification whereas the SIM mode was applied for quantitation.

The traditional GC-MS analysis has been improved by enhanced system settings such as adjusting oven temperature ramp to better separate the targeting PAHs in the column, and obtaining appropriate ion-source temperature by using the ultra-inert filament to provide a lower method detection limit (MDL). Three oven ramp programs (multiple/single) have been compared and two ion source temperatures (230 ℃/350 ℃) have been applied in the analysis. Table 3-3 shows the three scenarios of the system settings compared in this study for establishing the analytical method.

78

Table 3-3 Three Scenarios of the GC-MS System Settings

	Oven temperature ramp programs	Ion source temperatures
Scenario I[d]	45 min multiple ramp [a]	230 ℃
Scenario II	33 min multiple ramp [b]	230 ℃
Scenario III	60 min multiple ramp [c]	350 ℃

Note:

[a] - 45 min multiple ramp: 40 ℃ hold 4 min; 10 ℃/min to 270 ℃ hold 13 min

[b] - 33 min multiple ramp: 65 ℃ hold 1 min; 4 ℃/min to 115 ℃ hold 1 min; 25 ℃/min to 130 ℃ hold 0 min; 15 ℃/min to 280 ℃ hold 1 min; and 20 ℃/min to 320 ℃ hold 5 min

[c] - 60 min single ramp: at 60 ℃, 4 ℃/min to 300 ℃

[d] - Adapted from USEPA 8720D Method

3.2.3.1 Scenario I

The system settings with regard to the oven temperature ramp program and ion source temperature setting under Scenario I was adapted directly from the USEPA 8720D Method. Previous studies indicated that in the 16 PAHs analysis, 4 pairs of PAHs (i.e., PHE and ANT; BaA and CHR; BbF and BkF; IcdP and DahA) were difficult to be quantified because the retention time of the PAHs in each pair were close to each other and they had similar primary ions (Agilent, 2009). Therefore, special attention has been paid in the study to examine the performance of GC-MS analysis on these four pairs of PAHs. From **Figure 3-3 (a)**, the peaks of the last 3 pairs of PAH compounds (i.e., BaA and CHR; BbF and BkF; IcdP and DahA) were not well separated by the column under the oven temperature ramp in this scenario after 45 minutes. A zoomed in images of the 3 pairs of PAHs peaks are shown in **Figure 3-4 (a)**.
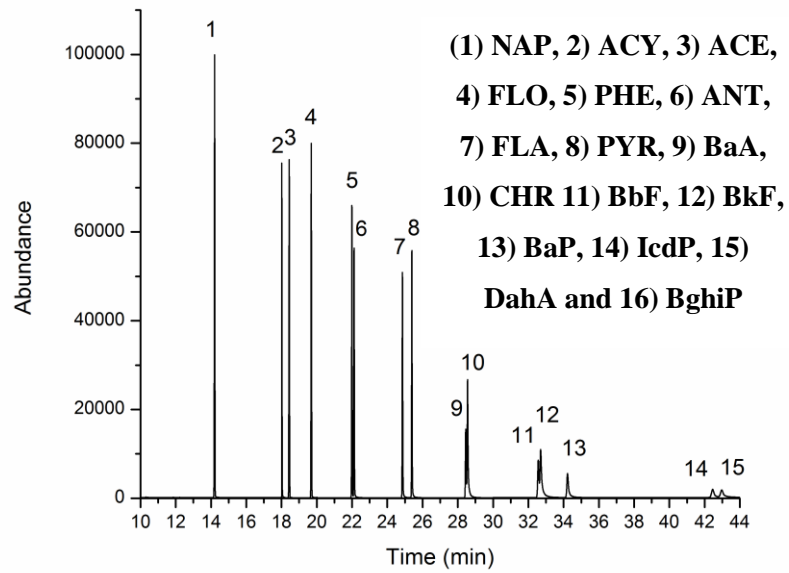
(a) Scenario 1
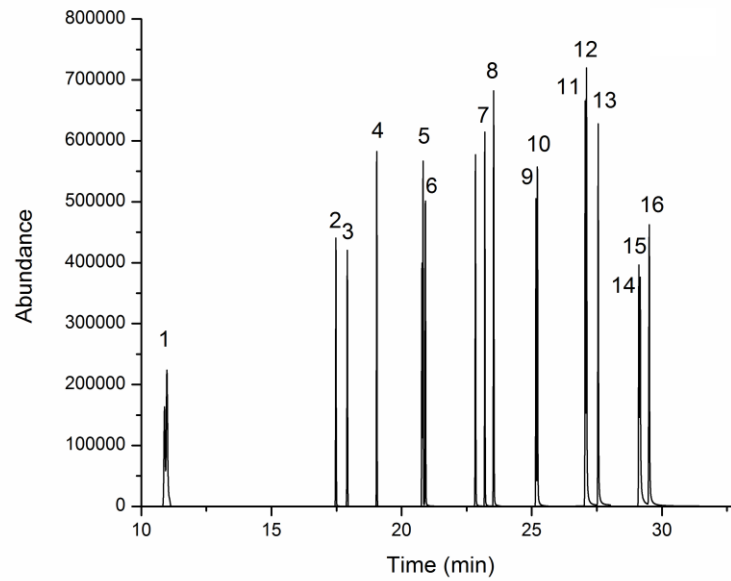
(b) Scenario 2

Figure 3-3 Chromatograph Peaks of the 16 PAHs Obtained through SIM Mode

81
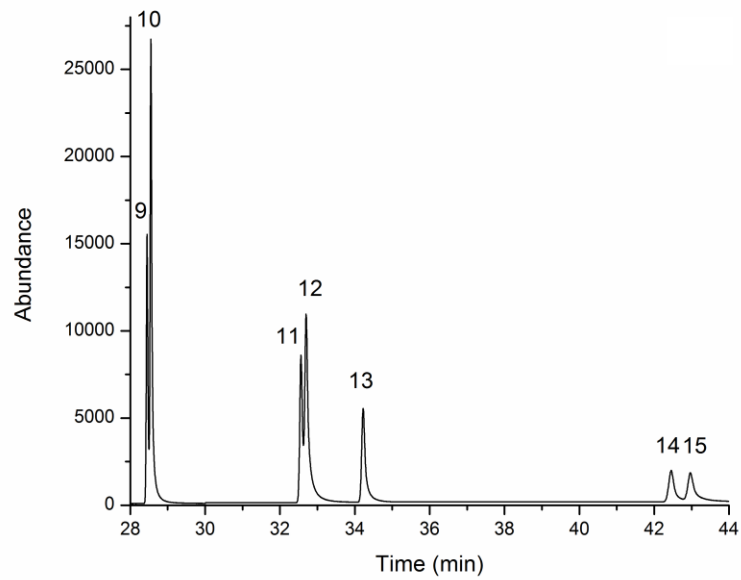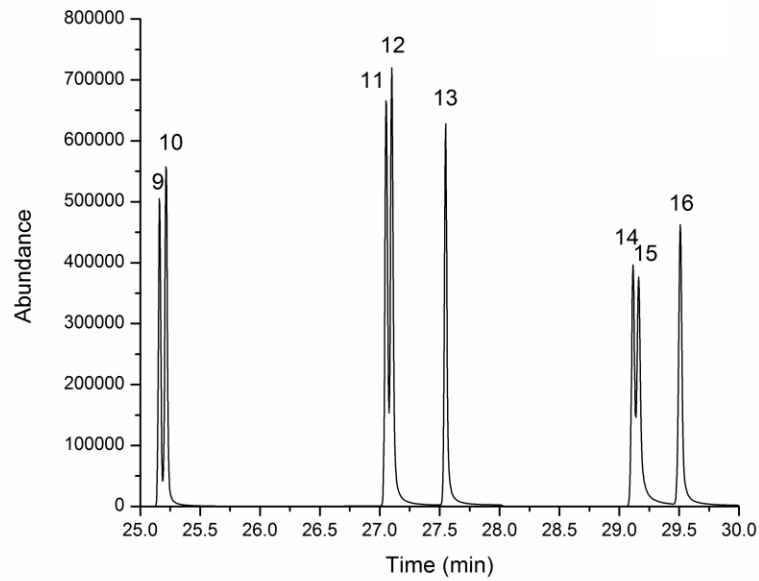
(a) Scenario 1

(b) Scenario 2

Figure 3-4 Zoomed in Images of the 3 pairs of PAHs Peaks

3.2.3.2 Scenario II

In order to better separate the last 3 peak pairs of late eluted PAHs and minimize the analysis duration, several attempts had been made and lead to a new method with the oven temperature ramp setting, which has been adjusted to the 33 min program. As can be seen from **Figure 3-3 (b)** and **Figure 3-4 (b)**, the adjusted ramp setting achieved much better separation of the 3 pairs of PAHs peaks and in the meantime with reduced time. Therefore, the system settings under the Scenario II were then applied to the analysis of PAHs (**Table 3-4** and **Table 3-5**). The distilled water was spiked with 16-PAHs stock solution to form 0.2 μg/l water samples for each individual PAH. Ions monitored for the quantitation and confirmation of PAHs under investigation and corresponding retention times are given in **Table 3-4**. The average recovery rates (RR) and repeatabilities (RSD) of the detected PAHs concentrations for the PAHs analysis in spiked distilled water samples are shown in **Table 3-5**. Analytical curves under Scenario II were drawn using seven pure PAH standards in DCM within the concentration range between 10 and 1,000 ng/ml. Each calibration standard contained the internal standard at level of 10 ng/ml. The coefficients of determination (R^2) for all studied PAHs under 230 °C ion source were between 0.9950 and 0.9995 (average ~ 0.9983) (**Table 3-4**). However, it was later found that the large MW PAHs had low recovery rate (e.g., BaP: 43; IcdP: 48; DahA: 53; and BghiP: 51) (**Table 3-5**). In general terms, method performance was worse for later eluting PAHs. This is typical of most trace level PAH analytical methods and is most likely due to inefficient or inconsistent transmission of less volatile PAHs through the transfer line or MSD chamber and chromatographic behavior (Hubschmann, 2000).

83

Table 3-4 GC-MS Analyses of PAHs: Retention Times of Studied Compounds, Ions Monitored and Method Linearity Ranges

PAHs	Ions (m/z) monitored for quantization	Ions (m/z) monitored for confirmation	GC-MS (Scenario 2)			GC-MS (Scenario 3)		
			Retention Times (33 min)	Calibration Range (ng/ml)	Linearity (R^2)	Retention times (60 min)	Calibration Range (ng/ml)	Linearity (R^2)
NAP	128	127,129	10.98	10-1,000	0.9995	11.26	0.1~20	0.9996
ACY	152	151	17.47	10-1,000	0.9995	19.55	0.1~20	0.9999
ACE	153	154	17.91	10-1,000	0.9975	20.56	0.1~20	0.9999
FLO	165	166	19.04	10-1,000	0.9995	23.53	0.1~20	0.9999
PHE	178	176	20.81	10-1,000	0.9995	28.91	0.1~20	0.9998
ANT	178	176	20.91	10-1,000	0.9990	29.2	0.1~20	0.9997
FLA	202	200	22.83	10-1,000	0.9990	35.74	0.1~20	0.9998
PYR	202	200	23.19	10-1,000	0.9985	36.92	0.1~20	0.9998
BaA	228	226	25.16	10-1,000	0.9990	44.01	0.1-20	0.9986

PAHs	Ions (m/z) monitored for quantization	Ions (m/z) monitored for confirmation	GC-MS (Scenario 2)			GC-MS (Scenario 3)		
			Retention Times (33 min)	Calibration Range (ng/ml)	Linearity (R^2)	Retention times (60 min)	Calibration Range (ng/ml)	Linearity (R^2)
CHR	228	226	25.21	10-1,000	0.9975	44.19	0.1-20	0.9985
BbF	252	250,253	27.05	10-1,000	0.9980	49.79	0.1-20	0.9987
BkF	252	250,253	27.1	10-1,000	0.9950	49.93	0.1-20	0.9962
BaP	252	250,253	27.55	10-1,000	0.9965	51.3	0.1-20	0.9985
IcdP	276	277,274	29.11	10-1,000	0.9985	56.35	0.1-20	0.9993
DahA	278	274	29.16	10-1,000	0.9975	56.62	0.1-20	0.9984
BghiP	276	274,277	29.51	10-1,000	0.9965	57.35	0.1-20	0.9981

Table 3-5 Method Performances on Analyzing PAHs Spiked (0.2 µg/l, n = 4) Distilled Water Samples

PAHs	GC-MS[*] (Scenario 2)		SPE-GC-MS (Scenario 3)		LPME-GC-MS (Scenario 3)	
	RR	RSD	RR	RSD	RR	RSD
	(%)	(%)	(%)	(%)	(%)	(%)
NAP	97	3.3	87	6.3	96	5.7
ACY	48	4.0	34	4.0	97	6.7
ACE	93	3.8	90	8.5	98	7.6
FLO	97	1.9	96	9.4	101	7.6
PHE	100	4.8	95	9.7	97	7.8
ANT	90	7.5	85	7.7	99	7.1
FLA	100	3.3	97	8.0	98	7.4
PYR	95	1.1	97	8.7	99	7.8
BaA	75	4.8	87	6.1	95	8.3
CHR	72	3.5	87	5.1	90	7.9

PAHs	GC-MS[*] (Scenario 2)		SPE-GC-MS (Scenario 3)		LPME-GC-MS (Scenario 3)	
BbF	69	5.6	85	5.1	91	7.1
BkF	60	4.9	89	4.3	88	7.1
BaP	43	7.2	84	4.2	99	6.0
IcdP	48	1.9	95	5.3	96	10.6
DahA	53	5.0	101	4.3	97	9.9
BghiP	51	3.2	95	4.6	98	7.5
Average	75	4.1	91	6.5	95	7.6

Note: [*] Pretreatment method under scenario 2 was the newly developed SPE.

3.2.3.3 Scenario III

To increase the recovery rates of PAHs with large molecular weights, adjustment of the GC-MS setting was further conducted generating a 60 minutes oven ramp program. Although this setting had a longer separation time, which achieved even better resolution compared to the 33 min program (**Figure 3-5**), it still produced lag tails for some large MW PAHs (**Figure 3-6 (a)**). Instead of adjusting the oven ramp program again, the temperature of the MS ion source which was set at 230 ^{o}C before was increased to 350 ^{o}C under this scenario. With the increased ion source temperature, the lag tail for the large molecular weight PAHs generated has been eliminated (**Figure 3-6 (b)**). **Figure 3-7** shows the peaks of the three pairs of PAHs (i.e., BaA and CHR; BbF and BkF; IcdP and DahA) under Scenario II and III. The results indicated that compared with the results obtained from Scenario II, the system settings under Scenario III fulfilled better performance in the PAH separation with low concentration range as well as the peak-shapes.
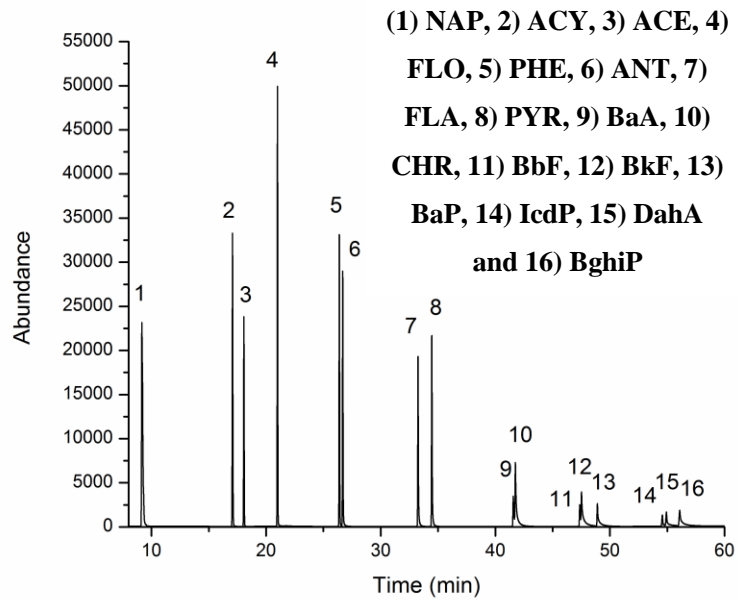
(a) 16 PAHs
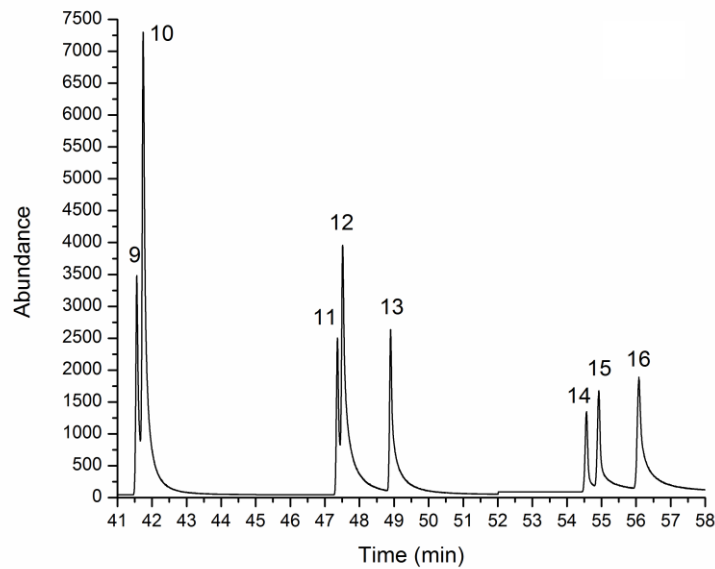
(b) The last Three Pairs of PAHs

Figure 3-5 Chromatograph Obtained through 60 Minutes Oven Ramp Program
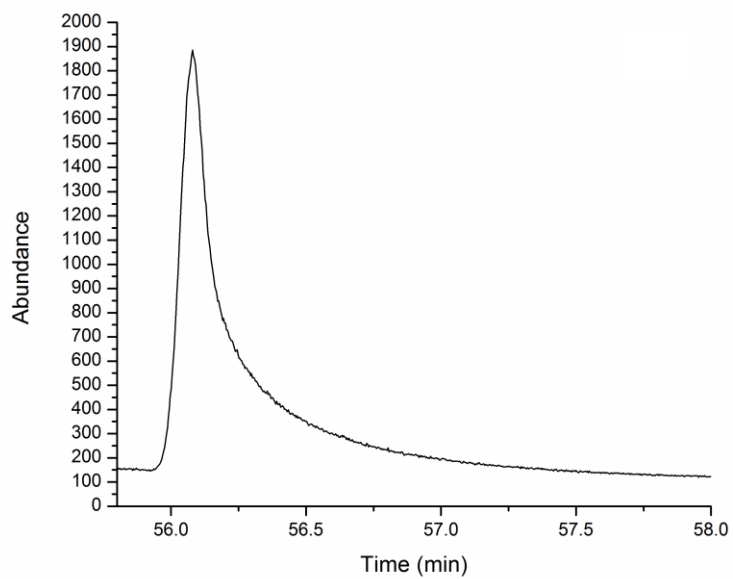
(a) 230 ℃ Ion Source Temperature
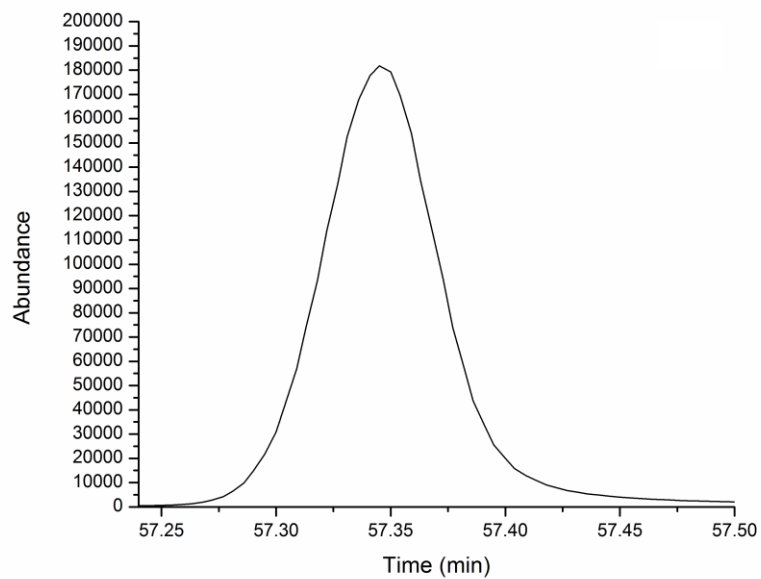
(b) 350 ℃ Ion Source Temperature

Figure 3-6 Lag Tail for the BghiP

90
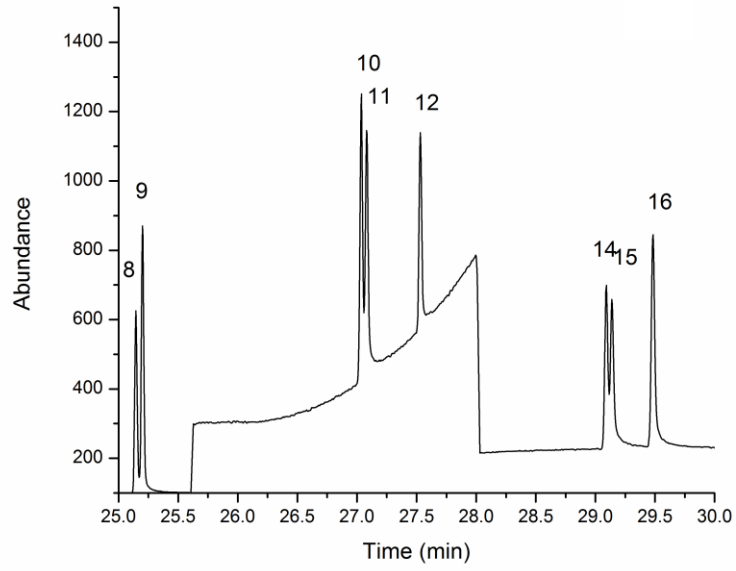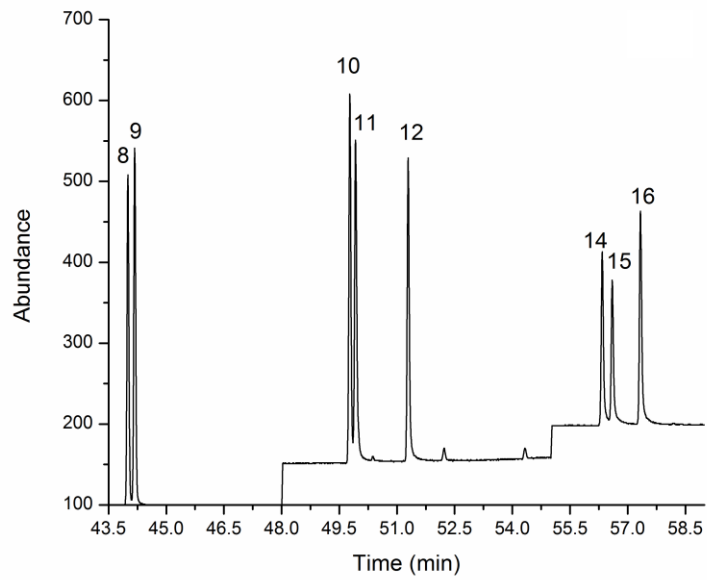
(a) Scenario 2

(b) Scenario 3

Figure 3-7 The Chromatograph Peaks of the Last Three Pairs of PAHs

Analytical curves under the Scenario III were also drawn using eight pure PAH standards in DCM within the concentration range between 0.1 and 20 ng/ml for the purpose of elaborating the enhanced performance in lower concentration detection of PAHs. Each calibration standard contained the internal standard at level of 10 ng/ml. The coefficients of determination (R^2) for all studied PAHs under Scenario III were between 0.9962 and 0.9999 (average ~ 0.9991) (**Table 3-4**). Comparing to the system performance under Scenario II, even though the calibration range was 100 times lower, similar R^2 values were achieved under the scenario III settings. This is because the increase of ion source temperature significantly improved the shape of the PAHs peaks, thus leading to high sensitivity in the analysis of trace level injected PAHs. The lowered level of calibration range not only decreases the MDLs, but also can improve the accuracy for trace level quantitation of PAHs. As shown on **Table 3-5**, the recovery rates under Scenario III were much higher than the ones detected under Scenario II, especially for the less volatile PAHs. By applying 350 ℃ ion source, most recovery rates of the targeting PAHs were close to 100%.

To sum up, by applying the new oven ramp program and ion source temperature under Scenario III, three major improvements have been achieved: 1) the enhanced resolution by eliminating the lag tail for the large molecular weight PAHs; 2) the lowered MDL; and 3) the increased recovery rate of the large molecular weight PAHs. The enhanced GC-MS method was thus developed.

3.3 Performance Evaluation and Discussion

3.3.1 PAHs Analysis in Spiked Distilled Water Samples

In addition to the RR and RSD (**Table 3-5**), the MDLs of the 16 PAHs obtained from the established SPE-GC-MS and LPME-GC-MS ranged in 4-28 ng/ml (average ~ 6.8) and 2-5 ng/ml (average ~ 3), respectively, which is better or comparable with other more expensive and complex methods list in **Table 3-6**. In specific, the average MDL achieved through USAEME-GC-MS by Ozcan et al. (2010) was around 24 ng/l; the average MDL achieved through SPME-GC-MS by King et al. (2004) was 12 ng/l; the average MDL achieved through SPE (C_{30})-GC-MS Li et al. (2007) was 80 ng/l; the average MDL achieved through HF-LPME-GC-MS by Charalabaki et al. (2005) was 8 ng/l. All these average MDLs are higher/much higher than the ones obtained from the current study except limited cases of lower MDLs when compared individually. It was also found that the developed LPME-GC-MS method showed even better sensitivity than the developed SPE-GC-MS method in analyzing spiked distilled water sample in the current spiking level (0.01μg/l).

3.3.2 PAHs Analysis in Spiked OPW Samples

In **Table 3-7**, the RRs and MDLs of the PAHs concentrations in the PAHs fortified (0.2 μg/l) OPW samples are presented. Data were generated based on four replicates. The results show that the detection of the PAHs in the spiked produced water samples can be done well by applying both analysis methods developed in this study. The RR, somewhat

93

matrix dependent when compared with the data generated from spiked OPW sample, ranged from 60 % to 114 % (except ACY) for SPE-GC-MS and from 64 % to 85 % for LPME-GC-MS, respectively. The special case of ACY by using SPE treatment (i.e., 8% recovery) could be due to the incapability of the ENVI-18 solid phase in extracting the individual PAH, ACY, from the water samples. In other words, the identification/development of a solid phase that is capable for all target PAHs in the SPE process deserves further studies.

Table 3-6 Comparison of MDLs of 16 PAHs in Spiked Distilled Water Samples

PAHs	Enhanced SPE-GC-MS (ng/l) (Current study)	Enhanced LPME-GC-MS (ng/l) (Current study)	USAEME-GC-MS [a] (ng/l) (Ozcan et al., 2010)	SPME-GC-MS [b] (ng/l) (King et al., 2004)	SPE (C$_{30}$)-GC-MS [c] (ng/l) (Li et al., 2007)	HF-LPME-GC-MS [c] (ng/l) (Charalabaki et al., 2005)
NAP	28	2	1	3	7	5
ACY	4	2	23	3	24	N/A
ACE	4	2	21	6	30	10
FLO	5	2	22	2	27	N/A
PHE	6	2	30	17	100	8
ANT	4	2	31	20	210	N/A
FLA	5	3	28	1	63	11
PYR	6	3	15	1	34	6
BaA	6	3	13	29	45	N/A

PAHs	Enhanced SPE-GC-MS (ng/l) (Current study)	Enhanced LPME-GC-MS (ng/l) (Current study)	USAEME-GC-MS [a] (ng/l) (Ozcan et al., 2010)	SPME-GC-MS [b] (ng/l) (King et al., 2004)	SPE (C_{30})-GC-MS [c] (ng/l) (Li et al., 2007)	HF-LPME-GC-MS [c] (ng/l) (Charalabaki et al., 2005)
CHR	7	2	29	5	30	N/A
BbF	8	3	28	27	110	N/A
BkF	7	4	24	13	110	N/A
BaP	6	4	29	18	180	N/A
IcdP	5	5	36	21	56	N/A
DahA	5	5	32	14	190	N/A
BghiP	4	4	29	12	55	N/A

Note:

[a] - USAEME-GC-MS: Ultrasound-assisted emulsification-microextraction and GC-MS

96

As can be seen in **Table 3-7**, the MDLs range from 2 to 124 ppt with LPME-GC-MS and even lower with SPE-GC-MS from 0.73 to 28 ppt. It should be noted that, the sample might be used as is for determining the MDL if the analyte level does not exceed 10 times the MDL of the analyte in reagent water. Since there exist significant amount NAP (conc. 6.546 μg/l >>10 times of MDL = 28 ng/l) in the original produced water matrix, the MDL determined under this circumstance may not truly reflect method variance, therefore, the MDL data of NAP was not presented and the MDL of NAP shown in **Table 3-7** is the MDL from **Section 3.3.1**. Since most of the PAHs were detected in the unfortified produced water sample except BaA and BkF, the spiking recoveries of the other 14 existing PAHs were calculated after deducting the background concentration. From the results, the method performance is comparable or better comparing to other methods summarized in **Table 3-7**. The calculated recoveries are all acceptable with good repeatability, and there is no significant increase of MDLs. Comparing to the HF-LPME-GC-MS method developed by Charalabaki et al. (2005), the enhanced methods have significant higher recoveries. Comparing to the advanced and more expensive SBSE-GC×GC-TOF-MS method developed by Gomez et al. (2011), the currently developed methods show higher recoveries and repeatability despite SBSE-GC×GC-TOF-MS having lower MDLs due to the application of high resolution time of flight MS.

Table 3-7 Comparison of Method Performance in Fortified OPW Samples

PAHs	SPE-GC-MS (Current study)		LPME-GC-MS (Current study)		HF-LPME -GC-MS Charalabaki et al., 2005)		SBSE-GC×GC -TOF-MS [a] (Gomez et al., 2011)	
	RR (%)	MDLs (ng/l)	RR (%)	MDLs (ng/l)	RR (%)	MDLs (ng/L)	RR (%)	MDLs (ng/L)
NAP	N/A	N/A	N/A	N/A	82 ±18	N/A	132 ±13	0.15
ACY	8 ±22	0.98	77 ±2	92.10	N/A	N/A	17 ±4	0.16
ACE	60 ±4	1.44	71 ±7	98.19	63 ±18	N/A	79 ±7	0.10
FLO	94 ±8	4.51	85 ±9	124.33	N/A	N/A	138 ±10	0.15
PHE	93±7	6.19	81 ±11	119.16	86 ±10	N/A	150 ±14	0.02
ANT	92 ±1	0.71	68 ±11	104.90	N/A	N/A	121 ±17	0.02
FLA	114 ±1	0.73	70 ±10	103.61	84 ±4	N/A	141 ±16	2.02
PYR	98 ±8	4.76	66 ±14	108.92	76 ±4	N/A	135 ±15	0.11
BaA	110 ±2	1.35	71 ±8	96.18	N/A	N/A	54 ±21	0.13
CHR	113 ±5	3.24	72 ±10	100.11	N/A	N/A	81 ±27	0.30
BbF	80 ±10	4.55	70 ±9	90.33	N/A	N/A	N/A	N/A
BkF	83 ±6	2.82	68 ±8	83.74	N/A	N/A	22 ±18	0.18
BaP	88 ±5	2.60	68 ±10	86.21	N/A	N/A	21 ±17	0.18
IcdP	65 ±6	2.28	64 ±8	77.96	N/A	N/A	18 ±17	1.16
DahA	90 ±11	6.21	65 ±8	81.79	N/A	N/A	17 ±17	1.06

99

PAHs	SPE-GC-MS (Current study)		LPME-GC-MS (Current study)		HF-LPME -GC-MS Charalabaki et al., 2005)		SBSE-GC×GC -TOF-MS [a] (Gomez et al., 2011)	
	RR (%)	MDLs (ng/l)	RR (%)	MDLs (ng/l)	RR (%)	MDLs (ng/L)	RR (%)	MDLs (ng/L)
BghiP	66 ±7	2.80	64 ±7	74.93	N/A	N/A	17 ±11	0.99

Note:

N/A - Not available;

[a] - SBSE-GC×GC-TOF-MS: sorptive extraction followed by comprehensive two dimensional GC-time-of-flight-MS.

3.3.3 Feasibility Analysis of On-Site Real-Time PAHs Testing

According to the above performance evaluation, the SPE-GC-MS and LPME-GC-MS methods developed in this study have both shown high selectivity and recovery on PAHs analysis (except the case of ACY with SPE). The low recovery rate of ACY has become the only limitation for the SPE-GC-MS analysis, which cannot be eliminated in the current study until another more efficient sorbent material has been developed. The LPME-GC-MS showed better sensitivity than the SPE-GC-MS in analyzing spiked distilled water sample in the current spike level (0.01 µg/l) but it was more suspect to matrix impacts, while SPE-GC-MS showed lower MDLs in analyzing spiked OPW samples. Although the addition of HCl was applied to reduce the emulsion during LPME process, the influence of the OPW matrix on PAHs determination could not be eliminated.

In addition to the improved sensitivity and selectivity, when discussing the potential of applying the developed analytical approaches to the on-site real-time PAHs monitoring in OPW, there are still other perspectives need to be considered. **Table 3-8** summarizes the comparison between the two analysis approaches related to time consumption, cost, labour intensity, etc. In point of time consumption in case of real-time monitoring, the sample pre-treatment through either SPE or LPME could be done when a previous sample is running in GC since both methods require only half an hour for pre-treating one sample and about one hour for GC/MS analysis. In terms of the cost and solvent consumption, the SPE-GC-MS consumes non-reusable SPE tubes for the pre-treatment and need approximate 20 ml solvent for conditioning and elution of each test, while the LPME-GC-

MS only consumes 0.25 ml solvent as the extraction reagent per test, resulting in a much lower analytical cost as well as human health risk from solvent than the SPE-GC-MS. As for sample consumption, LPME also requires less water sample than SPE. On the part of labor intensity, the fully automated SPE apparatus with online injection has recently been in the market (Stevens et al., 2010). The automated online system can control the sample-loading rate accurately without human induced operational errors. In addition, the fully automated system consumes little labor, which can lead to the 24 hours continuously monitoring in reality. After integration with the refined GC-MS method, the real-time PAHs data with good accuracy and precision can be obtained. On the other hand, the operational difficulty of the LPME treatment is higher than the SPE since the operator has to manually extract solvent from the bottom of the centrifuge tube with syringes. The LPME has not been automated yet with online injection, which means intensive labor is required for real-time monitoring purpose. The development of a fully automated online system based on the LPME-GC-MS analysis thus has a great market value. More comprehensive monitoring of organic pollutants could be achieved by this development since LPME has much lower selectivity issue (e.g., with ACY).

Table 3-8 LPME-GC/MS and SPE-GC/MS Detection Performance

Performance	SPE-GC-MS	LPME-GC-MS
Processing Time	Approx.30 min/sample	Approx. 30 min/sample
Cost	Moderate	Low
Sample consumption	200 ml/sample	10 ml/sample
Solvent consumption	Moderate (20 ml)	Low (0.25 ml)
Operational difficulty	Low	Moderate
Automation	Fully-automated	Semi-automated
Selectivity	Moderate	Low
Matrix dependency	Low	Moderate

To sum up, both the developed methods have been demonstrated to be feasible for offshore real-time monitoring purpose. The SPE-GC-MS method is a more accurate one comparing to the LPME-GC-MS method especially for the applications to real-seawater samples. Its automation is another advantage, which can significantly reduce the labor intensity. However, the selectivity issue limits its application to a certain extent because the industry might prefer to monitor not only PAHs but also more comprehensive compounds simultaneously. In addition, the relative higher cost and larger solvent consumption are other drawbacks of SPE method. On the other hand, the refined LPME-GC-MS is a simpler, less solvent consumption method. The interference of selectivity issue is usually insignificant, thus it can monitor comprehensive organic compounds and identify unknown pollutants. But still, there are two major drawbacks for this method. One is that it can be easily interfered by sample matrix, leading to less accurate results; the other one is that it has not been fully automated yet, resulting in high labor intensity. Nevertheless, LPME-GC-MS would be more feasible than SPE-GC-MS after automation. Generally speaking, both the developed methods have their own advantages and limitations, and they can be utilized under different circumstances to support each other and they both deserved further studies for addressing the current limitations due to their high marketing potential.

3.4 Summary

This chapter has developed simple, low-cost, time efficient, highly selective and sensitive methods based on SPE, LPME and GC-MS for offshore real-time PAHs testing in OPW.

104

In order to make the analytical method streamlined and cost efficient, two pre-treatment methods were developed by refinement and optimization based on traditional or commercial SPE and LPME methods. The GC-MS settings were also significantly improved by this research. In the developed approach: 1) a refined SPE system was developed to extract PAHs from the sample water through screening of conditioning/elution solvents and their appropriate volumes and the suitable pH value; 2) parameters affecting the extraction efficiency of LPME, such as solvent selection, organic solvent volume, shaking rate and time, content of salts and centrifuge speed were optimized and have been kept constant during the procedure of analysis; 3) the traditional GC-MS analysis has been improved by enhanced system settings such as the refined multiple ramp oven program to better separate the targeting PAHs in the DB-5MS UI fused silica capillary column, and increased high ion-source temperature by using the ultra-inert filament to provide a shorter run time and ppt MDL. All sample pre-treatment and analysis procedures follow the QA/QC requirements of accuracy and reproducibility. The developed methods have been applied to analyze the artificial and real OPW samples. Results indicated that the developed analytical approaches provide precise, stable and clean methodologies which are better or comparable with other more expensive and complex method in qualifying and quantitating PAHs in OPW with low volume demand of sample, which is especially useful for the purpose of continuous lab testing, thus showing a great potential for monitoring water samples containing PAHs in marine environment.

This chapter also evaluated the newly developed methods from the perspectives of feasibility and efficiency for real-time PAHs testing in OPW. The developed methods were demonstrated to be robust, viable, simple, rapid, easy to use, cost efficient and environmental friendly for the determination of PAHs in OPW samples. Results indicated that the SPE-GC-MS method is recently more suitable for real-time monitoring, whereas LPME-GC-MS method has the potential to achieve higher efficiency and lower cost.

Chapter 4 Removal of PAHs from OPW by Direct Photolysis and Photocatalysis

4.1 Experimental Facilities Design and Fabrication

The design and fabrication of the experimental facilities were based on a rule of thumb to optimize the treatment reactors as much as possible while taking the variations of the environmental and system conditions into account. The photochemical oxidation reactors have then been fully developed and ready for lab tests under different environmental conditions. **Figure 4-1** shows the experimental apparatus for UV irradiation (PS: a disclosure is filed and patent is under preparation). The main body of the reactor is a portable and detachable airtight quartz jar fitted with insertable stainless steel (SS) sparger. The UV grade quartz jar, with a 20 cm internal diameter (I.D.), a 4 mm wall thickness, and a 25 cm height, is able to contain approximately 6.5 L sample water. During the experiments, the contents will be stirred by a double layer six-bladed paddle-type SS impeller for thorough agitation. The top and an extra bottom plate are made of 1 cm thick Teflon plates. Four pillars are evenly fixed with the top and bottom plates around the reactor. The Teflon top is fitted with stirring motor (with speed controller), aquarium heater (with temperature control), ozone inlets (extended to the bottom of the reactor) and outlets, pH meter, and sampling port. The top is sealed by a 6 mm thick O-ring with a 20 cm I.D. The top could be also opened for feeding. Teflon fittings and tubing are used for all connections.
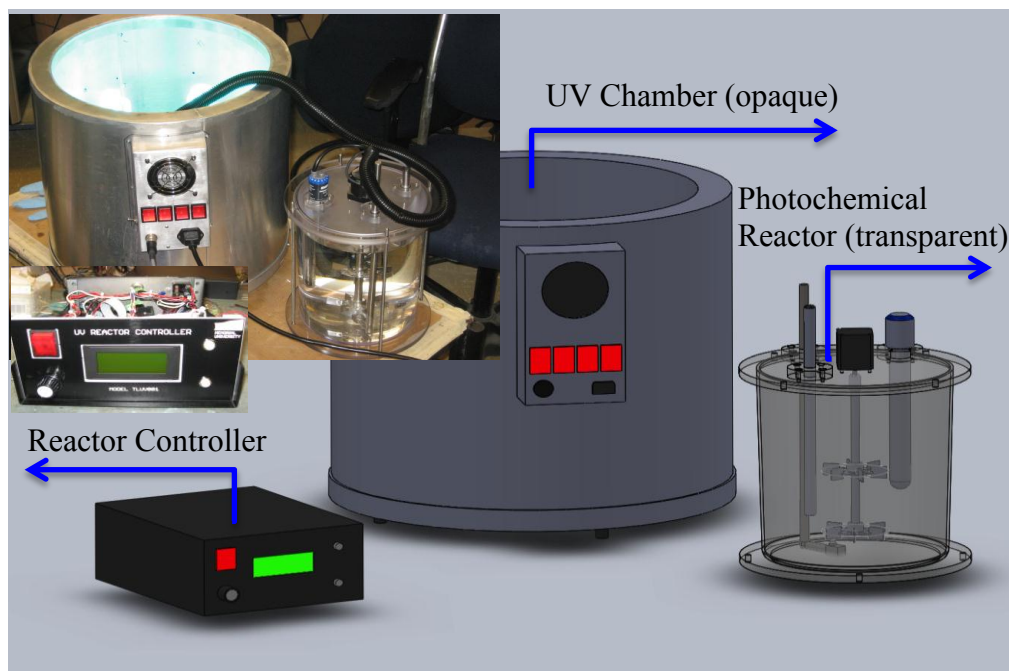
Figure 4-1 Photochemical Oxidation Reactor

The transparent UV grade quartz reactor could be lowered into an opaque UV chamber with the UV sleeves in which a maximum of 8 UV lamps could be mounted. The main body of the chamber is made of double layer SS with a 30 cm I.D., a 4 cm wall thickness, and a 38 cm height, and mounted with cooling fan to disseminate the extra heat generated by UV lamps during the irradiation experiments. The outer jacket has an aluminum lid that can be firmly sealed to provide heat and light insulation. The UV lamps with different wavelengths (i.e., UVA, UVB, and UVC) emit principally at 365 nm, 302 nm, and 254 nm respectively are rated at designed strength. In the course of this work, six lamps will be used. Wheels have been also installed on the bottom of the UV chamber for the reactor mobility.

The developed reactor has several unique features including: 1) a double chamber system to separate the UV unit and the reaction unit; 2) full-angle UV lighting setup to ensure highly efficient and adjustable radiation environment; 3) transparent inner chamber to facilitate observation of reactions; 4) multiple parameter control console to help optimize experimental conditions; 5) bottom-up gas disperser to enhance dispersion of induced gases (e.g., O_2/O_3) and uniform condition of reaction; and 6) multiple ports on the top to support mixing, sampling, and monitoring options.

4.2 Sample Preparation

For better understanding the reaction dynamics, degradation mechanisms as well as the matrices impacts, artificial OPW samples have been used based on the knowledge

109

obtained from real sample testing and literature tested under the UV photolysis system. Artificial samples were prepared by spiking distilled water with two typical PAHs in OPW to give varied concentrations of water solution (i.e., NAP at 2 mg/l; and FLO at 8 µg/l based on the sample analysis results and the confidential data of NAP and FLO concentrations in OPW from a few wells in Atlantic Canada). NAP and FLO were chosen because they are major contaminants in OPW, have been considered as a possible carcinogen to humans, and contribute most to OPW's toxicity as the most abundant PAHs in OPW (Neff 2002; 2005; 2010; Lee et al., 2011). They are relatively more soluble and less hydrophobic than other high MW PAHs that raises a critical bioavailability issue due to their high concentrations. The salinity of the water sample has been adjusted by sodium chloride (NaCl at 35g/l) on purpose of simulating the salty matrix water as this is the key difference between freshwater and OPW and the presence of NaCl was reported to enhance the photodegradation efficiency of NAP in freshwater (Damle, 2008; Zheng et al., 2012). All prepared samples were stored in the dark and cold (at 4 $^{\circ}$C) chromatograph fridge before analysis/treatments.

4.3 Experimental Methodology

Batches of direct photolysis and photocatalysis experiments were performed in the developed reactors to evaluate the efficiency of these processes in the degradation of the targeting PAHs. The influences of selected process variables (i.e., UV wavelength, radiation duration, pH value, oxygen, radical scavenger, and catalyst doses) on the photoreaction course have been evaluated through systematic one-factor-at-a-time (OFAT)

110

analysis. During the experiment, water samples were transferred into the reactors and exposed to UV irradiation under varied environmental conditions. The whole process of irradiation was carried out in a dark environment under the fume hood with all the other light sources turned off. Water samples from each container collected before, during (at designed intervals) and after irradiation, were pretreated and analyzed by the developed SPE-GC-MS approach, which qualify and quantify the background and residual contaminants for calculating the removal rates (%):

$$RR = \frac{c_0 - c_t}{c_0}$$ (4-1)

Where,

c_t = instant concentrations of the target PAH, ppm; and

c_0 = initial concentrations of the target PAH, ppm.

All experimental designs strictly follow the Quality Assurance (QA)/Quality Control (QC) requirements by integrating process parallel (PP), process blank (PB), sample parallel (SP), and experimental control (Ctrl) into the experimental framework (**Table 4-1**). The exact dose levels settings have been tested based on literature data and finally determined based on a series of preliminary tests conducted before the actual start of this round. Adjustment of the sampling frequency has been made based on the half-life (or the time taken for the initial concentration to be reduced by 50%), and time needed to achieve 90%-100% removal under the UV radiation with the most efficient wavelength.

111

Table 4-1 Experimental Design in Testing Influence of Photolysis Process Variables

(Sampling frequency: 10 minutes; size of sample: 200ml)

UV Wavelength	pH	Radical Scavenger Dose	Oxygen Dose	Catalyst Does
(nm)		(ppm)	(ml/min)	(g/l)
UVA (peak: 365)	3	0.01	20	0.5
UVB (peak: 302)	7	0.02	30	1
UVC (peak: 254)	10	0.04	40	2
SP (UVC)	SP (7)	SP (0.02)	SP (40)	SP (2)
PP (UVA)	PP (3)	PP (0.01)	PP (20)	PP (0.5)
PB (UVB)	PB (10)	PB (0.04)	PB (30)	PB (1)
Ctrl	Ctrl	Ctrl	Ctrl	Ctrl

4.3.1 Direct Photolysis of PAHs under Varied UV Wavelength

This group of tests is to examine the influence of the type of UV source with varied wavelengths on PAHs' removal rate. The one achieving the higher rate of destruction will indicate to be more efficient. Nevertheless, from this round of experiments, the half-life, and the treatment time needed to achieve 90%-100% removal under the UV radiation with the most efficient wavelength will be recorded for determining the sampling interval and exposure duration settings of the following tests.

4.3.2 Direct Photolysis of PAHs under Varied pH Value

From the literature, changes in acidity and alkalinity of the reaction medium often influence the photoreaction rate, mainly due to various electron distributions in the molecule, depending on pH. For some of the pollutants, which are weakly acidic, rate of photolysis increases at lower pH due to an increase in the extent of adsorption under acidic conditions (Andreozzi et al., 2000; Tanaka et al., 2000; Vohra and Davies, 2000); and some other pollutants, which undergo hydrolysis under alkaline conditions or undergo decomposition over a certain pH range, may show an increase in the rate of photolysis with an increase of pH (Trillas et al., 1996; Choi and Hoffmann, 1997). Since the effect of pH cannot be generalized considering of different PAHs along with the matrix impacts, laboratory scale studies are required for establishing the optimum conditions for the operating pH under the particular systems.

4.3.3 Direct Photolysis of PAHs under Varied Doses of Radical Scavenger

The effect of radical scavengers depends on the mechanism of the degradation. If the destruction is by direct attack of photon on the chemical bonds, not much effect is there, but if it is through the free radicals, presence of radical scavengers may affect the degradation process via reaction with hydroxyl radical ions. The study of photolytic reaction with the addition of radical scavenger (i.e., t-BuOH, a strong hydroxyl radical scavenger) should indicate the dominant type of degradation reaction (direct photolysis or hydroxyl radical reaction pathways). If a significant retarding effect (i.e., an increase of t-BuOH concentration follows a decrease in the reaction rate) was observed, probably the removal of PAHs occurs mainly according to a radical mechanism. In this case, presence of radical scavengers is a crucial factor in deciding the overall efficiency of the process. This is a very important point that needs to be considered as the OPW will have different types of salts at different levels of concentration act as radical scavengers and if this significantly affects the rates of advanced oxidation processes, development of kinetic models for predicting the rates of degradation must consider the presence of these substances.

4.3.4 Direct Photolysis of PAHs under Varied Doses of Oxygen

Presence of electron acceptors is recommended to help in maintaining for scavenging the electrons to prevent the recombination reaction between the generated positive holes and electrons. The contribution of oxygen in the photolysis system is unclear based on the data obtained from previous studies. Dijkstra et al. (2001) claimed that there was no

114

appreciable destruction in the absence of oxygen, while Miller and Olejnik (2000) stated that oxygen had influence on some of PAHs but not all. A recent report by Comber et al. (2013) indicated that in the case of individual PAHs the interpretation of historical laboratory studies regarding the impact of dissolved oxygen maybe confounded by matrix effects, differences in light intensity and wavelength, etc. It should be also noted that the removal of the PAHs will also be dependent on the driving force available for the reaction and hence the exact dependency should be established with the laboratory scale studies.

4.3.5 Photocatalysis of PAHs under Varied Doses of Catalyst

The photocatalytic mechanism occurring at the surface of semiconductors may substantially enhances the rate of generation of free radicals and hence the rates of degradation (Mazzarino et al., 1999). In photocatalysis process, a semiconductor absorbs UV light and generates hydroxyl radicals. From the literature, the best photocatalytic performances with maximum quantum yields have been always with titanium (Yu et al., 2002). In addition, the surface area and the number of active sites offered by the catalyst for the adsorption of pollutants plays an important role in deciding the overall rates of degradation as usually the adsorption step is the rate controller (Xu et al., 1999). Some studies have found the Degussa P-25 catalyst to be the most active form (75% anatase/25% rutile) among the various ones available and generally give better degradation efficiencies (Sakthivel et al., 2000; Yamazaki et al., 2001; Liu et al., 2014). Therefore, at this round of test, the Degussa P-25 TiO_2 has been evaluated and compared at varied dose level. The photocatalytic process was carried out by using slurry of the fine particles of the Degussa

P-25 TiO$_2$ dispersed in the liquid phase in a reactor irradiated with UVC light. The proper

dispersion of the catalyst in the liquid phase was achieved using the SS sparger.

4.3.6 Kinetic Analysis

The kinetics of degradation of the targeting PAHs in artificial OPW solution using UV

irradiation energy can tell basic information on effective removal of these low ring

numbered pollutants.

The simplified reaction rate equation of the photodegradation of PAHs can be expressed

as follows:

$$r = \frac{dc}{dt} = -k \cdot c^n \qquad \textbf{(4-2)}$$

Where,

r = reaction rate (μg l^{-1} min^{-1} / mg l^{-1} min^{-1});

t = time (min);

c = concentration of PAHs (μg l^{-1} / mg l^{-1});

k = reaction rate constant (min^{-1}); and

n = reaction order.

The reaction order has been generally accepted as equal to 1 (first order kinetics) for

lowly concentrated PAHs with small numbered aromatic rings (Kwon et al., 2009; Kong

116

et al., 2012, Jing et al., 2013). **Equation** (**4-2**) can be rearranged as:

$$dc = -kc \cdot dt \qquad \text{(4-3a)}$$

$$\Rightarrow -\frac{1}{k}\frac{1}{c}dc = dt \qquad \text{(4-3b)}$$

$$\Rightarrow -\frac{1}{k}\int \frac{1}{c}dc = \int dt \qquad \text{(4-3c)}$$

$$\Rightarrow \frac{1}{k}\ln \frac{c_t}{c_0} = t \qquad \text{(4-3d)}$$

$$\Rightarrow \ln \frac{c_t}{c_0} = -kt \qquad \text{(4-3e)}$$

Where,

c_t = instant concentrations of the target PAH, ppm; and

c_0 = initial concentrations of the target PAH, ppm.

In this section, kinetic analysis has been conducted based on the assumption of pseudo first order reaction for the basic understanding of the effects of different process parameters.

4.4 Results and Discussion

4.4.1 Effects of UV Wavelength

Figure 4-2 shows the comparison of degradation of NAP and FLO with time under

117

different UV wavelengths. The tests demonstrated that UV irradiation was able to enhance the natural degradation of the targeting PAHs. After 60-min irradiation, the concentrations of both the individual PAHs were significantly reduced. The removal rates ranged from 75.12% under UVA to 98.62% under UVC for NAP, and from 67.27% under UVA to 98.99% under UVC for FLO. The results also indicated a relatively higher treatment efficiency of UVC for both PAHs, followed by UVB, and then UVA. The higher efficiency of UVC could be due to its stronger energy level, which may lead to faster degradation of PAHs. While comparable removal rates were achieved for both the targeting PAHs under UVC, relatively higher photodegradation capacity of NAP was detected under UVA and UVB. This infers that the effectiveness of the different types of UV irradiation is also dependent on the type of the pollutants.

As can be seen from **Figure 4-3**, semi-log plots of PAHs concentration versus degradation time appear to be linear with most regression coefficients greater than 0.98. Reaction rate constants are then obtained for the two PAHs exposed to UV irradiation assuming the pseudo first order reaction. As the UV wavelengths increased, the reaction rate constant K decreased accordingly. For example, NAP could be degraded about twice times faster under UVC than under UVB, and about twice times faster under UVB than under UVA. The reduced rate constants might be attributed by the absorption spectra of the target PAHs. Regression equations of PAHs degradation at varied UV wavelength are summarized in **Table 4-2**.

118

It should be noted that the key requirement to be met in a successful direct photolysis is that the emission spectra of the light source should overlap the absorption spectra of the target compound. According to the Beer-Lambert law (Miller et al., 2001):

$$A = \varepsilon cl$$

(4-4)

Where,

A = Absorbance;

ε = Molar attenuation coefficient, cm^2/mol;

c = Concentration of PAHs, mol/l; and

l = Light path length, cm.

The Molar attenuation coefficient can be calculated by:

$$\varepsilon = \frac{\sigma}{3.82} \times 10^3$$

(4-5)

Where,

σ = Absorption cross section, Mb or $10^{-18}\,cm^2$

In the meantime, according to the Planck–Einstein relation (French and Taylor, 1978):

119
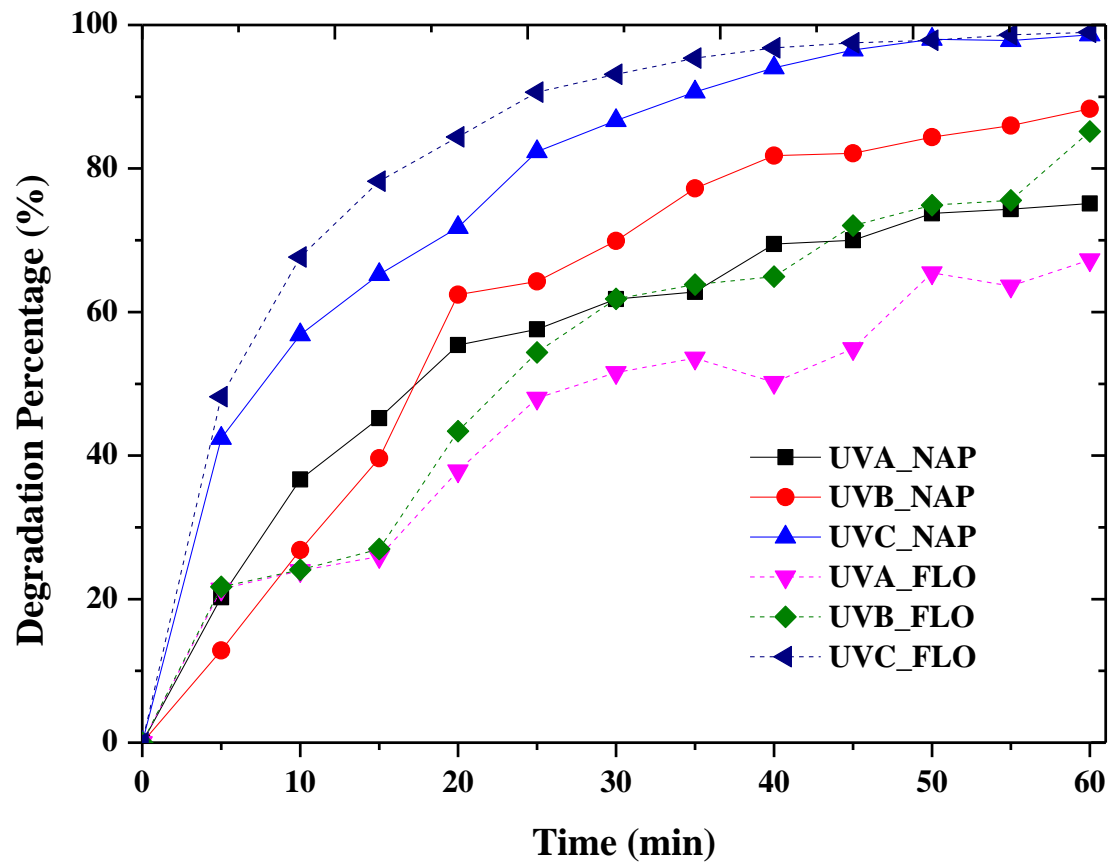
Figure 4-2 PAHs Degradation with Time under Varied UV Wavelengths
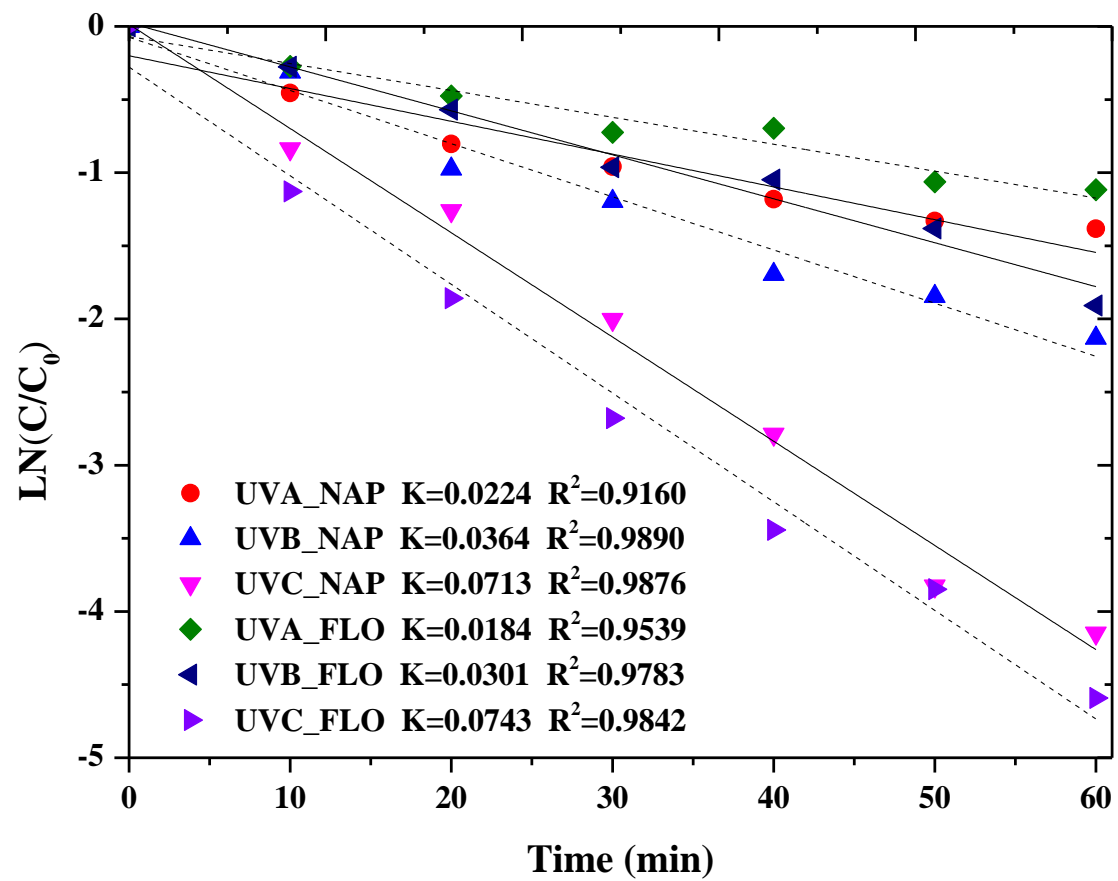
Figure 4-3 Reaction Rate Constants of PAHs under Varied UV Wavelengths

121

Table 4-2 Regression Equations of PAHs Degradation at Varied UV Wavelength

Experimental Settings	Regression Equations
UVA_NAP	$\ln\left(\dfrac{c}{c_0}\right) = -0.2241t - 0.20067$
UVB_NAP	$\ln\left(\dfrac{c}{c_0}\right) = -0.0364t - 0.0743$
UVC_NAP	$\ln\left(\dfrac{c}{c_0}\right) = -0.0713t - 0.0142$
UVA_FLO	$\ln\left(\dfrac{c}{c_0}\right) = -0.0184t - 0.0700$
UVB_FLO	$\ln\left(\dfrac{c}{c_0}\right) = -0.0301t - 0.0234$
UVC_FLO	$\ln\left(\dfrac{c}{c_0}\right) = -0.0743t - 0.2785$

$$E = h\nu = \frac{hC}{\lambda} \tag{4-6}$$

$$\Rightarrow \lambda = \frac{hC}{E} \times 10^9 \tag{4-7}$$

Where,

λ = Wavelength, nm;

h = Planck's constant, 6.626×10^{-34};

C = Light speed, 3×10^8 m/s;

ν = Frequency, Hz or s^{-1}

E = Energy, eV.

Using the photo absorption cross sections (σ) and the matching energy (E) data from the theoretical spectral database of PAHs (Mallocl, 2007), the attenuation coefficients and the related wavelengths of the selected PAHs (i.e., NAP and FLO) were calculated by applying Error! Reference source not found.) and (4-7). The corresponding absorption alue were then computed according to Error! Reference source not found.) under the specific experimental settings (i.e., $c_{NAP}=1.56\times10^{-5}$ mol/l; $c_{FLO}=4.82\times10^{-8}$mol/l; $l_{NAP/FLO}=10$cm)) and were finally plotted against the obtained wavelengths for each PAH (**Figure 4-4** and **Figure 4-5**). It was found that the experimental results are in accordance with the conclusion drawn by comparison of the individual PAH's absorption spectra with emission spectra of the right wavelength. The absorption peaks at the lower UV wavelengths, i.e., 220nm of NAP and 205nm of FLO, explained the higher efficiency of

UVC in this experiment. The second peak of photon absorption of FLO under UVB sparks an idea that UVB could be more effective for FLO than NAP. However, this phenomenon was not detected in this experiment possibly due to the significantly lower concentration of FLO.

4.4.2 Effects of pH Value

The effect of pH on the photodegradation of NAP and FLO is presented in **Figure 4-6**. The removal rates ranged from 85.41% under pH=3 to 92.51% under pH=10 for NAP; and from 46.41% under pH=3 to 99.23% under pH=10 for FLO. A clear trend can be identified that the performance of UVC irradiation increased at higher pH values. The increase of pH leads to an increase of OH$^-$, which plays key role in the formation of alcohol radical $(PAH(H) \cdot (OH))$, therefore, speed the photo degradation course. The results also indicated a much more significant impact of pH on the photolysis of FLO than that of NAP.

Semi-log plots of PAHs concentration versus degradation time (**Figure 4-7**) seem again to be linear according to good R^2 value. The photolytic kinetic rate constants of degraded FLO at pH = 7 was 0.0487 min^{-1}, whereas the photolytic kinetic rate constants of degraded FLO at pH = 3 was about 5 times slower i.e., 0.0097 min^{-1}. The differences between reaction rate constants at varied pH values for NAP were not as remarkable as those for FLO. For example, FLO could be degraded about twice time faster than NAP under pH 10, but about three times slower than NAP under pH 3. This behavior becomes

124

clear when attenuation coefficients depending on pH are measured. According to a couple of previous studies (Beltran et al., 1995; Heavey, 1998), NAP was reported to show no significant change of the attenuation coefficient with respect to pH, which confirms the experimental results from the current research. **Table 4-3** summarized the regression equations of PAHs degradation at varied pH.

4.4.3 Effects of Radical Scavenger

Figure 4-8 manifested all the time-varying change of PAHs for different dose of radical inhibitors. The removal rates decreased with increased t-BuOH concentration. Compared to the degradation data without the radical scavenger (i.e., BuOH=0M), a discernable retarding effect by adding t-BuOH was observed and hence verifying the radical mechanism. The t-BuOH is supposed to compete with the dissolved oxygen in the matrix, which increases the opportunity of the recombination reaction between the generated positive holes and electrons.

From **Figure 4-9**, the kinetic rate constants for the PAHs degradation process were observed to be inversely proportional to the concentration of t-BuOH. The regression equations of PAHs degradation are also available at **Table 4-4**. Within the tested dose range, the reduction in the rates of degradation is marginal as the differences between reaction rate constants at different concentration of t-BuOH were not as remarkable as those between different UV wavelengths. This deserves certain postulation relating to the presence of additional oxidant species (e.g., singlet oxygen).

125
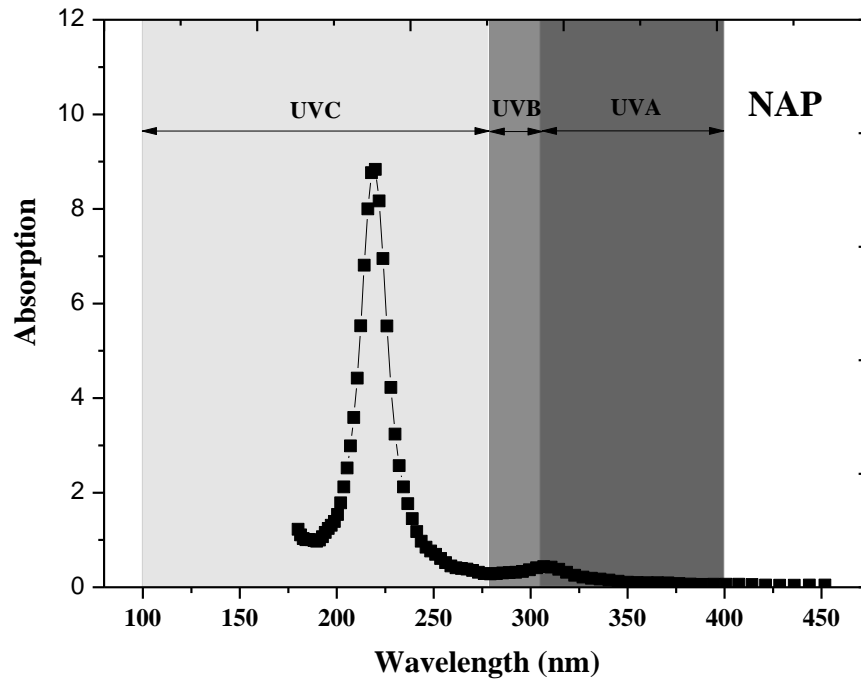
Figure 4-4 Photon Absorption of NAP at Different Wavelength
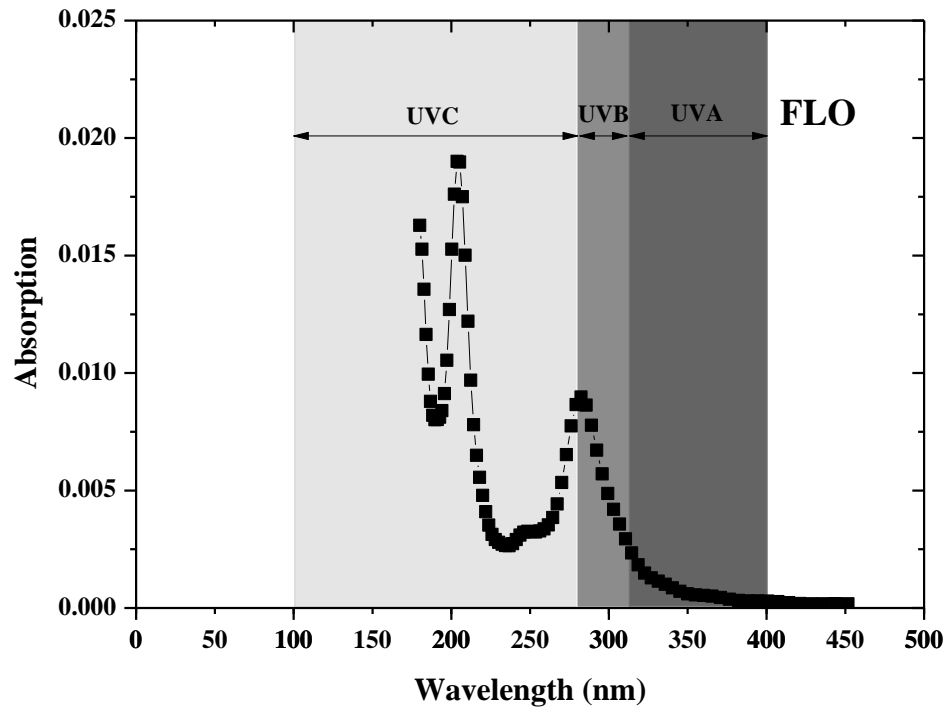
Figure 4-5 Photon Absorption of FLO at Different Wavelength
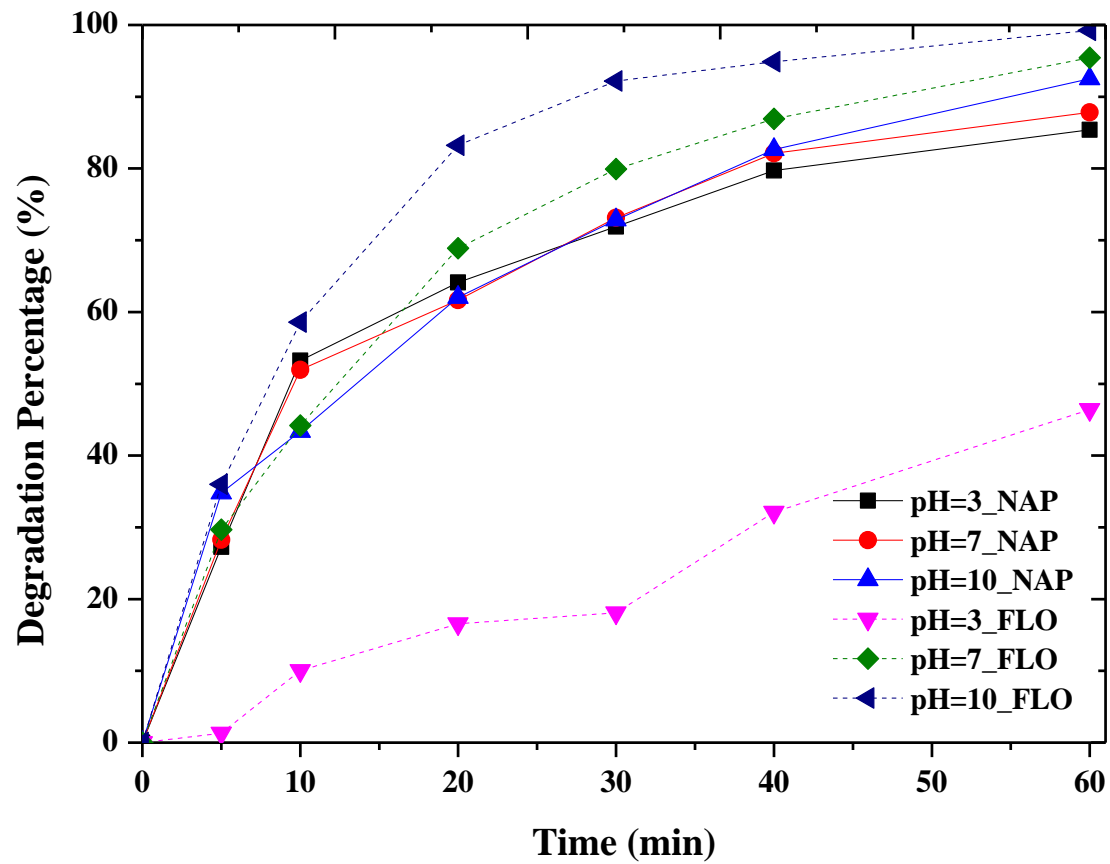
Figure 4-6 PAHs Degradation with Time under Varied pH Values

128
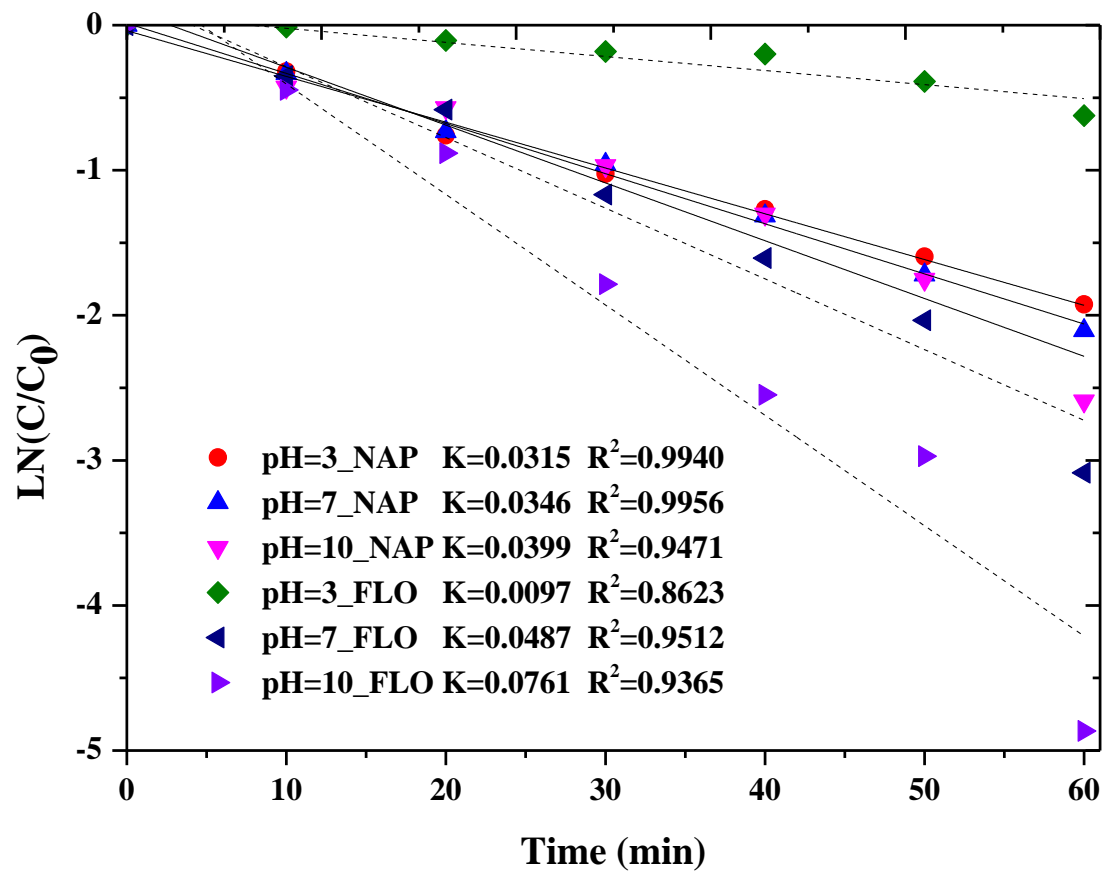
Figure 4-7 Reaction Rate Constants of PAHs under Varied pH
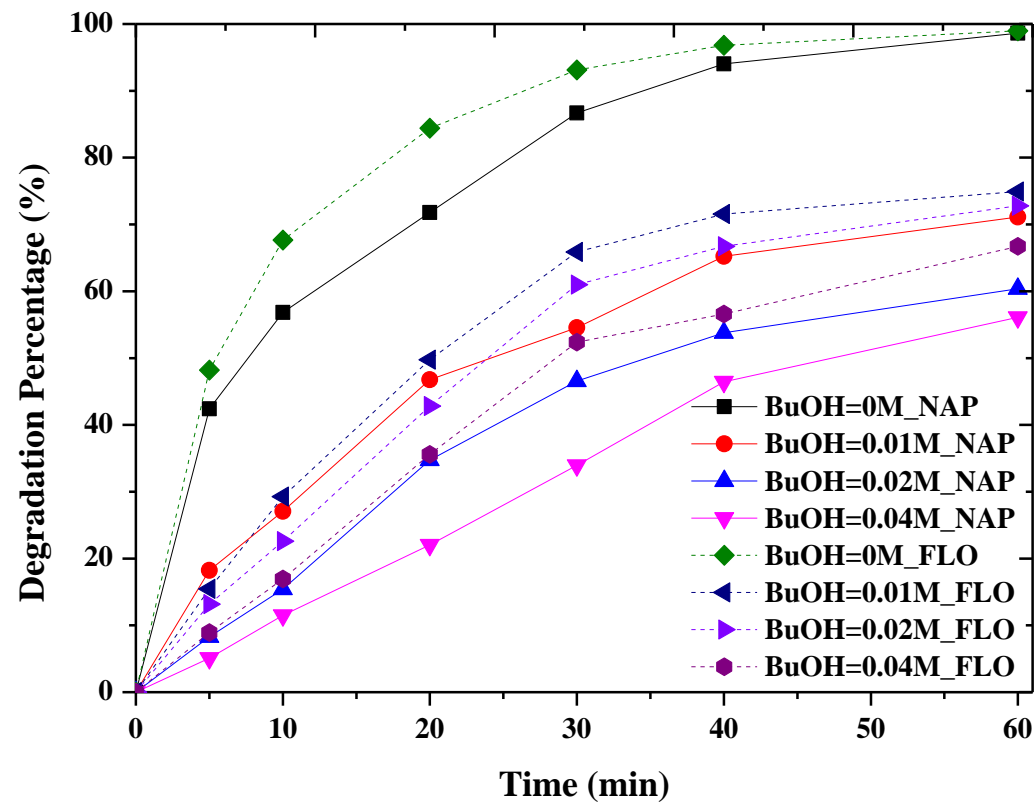
Figure 4-8 PAHs Degradation with Time under Varied Radical Scavenger Doses

Figure 4-9 Reaction Rate Constants of PAHs under Varied Radical Scavenger Doses

Table 4-3 Regression Equations of PAHs Degradation at Varied pH

Experimental Settings	Regression Equations
pH=3_NAP	$\ln\left(\dfrac{c}{c_0}\right) = -0.0316t - 0.0379$
pH=7_NAP	$\ln\left(\dfrac{c}{c_0}\right) = -0.0346t - 0.0131$
pH=10_NAP	$\ln\left(\dfrac{c}{c_0}\right) = -0.0399t - 0.1080$
pH=3_FLO	$\ln\left(\dfrac{c}{c_0}\right) = -0.0097t - 0.0749$
pH=7_FLO	$\ln\left(\dfrac{c}{c_0}\right) = -0.0487t - 0.2007$
pH=10_FLO	$\ln\left(\dfrac{c}{c_0}\right) = -0.0761t - 0.3551$

Table 4-4 Regression Equations of PAHs Degradation at Varied BuOH Dose

Experimental Settings	Regression Equations
BuOH=0M_NAP	$\ln\left(\dfrac{c}{c_0}\right) = -0.0702t - 0.4683$
BuOH=0.01M_NAP	$\ln\left(\dfrac{c}{c_0}\right) = -0.0210t - 0.1103$
BuOH=0.02M_NAP	$\ln\left(\dfrac{c}{c_0}\right) = -0.0165t - 0.0412$
BuOH=0.04M_NAP	$\ln\left(\dfrac{c}{c_0}\right) = -0.0144t - 0.0129$
BuOH=0M_FLO	$\ln\left(\dfrac{c}{c_0}\right) = -0.0720t - 0.8106$
BuOH=0.01M_FLO	$\ln\left(\dfrac{c}{c_0}\right) = -0.0247t - 0.1195$
BuOH=0.02M_FLO	$\ln\left(\dfrac{c}{c_0}\right) = -0.0232t - 0.0675$
BuOH=0.04M_FLO	$\ln\left(\dfrac{c}{c_0}\right) = -0.0193t - 0.0308$

4.4.4 Effects of Oxygen

This round of experiment targets in comparing the effects of oxygen at varied dose levels. **Figure 4-10** depicted the time change of PAHs breakdown in artificial OPW under different oxygen doses when UVC was irradiated. It was found that the oxygen should be maintained at an optimum level in order to reach the highest degradation efficiency. In the current study, for both NAP and FLO, the highest degradation rates were achieved at 30 ml/min oxygen flow rate. At either the lower (i.e., 20 ml/min) or upper (i.e., 40 ml/min) level of oxygen flow rates, the performances were even not comparable with that under the ambient environment without adding extra oxygen.

The slight difference between the degradation rates (Figure 4-10) with and without oxygen indicated that oxygen concentration had minor effects upon the photo degradation rates of the selected PAHs. Besides, the decaying rates shown in **Figure 4-11** turned out to be in the pattern that those for NAP were a little higher than those for FLO at each O_2 dose level, which again reaffirmed that the effectiveness of oxygen is also dependent on the type of the pollutants. The photosensitized oxygenation of FLO in the sample waters could be slower than that of NAP compared with direct photolysis and consequently, that singlet oxygen might play less significant role in the photochemical transformation of FLO. Table 4-5 lists the regression equations of PAHs degradation at varied O_2 doses. More discussions on the degradation mechanism can be found in Section **4.2.3.6**.

134
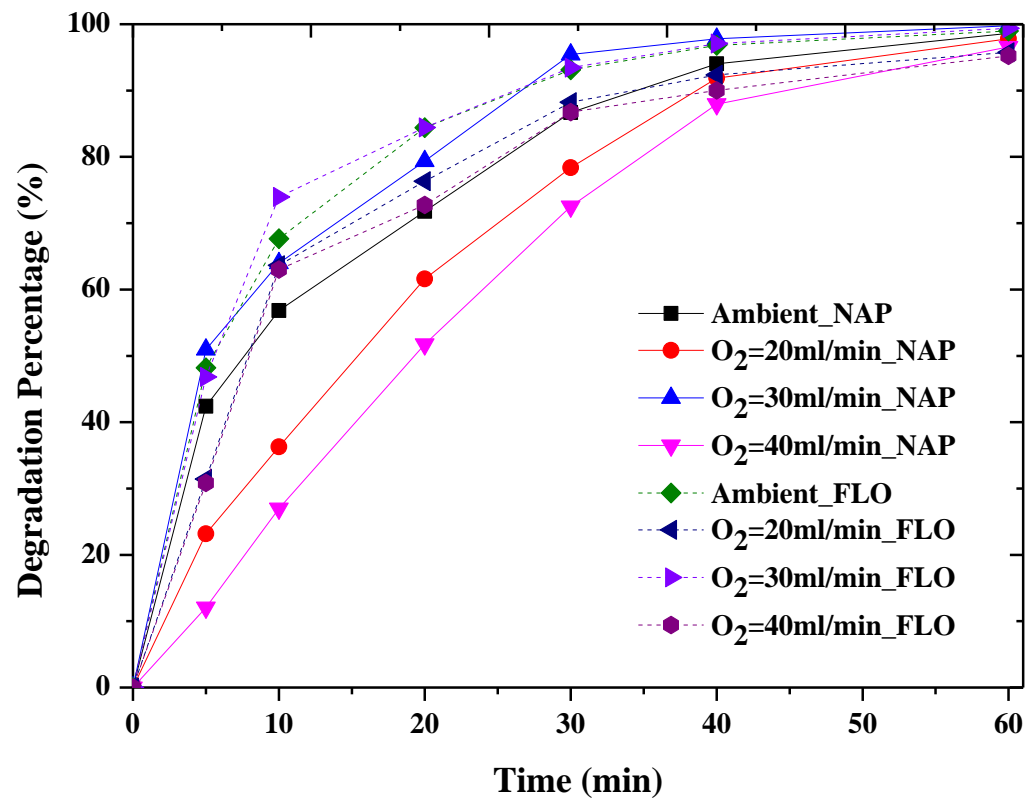
Figure 4-10 PAHs Degradation with Time under Varied Oxygen Doses

135
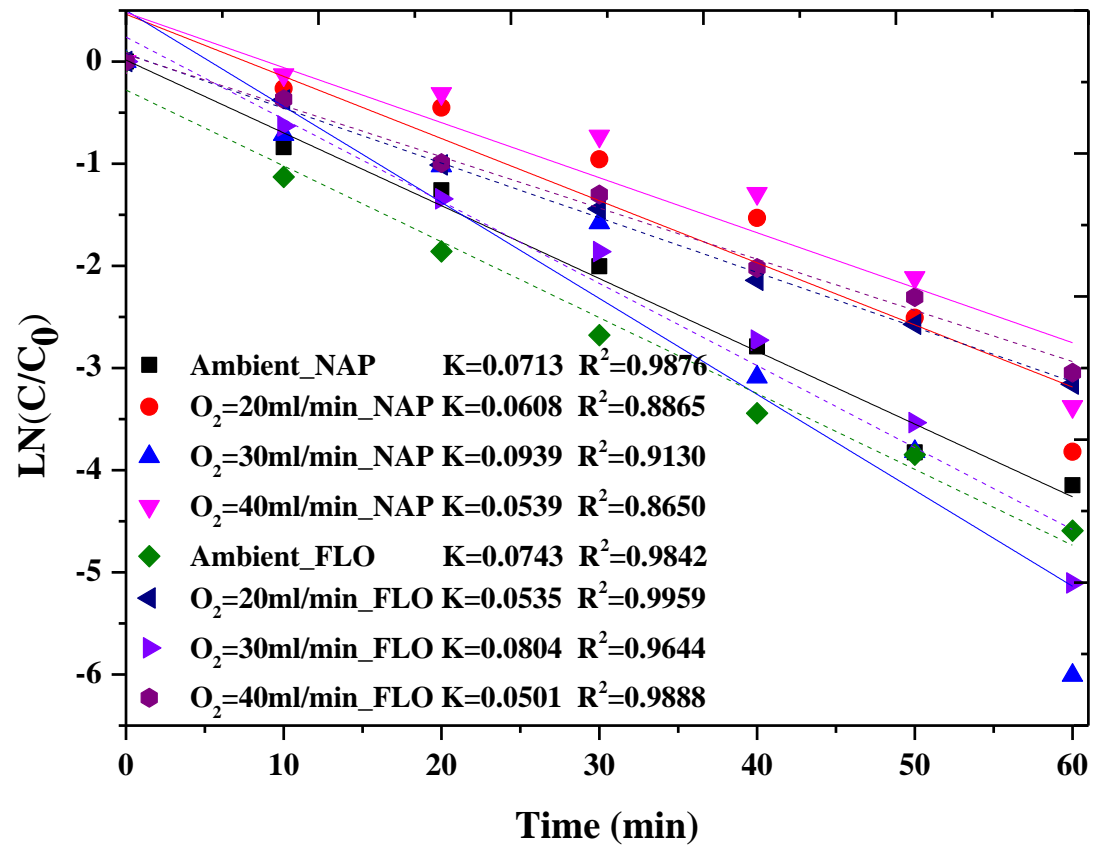
Figure 4-11 Reaction Rate Constants of PAHs under Varied Oxygen Doses

Table 4-5 Regression Equations of PAHs Degradation at Varied O_2 Doses

Experimental Settings	Regression Equations
Ambient_NAP	$\ln\left(\dfrac{c}{c_0}\right) = -0.2241t - 0.20067$
O_2=20ml/min_NAP	$\ln\left(\dfrac{c}{c_0}\right) = -0.0364t - 0.0743$
O_2=30ml/min_NAP	$\ln\left(\dfrac{c}{c_0}\right) = -0.0713t - 0.0142$
O_2=40ml/min_NAP	$\ln\left(\dfrac{c}{c_0}\right) = -0.0184t - 0.0700$
Ambient_FLO	$\ln\left(\dfrac{c}{c_0}\right) = -0.0301t - 0.0234$
O_2=20ml/min_FLO	$\ln\left(\dfrac{c}{c_0}\right) = -0.0743t - 0.2785$
O_2=30ml/min_FLO	$\ln\left(\dfrac{c}{c_0}\right) = -0.0316t - 0.0379$
O_2=40ml/min_FLO	$\ln\left(\dfrac{c}{c_0}\right) = -0.0346t - 0.0131$

4.4.5 Effects of Catalyst Dose

It is clear from **Figure 4-12** and **Figure 4-13** that the lowest Degussa P-25 TiO_2dose (0.5 g/l) shows the highest PAHs removal among the three dose settings. Table 4-6 shows the regression equations of PAHs degradation at varied doses. It is reasonable as using excess catalyst reduces the amount of photo-energy being transferred in the medium due to opacity offered by the catalyst particles. Trials of experiments have been further conducted with lower catalyst dose settings for investigating the optimum catalyst dose level, however, the results showed high fluctuation or uncertainty under the current experimental condition, and thus there is a tradeoff between finding the optimum catalyst dose value and achieving the reliability of the results. The experimental finding also brings attention to the fact that the effectiveness of the catalyst is strongly dependent on the type of the pollutant, as even higher degradation of FLO was found under direct photolysis without the catalyst. Further studies on the TiO_2 effects on PAHs degradation are led by a team member at the NRPOP lab (Liu et al., 2014).

138
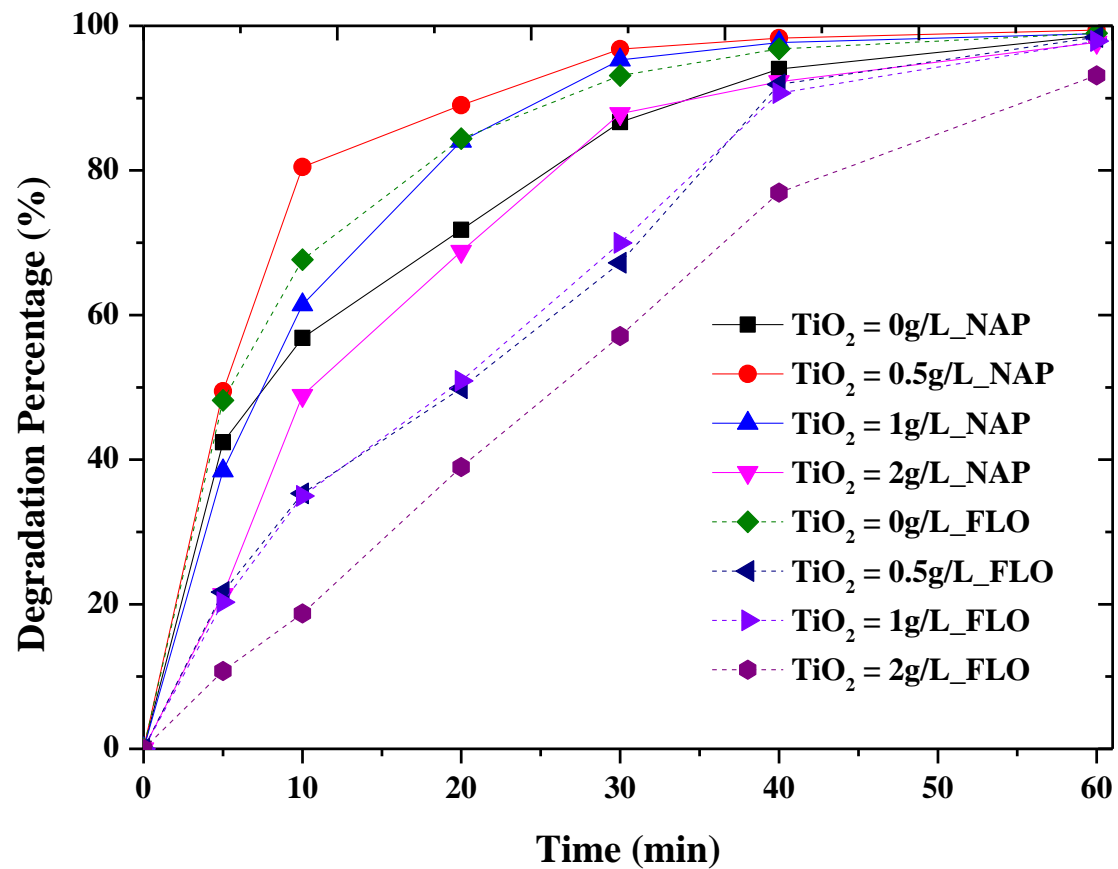
Figure 4-12 PAHs Degradation with Time under Varied Catalyst Doses
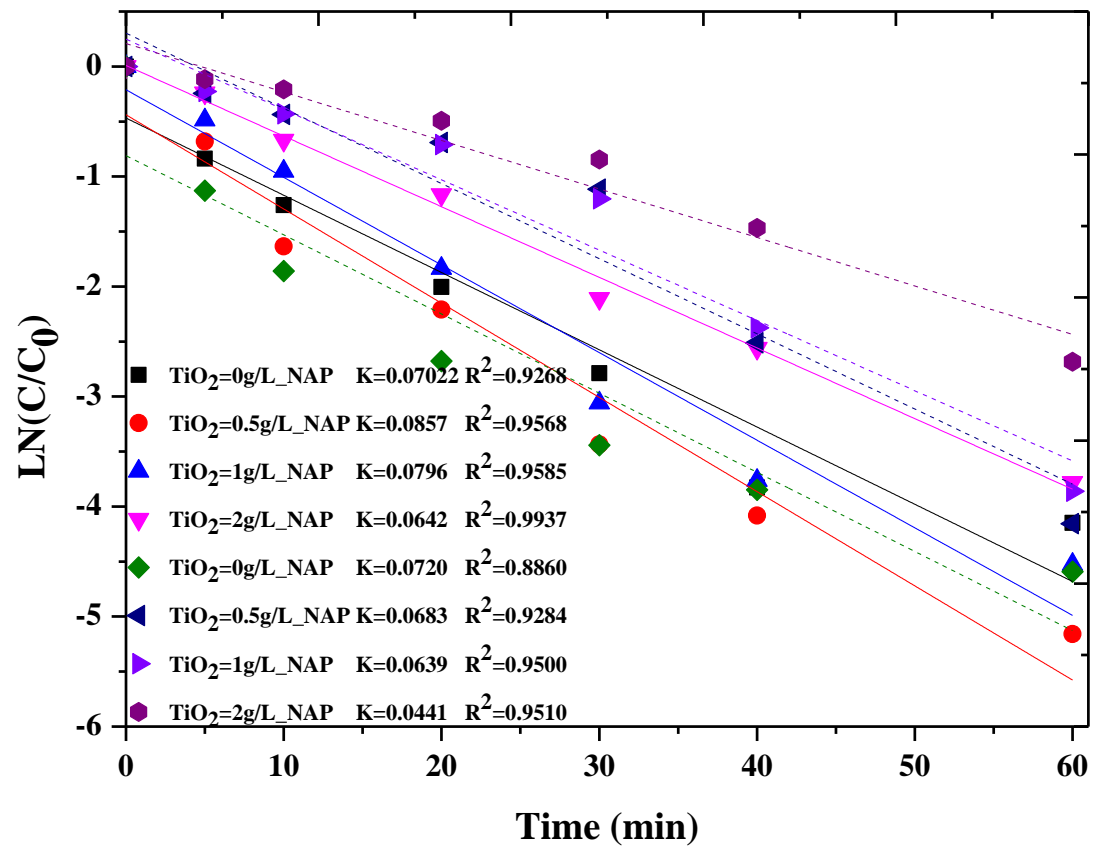
Figure 4-13 Reaction Rate Constants of PAHs under Varied Catalyst Doses

140

Table 4-6 Regression Equations of PAHs Degradation at Varied Catalyst Doses
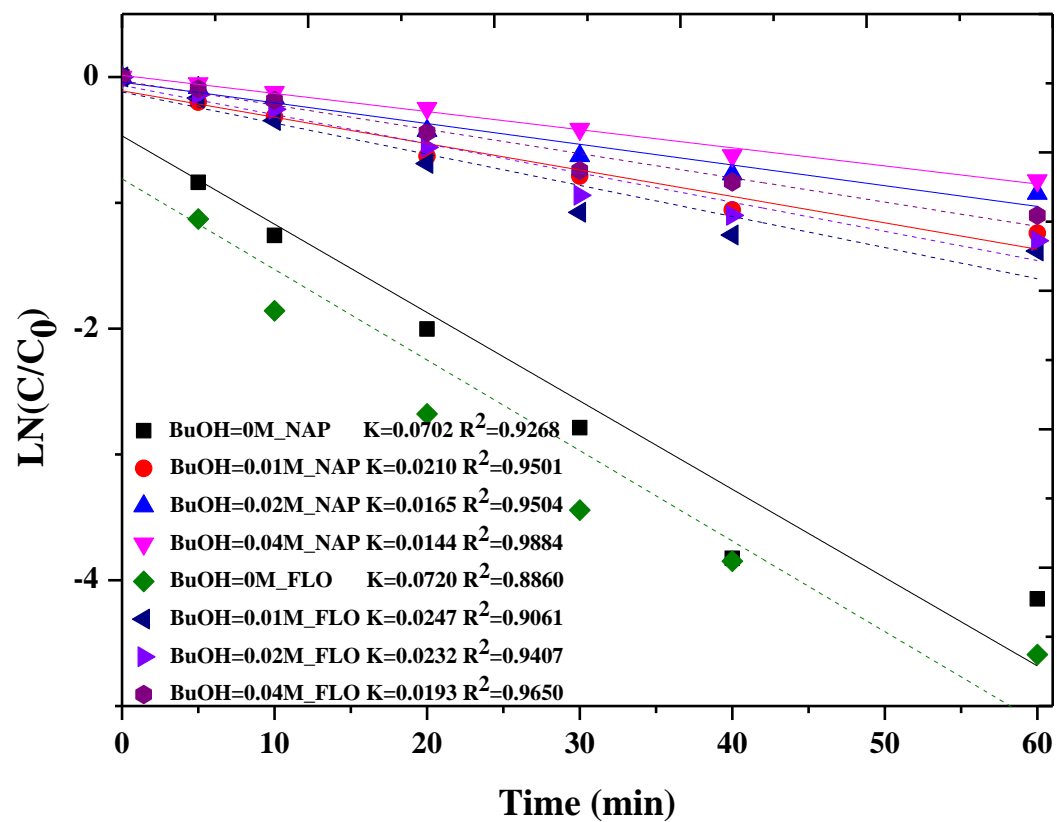
Experimental Settings	Regression Equations
TiO$_2$=0g/l_NAP	$\ln\left(\frac{c}{c_0}\right) = -0.0399t - 0.1080$
TiO$_2$=0.5g/l_NAP	$\ln\left(\frac{c}{c_0}\right) = -0.0097t - 0.0749$
TiO$_2$=1g/l_NAP	$\ln\left(\frac{c}{c_0}\right) = -0.0487t - 0.2007$
TiO$_2$=2g/l_NAP	$\ln\left(\frac{c}{c_0}\right) = -0.0761t - 0.3551$
TiO$_2$=0g/l_FLO	$\ln\left(\frac{c}{c_0}\right) = -0.0713t - 0.0142$
TiO$_2$=0.5g/l_FLO	$\ln\left(\frac{c}{c_0}\right) = -0.0608t - 0.4630$
TiO$_2$=1g/l_FLO	$\ln\left(\frac{c}{c_0}\right) = -0.0939t - 0.5002$
TiO$_2$=2g/l_FLO	$\ln\left(\frac{c}{c_0}\right) = -0.0539t - 0.4796$

4.4.6 Degradation Mechanism

4.4.6.1 Direct Photolysis of PAHs in Water

The mechanism study aims to choose the most probable pathway of PAHs' decomposition considering experimental results. There are three main initial pathways of PAHs' degradation: 1) direct photolysis through radical cation (PAH(H) $\cdot^+$); 2) "self-sensitized" photolysis via a singlet oxygen ($^1O_2$); or 3) indirect or "sensitized" photolysis initiated via light absorption by matrix substances which subsequently react with PAHs via a hydroxyl radical ($\cdot$ OH). **Figure 4-14** shows the possible reaction of a PAH molecule in water with dissolved oxygen (DO) under UV irradiation (adapted from Miller and Olejnik, 2001).

Pathway 1: Photon absorbed by the PAH molecule caused its excitation ($PAH(H) + hv \rightarrow PAH(H)^*$). Such a molecule can undergo chemical changes, for example, electron transfer. In proper conditions an electron (e_{aq}) can be transferred to oxygen yielding $PAH(H) \cdot^+$ and a superoxide anion ($O_2 \cdot^-$). The radical cation reacts with water (H_2O) or hydroxide ion (OH^-) to give the alcohol radical ($PAH(H) \cdot (OH)$)), which then either polymerizes in deoxygenated solutions or reacts with oxygen to yield quinone ($PAH(H)(OH)(OO) \cdot$) which decomposes producing $O_2 \cdot^-$ and alcohol ($PAH(H)^+(OH)$). According to the experimental results from the effects of oxygen, direct photolysis appears to be significant relative to self-sensitized photo degradation.

142
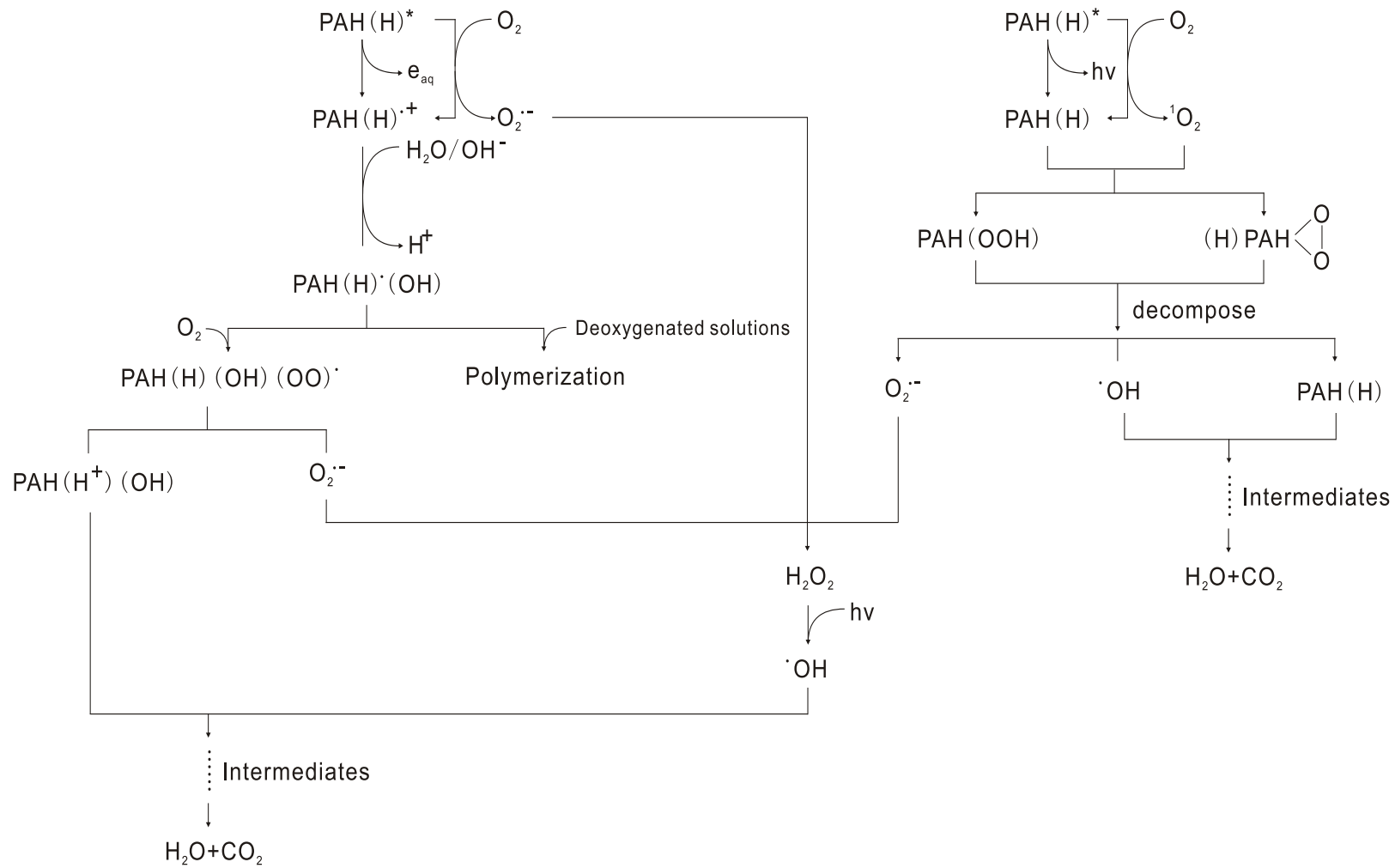
Figure 4-14 Schemes of PAHs Photolysis Pathways in the O$_2$/H$_2$O System

143

Pathway 2: The excited molecule can also return to the ground state dissipating energy in various ways, mostly photophysical processes such as internal conversion, fluorescence, intersystem crossing, phosphorescence and by energy transfer to other molecules, for example, to oxygen giving $^1O_2$. PAHs are known as good sensitizers for singlet oxygen formation (Liu et al., 2011; Comber et al, 2013). Oxygen in the ground triplet state needs above 94 kJ/mol to transform into a very reactive singlet state. This energy can be delivered to oxygen exactly by encountering an excited PAH molecule. The investigated PAHs have sufficient energy levels in the excited state, as well as in the singlet and triplet state (Murov et al., 1993). Singlet oxygen can attack a PAH molecule in the ground state which mainly causes formation of endoperoxides ($PAH(OOH)$) and hydroperoxides ($(H)PAH(OO)$) and these compounds in turn initiate radical reactions. Considering experimental results from the minor effects of oxygen, the primary photochemical processes in this experiment may not involve singlet oxygen.

Pathway 3: Organic peroxides and hydroperoxides can also decompose producing $O_2 \cdot^-$ or $\cdot OH$. The first species, which may also be formed by the electron transfer from the excited PAH to O_2, is rather unreactive. But it can transform to a hydroperoxide radical ($HO_2 \cdot$) which in turn in sequence of reactions via hydrogen peroxide (H_2O_2) gives a very reactive $\cdot OH$. The experimental results from the effects of radical inhibitor verified the presence of hydrogen peroxide during the photolysis of NAP and FLO and its importance. Thus, the third pathway of the PAHs' degradation appeared to be valid in this experiment. The cases described above led to the following reaction scheme:

144

$$PAH + hv \longrightarrow PAH^* \qquad\qquad r_1 = k_1 I_a \qquad \text{(4-8)}$$

$$PAH^* \longrightarrow PAH + hv \qquad\qquad r_2 = k_2 C^* \qquad \text{(4-9)}$$

$$PAH^* + O_2 \longrightarrow PAH + {}^1O_2 \qquad r_3 = k_3 [O_2] C^* \qquad \text{(4-10)}$$

$$PAH + {}^1O_2 \longrightarrow products \qquad r_4 = k_4 \left[{}^1O_2 \right] C \qquad \text{(4-11)}$$

$$PAH^* \longrightarrow PAH^{\cdot +} + e_{aq}^- \qquad\qquad r_5 = k_5 C^* \qquad \text{(4-12)}$$

$$PAH^* + O_2 \longrightarrow PAH^{\cdot +} + O_2 {}^{\cdot -} \qquad r_6 = k_6 [O_2] C^* \quad \text{(4-13)}$$

$$PAH + O_2 {}^{\cdot -} \longrightarrow products \qquad r_7 = k_7 [O_2 {}^{\cdot -}] C \qquad \text{(4-14)}$$
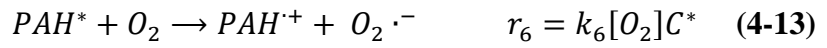
Where,

r = Reaction rate;

I_a = Intensity of absorbed light (quanta l^{-1} s^{-1}); and

k = Rate constant.

Taking into consideration the experimental results, i.e., the influence of oxygen and t-BuOH on the removal rates of the targeting PAHs, the superoxide pathway of the NAP and FLO decomposition was proposed and the PAH's elimination can be expressed by the following equation:

$$-\frac{dC_{PAH}}{dt} = r_1 - r_2 - r_6 + r_7 \qquad\qquad \text{(4-15)}$$

Based on the stationary state assumption for concentrations of exited PAHs and $O_2 \cdot^-$:

$$r_1 = r_2 + r_6$$

$$\Rightarrow k_1 I_a = k_2 C^* + k_6 [O_2] C^*$$

$$\Rightarrow C^* = \frac{k_1 I_a}{k_2 + k_6 [O_2]} \tag{4-16}$$

$$r_6 = r_7$$

$$\Rightarrow -\frac{dC_{PAH}}{dt} = r_1 - r_2 = k_1 I_a - k_2 C^*$$

$$\Rightarrow -\frac{dC_{PAH}}{dt} = I_a \frac{k_2 k_6 [O_2]}{k_2 + k_6 [O_2]} = I_a \Phi_{PAH} \tag{4-17}$$

where,

$$\Phi_{PAH} = \frac{k_1 k_6 [O_2]}{k_2 + k_6 [O_2]} \tag{4-18}$$

Weather different pH lead to any variation of oxidation rate is another way confirms whether the individual PAH is oxidized by hydroxyl radicals. According to the experimental results, at a given time the increase of pH leads to an increase of the oxidation rate of the targeting PAHs, this confirms that at pH values higher than 3 FLO is partially oxidized by hydroxyl radicals. In reaction **(4-14)**, $O_2 \cdot^-$ converts into a hydroxyl radical and finally it reacts with the PAH to produce H_2O and CO_2.

The rate of photolysis is usually described by **(4-19)**, which is a combination of Stark-

146

Einstein law and Lambert-Beer law:

$$r = \phi I_0[1 - \exp(-2.303\epsilon bC)] \tag{4-19}$$

Where,

r = Reaction rate;

ɸ = Quantum yield;

ϵ = Attenuation coefficient, $lM^{-1}cm^{-1}$;

b = Light path length, cm; and

C = PAHs concentration, lM.

When the concentration of the absorbing substance, exactly absorbance, is small, **(4-19)** can be simplified to the familiar first-order expression:

$$r = 2.303\phi I_0\epsilon bC = kC \tag{4-20}$$

This form of equation is very often used for the determination of a quantum yield.

For the initial reaction time, when PAH molecules are the solely absorbing species, absorbed UV light I_a can be expressed using the Lambert-Beer law:

$$I_a = I_0[1 - \exp(-2.303b\epsilon C)] \tag{4-21}$$

147

Substituting (**4-21**) to (**4-17**) gives equation (**4-19**) in general form, which after integration in the limits C_0 for time 0 and C for t, results in:

$$\ln \frac{1 - \exp(-2.303 b\epsilon C_0)}{1 - \exp(-2.303 b\epsilon C)} = \phi I_0 \text{t} \qquad\qquad \textbf{(4-22)}$$

A plot of the left-hand-side of **Equation (4-22)**, denoted Γ, versus time should give a straight line with the slope ϕI_0. Knowing I_0 from actinometry it is possible to calculate an apparent quantum yield. By plotting the theoretical kinetic model with experimental data, the calculated slopes (i.e., ϕI_0) are quite close to the reaction rate constant obtained in the experimental section assuming the pseudo first order kinetic.

Table 4-7 shows an example in comparing the reaction rate constants of PAHs obtained from the two kinetic models of UVC irradiation at varied environmental settings. T test has been performed to determine if there is significant difference between the data obtained from the two kinetic models. Probability associated with the t-Test, with a two-tailed distribution (0.72252 (FLO)/0.936081 (NAP)) was > 0.05, t_{obs} = 0.08275(NAP)/0.36786(FLO) < 2.31 = t_{crit}, the null hypothesis was retained: i.e., it is 95% confident to conclude that any difference between the two groups is due to chance. The results also verified the efficiency of the pseudo first order kinetic model in analyzing the OFAT experimental results of the photolysis/photocatalysis process.

148

Table 4-7 Reaction Rate Constants of PAHs from Two Kinetic Models

Models	PAHs	UVC				
		Ambient	pH=10	BuOH =0.01 M	O_2=30 ml/min	TiO_2=0.5 g/l
Pseudo	NAP	0.0713	0.0368	0.0210	0.0939	0.0857
First Order	FLO	0.0743	0.067	0.0247	0.0804	0.0683
Theoretical	NAP	0.0678	0.0398	0.0187	0.0913	0.083
Model	FLO	0.0675	0.0761	0.0182	0.072	0.0544

4.4.6.2 Photocatalytic Degradation of PAHs in Water

The Degussa P-25 TiO_2 selected in this research is a high efficient semiconductor that under UV irradiation can promote an electron (e⁻) from the valence band (VB) to the conduction band (CB), leaving a positive hole (h⁺) at the site where the electron was originally captured. Photoreduction, photooxidation and adsorption occur on or near the particle surface. A competition reaction occurs between water, oxygen, organic molecules and other chemicals, which may be present in the system. When TiO_2 is suspended in water, band electrons interact with surface adsorbed molecular oxygen to yield superoxide radical anions, while valence band holes interact with water to produce hydroxyl radical, both are very active in the oxidative degradation of PAHs in water (**4-23**).

$$TiO_2 + hv \rightarrow h^+ + e^- \qquad \text{(4-23)}$$

$$h^+ + e^- \rightarrow heat \qquad \text{(4-24)}$$

$$h^+ + H_2O \rightarrow \cdot OH + H^+ \qquad \text{(4-25)}$$

$$h^+ + OH^- \rightarrow \cdot OH \qquad \text{(4-26)}$$

$$e^- + O_2 \rightarrow O^{2-} \qquad \text{(4-27)}$$

$$O^{2-} + O^{2-} + 2H^+ \rightarrow H_2O_2 + O_2 \qquad \text{(4-28)}$$

$$O^{2-} + H^+ \rightarrow HO_2 \cdot \qquad \text{(4-29)}$$

$$HO_2 \cdot + H^+ + e^- \rightarrow H_2O_2 \qquad \text{(4-30)}$$

150

$$H_2O_2 + hv \rightarrow 2 \cdot OH \qquad \text{(4-31)}$$

$$H_2O_2 + e^- \rightarrow \cdot OH + OH^- \qquad \text{(4-32)}$$
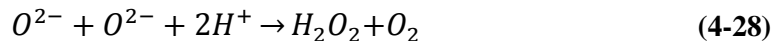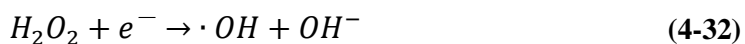
Although the transformation of PAHs in the presence of TiO_2 dispersion occur through various more or less complex steps, it basically is expected to go through hydroxyl attaching, aromatic ring break down, generating alcohol, carboxyl acid, finally breaks down to CO_2 and H_2O in the presence of oxygen excess and may be usually described by an over-all mineralization equation, which is valid after long-term irradiation:

$$C_xH_y + 12O_2 + hv \xrightarrow{TiO_2} [intermediates]$$
$$\rightarrow 10CO_2 + 4H_2O \qquad \text{(4-33)}$$
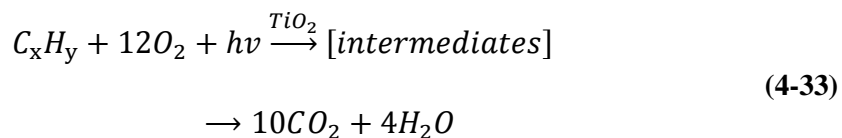
Since the primary process is always faster than the stoichiometric CO_2 formations, it confirms that other carbon-containing products exist after the substrate disappearance and that those intermediates undergo further degradation to CO_2. The attention will be focused on aromatic compounds formed during the treatment, in order to identify them and to verify that no accumulation of toxic reaction products is produced in the reaction media. The sampling time will be chosen within the time range when the intermediate concentrations are found to be higher experimentally.

Due to the general complexity of the radical-induced processes it is difficult to draw a

complete and unique reaction scheme, linking all the identified intermediates through a well-defined sequence of chemical processes. However, it is possible to indicate a limited number of pathways capable of explaining the formation and evolution of some of the observed compounds. In order to examine these reactions, take NAP as an example, the transient species have been divided into three groups (**Figure 4-15,** adapted from Pramauro et al., 1998).
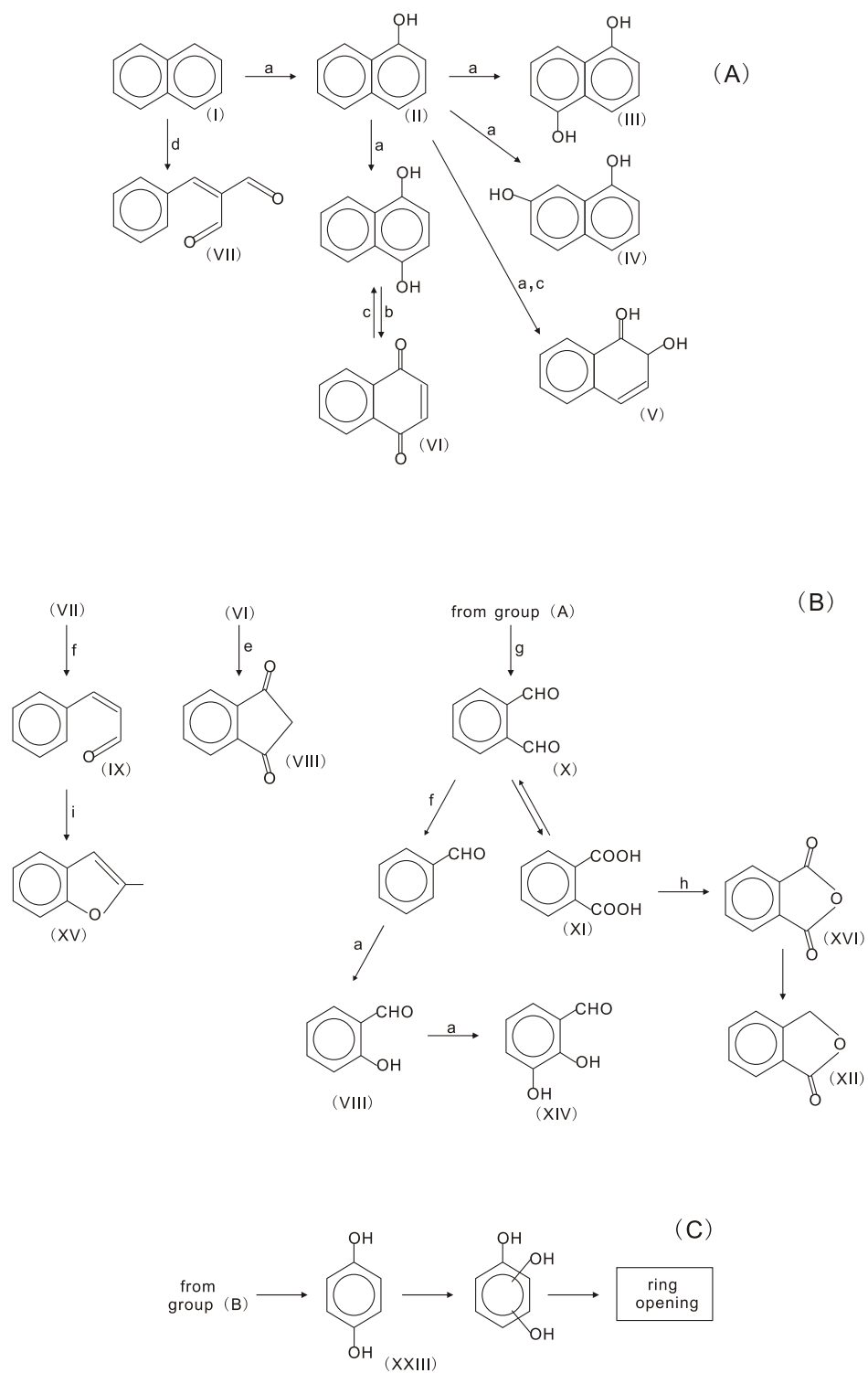
Figure 4-15 Plausible Photocatalytic Degradation Pathways of NAP

Path a – Hydroxylation: The first group of compounds (A) accounts for the simultaneous attack of reactive radicals (mainly $\cdot OH$) to different points of the starting NAP molecule, being hydroxylation reactions assumed as the initial events.

Path b – Oxidation of diols: The oxidation of o- and p-diols to the corresponding quinones usually follows at a rate depending on the redox potential of the couple diol/quinone. A fast transformation of the hypothesized compound 1,4-dihydroxynaphthalene (VI) can occur in the oxidizing reaction media, avoiding its accumulation at measurable concentration levels.

Path c – Reduction of diols: Together with oxidation, reduction of diols (e.g., originated from their reaction with $\cdot H$) can also occur at the semiconductor/solution interface.

Path d – Isomerization + carbon oxidation: The opening of one of the aromatic rings, with isomerization and carbon oxidation, is another major route of transformation of NAP, giving rise to the formation of the abundant product (VII).

Path e – Hydrogenation + carbon loss: Further chemical processes (group B) must involve the above-mentioned derivatives. Intermediate (VIII) originates mainly from the precursor (VI) through a reaction step involving hydrogenation and carbon loss.

Path f – Oxidation of aldehyde + decarboxylation: Moreover, compound (IX) may be

154

formed by oxidation of one aldehyde group of (VII), followed by decarboxylation.

Path g – Opening of rings + redox + decarboxylation: The opening of the oxidized rings in compounds of group (A), coupled with reduction/oxidation and decarboxylation reactions may give rise to the formation of compounds (X) and (XI), which can convert one to another through redox reactions.

Path h – Dehydration: Similar oxidized derivatives containing either a keto- and a carboxylic group may be detected during the photocatalytic transformation of substituted NAP over TiO_2 suspensions in oxygen-saturated acetonitrile. The intermediate (XVI) could be obtained from (XI) by dehydration or on the contrary could originate (XI) by hydrolysis. The reduction of one of the keto groups of (XVI) may, in turn, give rise to the formation of intermediate (XII).

Path i – Isomerization and cyclization: Some intermediates of group (B), such as (IX), may also give rise to the formation of (XV) through isomerization and cyclization reactions.

From compound (X) the formation of benzaldehyde can occur through an oxidation/decarboxylation step (path f). Hydroxylation of benzaldehyde may be invoked to explain the possible formation of the compounds (XIII) and (XIV) (path a).

155

Oxidation and decarboxylation of aliphatic substituents in compounds of group (B) (path f), together with simultaneous hydroxylation of the benzene ring (path a), may form hydroxybenzenes. These compounds, indicated under the group (C), are typical precursors of the ring opening. Hydroquinone (XXIII) can be in turn hydroxylated. Further attack of trihydroxybenzenes leads to the ring opening and to the formation of various aliphatic derivatives, which in turn undergo oxidation and decarboxylation steps with the formation of CO_2 as final product.

4.5 Summary

In this chapter, batches of lab-scale bench-top experiments have been conducted to evaluate the efficiency of UV-enhanced treatment in the degradation of PAHs. The key technology is to develop in situ photolysis enhanced oxidation approaches to remove PAHs from OPW. The major activities are based on the development of optimized direct photolysis and photocatalysis systems.

OPW samples have been transferred into chambers of the developed UV reactors for process optimization. OFAT experimental design has been applied for the analysis of significant environment parameters during the direct photolysis and photocatalysis processes. The key testing parameters during the experiments include UV wavelength, pH value, photo-catalysts, radical inhibitors, O_2 concentration. After treatment, the PW sample have been collected and pretreated and analyzed based on the developed analytical methods. The half-life was suggesting that photolysis-enhanced oxidation was

156

a significantly fast reaction for removal of the targeting PAHs from OPW under certain conditions. Nevertheless, process dynamics and mechanisms have also been discussed based on the experimental results.

Chapter 5 Removal of PAHs from OPW by Hybrid Oxidation Systems

Simultaneous applications of different AOPs have been widely promoted such as UV/O_3, UV/H_2O_2, UV/TiO_2/O_3, UV/TiO_2/H_2O_2, etc. The main objective of using coupled AOPs aims at increasing the formation rate of highly reactive species such as (primarily but not exclusively) hydroxyl radicals leading to the destruction of the target pollutant. Synergism between UV photolysis and H_2O_2 or O_3 may lead to treatment efficiencies that are greater than the sum of efficiencies that could be achieved by the individual processes applied alone (Jing et al., 2012). Another advantage of using hybrid systems is the presence of additional oxidation species (e.g., O_3 and H_2O_2) which are relatively unaffected by the presence of radical scavengers.

Among the AOPs, the combination between O_3 and UV irradiation deserves special consideration because of its possibilities (Beltran et al., 1995b, Corrêa et al., 2010). O_3 has high oxidant capacity and electrophilic character, seems most appropriate oxidant to degrade PAHs, advisable due to its two-component attack of the organic matter in water, through direct and radical reactions (Gogate and Pandit, 2004). To further enhance the treatment efficiency, combination of UV radiation with ozonation was studied. An O_3 oxidization chamber was incorporated into the UV treatment system. The simultaneous application of O_3 and UV radiation were expected to generate more hydroxyl radicals and increase the rate of degradation, plus direct ozonation of the PAHs, thus resulting in a positively synergistic effect on destroying PAHs than the use of either O_3 or UV on its own.

158

Another potentially powerful oxidation system is the addition of H_2O_2 to generate hydroxyl radicals, which also deserves specific studies. The combinations of hydrogen peroxide with UV radiation (UV/H_2O_2) can be more practical from the economic point of view since electric energy requirements are lower. Based on previous work the use of the UV/H_2O_2 system to eliminate pollutants from water, this oxidation technology seems to be very attractive if optimum conditions are applied (Beltran et al., 1995c; Cater et al., 2000; and Fung et al., 2000b).

Therefore, the objective of this Chapter is to develop photolysis enhanced oxidation systems by integrating the effects from O_3 and H_2O_2.

5.1 Sample Preparation

Same as above, artificial PW samples were prepared by spiking distilled water with 2mg/l NAP and 8 μg/l FLO. By adding NaCl, the salinity of the water sample has been adjusted to 35g/l. All prepared water samples were stored in the dark and cold (at 4 ^{o}C) chromatograph fridge before analysis and treatments.

5.2 Experimental Methodology

Preliminary tests were firstly conducted in the developed reactors to evaluate the synergism between UV photolysis and ozonation or hydrogen peroxide and the possibility of enhanced treatment efficiency. O_3 generator was incorporated into the existing
159

photochemical reactor, and O_3 was introduced into the water sample by ozone inlets extended to the bottom of the reactor, and the residual gas was directed through the O_3 outlet for post absorption. Again for safety reason, the whole process was carried out under the fume hood. Although limited ability from TiO_2 was observed in the above tests (i.e., **Section 4.3.5**), the Degussa P-25 TiO_2 still was added to the new systems at 0.5g/l to simulate a popular photocatalysis environment under which for comparing the effects of varied combination of selected process parameters. Influence of temperature and radical scavenger has been further explored either for the purpose of offshore application or for the better understanding of the reaction mechanism in the hybrid systems.

As the proposed systems were expected to have greater potential in on-site real-time applications, rather than the above OFAT experiments for the basic understanding of the photolysis and photocatalysis system, the proposed hybrid systems deserve more discussions on interactions between their process variables and their systems modeling and optimization. Ideally, a comprehensive experimental design for all possible combinations of contributing factors at their varied levels is optimum, however, the number of possible combinations of the potential parameters at multiple levels are likely too numerous (i.e., the product of the number of levels for all parameters) to be tested empirically. Therefore, an appropriate experimental design needs to be streamlined in order to reduce the scale of the experiment while maintaining its potential to provide information that yield to valuable conclusions.

5.2.1 Response Surface Methodology (RSM) and Central Composite Design (CCD)

As discussed in **Chapter 3**, the concept of experimental design is to yield the most information from the fewest runs of an experiment. In order to investigate and optimize the response of different models, as a collection of mathematical and statistical techniques, the Response Surface Methodology (RSM) is commonly applied in practice (Lye, 2009; Plesu et al., 2009; Wu et al., 2012) to address the insufficiency of factorial design to nonlinear models. Central Composite Design (CCD) is one of the most popular RSM techniques, and can investigate the curvature of the nonlinear model and catch its maximum or minimum response. A CCD has three groups of design points (Ramlan, May 2008): a) two-level factorial or fractional design points consisting of all possible combinations of the +1 and -1 levels of the factors; b) axial/start points having all of the factors set to 0, the midpoint, except one factor, which has the value +/- alpha (α) forming a sphere shape which allows the estimation of curvature (α); and c) center points with all levels set to coded level 0 (the midpoint of each factor range) providing information about the existence of curvature. A CCD uses the method of least squares regression to fit the data to a quadratic model. The quadratic model for the response (removal efficiency, R) was as follows:

$$Y = a_0 + \sum_{i=1}^{3} a_i X_i + \sum_{i=1}^{3} a_{ii} X_{ii} + \sum_{i=1}^{3} a_{ij} X_{ij} \qquad \text{(5-1)}$$

Where,

Y = response variable;

a_0 = constant;

a_i, = linear coefficient;

a_{ii} = quadratic coefficient;

a_{ij} = interactive coefficient; and

X_i , X_j = levels of the independent variables.

Assuming the nonlinearity of the hybrid advanced oxidation process, the CCD based RSM with five levels was conducted on the selected key factors based on the purpose of the study.

5.2.2 Parameters Selection and Levels Determination

Although it is known that the removal efficiencies for PAHs could be impacted by many other factors in the hybrid treatment systems, considering the ease of manipulation during an offshore operation, the cost-effective enhancement of the conventional physical process, and the possible scale of current study, three types of process parameters, i.e., oxidant (O_3/H_2O_2) concentration, pH value, and UV wavelength, have been selected to test their contribution to the proposed systems. Oxidants concentration is always one of the key components to be tested for optimizing the oxidation process; the effectiveness of different UV wavelengths require further test with regard to the hybrid situation; the increase of pH leads, on one hand, to an increase of the hydroxyl ion catalyzed

162

decomposition of O_3/H_2O_2 into hydroxyl radicals and, on the other hand, to a decrease of the oxidants available to undergo direct photolysis and produce hydrogen peroxide and eventually more hydroxyl radicals, which is particularly important at pH 10 (Gogate and Pandit, 2014). Given the importance of these variables more studies are needed to clarify their effects, especially under basic conditions.

In this design, numerical factors include O_3 dosage (for UV/O_3 system), H_2O_2 dosage (for UV/H_2O_2 system), and the pH value; categorical factor is the UV wavelength including UVA, UVB and UVC. The lower and upper bonds of the numerical factors should be used to generate their five testing levels on the CCD experimental design. Based on the understanding of the preliminary experiments (i.e., **Section 5.3.1**), the range of O_3 flow rate were set between 25ml/min and 35ml/min; the range of H_2O_2 dosage were set between 10g/l and 30g/l. Considering the OFAT test result the pH value were set at relatively the higher end between 7 and 10. Using Design-Expert v8.0 software (Stat-Ease, Minneapolis, MN), for each of the hybrid system, a full CCD for three factors with 39 points (16 factorial points, 18 axial points, and 5 center points) with each run representing a unique combination of levels for the parameters was employed to evaluate the removal efficiencies of PAHs under varying system conditions (**Table 5-1** and **Table 5-2**).

Table 5-1 CCD Design for Testing the UV/TiO$_2$/O$_3$ System

Run	Factor A: O$_3$ Flow Rate (ml/min)	Factor B: pH Value	Factor C: UV Wavelength	Response 1: NAP Degradation (%)	Response 2: FLO Degradation (%)
1	30.00	8.50	UVB	89.95	94.18
2	25.00	10.00	UVC	90.29	94.95
3	30.00	6.38	UVC	91.94	95.76
4	35.00	10.00	UVB	88.92	94.58
5	30.00	8.50	UVB	89.92	95.13
6	37.07	8.50	UVB	88.24	93.81
7	30.00	8.50	UVA	87.26	94.18
8	30.00	8.50	UVC	98.35	100.00
9	30.00	6.38	UVA	90.49	92.76
10	30.00	8.50	UVB	94.22	94.44
11	30.00	8.50	UVB	94.29	94.23
12	25.00	10.00	UVA	92.46	95.04
13	30.00	10.62	UVA	94.25	93.85
14	35.00	10.00	UVC	95.88	99.61
15	35.00	7.00	UVB	88.48	95.19
16	30.00	8.50	UVA	91.15	93.62
17	30.00	8.50	UVC	98.34	99.99

Run	Factor A: O₃ Flow Rate (ml/min)	Factor B: pH Value	Factor C: UV Wavelength	Response 1: NAP Degradation (%)	Response 2: FLO Degradation (%)
18	25.00	7.00	UVA	87.79	93.93
19	35.00	7.00	UVA	90.61	94.92
20	22.93	8.50	UVB	89.89	94.55
21	30.00	8.50	UVA	90.78	94.51
22	30.00	8.50	UVC	98.36	99.98
23	25.00	7.00	UVB	85.6	92.32
24	35.00	7.00	UVC	93.91	95.88
25	30.00	6.38	UVB	91.19	94.82
26	30.00	8.50	UVA	91.43	94.62
27	30.00	10.62	UVB	89.85	97.22
28	22.93	8.50	UVC	94.80	98.76
29	30.00	8.50	UVA	90.60	96.04
30	35.00	10.00	UVA	88.13	94.83
31	30.00	8.50	UVB	87.26	94.41
32	25.00	7.00	UVC	96.04	99.79
33	25.00	10.00	UVB	87.42	94.9
34	37.07	8.50	UVC	95.28	98.89
35	30.00	8.50	UVC	98.35	99.98

Run	Factor A: O$_3$ Flow Rate (ml/min)	Factor B: pH Value	Factor C: UV Wavelength	Response 1: NAP Degradation (%)	Response 2: FLO Degradation (%)
36	37.07	8.50	UVA	91.70	94.05
37	30.00	10.62	UVC	92.15	95.70
38	22.93	8.50	UVA	90.26	94.28
39	30.00	8.50	UVC	98.36	99.98

166

Table 5-2 CCD Design for Testing the UV/TiO₂/H₂O₂ System

Run	Factor A: H$_2$O$_2$ Concentration (g)	Factor B: pH value	Factor C: UV Wavelength	Response 1: NAP Degradation (%)	Response 2: FLO Degradation (%)
1	5.00	7.00	UVC	92.40	97.06
2	15.00	7.00	UVA	89.78	90.76
3	15.00	10.00	UVC	95.61	98.37
4	15.00	7.00	UVB	84.12	95.46
5	5.00	10.00	UVC	93.55	97.86
6	5.00	7.00	UVB	84.11	94.81
7	10.00	8.50	UVC	94.50	97.46
8	15.00	7.00	UVA	85.32	89.36
9	10.00	8.50	UVC	93.16	98.60
10	10.00	8.50	UVC	94.62	96.11
11	10.00	6.38	UVB	85.98	93.69
12	5.00	7.00	UVA	81.86	88.35
13	2.93	8.50	UVA	88.57	88.28
14	17.07	8.50	UVA	85.72	88.41
15	10.00	6.38	UVA	83.67	88.45
16	10.00	8.50	UVA	83.07	86.78
17	10.00	8.50	UVC	97.13	97.81

167

Run	Factor A: H$_2$O$_2$ Concentration (g)	Factor B: pH value	Factor C: UV Wavelength	Response 1: NAP Degradation (%)	Response 2: FLO Degradation (%)
18	10.00	8.50	UVA	83.14	85.88
19	17.07	8.50	UVC	95.28	98.00
20	10.00	10.62	UVC	95.61	97.76
21	2.93	8.50	UVB	88.00	93.70
22	10.00	6.38	UVC	89.89	96.81
23	15.00	10.00	UVB	91.16	95.51
24	10.00	10.62	UVA	87.90	88.78
25	10.00	8.50	UVB	86.29	95.22
26	10.00	8.50	UVB	86.55	95.32
27	10.00	8.50	UVA	81.66	86.32
28	10.00	8.50	UVB	86.38	95.31
29	15.00	7.00	UVC	90.14	97.77
30	2.93	8.50	UVC	92.47	96.76
31	10.00	8.50	UVA	85.61	90.53
32	10.00	8.50	UVC	94.56	98.78
33	10.00	8.50	UVB	86.83	94.58
34	10.00	10.62	UVB	87.89	95.39
35	5.00	10.00	UVA	87.62	89.35

168

Run	Factor A: H₂O₂ Concentration (g)	Factor B: pH value	Factor C: UV Wavelength	Response 1: NAP Degradation (%)	Response 2: FLO Degradation (%)
36	10.00	8.50	UVA	85.43	89.15
37	17.07	8.50	UVB	89.92	95.90
38	10.00	8.50	UVB	87.07	95.21
39	5.00	10.00	UVB	87.10	90.05

5.2.3 Data Analysis and System Optimization

RSM was applied to evaluate the effects of O_3 dose, H_2O_2 dose, pH value, and UV wavelength on the removal efficiencies of PAHs removal by the two proposed hybrid oxidation systems. The Design-Expert software program version 8.0 (Stat-Ease) was used to analyze the data generated based on the experimental design (**Table 5-1** and **5-2**). Experimental data was analyzed by multiple regressions to fit the quadratic equation to all independent variables. The software uses the quadratic model to build the response surface. The adequacy of the model was determined by evaluating the lack of fit, coefficient of determination (P-value) and the Fisher test value (F-value) obtained from the analysis of variance (ANOVA) that was generated by the software. Statistical significance of the model and model parameters was determined at the 5% probability level ($\alpha = 0.05$). To visualize the relationship between the responses and the independent variables, three-dimensional surface response and contour plots of the fitted quadratic regressions were also generated by varying the variables within the experimental range and holding the other constant at the central point.

After RSM were conducted, the final model with key parameters was shown to model the hybrid oxidation systems. In order to improve the simulation efficiency, the linear/nonlinear optimization can be applied to optimize the results of final model. By making use of the results, the combination of the values of each parameter, which can achieve the optimized value, can be calculated. In this case, the degradation percentage was selected as the final response in CCD for the targeting systems. The greatest

170

degradation value means the best performance of treatment. In order to maximize the degradation value, the nonlinear optimization was used to calculate the greatest value for degradation from the final model, and to get the values for each factors in final model at the same time.

5.2.4 Model Verification

When the results obtained from optimization software, the verification from the experiment should be conducted to make sure the accuracy and feasibility of the final model which was generated by the RSM model. In this study, the new combination of each key parameter was used as new input values for carrying the experiment under the hybrid systems to verify feasibility of the CCD model. By using new combination of the values of each parameter, the final response predicted by CCD model should be close to the results obtained from the experiment, which will demonstrate that the CCD model had an ability to adequately represent the hybrid process. The developed model would be especially helpful in evaluating the interactive influence of the key process variables on treatment efficiency, which will provide significant support on the design and choose of appropriate treatment processes as well as better understandings of the reaction mechanisms of the proposed hybrid AOP systems.

5.3 Results and Discussion

171

5.3.1 Preliminary Tests

Preliminary tests of the synergism of UV/O_3 and UV/H_2O_2 were conducted at room temperature in the prepared PW sample with pH unadjusted. Figure 5-1 shows the comparison of degradation of NAP and FLO with time under varied dose of O_3. The test demonstrated that the participation of O_3, at appropriate dose setting, was able to accelerate the PAHs degradation under the photo catalysis system. After 60-min UVC irradiation, the removal rates reached 99.73% for NAP and 99.45% for FLO when the flow rate of O_3 was set at 30ml/min. However, the degradation rates of both PAHs reduced when the O_3 flow rate either increased to 40ml/min or reduced to 20ml/min. The result also indicated that NAP was more sensitive to the dose change of O_3 than FLO, as the difference between the kinetic rates of NAP at varied O_3 dose were relatively greater than that of FLO (**Figure 5-2**). The regression equations of PAHs degradation at varied O_3 doses are available at **Table 5-3**.
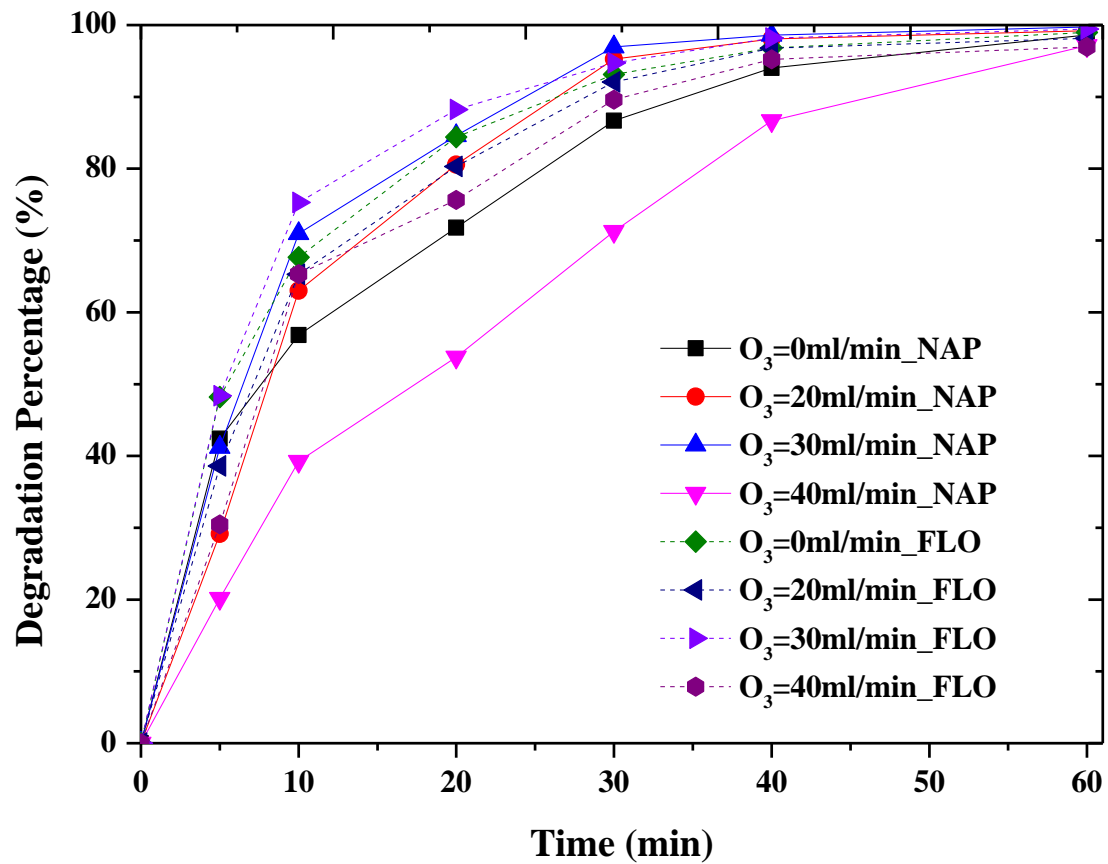
Figure 5-1 PAHs Degradation with Time under Varied Ozone Doses
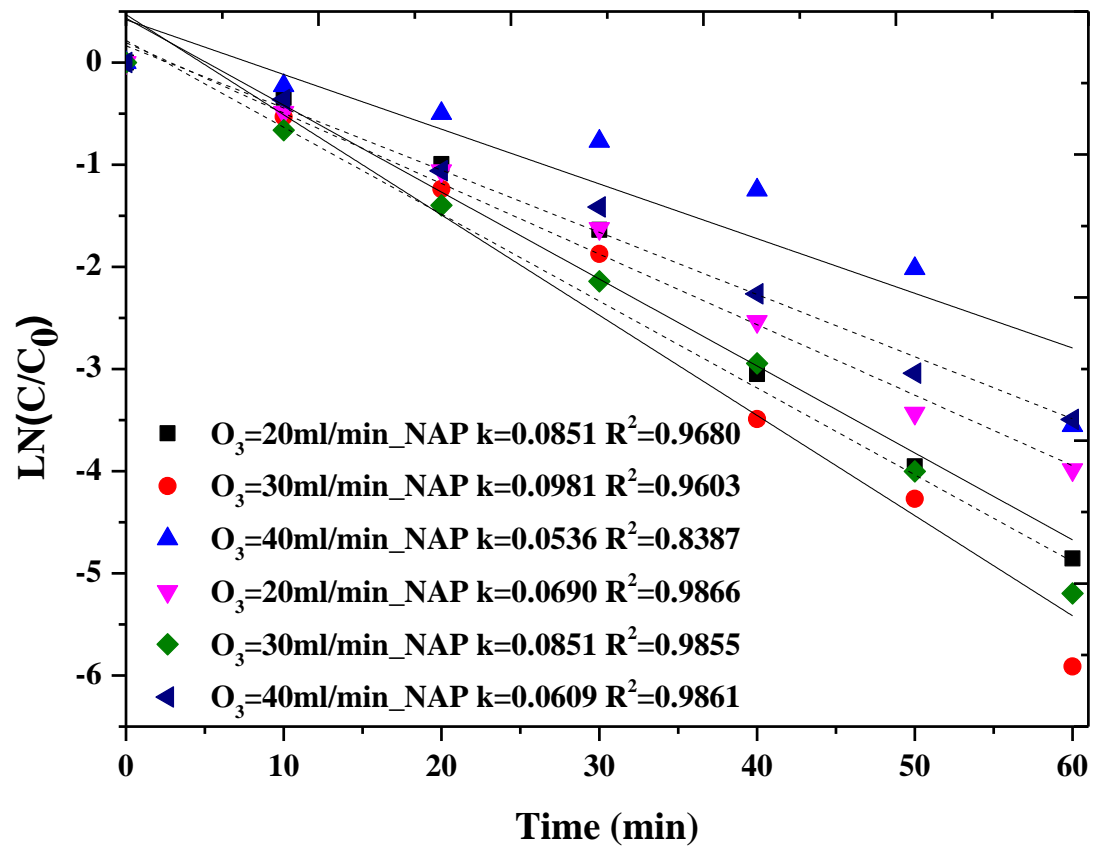
Figure 5-2 Reaction Rate Constants of PAHs under Varied Ozone Doses

174

Table 5-3 Regression Equations of PAHs at Varied O_3 Doses

Experimental Settings	Regression Equations
Ambient_NAP	$\ln\left(\dfrac{c}{c_0}\right) = -0.0713t - 0.0142$
O_3=20ml/min_NAP	$\ln\left(\dfrac{c}{c_0}\right) = -0.0851t - 0.4346$
O_3=30ml/min_NAP	$\ln\left(\dfrac{c}{c_0}\right) = -0.0981t - 0.4697$
O_3=40ml/min_NAP	$\ln\left(\dfrac{c}{c_0}\right) = -0.0536t - 0.4190$
Ambient_FLO	$\ln\left(\dfrac{c}{c_0}\right) = -0.0743t - 0.2785$
O_3=20ml/min_FLO	$\ln\left(\dfrac{c}{c_0}\right) = -0.0690t - 0.1955$
O_3=30ml/min_FLO	$\ln\left(\dfrac{c}{c_0}\right) = -0.0851t - 0.2170$
O_3=40ml/min_FLO	$\ln\left(\dfrac{c}{c_0}\right) = -0.0609t - 0.1637$

The effect of H_2O_2 on the removal of NAP and FLO is presented in **Figure 5-3**. The test demonstrated that the participation of H_2O_2, at appropriate dose setting, was also able to speed the PAHs degradation under the photo catalysis system. After 60-min UVC irradiation, the NAP removal rates reached the highest of 99.88% with 0.001M H_2O_2, and the FLO removal rate reached the highest of 99.73% with 0.1M H_2O_2. A clear trend can be identified that the FLO removal rates increased by increasing dose of H_2O_2, while the NAP removal rates were observed to be inversely proportional to the concentration of H_2O_2 (**Figure 5-4**), which restated that the effectiveness of H_2O_2 is strongly dependent on the type of the individual PAH. The optimum dose of H_2O_2 to achieve the highest removal of NAP could be under 0.001M. The regression equations of PAHs degradation at varied H_2O_2 doses are presented at **Table 5-4**.

5.3.2 Effects of Temperature

Usually photolysis systems are operated at room temperature, as with most photoreactions, temperature is not the major driving force to enhance UV-induced photodegradation (Gogate and Pandit, 2004; Nadal et al., 2006; Lee et al., 2011; Jing et al., 2013). However, the temperature of OPW is usually high (average: 50-90 ^{0}C) (Ayers and Parker, 2001; Arthur et al., 2005; Li, 2014) and with the release of energy in the destruction process the temperature might also increase. A temperature increase may accelerate the degradation of PAHs in OPW because of the increased collisions between photons and molecules; however, it is also expected to result in a decrease in oxygen solubility that lowers the generation of singlet oxygen and superoxide anion radical, which could impede the

176

oxidation process. Therefore, when it comes to investigating the possibility of offshore onsite application, the dependence of the degradation rates on temperature in the specific hybrid processes should be examined to see if cooling and/or post treatment of ventilation from the wastewater stream is needed.

177
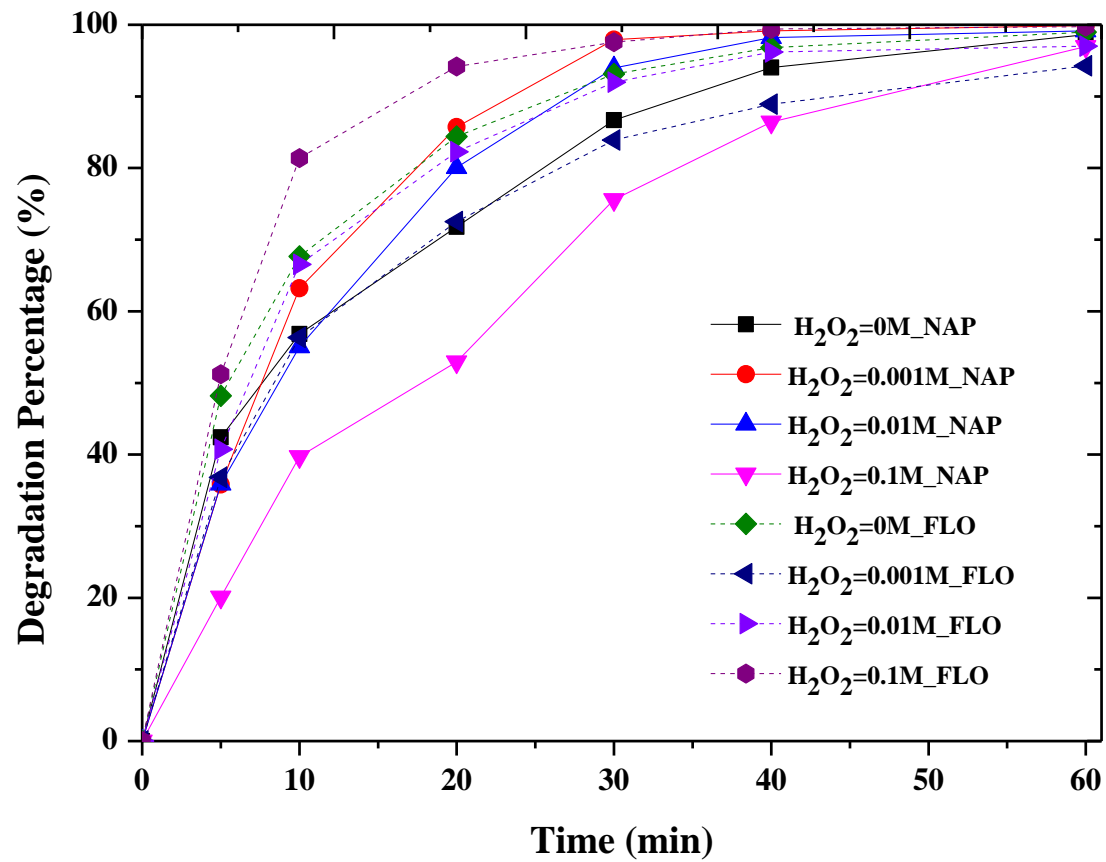
Figure 5-3 PAHs Degradation with Time under Varied H₂O₂ Doses
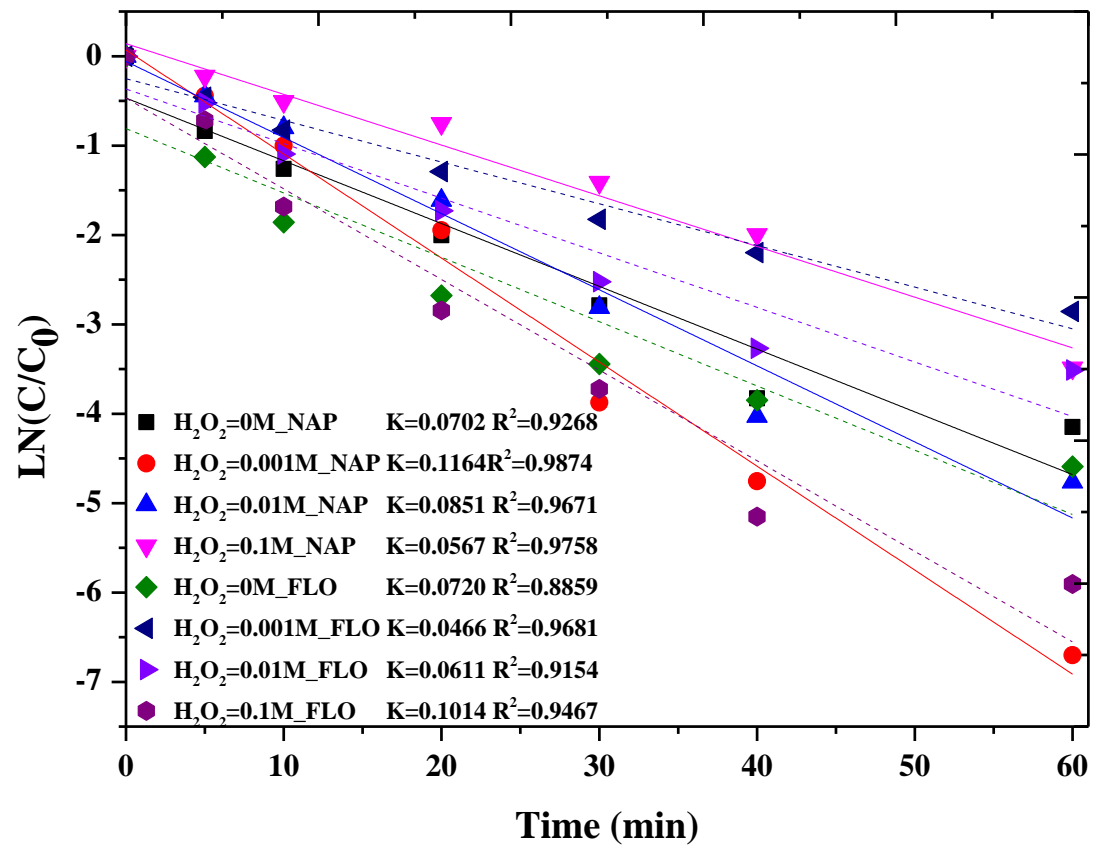
Figure 5-4 Reaction Rate Constants of PAHs under Varied H₂O₂ Dose

- ■ H_2O_2=0M_NAP   K=0.0702 R^2=0.9268
- ● H_2O_2=0.001M_NAP   K=0.1164 R^2=0.9874
- ▲ H_2O_2=0.01M_NAP   K=0.0851 R^2=0.9671
- ▼ H_2O_2=0.1M_NAP   K=0.0567 R^2=0.9758
- ◆ H_2O_2=0M_FLO   K=0.0720 R^2=0.8859
- ◀ H_2O_2=0.001M_FLO   K=0.0466 R^2=0.9681
- ▶ H_2O_2=0.01M_FLO   K=0.0611 R^2=0.9154
- ⬡ H_2O_2=0.1M_FLO   K=0.1014 R^2=0.9467

Table 5-4 Regression Equations of PAHs at Varied H_2O_2 Doses

Experimental Settings	Regression Equations
Ambient_NAP	$\ln\left(\dfrac{c}{c_0}\right) = -0.0702t - 0.4683$
H_2O_2=0.001M_NAP	$\ln\left(\dfrac{c}{c_0}\right) = -0.1164t + 0.0687$
H_2O_2=0.01M_NAP	$\ln\left(\dfrac{c}{c_0}\right) = -0.0851t - 0.0588$
H_2O_2=0.1M_NAP	$\ln\left(\dfrac{c}{c_0}\right) = -0.0567t + 0.1403$
Ambient_FLO	$\ln\left(\dfrac{c}{c_0}\right) = -0.0720t - 0.8106$
H_2O_2=0.001M_FLO	$\ln\left(\dfrac{c}{c_0}\right) = -0.0466t - 0.2526$
H_2O_2=0.01M_FLO	$\ln\left(\dfrac{c}{c_0}\right) = -0.0611t - 0.3675$
H_2O_2=0.1M_FLO	$\ln\left(\dfrac{c}{c_0}\right) = -0.1014t - 0.4707$

For the purpose of this research, experimental data were collected by running the hybrid systems under varied temperature that was adjusted and maintained at 23 (room temperature), 50, 70, and 90 ^{0}C, covering the reported typical temperature range of OPW. An interesting finding was observed (**Figure 5-5** to **Figure 5-8**) that the degradation rates of the target PAHs significantly decreased by increasing temperature from 23 to 50 ^{0}C, however, the reaction rates progressively "recovered" back with the elevation of temperature from 50 to 90 ^{0}C. Take the degradation of NAP in the UV/O$_3$ system as an example, the removal rates of NAP significantly decreased by 54% from 23 to 50 ^{0}C, but gradually increased by 25% and 41% from 50 to 70 ^{0}C, and 70 to 90 ^{0}C. On one hand, this result drove to the speculation that the decreased reaction rate by increasing the temperature from 23 to 50 ^{0}C could be due to the loss of oxidants in the matrix. For example, the solubility of O$_3$ decreases with the increase of temperature, the effect of this variable on the oxidation rate of PAHs is partially masked. On the other hand, the rates recovering phenomenon could simply because of the evaporation of the PAHs at high temperature due to their semi-volatile feature. The regression equations of PAHs degradation at varied temperature settings in the hybrid systems are shown in **Table 5-5** and **Table 5-6**. Based on the experimental results, a conclusion can be drawn that unless post treatment of the ventilated gas stream from the treatment process is conducted, cooling system need to be incorporated in order to maintain good treatment results and in the meantime preventing the health/environmental risks from the waste stream.

181
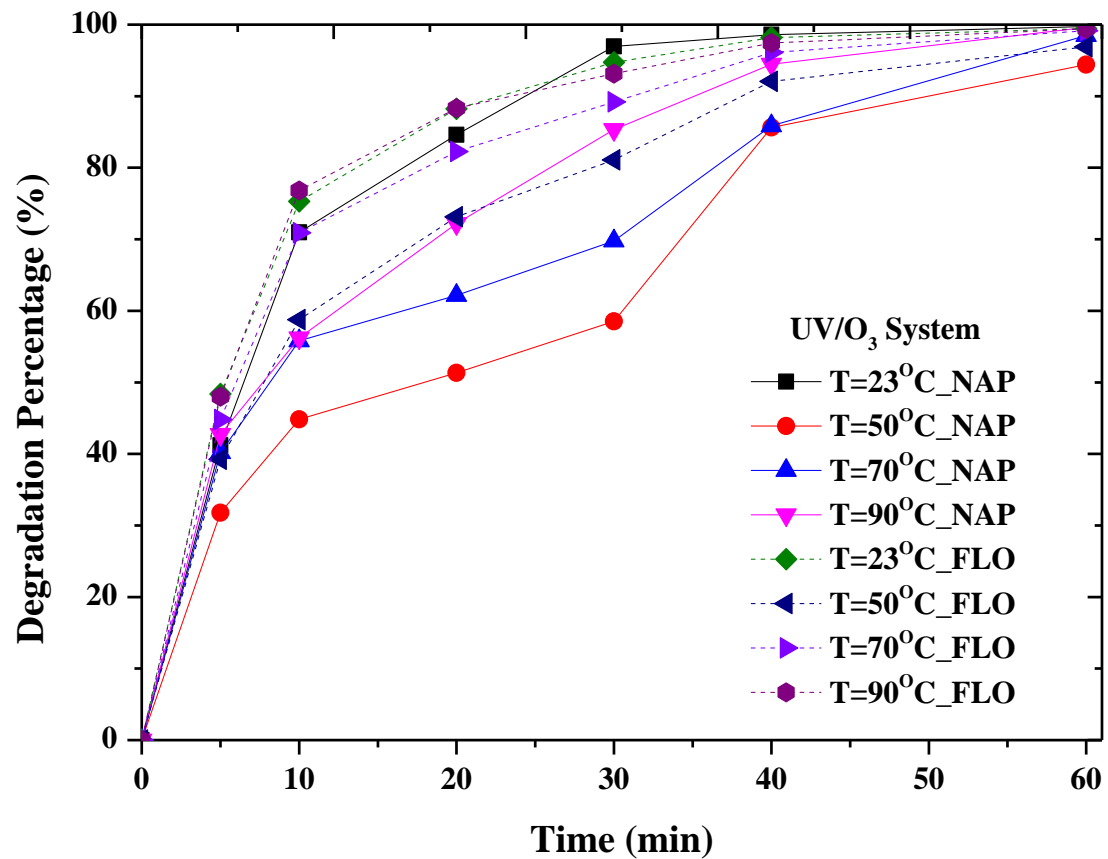
Figure 5-5 PAHs Degradation with Time under Varied Temperature at the UV/O$_3$ System

182
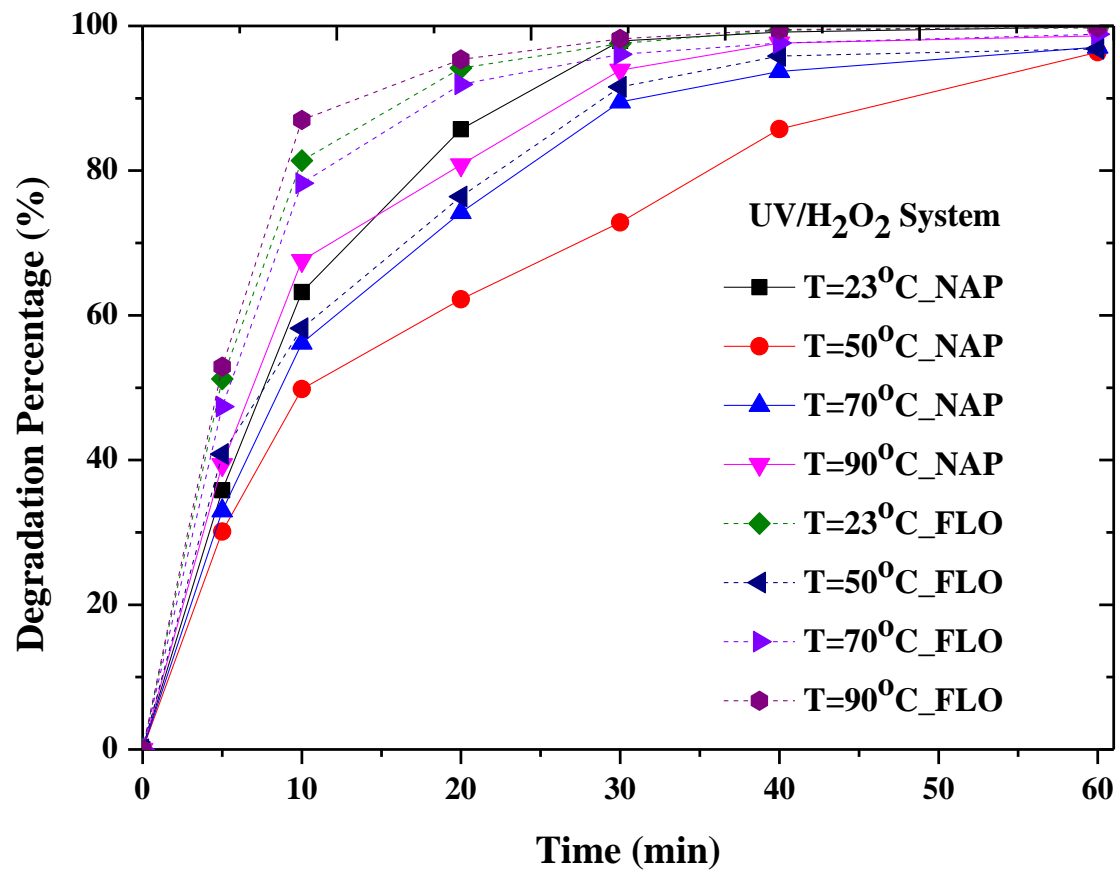
Figure 5-6 PAHs Degradation with Time under Varied Temperature at the UV/H$_2$O$_2$ System
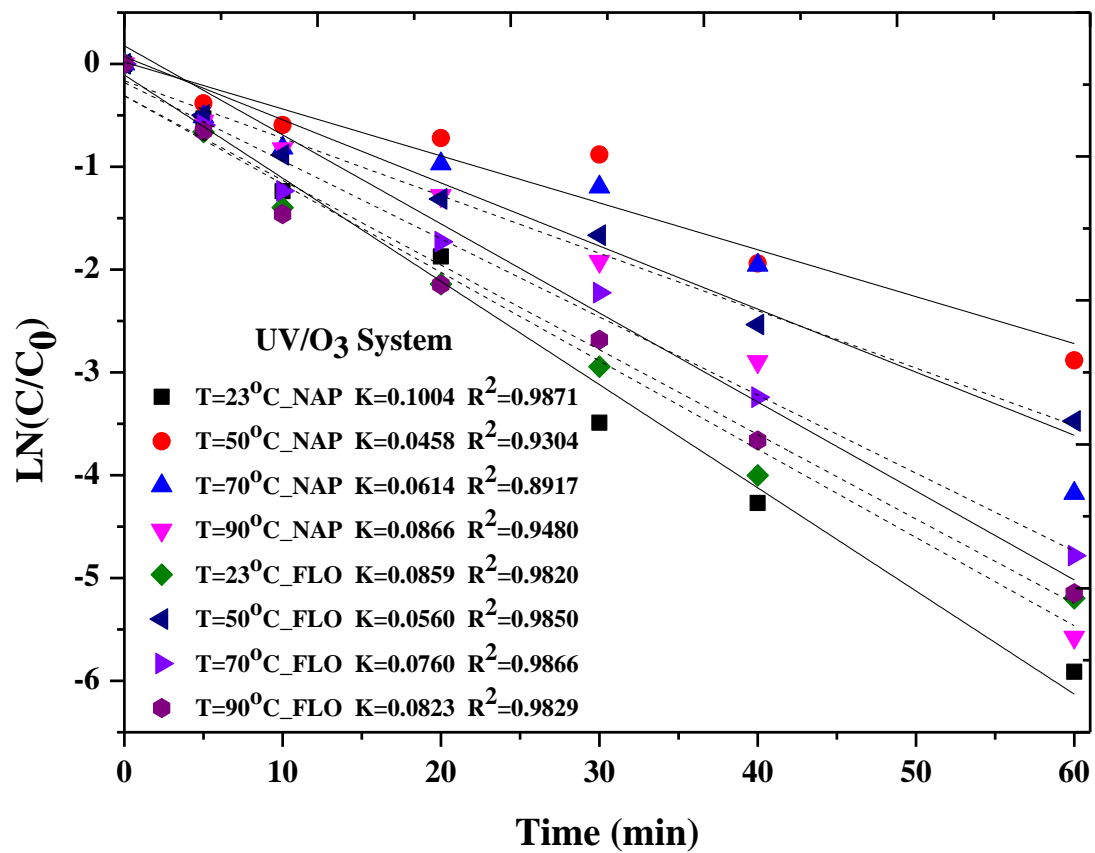
Figure 5-7 Reaction Rate Constants of PAHs under Varied Temperature at the UV/O₃ System

184
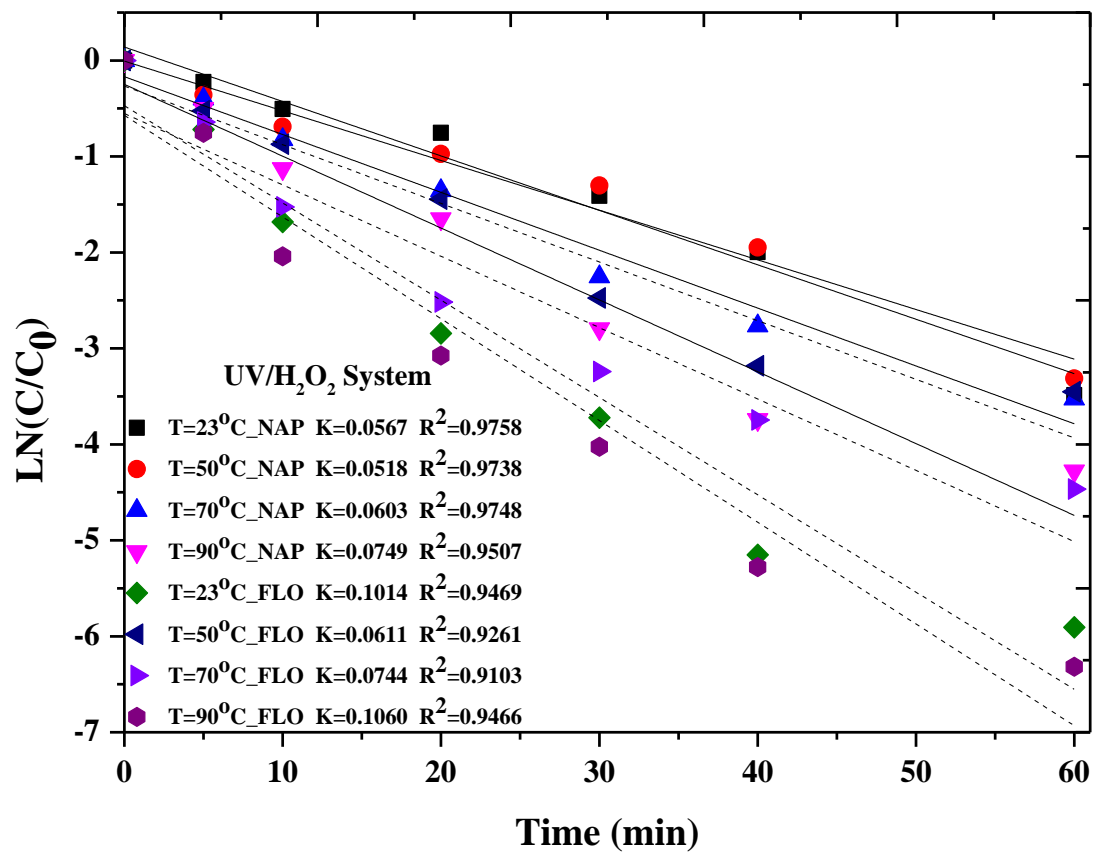
Figure 5-8 Reaction Rate Constants of PAHs under Varied Temperature at the UV/H₂O₂ System

Table 5-5 Regression Equations of PAHs at Varied Temperature in UV/O$_3$ System

Experimental Settings	Regression Equations
UV/O$_3$_T=23°C_NAP	$\ln\left(\dfrac{c}{c_0}\right) = -0.1004t - 0.1071$
UV/O$_3$_T=50°C_NAP	$\ln\left(\dfrac{c}{c_0}\right) = -0.0456t + 0.0182$
UV/O$_3$_T=70°C_NAP	$\ln\left(\dfrac{c}{c_0}\right) = -0.0614t - 0.0704$
UV/O$_3$_T=90°C_NAP	$\ln\left(\dfrac{c}{c_0}\right) = -0.0866t + 0.1759$
UV/O$_3$_T=23°C_FLO	$\ln\left(\dfrac{c}{c_0}\right) = -0.0859t - 0.3094$
UV/O$_3$_T=50°C_FLO	$\ln\left(\dfrac{c}{c_0}\right) = -0.0559t - 0.1644$
UV/O$_3$_T=70°C_FLO	$\ln\left(\dfrac{c}{c_0}\right) = -0.0760t - 0.1823$
UV/O$_3$_T=90°C_FLO	$\ln\left(\dfrac{c}{c_0}\right) = -0.0823t - 0.3098$

Table 5-6 Regression Equations of PAHs at Varied Temperature in UV/H_2O_2 System

Experimental Settings	Regression Equations
UV/H_2O_2_T=23°C_NAP	$\ln\left(\dfrac{c}{c_0}\right) = -0.0567t + 0.1403$
UV/ H_2O_2_T=50°C_NAP	$\ln\left(\dfrac{c}{c_0}\right) = -0.0518t + 0.0063$
UV/ H_2O_2_T=70°C_NAP	$\ln\left(\dfrac{c}{c_0}\right) = -0.0603t - 0.1683$
UV/ H_2O_2_T=90°C_NAP	$\ln\left(\dfrac{c}{c_0}\right) = -0.0749t + 0.2483$
UV/ H_2O_2_T=23°C_FLO	$\ln\left(\dfrac{c}{c_0}\right) = -0.1014t - 0.4707$
UV/ H_2O_2_T=50°C_FLO	$\ln\left(\dfrac{c}{c_0}\right) = -0.0611t - 0.2667$
UV/ H_2O_2_T=70°C_FLO	$\ln\left(\dfrac{c}{c_0}\right) = -0.0744t - 0.5525$
UV/ H_2O_2_T=90°C_FLO	$\ln\left(\dfrac{c}{c_0}\right) = -0.1060t - 0.5705$

5.3.3 Effects of Radical Inhibitors

The decomposing of PAHs in the hybrid processes may be attributed to either direct oxidant attack, or radical reactions. In this round of experiment, a series of UV/O_3 and UV/H_2O_2 reactions were then carried out in the absence and presence of different t-BuOH concentrations. Figure 5-9 toFigure 5-12 present the variations of the removal of NAP and FLO versus time corresponding to varied t-BuOH concentrations, as well as the corresponding oxidation rate.

It can be observed that the oxidation rate of both NAP and FLO is clearly retarded. This result suggests that the studied PAHs are at least partially oxidized by hydroxyl radicals, and the investigation of the PAHs oxidation through radicals seems to be necessary. Moreover, comparing with the results under direct photolysis system (**Figure 4-8** and **4-9**), the retarding effects are more significant in the hybrid systems, which reaffirm the role of hydroxyl radicals.
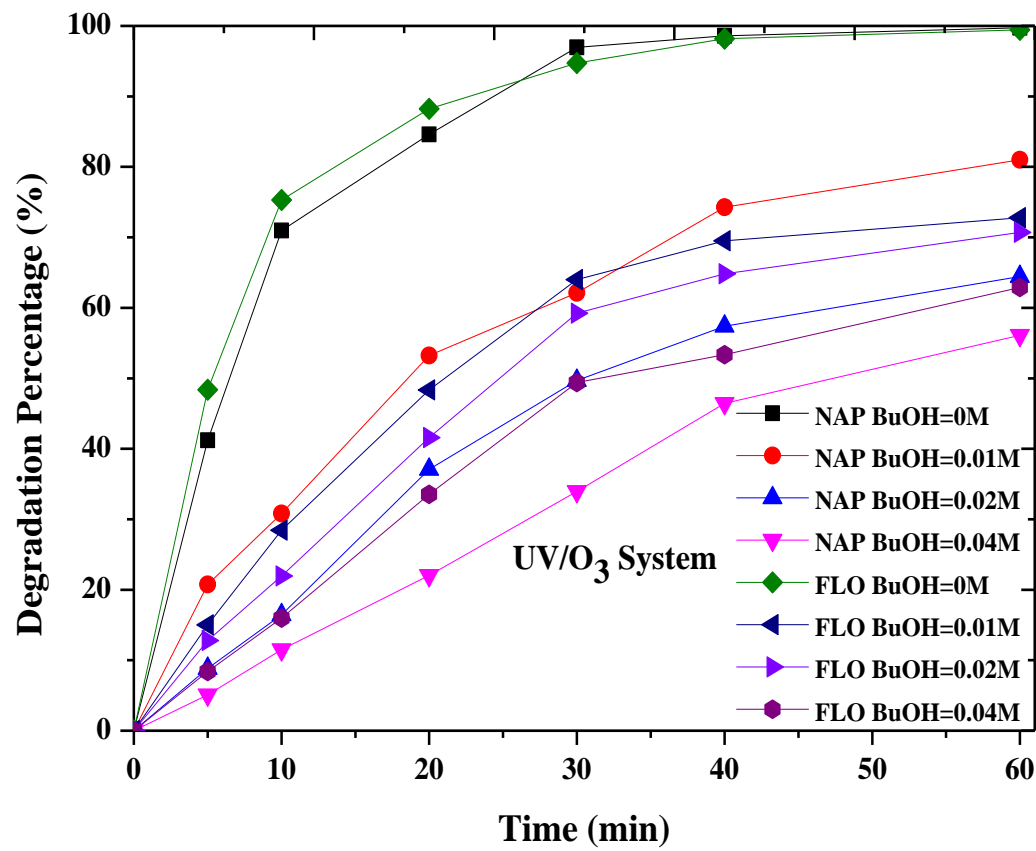
Figure 5-9 PAHs Degradation with Time at Varied BuOH Dose in UV/O$_3$ System
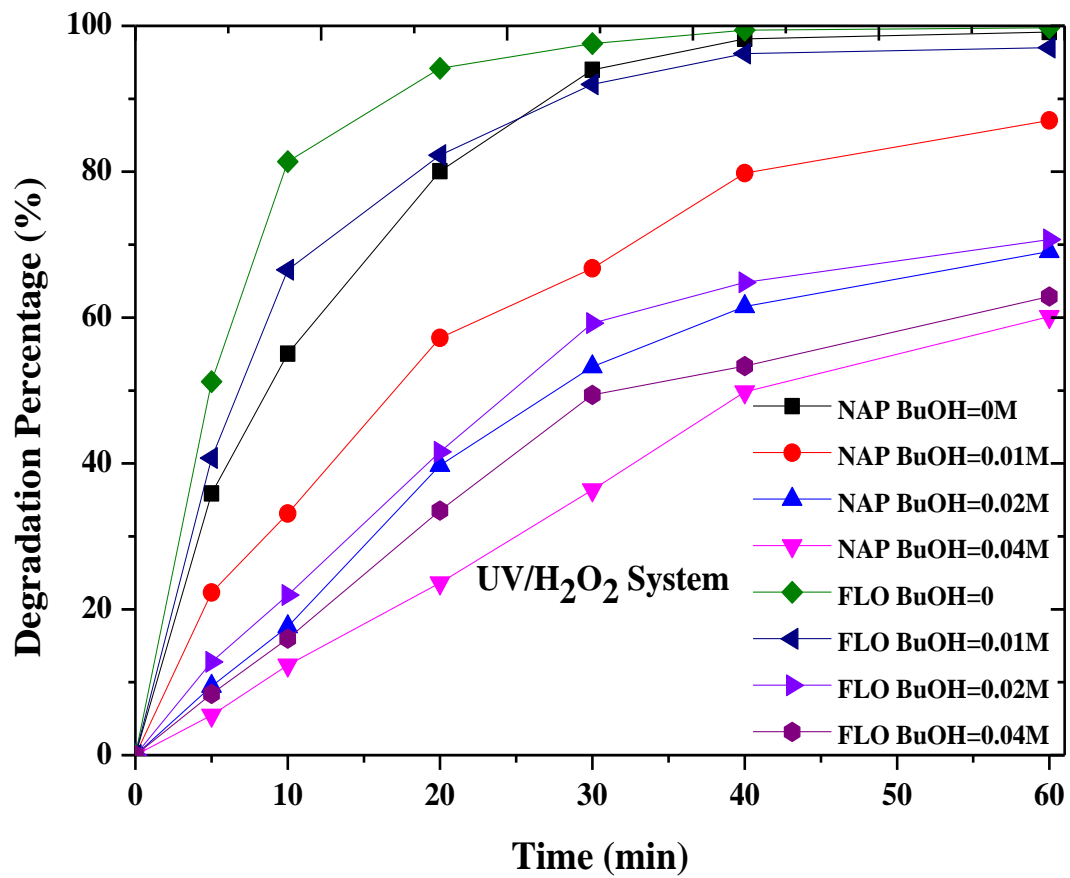
Figure 5-10 PAHs Degradation with Time at Varied BuOH Dose in UV/H$_2$O$_2$ System

190
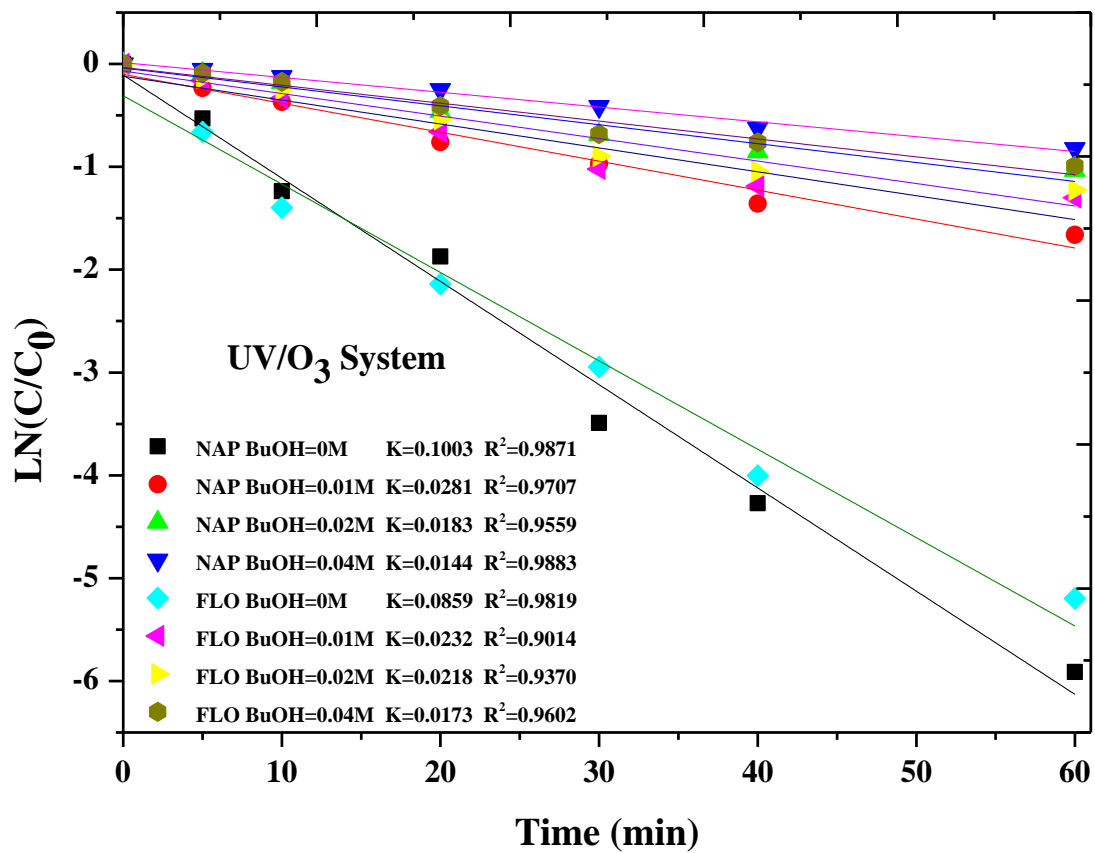
Figure 5-11 Reaction Rate Constants of PAHs at Varied Radical Scavenger Doses in UV/O$_3$ System
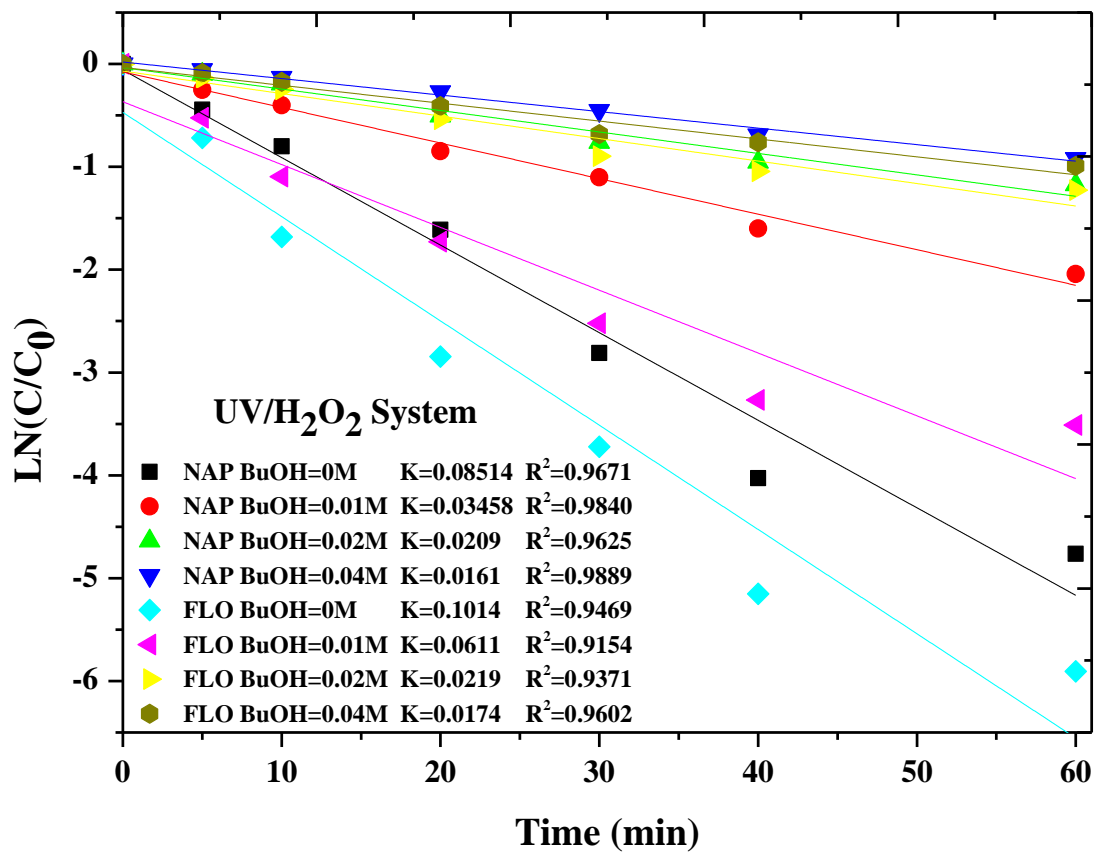
Figure 5-12 Reaction Rate Constants of PAHs at Varied Radical Scavenger Doses in UV/H₂O₂ System

192

Table 5-7 Regression Equations of PAHs at Varied BuOH Doses in UV/O$_3$ System

Experimental Settings	Regression Equations
UV/O$_3$_BuOH=0M_NAP	$\ln\left(\frac{c}{c_0}\right) = -0.1004t - 0.1071$
UV/ O$_3$_ BuOH=0.01M _NAP	$\ln\left(\frac{c}{c_0}\right) = -0.0282t + 0.1009$
UV/ O$_3$_ BuOH=0.02M _NAP	$\ln\left(\frac{c}{c_0}\right) = -0.0184t - 0.0395$
UV/O$_3$_ BuOH=0.04M _NAP	$\ln\left(\frac{c}{c_0}\right) = -0.0144t + 0.0129$
UV/O$_3$_ BuOH=0M _FLO	$\ln\left(\frac{c}{c_0}\right) = -0.0859t - 0.3094$
UV/O$_3$_ BuOH=0.01M _FLO	$\ln\left(\frac{c}{c_0}\right) = -0.0232t - 0.1192$
UV/O$_3$_ BuOH=0.02M _FLO	$\ln\left(\frac{c}{c_0}\right) = -0.0219t - 0.0691$
UV/O$_3$_ BuOH=0.04M _FLO	$\ln\left(\frac{c}{c_0}\right) = -0.0174t - 0.0338$

Table 5-8 Regression Equations of PAHs at Varied BuOH Doses in UV/H₂O₂ System

Experimental Settings	Regression Equations
UV/H₂O₂_BuOH=0M_NAP	$\ln\left(\dfrac{c}{c_0}\right) = -0.0851t + 0.0588$
UV/ H₂O₂_ BuOH=0.01M _NAP	$\ln\left(\dfrac{c}{c_0}\right) = -0.0346t + 0.0774$
UV/ H₂O₂_ BuOH=0.02M _NAP	$\ln\left(\dfrac{c}{c_0}\right) = -0.0209t - 0.0355$
UV/ H₂O₂_ BuOH=0.04M _NAP	$\ln\left(\dfrac{c}{c_0}\right) = -0.0161t + 0.0189$
UV/ H₂O₂_ BuOH=0M _FLO	$\ln\left(\dfrac{c}{c_0}\right) = -0.1014t - 0.4707$
UV/ H₂O₂_ BuOH=0.01M _FLO	$\ln\left(\dfrac{c}{c_0}\right) = -0.0611t - 0.3675$
UV/ H₂O₂_ BuOH=0.02M _FLO	$\ln\left(\dfrac{c}{c_0}\right) = -0.0219t - 0.0691$
UV/ H₂O₂_ BuOH=0.04M _FLO	$\ln\left(\dfrac{c}{c_0}\right) = -0.0174t - 0.0338$

5.3.4 System CCD and Optimization

5.3.4.1 NAP degradation in the UV/TiO$_2$/O$_3$ reaction system

Fit all the experimental data to the CCD model, the ANOVA for the quadratic model is shown in **Table 5-9**. The model F-value of 4.88 implies the model is significant. There is only a 0.04% chance that a "Model F-Value" this large could occur due to noise. The "lack of fit F-value" of 1.82 implies there is a 14.99% chance that a "lack of fit F-value" this large could occur due to noise. Non-significant lack of fit is good, as the model is expected to fit. "Adeq Precision" measures the signal to noise ratio and the ratio of 6.316 (>4) indicates an adequate signal. However, the "Pred R-Squard" of 0.2501 is not as close to the "Adj R-Squared" of 0.5288 as is normally expected. This may indicate a large block effect or a possible problem with the model and/or data. Things to consider are model reduction, response transformation, outliers, etc.

As some insignificant model terms are included (not counting those required to support hierarchy), the model is refined by excluding the terms of AB, AC, C^2. From the ANOVA of the refined model (**Table 5-10**), the model F-value of 9.78 implies the model is significant. The "lack of fit F-value" of 1.47 implies the lack of fit is not significant relative to the pure error. "Adeq Precision" of 8.778 (>4) indicates an adequate signal. The "Pred R-Squared" of 0.4733 is now in reasonable agreement with the "Adj R-Squared" of 0.5809. This model can be used to navigate the design space.

195

Table 5-9 ANOVA of CCD Design of NAP Degradation in the UV/TiO$_2$/O$_3$ System

Source	Sum of Squares	df	Mean Square	F Value	p-value Prob > F
Model	318.66	11	28.97	4.8763	0.0004
A-Ozone flow rate	1.88	1	1.88	0.3160	0.5787
B-pH	0.80	1	0.80	0.1351	0.7160
C-UV Wavelength	263.61	2	131.81	22.1869	< 0.0001
AB	0.05	1	0.05	0.0092	0.9243
AC	0.82	2	0.41	0.0692	0.9333
BC	7.78	2	3.89	0.6544	0.5278
A^2	24.14	1	24.14	4.0631	0.0539
B^2	25.27	1	25.27	4.2542	0.0489
Residual	160.40	27	5.94		
Lack of Fit	111.49	15	7.43	1.8234	0.1499
Pure Error	48.91	12	4.08		
Cor Total	479.06	38			
Std. Dev.	2.44		R-Squared	0.6652	
Mean	91.90		Adj R-Squared	0.5288	
C.V. %	2.652131551		Pred R-Squared	0.2501	

Source	Sum of Squares	df	Mean Square	F Value	p-value Prob > F
PRESS	359.2260606		Adeq Precision	6.3157	

Table 5-10 ANOVA of Refined Model of NAP Degradation in the UV/TiO$_2$/O$_3$ Reaction System

Source	Sum of Squares	df	Mean Square	F Value	p-value Prob > F	
Model	310.01	6	51.67	9.7801	< 0.0001	Significant
A-Ozone flow rate	1.88	1	1.88	0.3553	0.5553	
B-pH	0.80	1	0.808	0.1520	0.6993	
C-UV Wavelength	263.61	2	131.81	24.9497	< 0.0001	
A^2	24.14	1	24.14	4.5691	0.0403	
B^2	25.27	1	25.27	4.7840	0.0361	
Residual	169.05	32	5.28			
Lack of Fit	120.14	20	6.01	1.4737	0.2476	Not significant
Pure Error	48.91	12	4.08			
Cor Total	479.06	38				
Std. Dev.	2.30		R-Squared	0.6471		
Mean	91.90		Adj R-Squared	0.5809		
C.V. %	2.50		Pred R-Squared	0.4733		

198

| Source	Sum of Squares	df	Mean Square	F Value	p-value Prob > F
PRESS	252.32		Adeq Precision	8.7780	

The diagnostic plots for residuals analysis (Figure 5-13) confirms the assumptions of the developed model. The normality plot of the residuals (a) are approximately a straight line, therefore, normal distribution assumption is satisfied; the residuals are distributed randomly within two lines on both the "residual Vs predicted" and "residual Vs run plots" (b and c), the independent assumption is satisfied; the relationship between the predicted and the actual (d) is approximately linear, as all the points are close to the straight line; as can be seen from the "Box-Cox plot" (e), it is unnecessary to apply "transformation"; the "residual Vs factor" plot (f), the variance, indicate equal value for different level of the factor, since the residuals distribute randomly within two lines, showing no visible pattern. The regression equation for the NAP degradation in the UV/TiO$_2$/O$_3$ reaction system in terms of actual factors are then obtained:

$$\text{NAP Degradation}_{\text{UVA}}$$
$$= 15.10 + 2.63 \times \text{Ozone flow rate} + 8.44$$
$$\times \text{pH} - 0.04 \times \text{Ozone flow rate}^2 - 0.49$$
$$\times \text{pH}^2$$

$$(5\text{-}34)$$

$$\text{NAP Degradation}_{\text{UVB}}$$
$$= 14.20 + 2.63 \times \text{Ozone flow rate} + 8.44$$
$$\times \text{pH} - 0.04 \times \text{Ozone flow rate}^2 - 0.49$$
$$\times \text{pH}^2$$

$$(5\text{-}35)$$

NAP Degradation$_{UVC}$

$$= 20.11 + 2.63 \times \text{Ozone flow rate} + 8.44$$
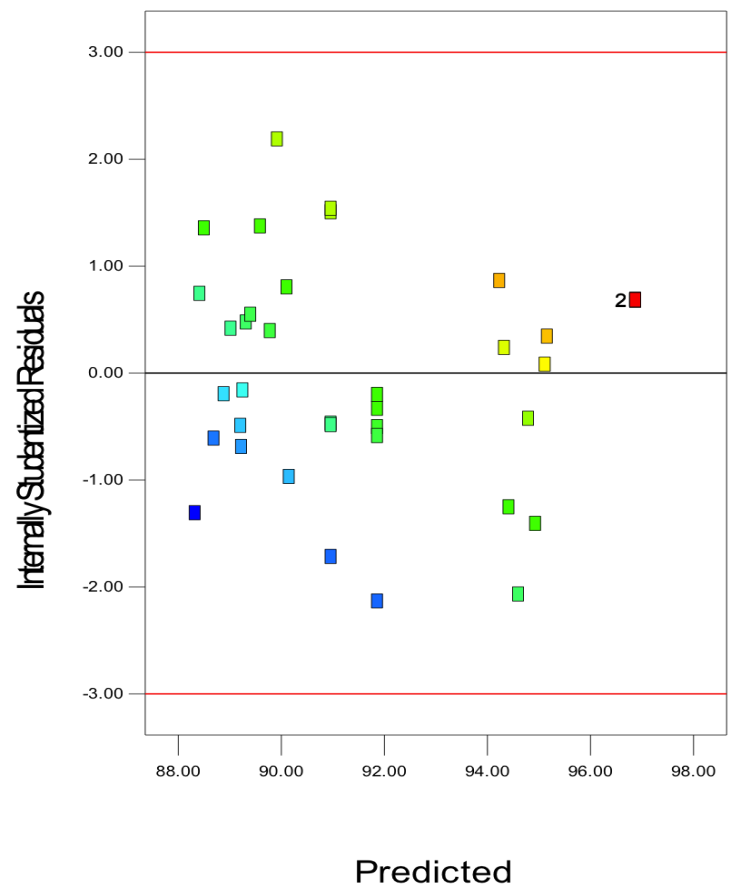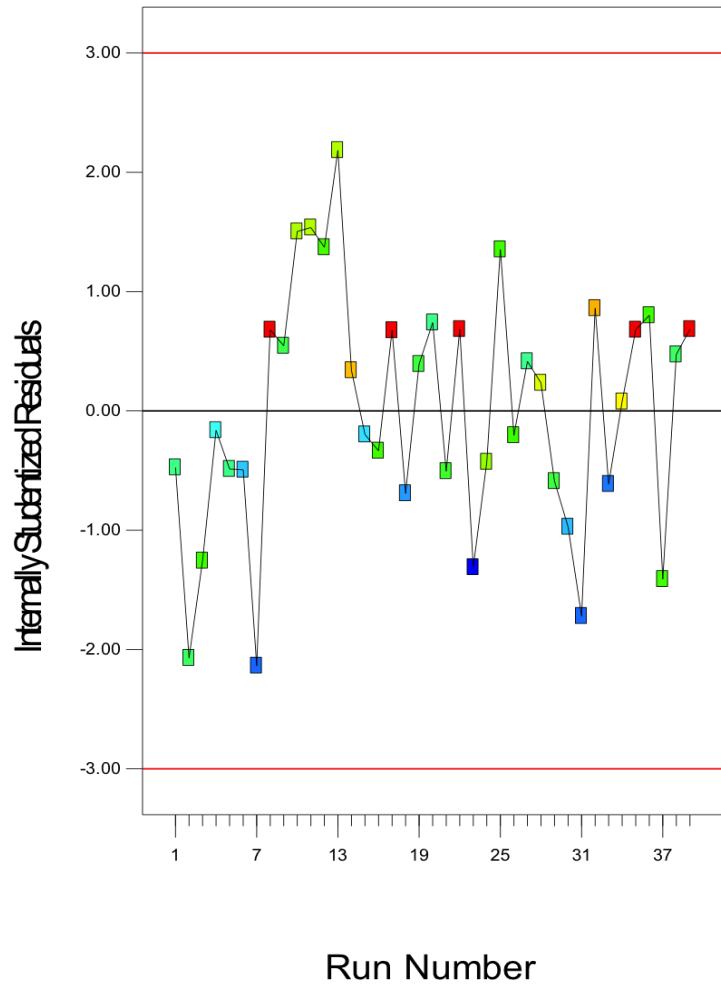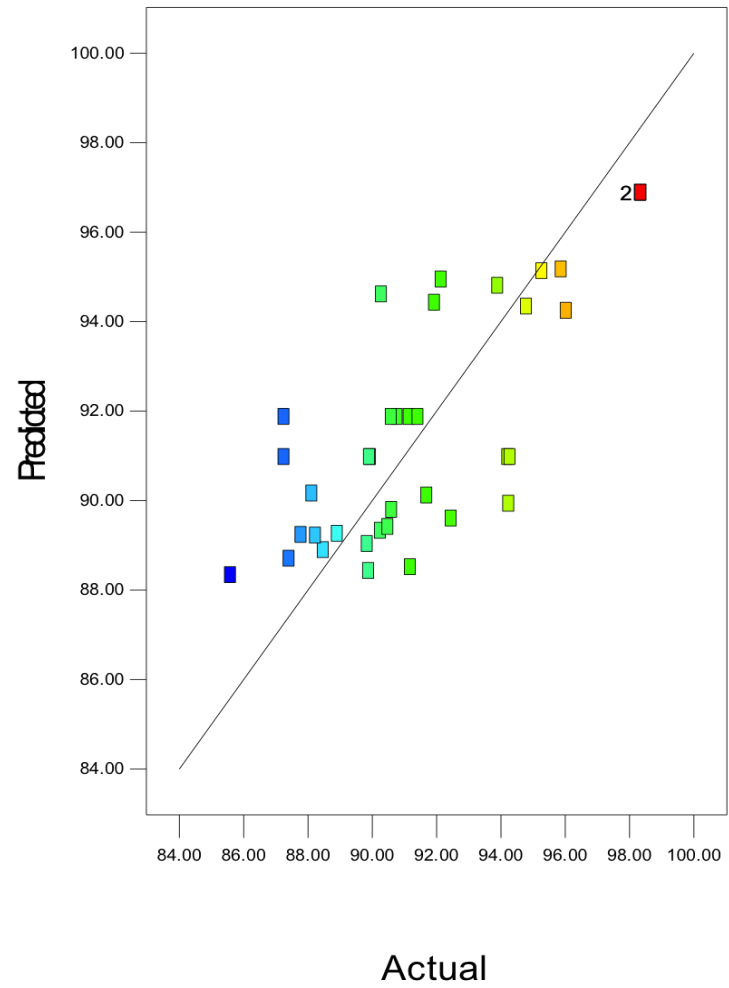$$\times \text{pH} - 0.04 \times \text{Ozone flow rate}^2 - 0.49$$
$$\times \text{pH}^2$$

(5-36)

(a)

(b)

(c)

(d)

203
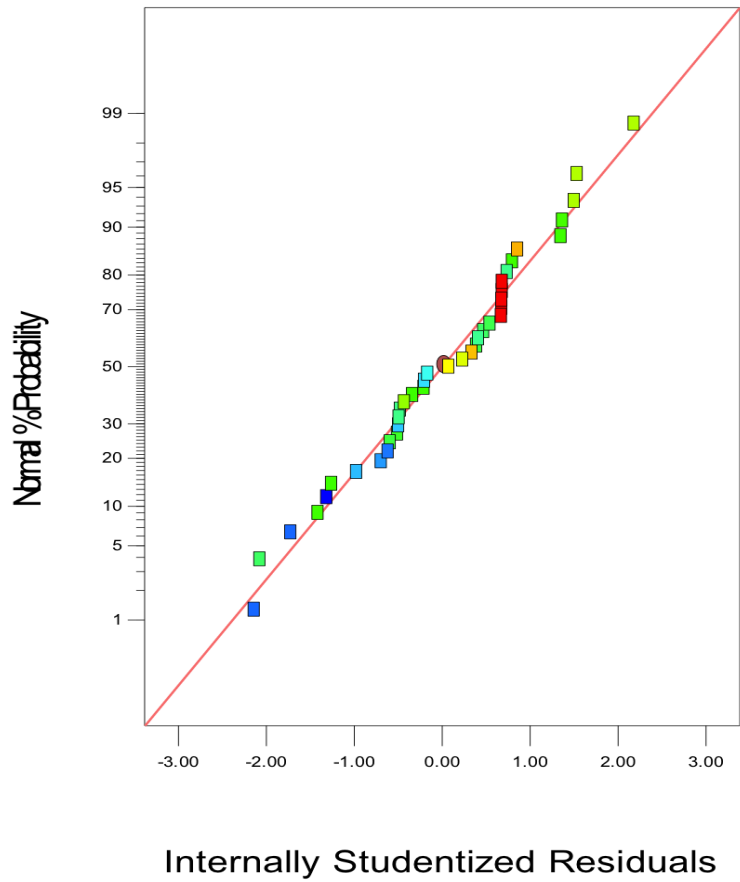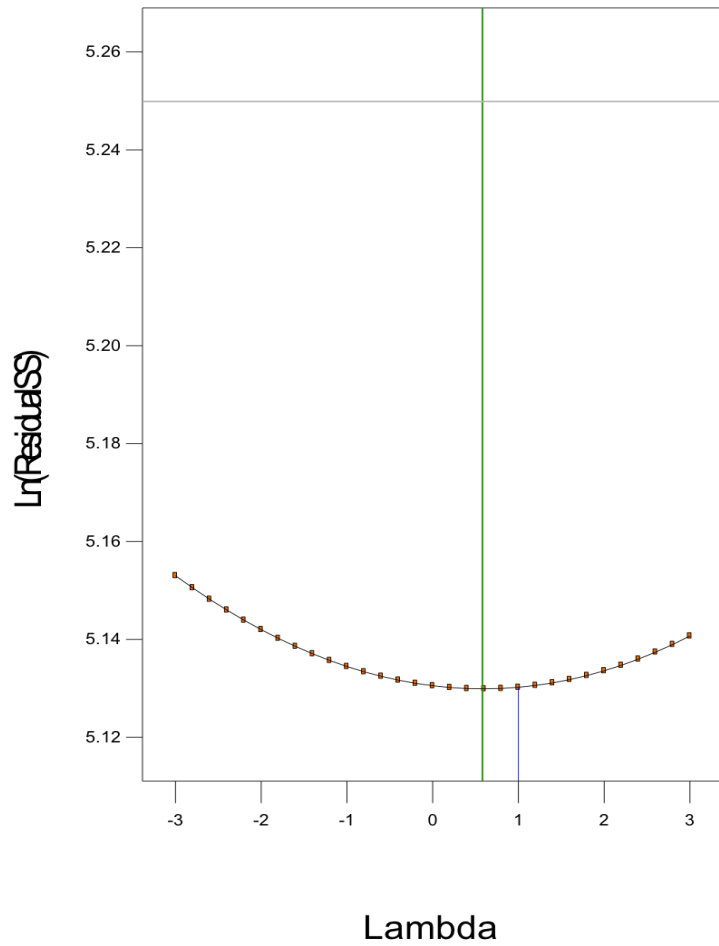
(e)
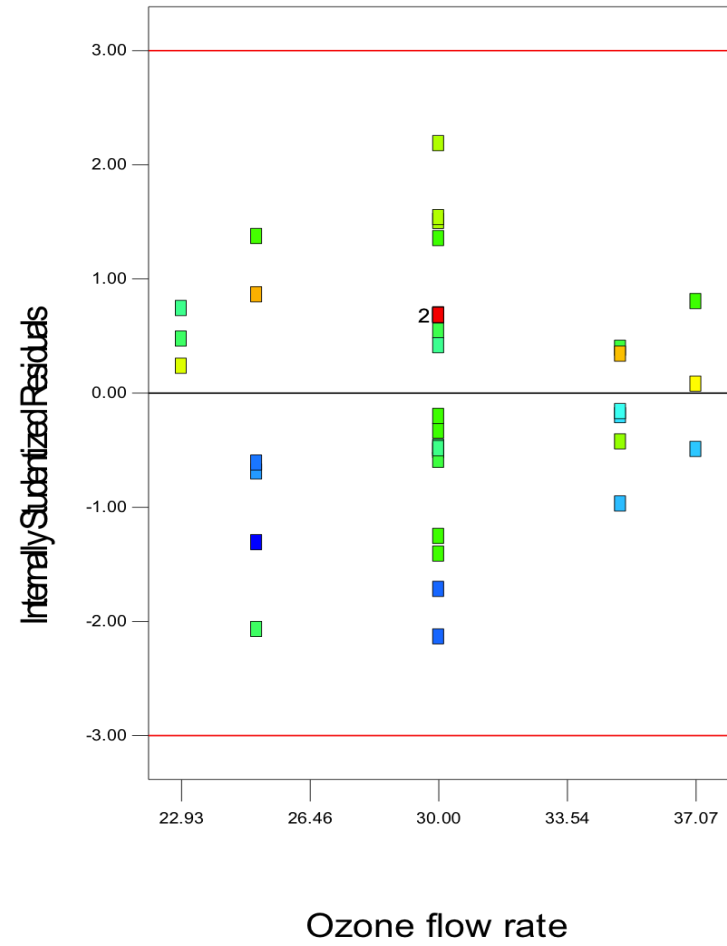
(f)

Figure 5-13 Diagnostics plots for Model Assumptions of NAP Degradation in the UV/TiO$_2$/O$_3$ Reaction System

Figure 5-14 showed the 3-D surface graphs of the interaction of O_3 dose and pH value under varied UV irradiation. It indicated that the CCD model could accurately capture the curvature of the NAP degradation response, and predicted the possible maximum. By using Design Expert v8, the optimum combinations of the three factors to achieve the highest NAP degradation were constructed. The solutions for 3 combinations of categoric factor levels are shown in **Table 5-11**.

5.3.4.2. FLO degradation in the UV/TiO₂/O₃ reaction system

Fit all the experimental data to a CCD model, the ANOVA for the quadratic model is shown in **Table 5-12**. The model F-value of 6.75 implies the model is significant. There is only a 0.01% chance that a "Model F-Value" this large could occur due to noise. The "lack of fit F-value" of 10.68 implies the lack of fit is significant. There is only a 0.01% chance that a "lack of fit F-value" this large could occur due to noise. Significant lack of fit is bad, as we want the model to fit. "Adeq Precision" measures the signal to noise ratio and the ratio of 7.647 (>4) indicates an adequate signal. However, the "Pred R-Squard" of 0.2912 is not as close to the "Adj R-Squared" of 0.6246 as is normally expected. This may indicate a large block effect or a possible problem with the model and/or data. Things to consider are model reduction, response transformation, outliers, etc.

(UVA)

206
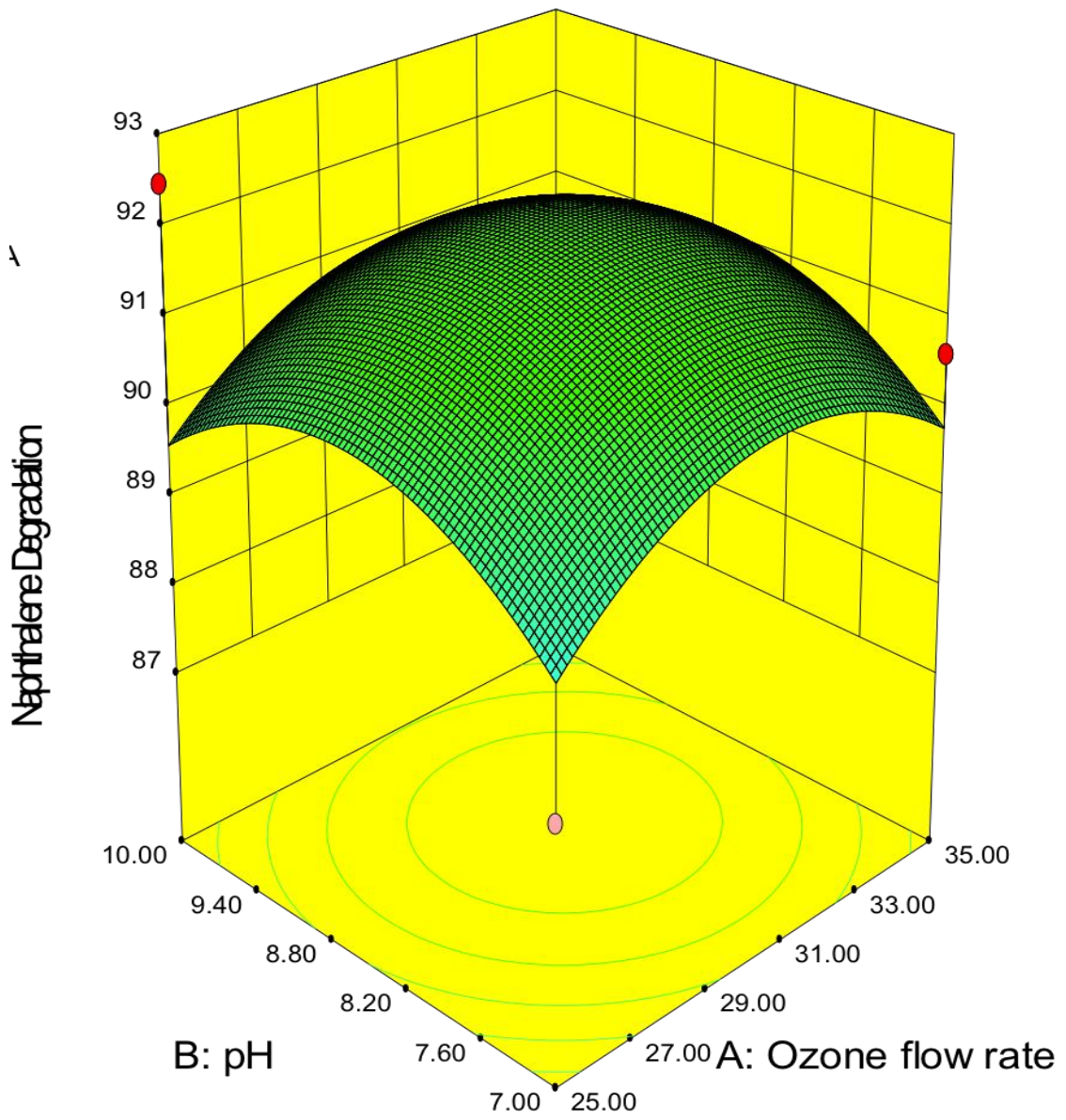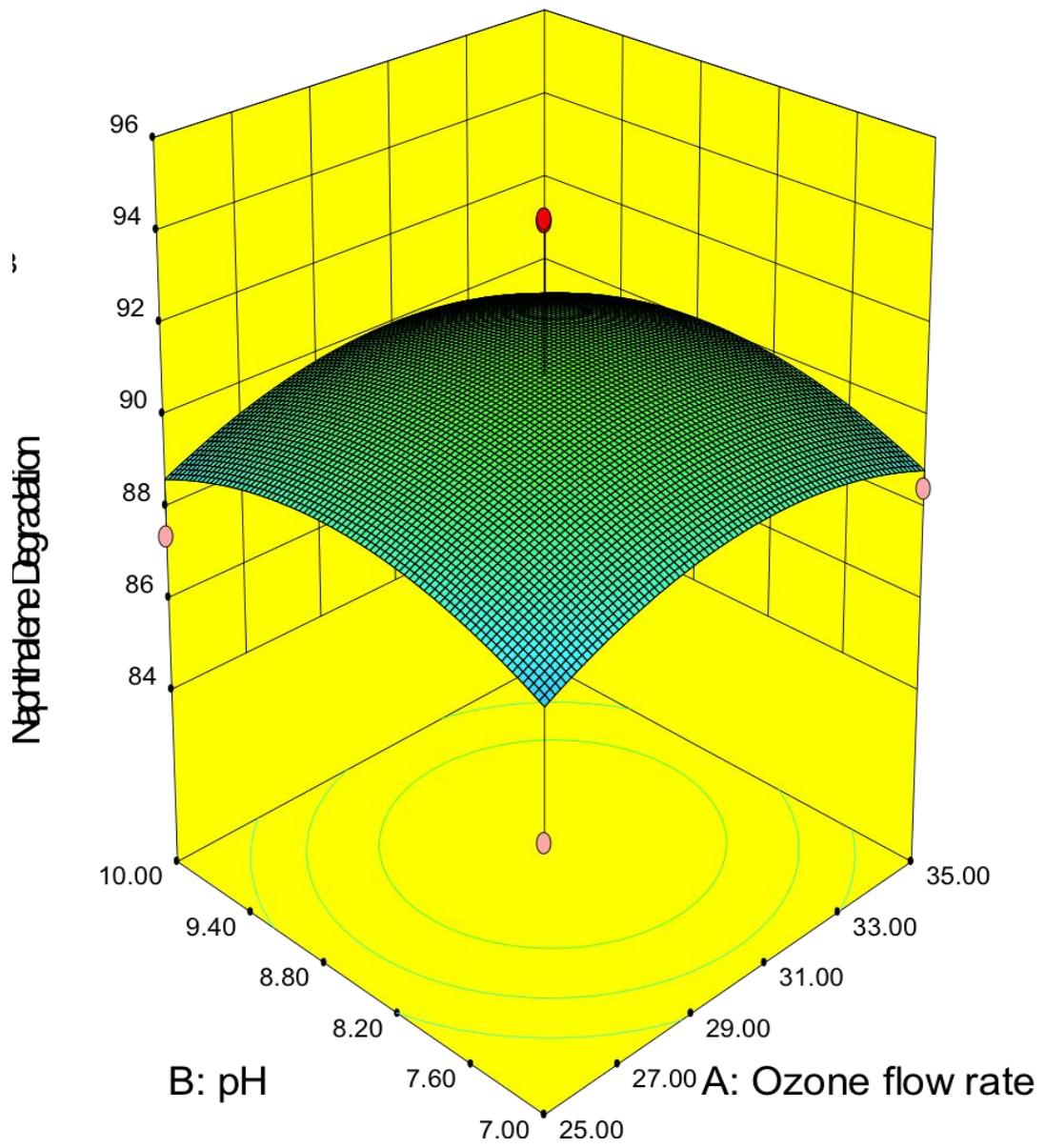
(UVB)
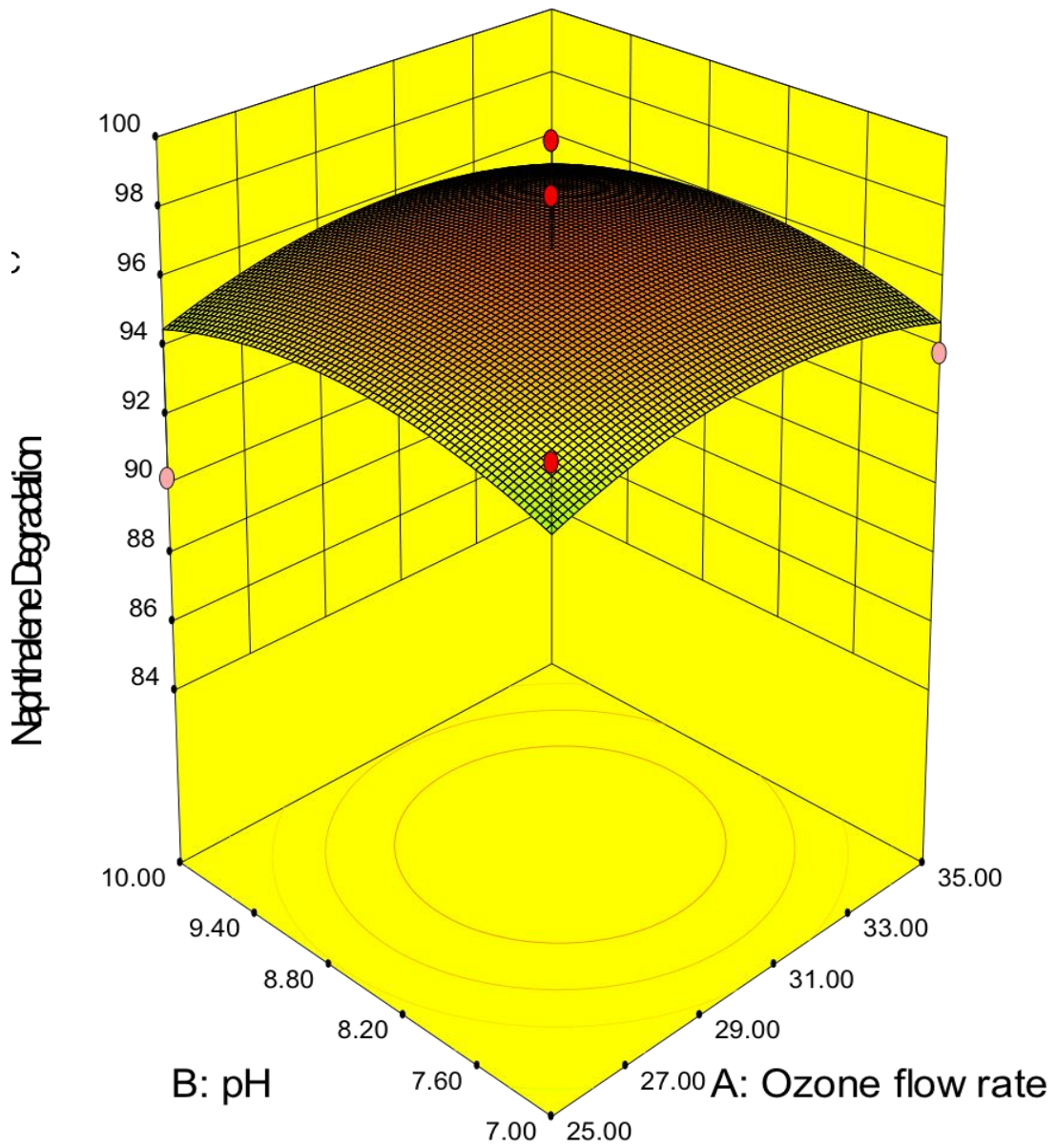
(UVC)

Figure 5-14 CCD 3D Surface Model Graphs for NAP Degradation Model in the UV/TiO₂/O₃
Reaction System

Table 5-11 Optimum Combination of Process Factors to Achieve the Highest Naphthalene Degradation in the UV/TiO$_2$/O$_3$ Reaction System

Number	Ozone flow rate (ml/min)	pH	UV Wavelength	NAP Degradation (%)	Desirability
1	31.20	8.53	UVC	96.89	0.84
2	32.27	9.55	UVB	90.46	0.38
3	32.14	9.42	UVA	91.49	0.38

Table 5-12 ANOVA of CCD Design of FLO Degradation in the UV/TiO$_2$/O$_3$ Reaction System

Source	Sum of Squares	df	Mean Square	F Value	p-value Prob > F
Model	149.87	11	13.62	6.7481	< 0.0001
A-Ozone flow rate	0.35	1	0.35	0.1726	0.6811
B-pH	1.89	1	1.89	0.9349	0.3422
C-UV Wavelength	134.11	2	67.05	33.2095	< 0.0001
AB	1.46	1	1.46	0.7211	0.4032
AC	0.07	2	0.03	0.0171	0.9831
BC	2.71	2	1.35	0.6705	0.5198
A^2	1.68	1	1.68	0.8315	0.3699
B^2	8.44	1	8.44	4.1825	0.0507
Residual	54.52	27	2.02		
Lack of Fit	50.72	15	3.38	10.6754	< 0.0001
Pure Error	3.80	12	0.32		
Cor Total	204.39	38			
Std. Dev.	1.42		R-Squared	0.7342	
Mean	95.79		Adj R-Squared	0.6246	
C.V. %	1.48		Pred R-Squared	0.2912	
PRESS	144.87		Adeq Precision	7.6470	

210

As some insignificant model terms are included (not counting those required to support hierarchy), the model is refined by excluding the terms of AB, AC, BC, and C^2. From the ANOVA of the refined model (**Table 5-13**), the model F-value of 13.22 implies the model is significant. The "lack of fit F-value" of 8.67 implies the lack of fit is not significant relative to the pure error. "Adeq Precision" of 9.961 (>4) indicates an adequate signal. The "Pred R-Squared" of 0.5525 is in reasonable agreement with the "Adj R-Squared" of 0.6587. However, the "lack of fit F-value" of 8.67 still implies the lack of fit is significant. There is only a 0.02% chance that a "lack of fit F-value" this large could occur due to noise.

The diagnostic plots for residuals analysis (**Figure 5-15**) confirm the assumptions of the developed model. The normality plot of the residuals (a) are approximately a straight line; the residuals are distributed within two lines on both the "residual Vs predicted" and "residual Vs run" plots (b & c), however, show some patterns; the relationship between the predicted and the actual (d) is approximately linear, but the points are not quite close to the straight line; as can be seen from the "Box-Cox plot" (e), it is unnecessary to apply "transformation"; the "residual Vs factor" plot (f), the variance, indicate equal value for different level of the factor, since the residuals distribute randomly within two lines, showing no visible pattern.

Table 5-13 ANOVA of Refined Model of FLO Degradation in the UV/TiO$_2$/O$_3$ Reaction System

Source	Sum of Squares	df	Mean Square	F Value	p-value Prob > F	
Model	145.64	6	24.27	13.2218	< 0.0001	Significant
A-Ozone flow rate	0.35	1	0.35	0.1898	0.6660	
B-pH	1.89	1	1.89	1.0282	0.3182	
C-UV Wavelength	134.11	2	67.05	36.5237	< 0.0001	
A^2	1.68	1	1.68	0.9144	0.3461	
B^2	8.44	1	8.44	4.6000	0.0397	
Residual	58.75	32	1.84			
Lack of Fit	54.95	20	2.75	8.6748	0.0002	Significant
Pure Error	3.80	12	0.32			
Cor Total	204.39	38				
Std. Dev.	1.35		R-Squared	0.7126		
Mean	95.79		Adj R-Squared	0.6587		
C.V. %	1.41		Pred R-Squared	0.5525		
PRESS	91.46		Adeq Precision	9.9612		

(a)

(b)

213

(c)

(d)

214
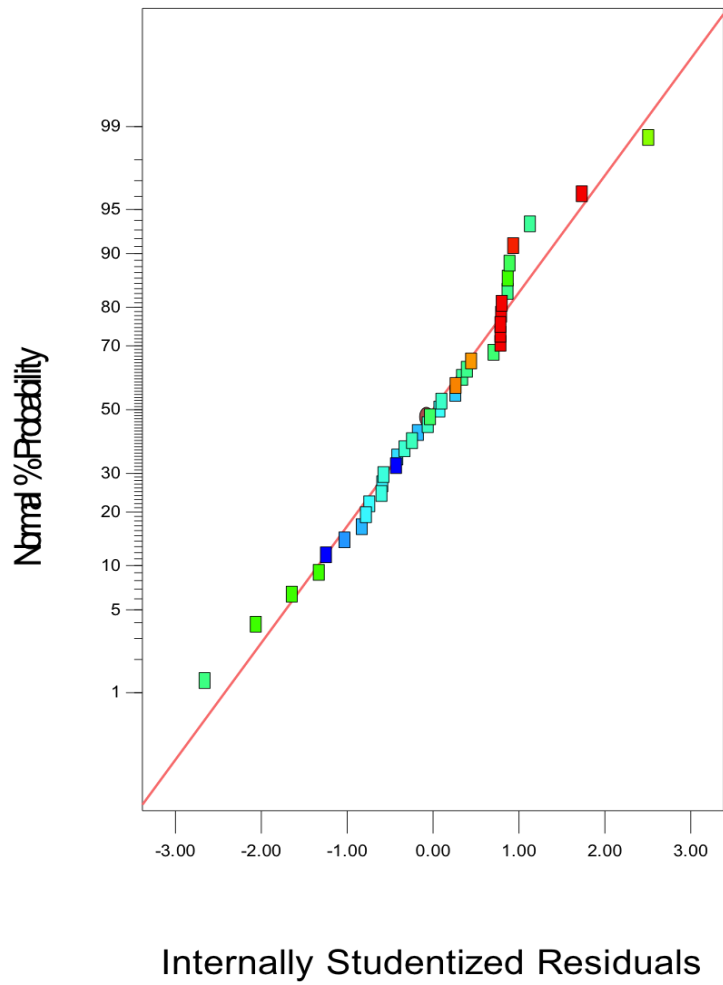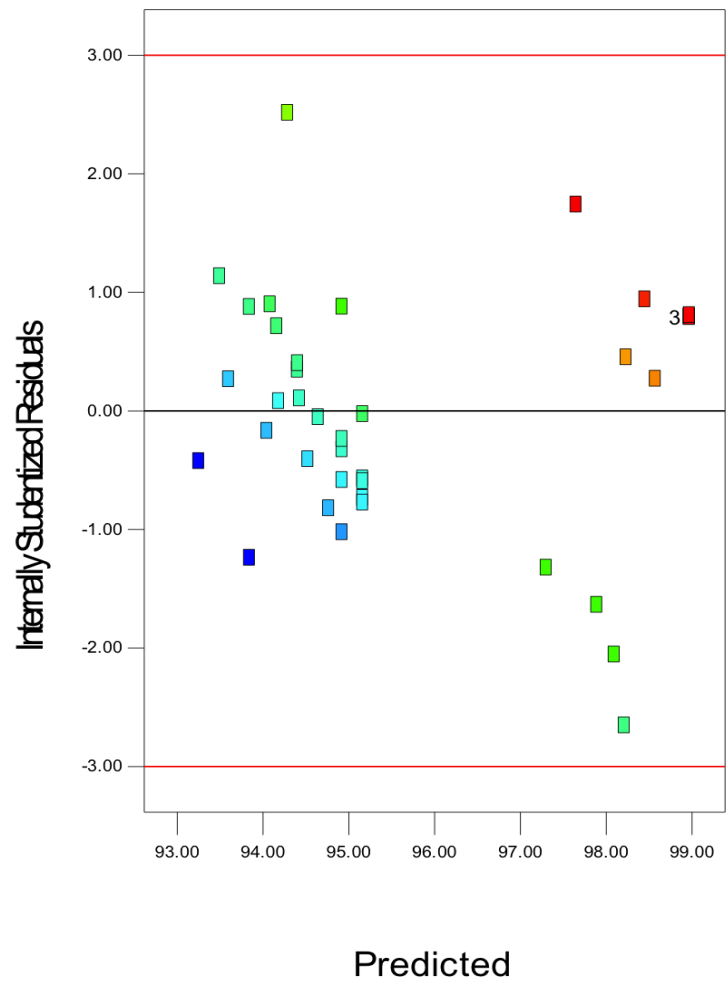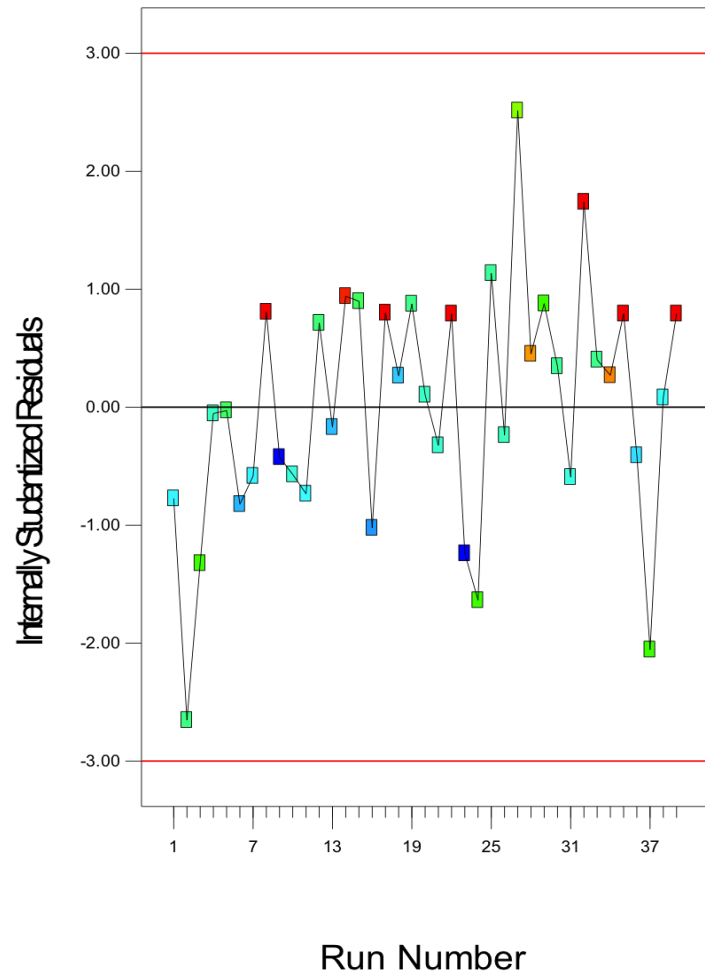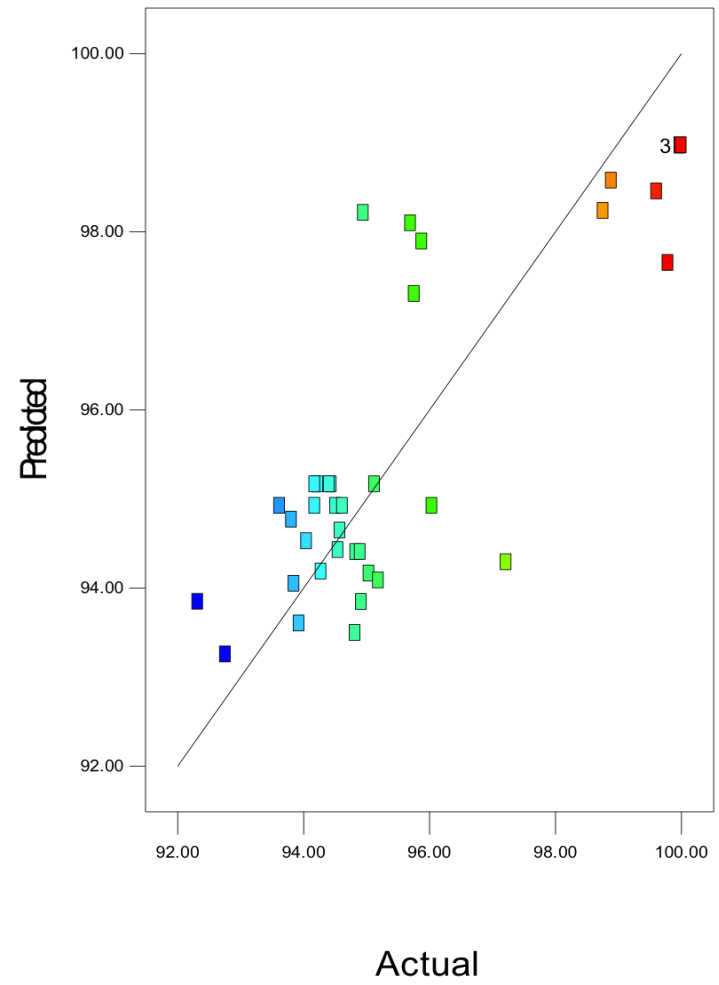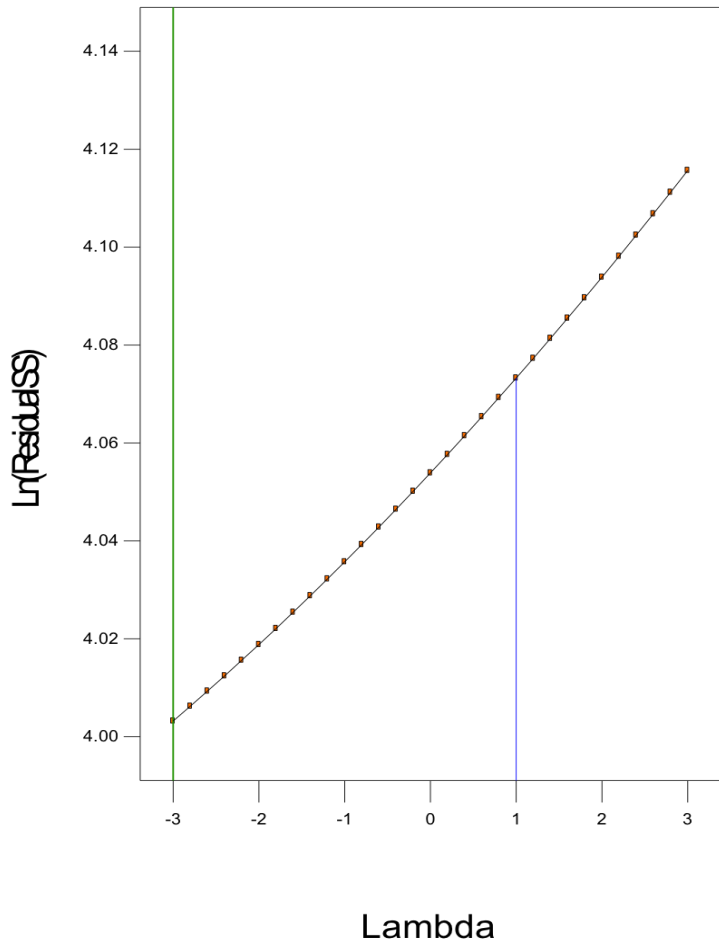
Lambda

(e)
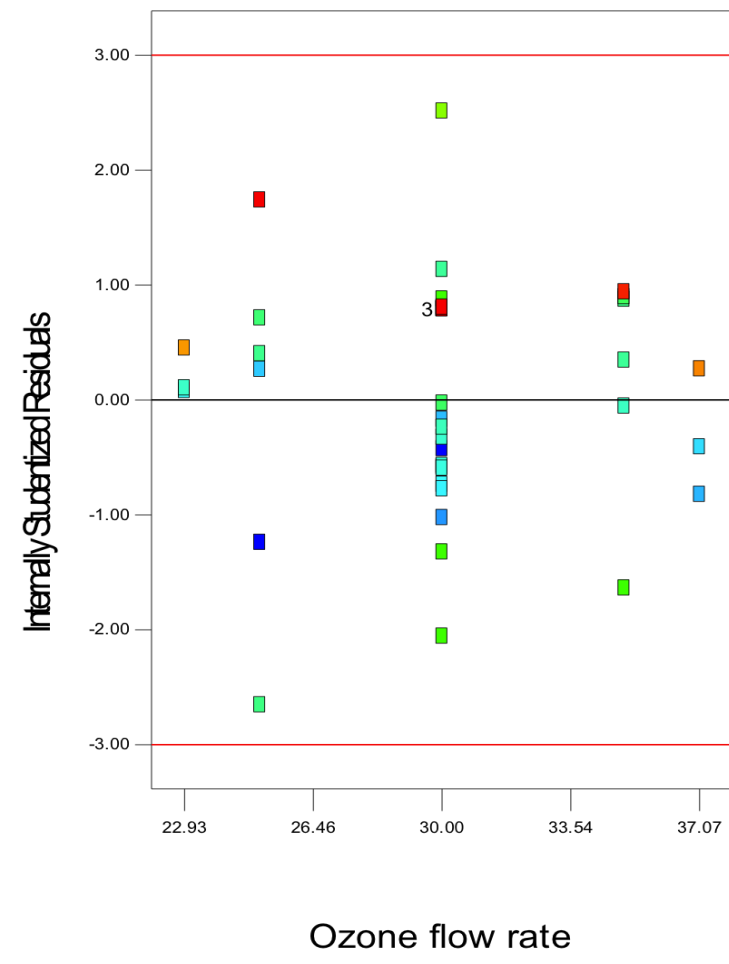
Ozone flow rate

(f)

Figure 5-15 Diagnostics plots for Model Assumptions of FLO Degradation in the UV/TiO$_2$/O$_3$ Reaction System

215

The regression equations for the FLO degradation under UV/TiO$_2$/O$_3$ scenario using the actual factors are given by:

FLO Degradation$_{UVA}$

$$= 61.21 + 0.70 \times \text{Ozone flow rate} + 4.99$$
$$\times \text{pH} - 0.01 \times \text{Ozone flow rate}^2 - 0.28$$
$$\times \text{pH}^2$$

(5-37)

FLO Degradation$_{UVB}$

$$= 62.21 + 0.70 \times \text{Ozone flow rate} + 4.99$$
$$\times \text{pH} - 0.01 \times \text{Ozone flow rate}^2 - 0.28$$
$$\times \text{pH}^2$$

(5-38)

FLO Degradation$_{UVC}$

$$= 66.02 + 0.70 \times \text{Ozone flow rate} + 4.99$$
$$\times \text{pH} - 0.01 \times \text{Ozone flow rate}^2 - 0.28$$
$$\times \text{pH}^2$$

(5-39)

Figure 5-16 (a) to **(c)** show the 3-D surface graphs of the interaction of O$_3$ does and pH value under varied UV irradiation. It indicated that the CCD model could accurately capture the curvature of the FLO degradation response, and predicts the possible maximum. By using Design Expert v8, the optimum combinations of the three factors to achieve the highest FLO degradation were obtained. The solutions for 3 combinations of categoric factor levels are shown in **Table 5-14**. It was found that UVC still performed

better than the other two UV levels in the hybrid system. Comparing with the results of NAP, under the modeled optimum conditions, FLO would show higher degree of degradation at each UV level in the UV/TiO$_2$/O$_3$ reaction system.

(UVA)

218

(UVB)

219

(UVC)
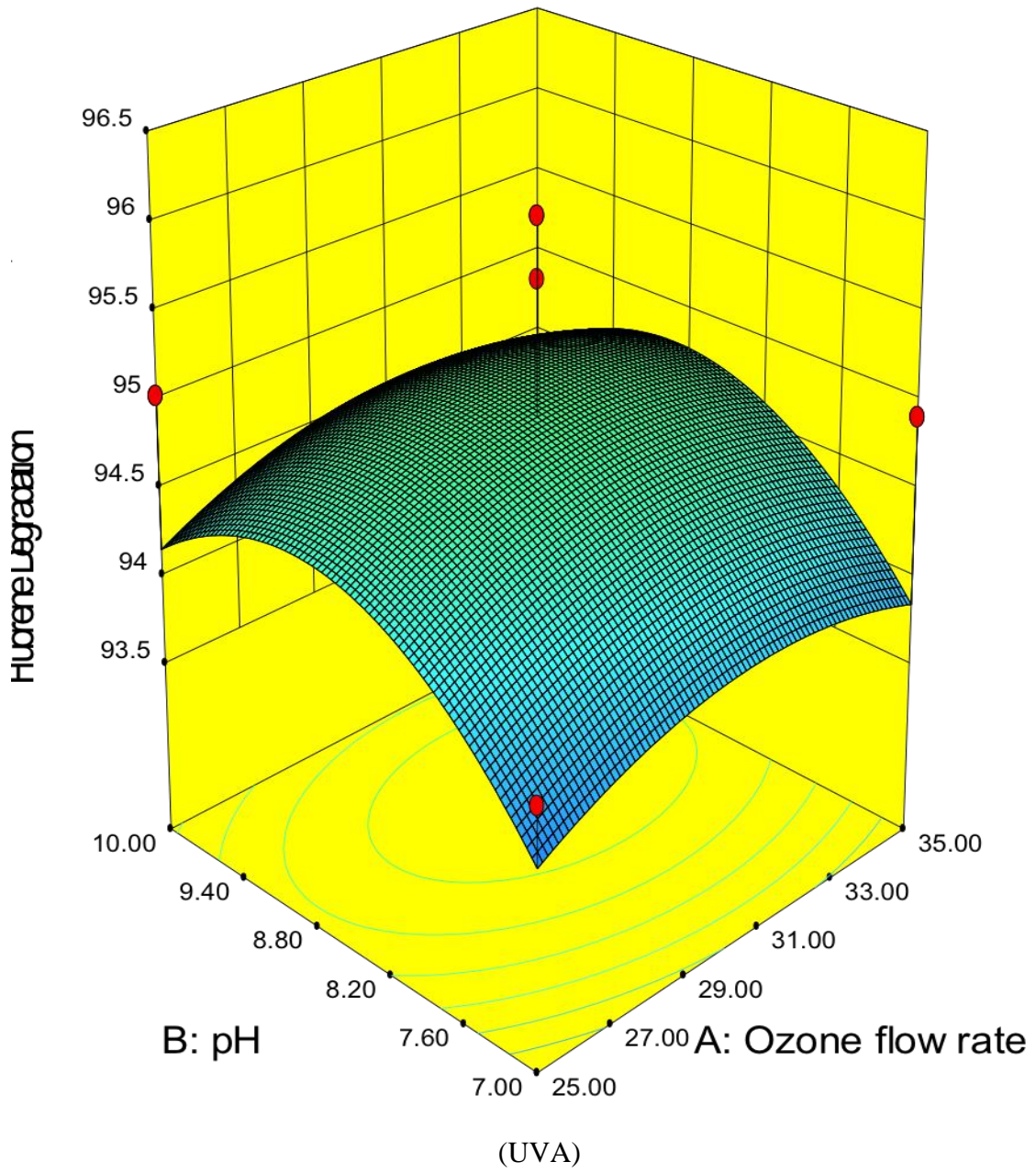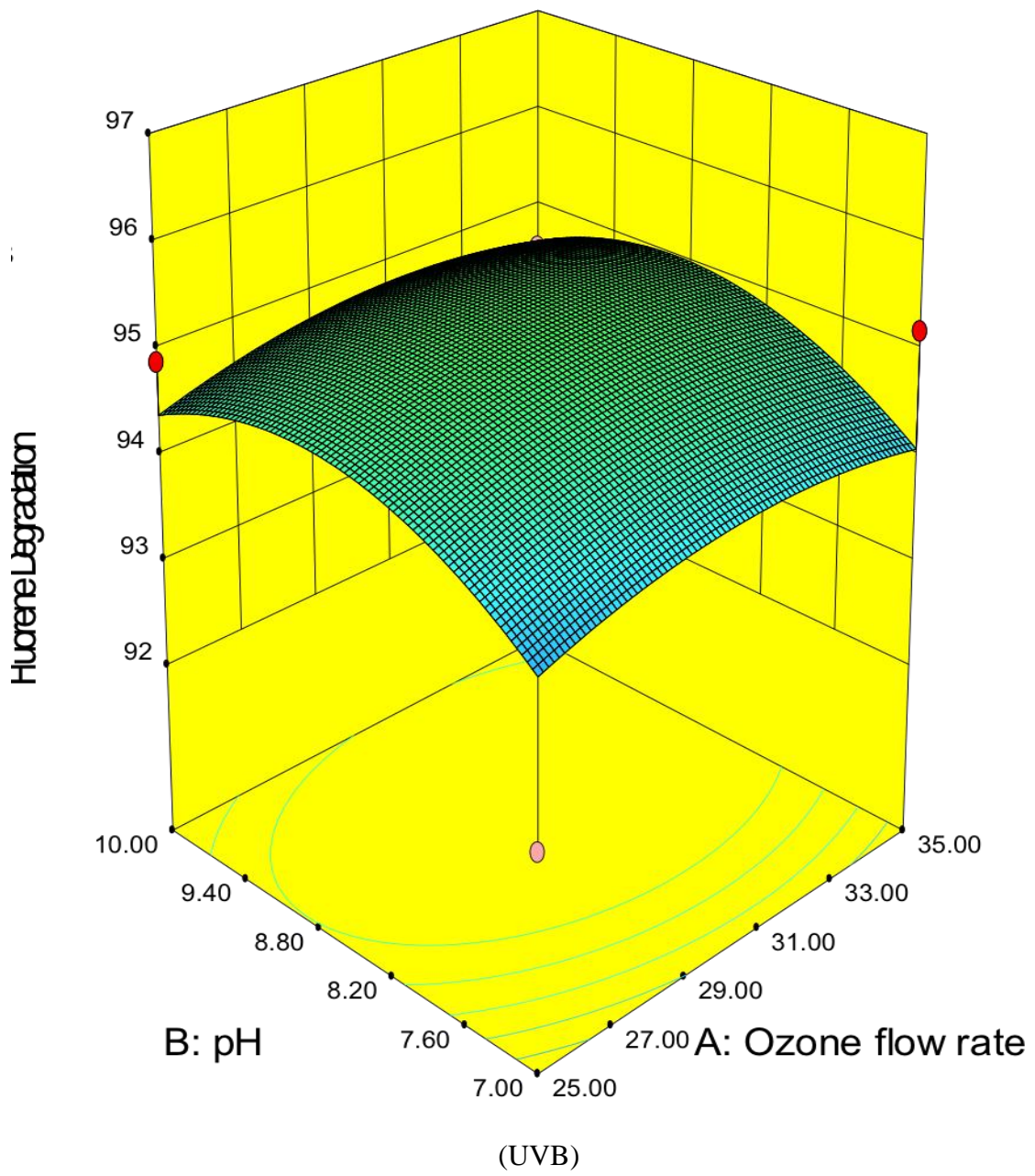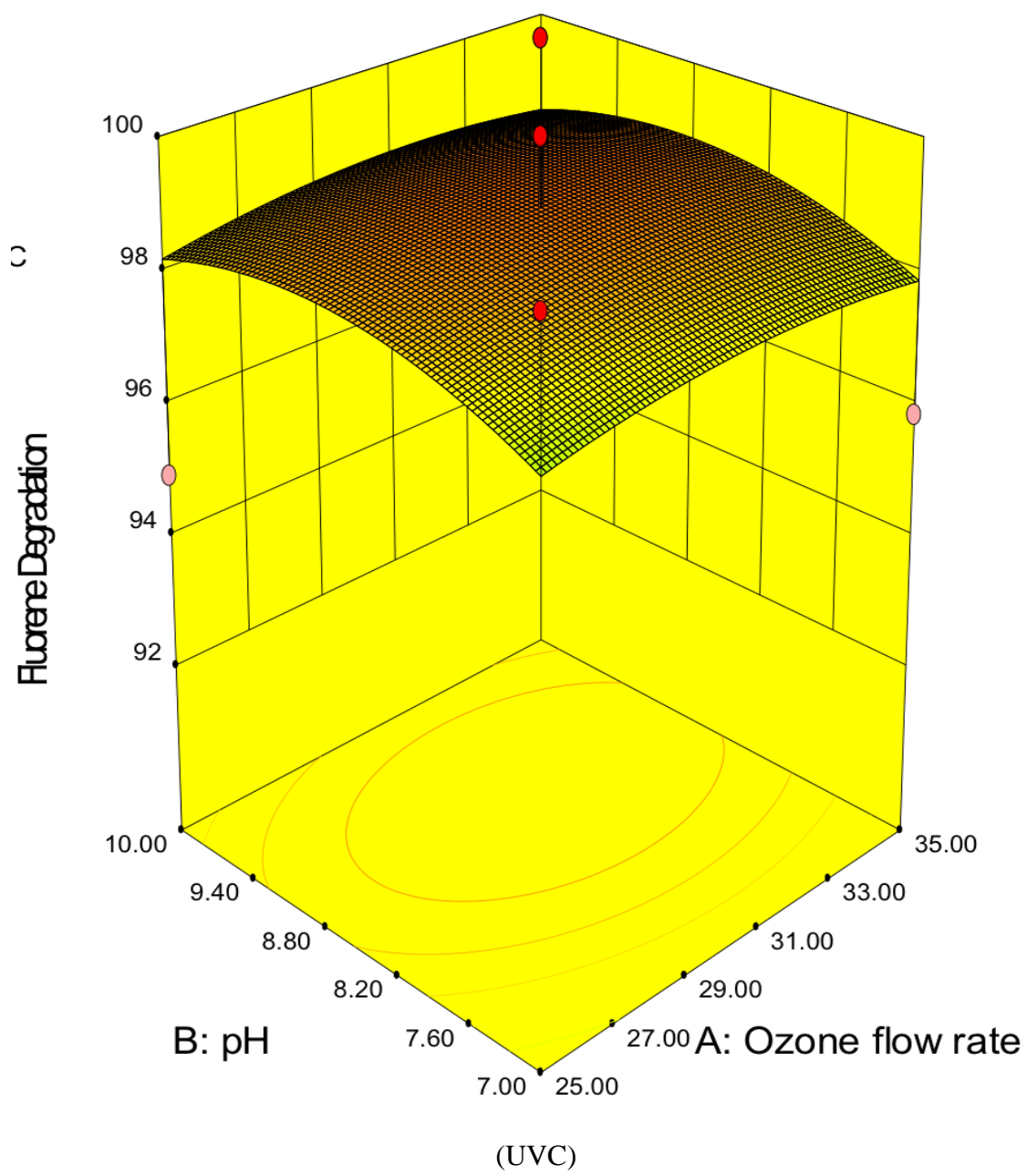
Figure 5-16 CCD 3D Surface Model Graphs for FLO Degradation Model in the UV/TiO$_2$/O$_3$ Reaction System

Table 5-14 Optimum Combinations of Process Factors to Achieve the Highest FLO Degradation in the UV/TiO$_2$/O$_3$ Reaction System

Number	Ozone flow rate (ml/min)	pH	UV Wavelength	FLO Degradation (%)	Desirability
1	30.78	8.73	UVC	99.01	0.88
2	30.84	8.72	UVC	99.01	0.88
3	30.81	8.74	UVA	94.96	0.41
4	30.79	8.73	UVB	95.20	0.40

5.3.4.3 NAP degradation in the UV/TiO$_2$/H$_2$O$_2$ reaction system

Fit all the experimental data to a CCD model, the ANOVA for the quadratic model is shown in **Table 5-15**. The model F-value of 18.92 implies the model is significant. There is only a 0.01% chance that a "Model F-Value" this large could occur due to noise. The "lack of fit F-value" of 2.38 implies the lack of fit is not significant. "Adeq Precision" of 15.633 (>4) indicates an adequate signal. The "Pred R-Squard" of 0.7439 is in reasonable agreement with the "Adj R-Squared" of 0.8384. This may indicate a large block effect or a possible problem with the model and/or data. Things to consider are model reduction, response transformation, outliers, etc. However, There is a 6.88% chance that a "lack of fit F-value" this large could occur due to noise. Lack of fit is bad as we want the model to fit. This relatively low probability (<10) is troubling.

As some insignificant model terms are included (not counting those required to support hierarchy), the model is refined by excluding the terms of AC, B^2, and C^2. From the ANOVA of the refined model (**Table 5-16**), the model F-value of 39.55 implies the model is significant. The "lack of fit F-value" of 1.86 implies the lack of fit is not significant relative to the pure error. There is a 13.43% chance that a "lack of fit F-value" this large could occur due to noise. Non-significant lack of fit is good as we want the model to fit. "Adeq Precision" of 21.34 (>4) indicates an adequate signal. The "Pred R-Squared" of 0.8217 is in reasonable agreement with the "Adj R-Squared" of 0.8589. This model can be used to navigate the design space.

222

Table 5-15 ANOVA of CCD Design of FLO Degradation in the UV/TiO$_2$/O$_3$ Reaction System

Source	Sum of Squares	df	Mean Square	F Value	p-value Prob > F
Model	617.96	11	56.18	18.9175	< 0.0001
A-H$_2$O$_2$ Concentration	6.15	1	6.15	2.0708	0.1616
B-pH	79.36	1	79.36	26.7244	< 0.0001
C-UV Wavelength	516.71	2	258.35	86.9985	< 0.0001
AB	4.17	1	4.17	1.4027	0.2466
AC	1.70	2	0.85	0.2865	0.7532
BC	0.76	2	0.38	0.1276	0.8807
A^2	8.21	1	8.21	2.7654	0.1079
B^2	0.32	1	0.32	0.1087	0.7442
Residual	80.18	27	2.97		
Lack of Fit	59.98	15	4.00	2.3761	0.0688
Pure Error	20.20	12	1.68		
Cor Total	698.14	38			
Std. Dev.	1.72		R-Squared	0.8852	
Mean	88.71		Adj R-Squared	0.8384	
C.V. %	1.94		Pred R-	0.7439	

Source	Sum of Squares	df	Mean Square	F Value	p-value Prob > F
			Squared		
PRESS	178.82		Adeq Precision	15.6334	

Table 5-16 ANOVA of Refined Model of FLO Degradation in the UV/TiO$_2$/O$_3$ Reaction System

Source	Sum of Squares	df	Mean Square	F Value	p-value Prob > F
Model	615.17	6	102.53	39.5473	< 0.0001
A-H$_2$O$_2$ Concentration	6.15	1	6.15	2.3720	0.1334
B-pH	79.36	1	79.36	30.6111	< 0.0001
C-UV Wavelength	516.71	2	258.35	99.6515	< 0.0001
AB	4.17	1	4.17	1.6067	0.2141
A^2	8.79	1	8.79	3.3912	0.0748
Residual	82.96	32	2.59		
Lack of Fit	62.77	20	3.14	1.8647	0.1343
Pure Error	20.20	12	1.68		
Cor Total	698.14	38			
Std. Dev.	1.61		R-Squared	0.8812	
Mean	88.71		Adj R-Squared	0.8589	
C.V. %	1.82		Pred R-Squared	0.8217	
PRESS	124.50		Adeq Precision	21.3404	

(a)

(b)

226

(c)

(d)

227

(e)
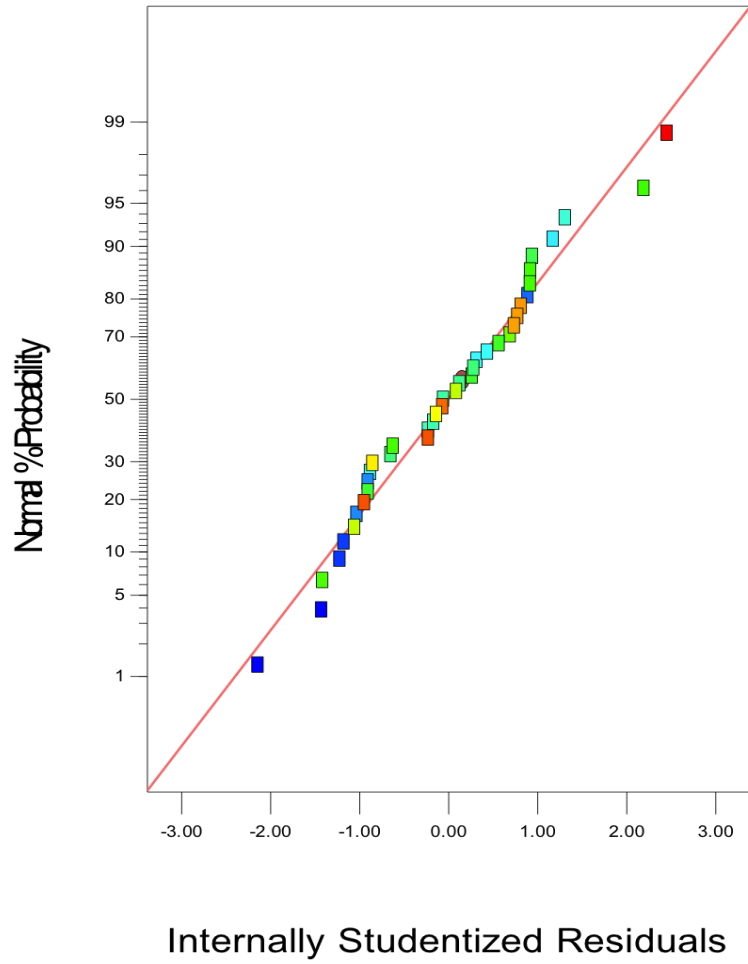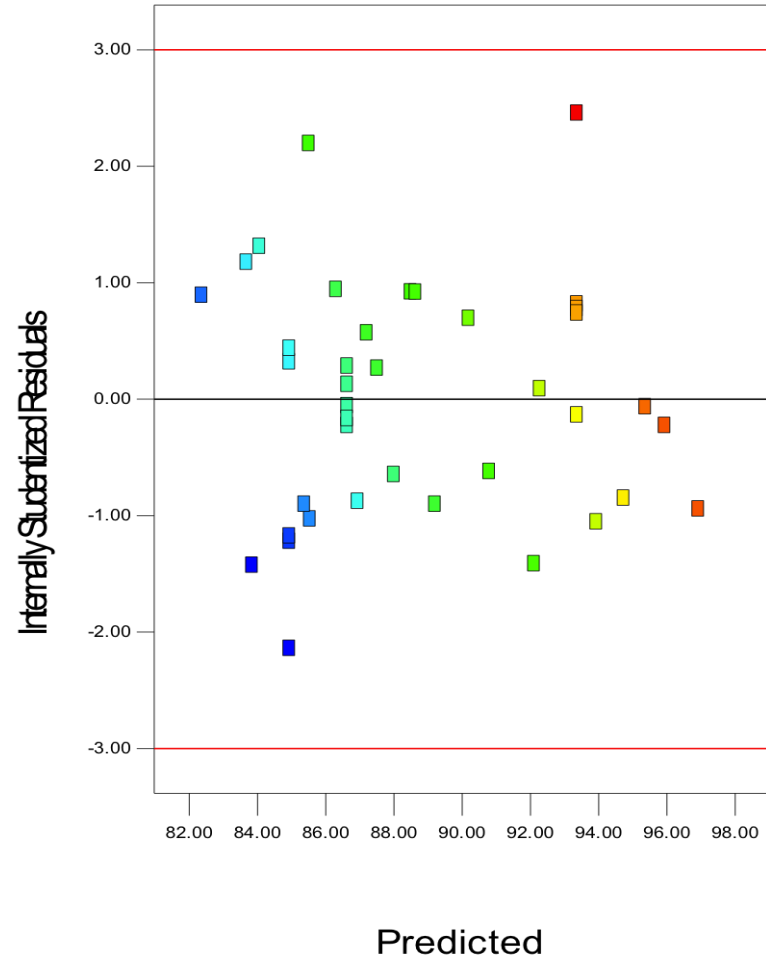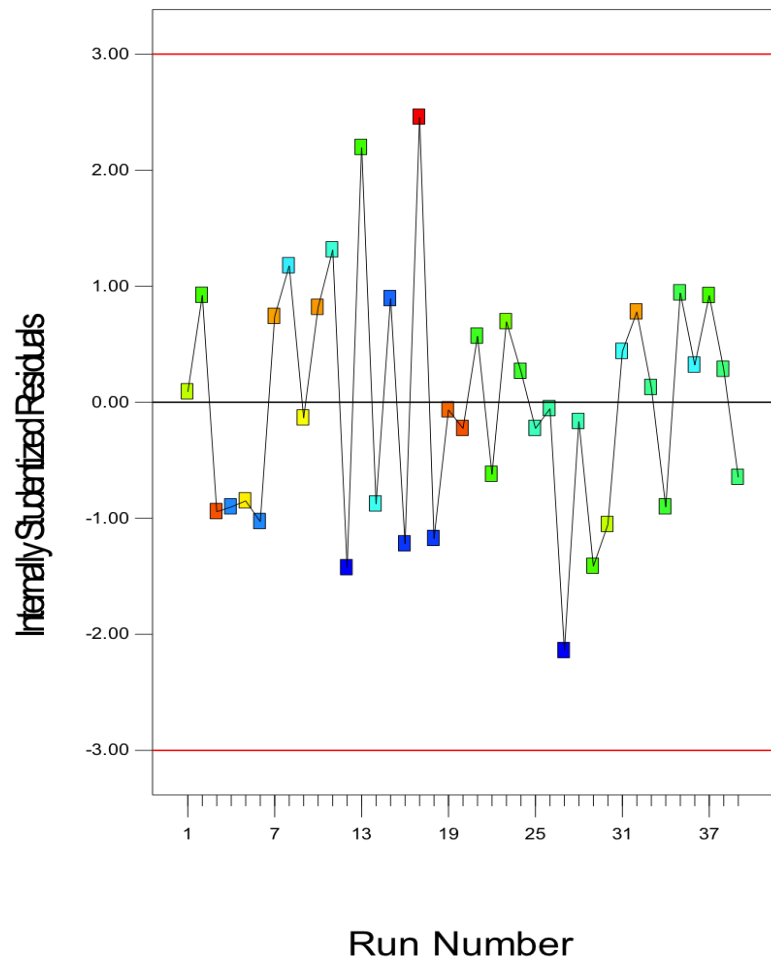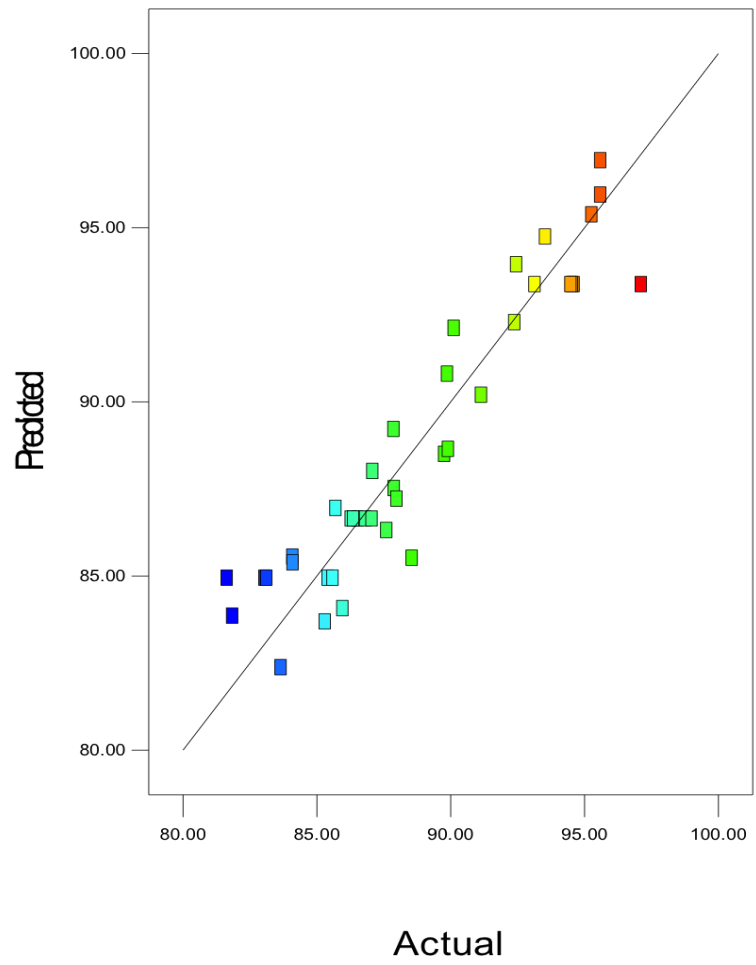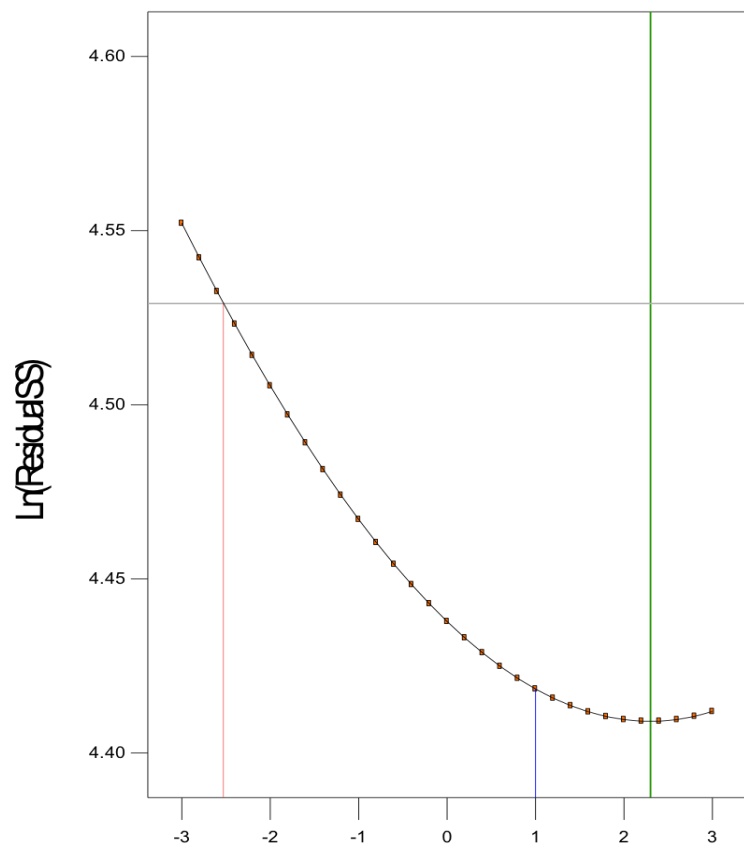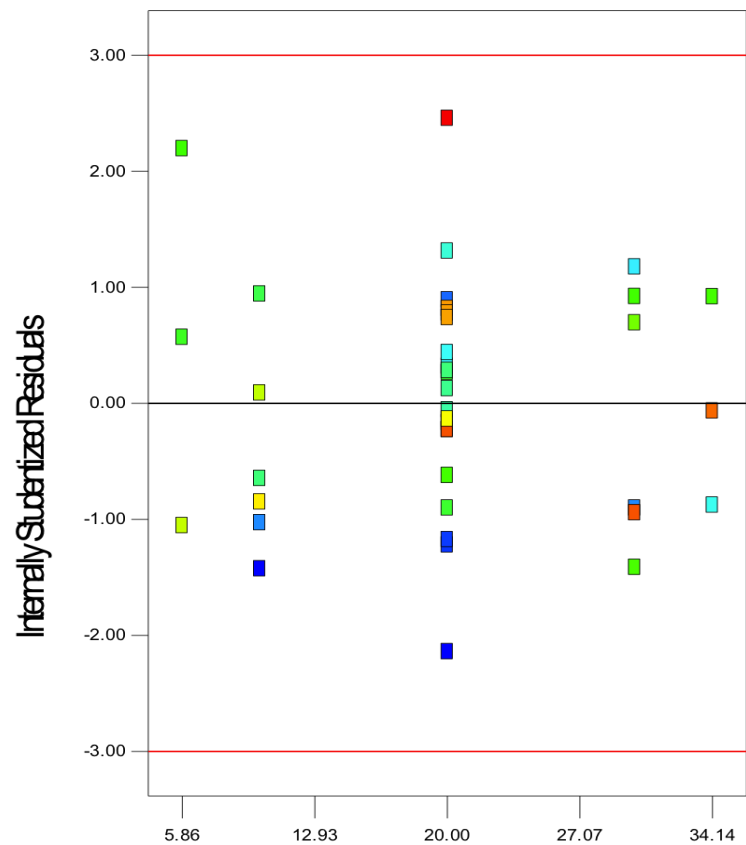
(f)

Figure 5-17 Diagnostics plots for Model Assumptions of NAP Degradation in the UV/TiO$_2$/H$_2$O$_2$ Reaction System

The diagnostic plots for residuals analysis (**Figure 5-17**) confirms the assumptions of the developed model. The normality plot of the residuals (a) are approximately a straight line; the residuals are distributed randomly within two lines on both the "residual Vs predicted" and "residual Vs run" plots (b & c); the relationship between the predicted and the actual (d) is approximately linear, and the points are close to the straight line; as can be seen from the "Box-Cox" plot (e), it is unnecessary to apply "transformation"; the "residual Vs factor" plot (f), the variance, indicate equal value for different level of the factor, since the residuals distribute randomly within two lines, showing no visible pattern.

The regression equations for the NAP degradation in the $UV/TiO_2/H_2O_2$ reaction system in terms of actual factors are then obtained:

$$\text{NAP Degradation}_{\text{UVA}}$$

$$= 82.87 - 0.54 \times H_2O_2 \text{Concentration}$$

$$+ 0.43 \times pH + 0.04 \times H_2O_2 \text{Concentration}$$

$$\times pH + 0.006 \times H_2O_2 \text{Concentration}^2$$

(5-40)

$$\text{NAP Degradation}_{\text{UVB}}$$

$$= 84.57 - 0.54 \times H_2O_2 \text{Concentration}$$

$$+ 0.43 \times pH + 0.04 \times H_2O_2 \text{Concentration}$$

$$\times pH + 0.006 \times H_2O_2 \text{Concentration}^2$$

(5-41)

NAP Degradation$_{UVC}$

$$= 91.3 - 0.54 \times H_2O_2 \text{Concentration}$$

$$+ 0.43 \times pH + 0.04 \times H_2O_2 \text{Concentration}$$

$$\times pH + 0.006 \times H_2O_2 \text{Concentration}^2 \qquad \textbf{(5-42)}$$

(UVA)

231

(UVB)

232

(UVC)
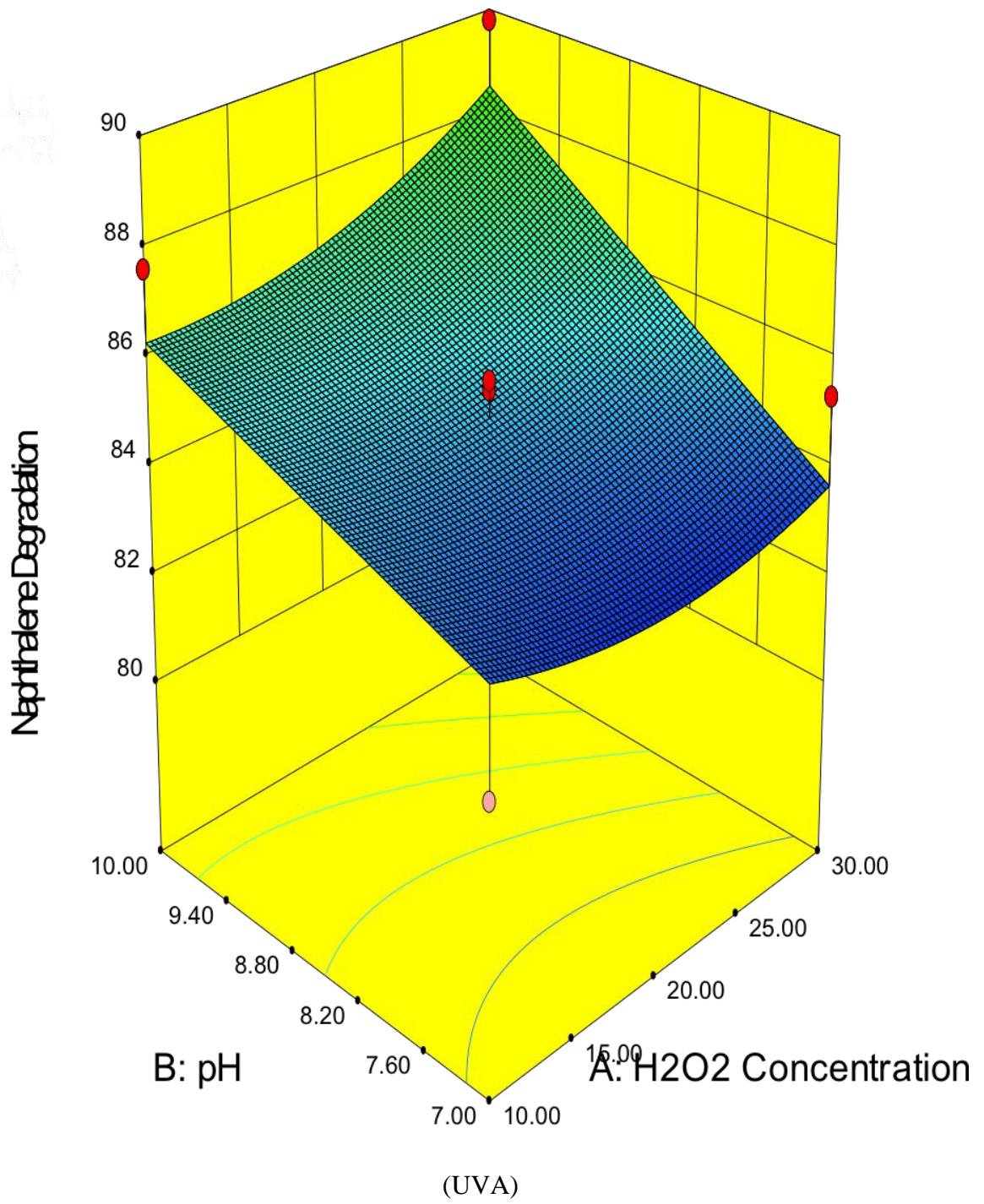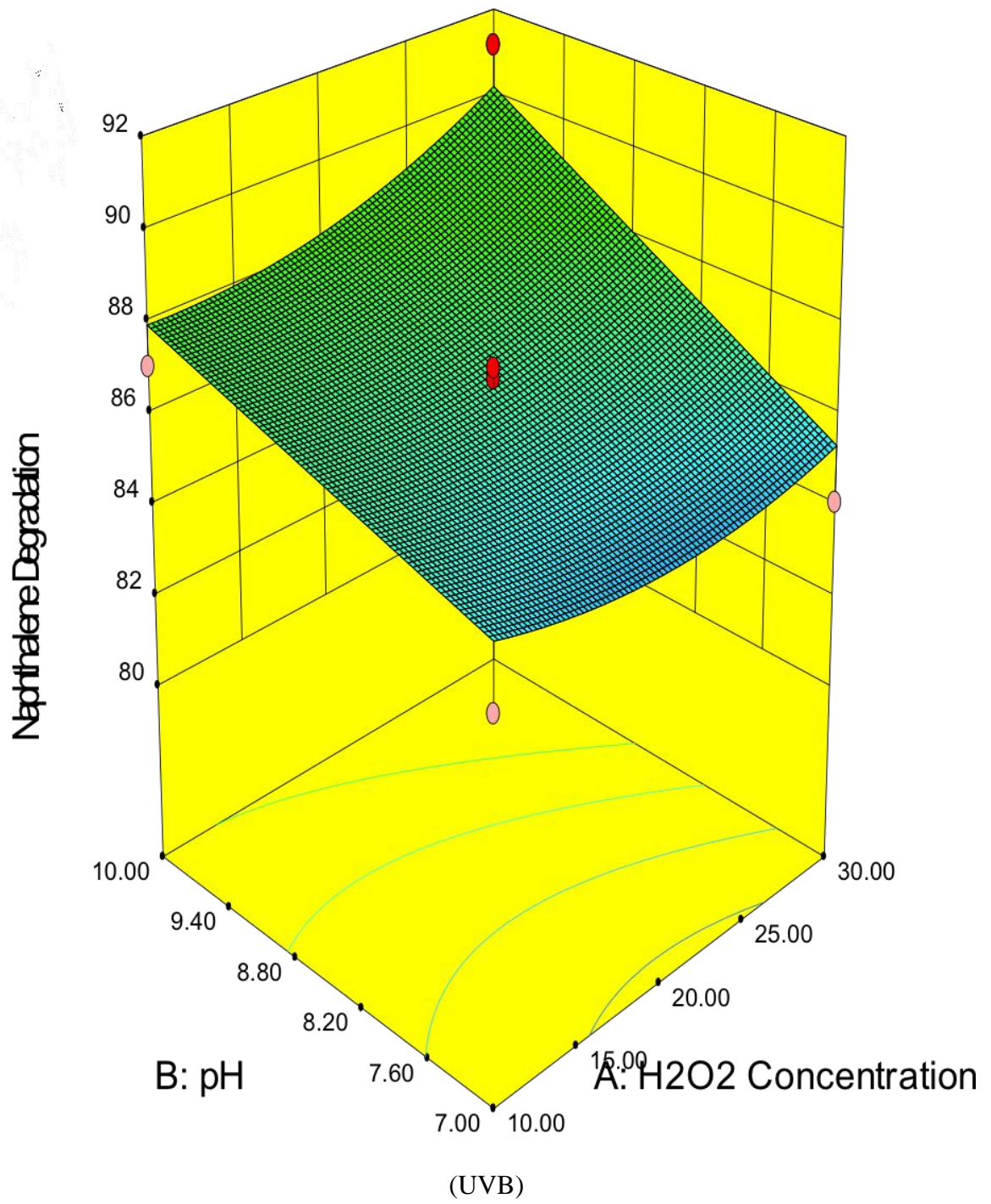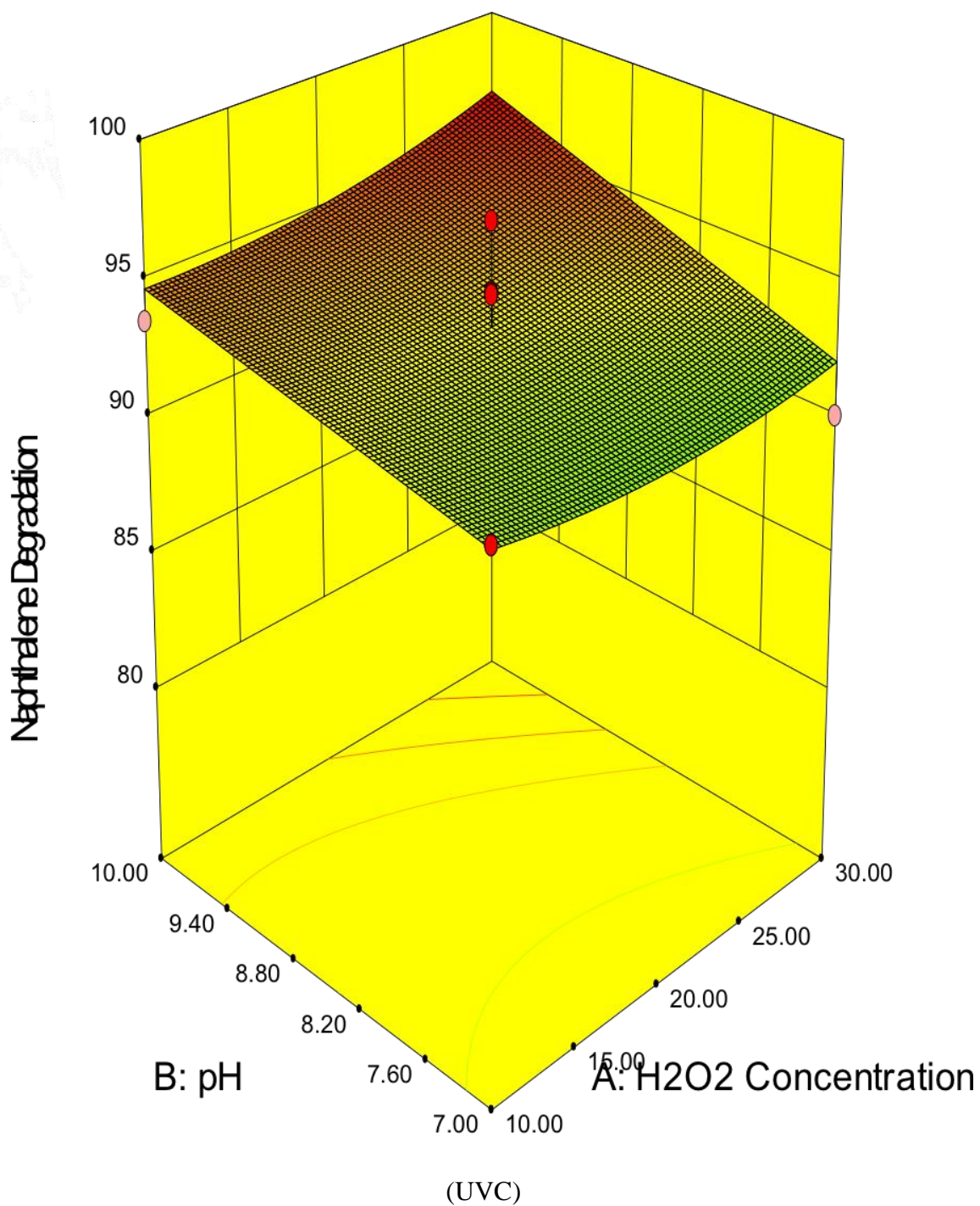
Figure 5-18 CCD 3D Surface Model Graphs for NAP Degradation Model in the

UV/TiO$_2$/H$_2$O$_2$ Reaction System

233

Table 5-17 Optimum Combination of Process Factors to Achieve the Highest NAP Degradation in the UV/TiO$_2$/H$_2$O$_2$ Reaction System

Number	H$_2$O$_2$ Concentration (g/l)	pH	UV Wavelength	NAP Degradation (%)	Desirability
1	30.00	10.00	UVC	96.92	0.98
2	29.90	10.00	UVC	96.90	0.98
3	30.00	9.92	UVC	96.80	0.98
4	30.00	10.00	UVB	90.19	0.67
5	28.32	10.00	UVB	89.81	0.65
6	30.00	9.38	UVB	89.19	0.62
7	30.00	10.00	UVA	88.50	0.35
8	30.00	9.99	UVA	88.47	0.35
9	30.00	9.85	UVA	88.25	0.34

Figure 5-18 show the 3-D surface graphs of the interaction of H_2O_2 concentration and pH value under varied UV irradiation. It indicated that the CCD model could accurately capture the curvature of the NAP degradation response, and predict the possible maximum. The developed models showed significant interaction between the H_2O_2 concentration and the pH value, and the positive impacts to the degradation. By using Design Expert v8, the optimum combinations of the three factors to achieve the highest NAP degradation were achieved. The solutions for 9 combinations of categoric factor levels are shown in Error! Reference source not found. Compared with the results from he UV/TiO_2/O_3 system, NAP achieved higher degree of degradation in the UV/TiO_2/H_2O_2 system in relative higher pH settings.

5.3.4.4 FLO degradation in the UV/TiO_2/H_2O_2 reaction system

Fit all the experimental data to a CCD model, the ANOVA for the quadratic model is shown in **Table 5-18**. The model F-value of 32.64 implies the model is significant. There is only a 0.01% chance that a "Model F-Value" this large could occur due to noise. The "lack of fit F-value" of 0.86 implies the lack of fit is not significant relative to the pure error. There is a 61.84% chance that a "lack of fit F-value" this large could occur due to noise. Non-lack of fit is good as we want the model to fit. "Adeq Precision" of 15.633 (>4) indicates an adequate signal. The "Pred R-Squard" of 0.8585 is in reasonable agreement with the "Adj R-Squared" of 0.9016. "Adeq Precision" of 15.288 indicates an adequate signal.

Table 5-18 ANOVA of CCD Design of FLO Degradation in the UV/TiO$_2$/H$_2$O$_2$ Reaction System

Source	Sum of Squares	df	Mean Square	F Value	p-value Prob > F
Model	581.01	11	52.82	32.6422	< 0.0001
A-H$_2$O$_2$ Concentration	9.13	1	9.13	5.6393	0.0249
B-pH	0.45	1	0.45	0.2812	0.6003
C-UV Wavelength	563.66	2	281.83	174.1686	< 0.0001
AB	2.09	1	2.09	1.2926	0.2656
AC	3.46	2	1.73	1.0681	0.3577
BC	2.18	2	1.09	0.6729	0.5186
A^2	0.04	1	0.04	0.0243	0.8773
B^2	0.02	1	0.02	0.0110	0.9171
Residual	43.69	27	1.62		
Lack of Fit	22.57	15	1.50	0.8553	0.6184
Pure Error	21.12	12	1.76		
Cor Total	624.70	38			
Model	581.01	11	52.82	32.6422	< 0.0001
Std. Dev.	1.27		R-Squared	0.9301	
Mean	93.58		Adj R-Squared	0.9016	

Source	Sum of Squares	df	Mean Square	F Value	p-value Prob > F
C.V. %	1.36		Pred R-Squared	0.8585	
PRESS	88.37		Adeq Precision	15.2884	

As some insignificant model terms are included (not counting those required to support hierarchy), the model is refined by excluding the terms of A^2, B^2, and C^2. From the ANOVA of the refined model (**Table 5-19**), the model F-value of 42.80 implies the model is significant. The "lack of fit F-value" of 0.76 implies the lack of fit is not significant relative to the pure error. There is a 70.85% chance that a "lack of fit F-value" this large could occur due to noise. Non-significant lack of fit is good as we want the model to fit. "Adeq Precision" of 17.324 (>4) indicates an adequate signal. The "Pred R-Squared" of 0.8728 is in reasonable agreement with the "Adj R-Squared" of 0.9083. Comparing the models before and after reduction, all the statistics in the refined model shows better performance. Thus, the refined model was used to navigate the design space.

The diagnostic plots for residuals analysis (**Figure 5-19**) confirms the assumptions of the developed model. The normality plot of the residuals (a) are approximately a straight line; the residuals are distributed randomly within two lines on both the "residual Vs predicted" and "residual Vs run" plots (b & c); the relationship between the predicted and the actual (d) is approximately linear, and the points are close to the straight line; as can be seen from the "Box-Cox" plot (e), it is unnecessary to apply "transformation"; the "residual Vs factor" plot (f), the variance, indicate equal value for different level of the factor, since the residuals distribute randomly within two lines, showing no visible pattern.

Table 5-19 ANOVA of Refined Model of FLO Degradation in the UV/TiO₂/H₂O₂

Reaction System

Source	Sum of Squares	df	Mean Square	F Value	p-value Prob > F
Model	580.96	9	64.55	42.7974	< 0.0001
A-H_2O_2 Concentration	9.13	1	9.13	6.0500	0.0201
B-pH	0.45	1	0.45	0.3016	0.5871
C-UV Wavelength	563.66	2	281.83	186.8512	< 0.0001
AB	2.09	1	2.09	1.3868	0.2485
AC	3.46	2	1.73	1.1459	0.3319
BC	2.18	2	1.09	0.7219	0.4943
Residual	43.74	29	1.51		
Lack of Fit	22.63	17	1.33	0.7563	0.7085
Pure Error	21.12	12	1.76		
Std. Dev.	1.23		R-Squared	0.9300	
Mean	93.58		Adj R-Squared	0.9083	
C.V. %	1.31		Pred R-	0.8728	

Source	Sum of Squares	df	Mean Square	F Value	p-value Prob > F
			Squared		
PRESS	79.45		Adeq Precision	17.3239	
			Precision		

(a)

(b)

241

(c)

(d)

242

(e)
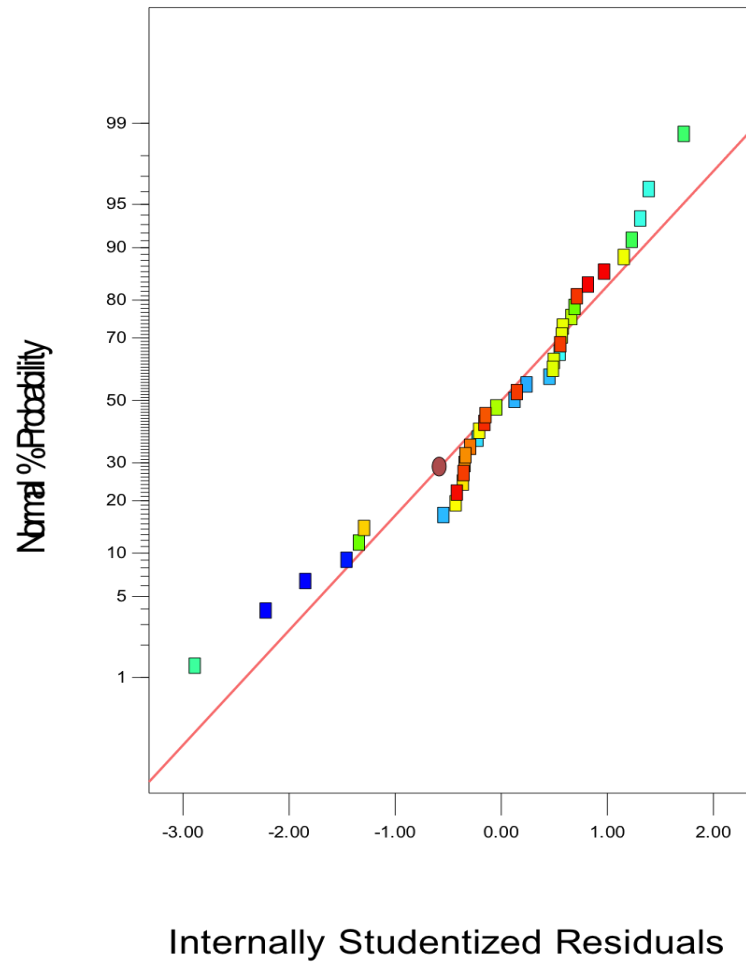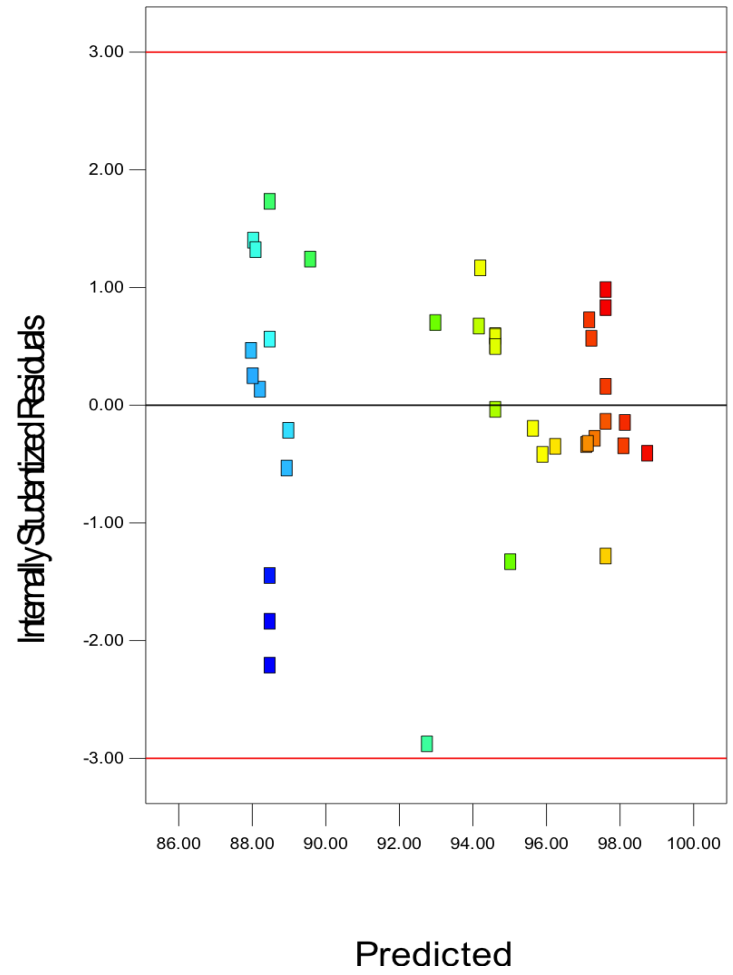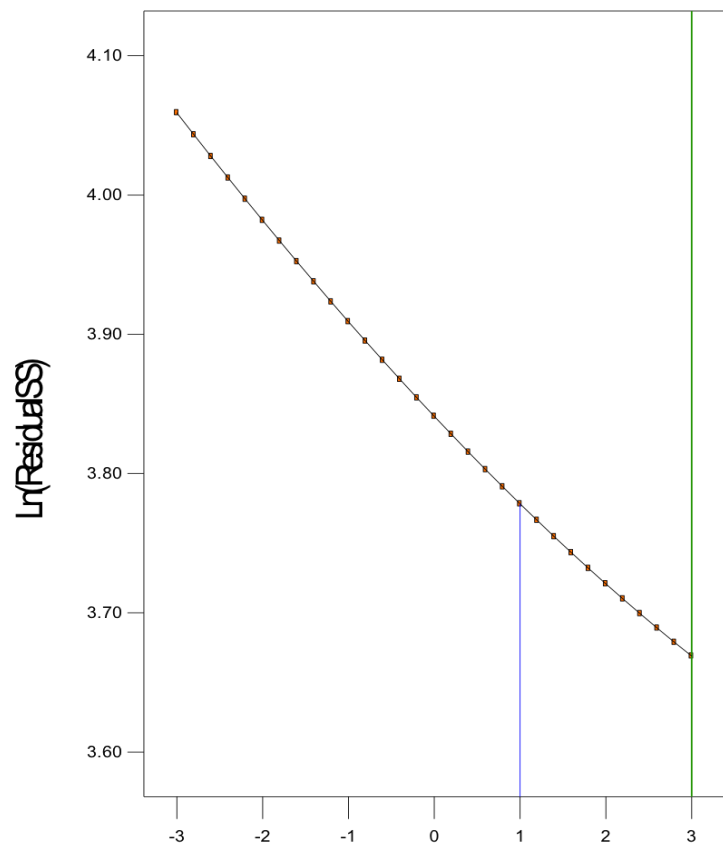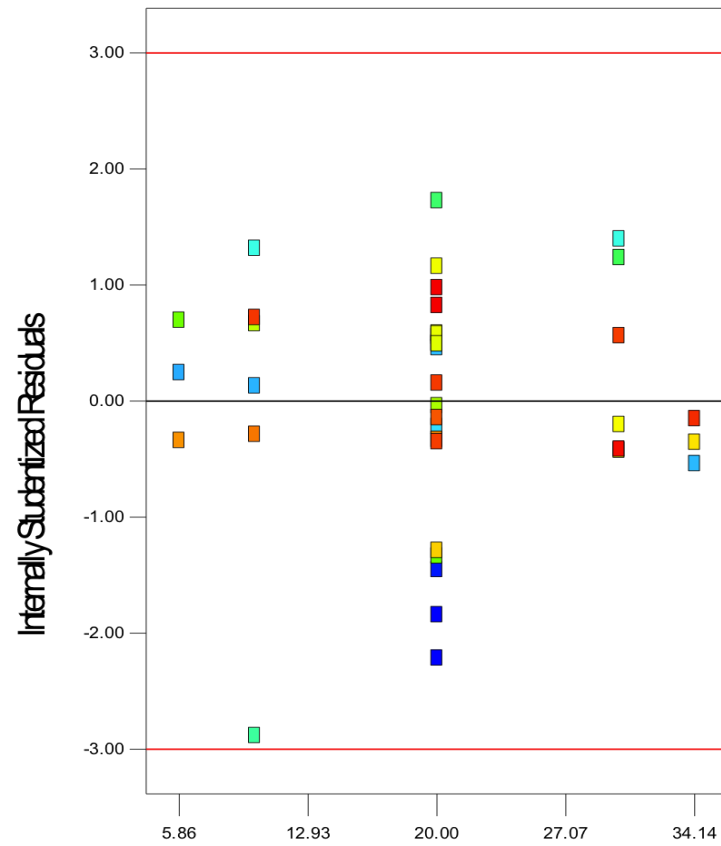
(f)

Figure 5-19 Diagnostics plots for Model Assumptions of FLO Degradation in the UV/TiO$_2$/H$_2$O$_2$ Reaction System

243

The regression equations for the FLO degradation under UV/TiO_2/H_2O_2 scenario using the selected factors in terms of actual factors are given by:

FLO Degradation$_{UVA}$

$$= 90.54 - 0.20 \times H_2O_2\,\text{Concentration}$$
$$- 0.32 \times pH - 0.27 \times H_2O_2\,\text{Concentration}$$
$$\times pH \tag{5-43}$$

FLO Degradation$_{UVB}$

$$= 98.69 - 0.12 \times H_2O_2\,\text{Concentration}$$
$$- 0.75 \times pH - 0.03 \times H_2O_2\,\text{Concentration}$$
$$\times pH \tag{5-44}$$

FLO Degradation$_{UVC}$

$$= 99.67 - 0.20 \times H_2O_2\,\text{Concentration}$$
$$- 0.33 \times pH - 0.03 \times H_2O_2\,\text{Concentration}$$
$$\times pH \tag{5-45}$$

Figure 5-20 show the 3-D surface graphs of the interaction of H_2O_2 concentration and pH value under varied UV irradiation. It indicated that the CCD model could accurately capture the curvature of the FLO degradation response, and predict the possible maximum. On contrary to the NAP model, the impact of interaction between the H_2O_2 concentration and pH value is negative for FLO. By using Design Expert v8, the optimum combinations of the three factors to achieve the highest FLO degradation. The solutions

for 10 combinations of categoric factor levels are shown in **Table 5-20**. Higher degradation of FLO than NAP was observed in this hybrid reaction system again at the high end of pH value. But the removal of FLO is less efficient than that in the UV/TiO$_2$/O$_3$ reaction system, while the degradation of NAP favored the UV/TiO$_2$/H$_2$O$_2$ reaction system.

(UVA)

246

(UVB)

247

(UVC)
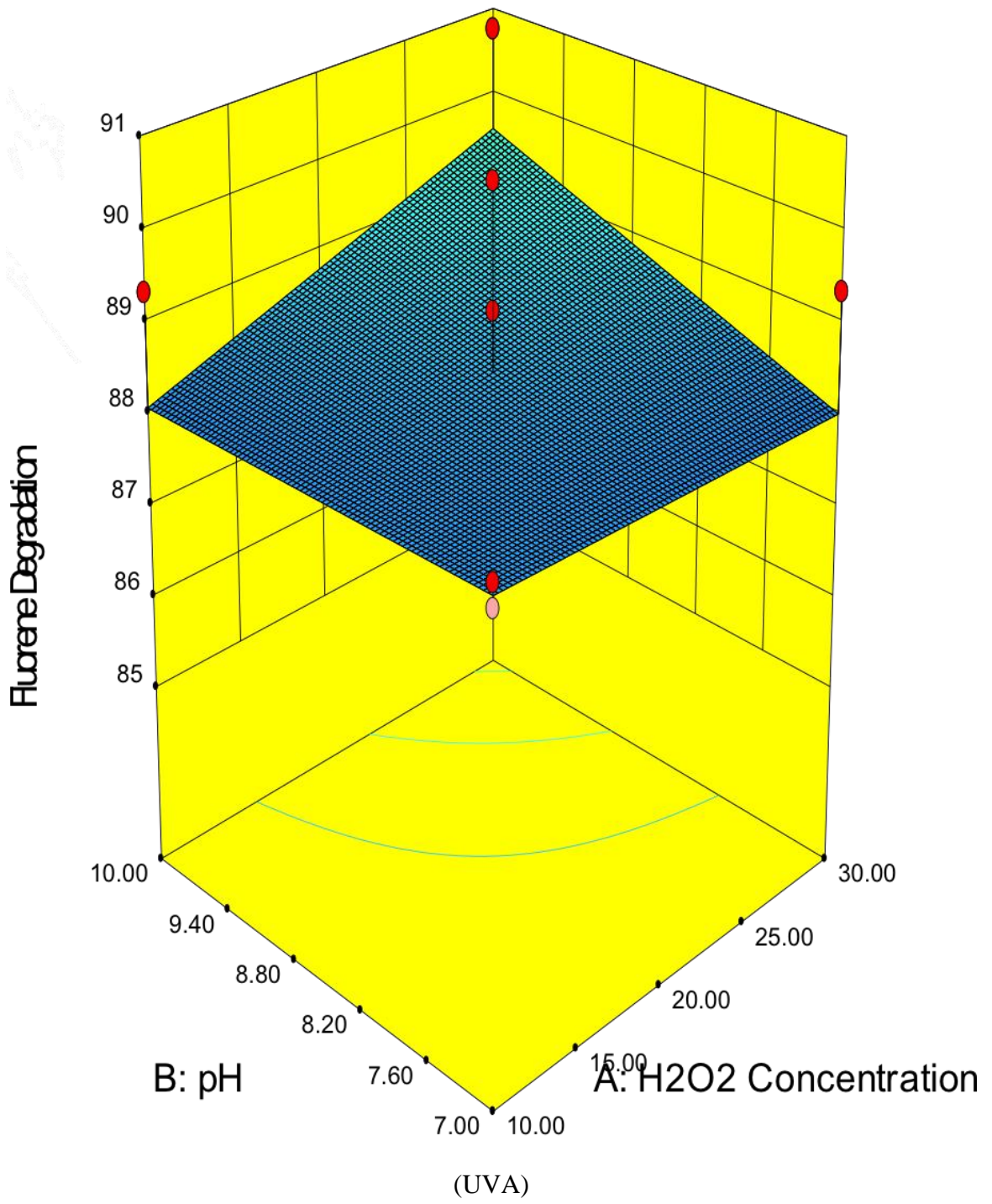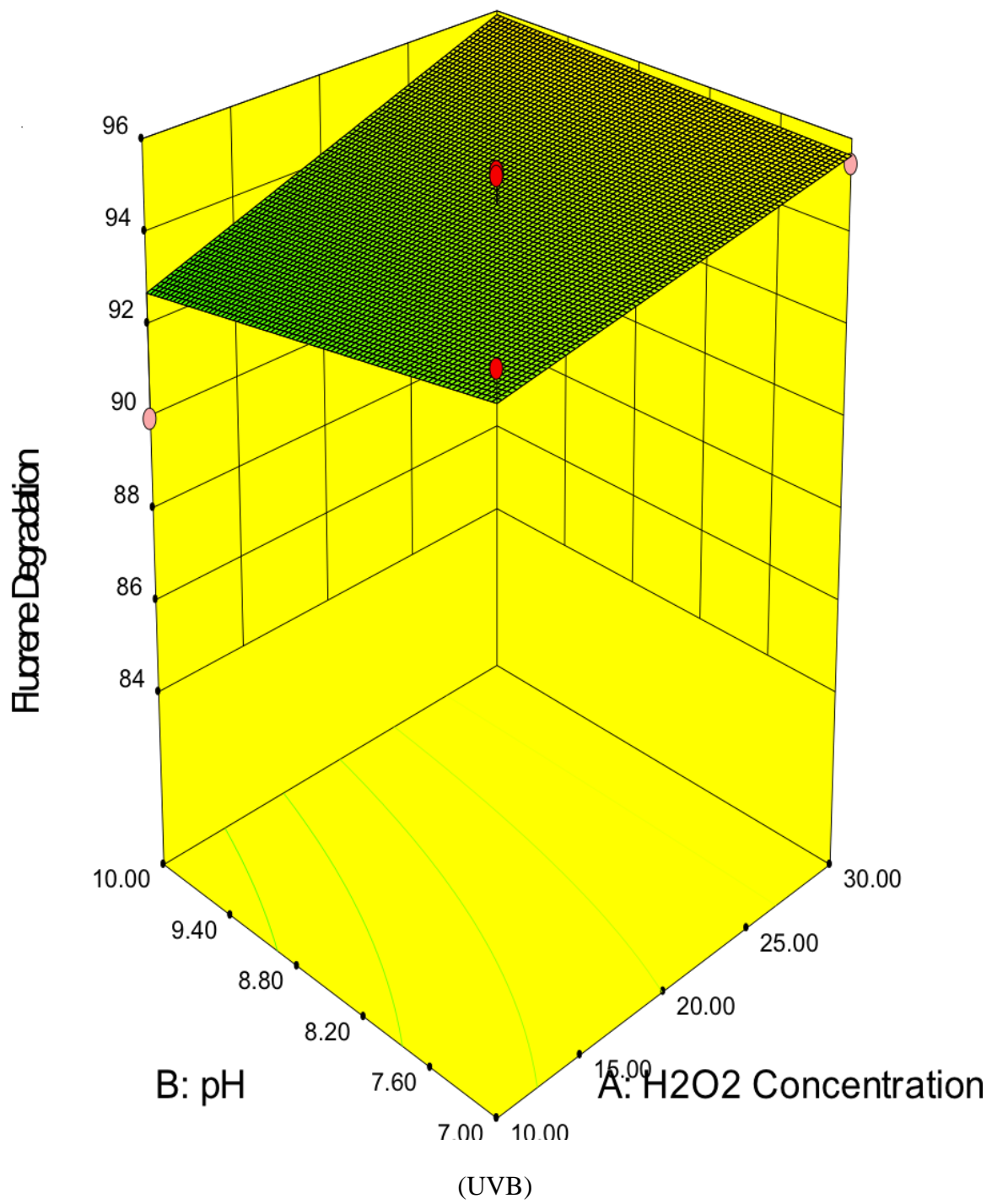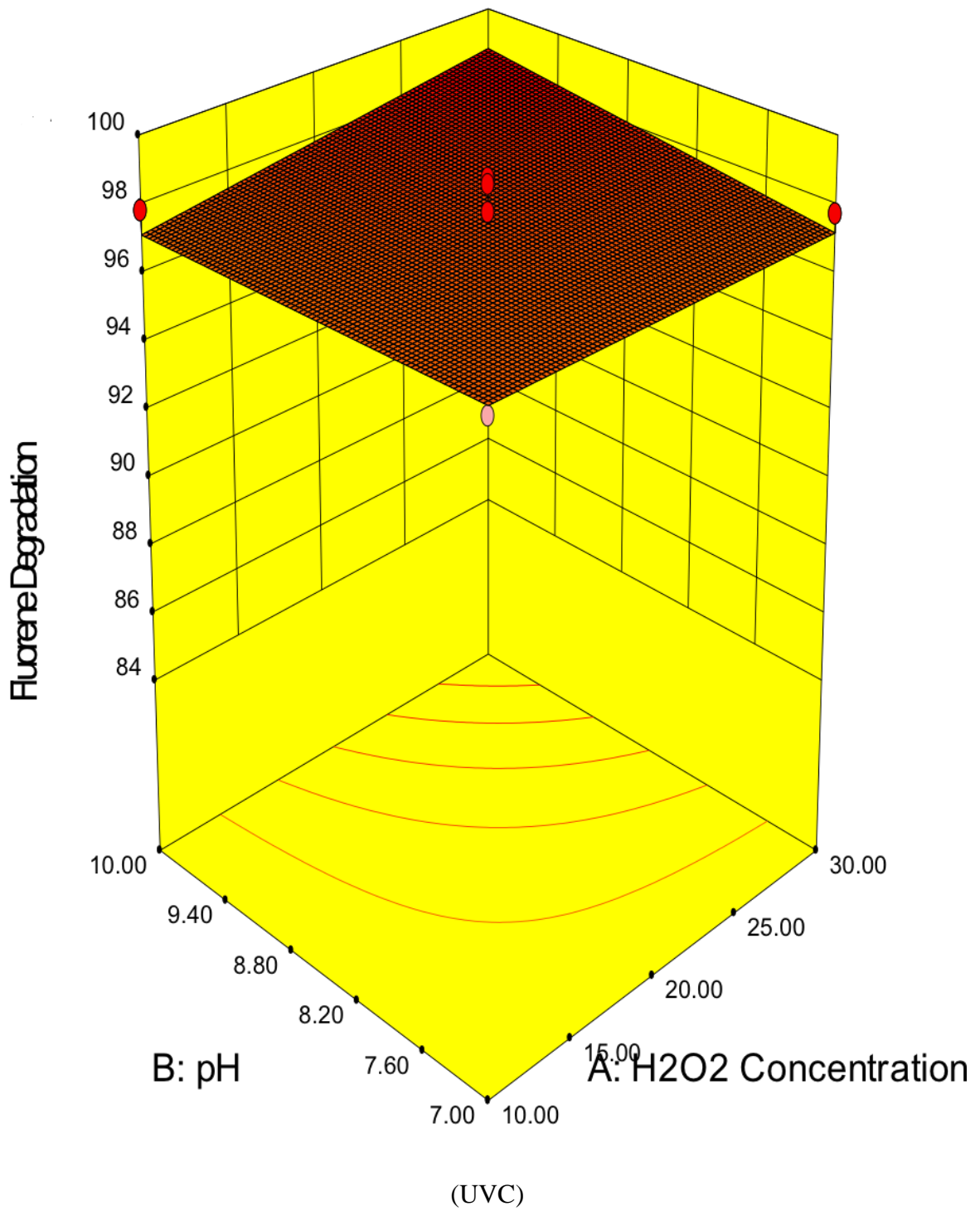
Figure 5-20 CCD 3D Surface Model Graphs for FLO Degradation Model in the UV/TiO$_2$/H$_2$O$_2$ Reaction System

Table 5-20 Optimum Combination of Process Factors to Achieve the Highest FLO Degradation in the UV/TiO$_2$/H$_2$O$_2$ Reaction System

Number	H$_2$O$_2$ Concentration (g/l)	pH	UV Wavelength	FLO Degradation (%)	Desirability
1	30.00	10.00	UVC	98.76	0.99
2	29.90	10.00	UVC	98.75	0.99
3	30.00	9.98	UVC	98.75	0.99
4	28.71	10.00	UVC	98.66	0.98
5	11.71	10.00	UVC	97.32	0.87
6	30.00	10.00	UVB	95.91	0.65
7	30.00	9.90	UVB	95.90	0.65
8	30.00	9.12	UVB	95.83	0.60
9	30.00	10.00	UVA	89.59	0.36
10	30.00	9.38	UVA	89.27	0.31

5.3.4.5 Validation of CCD models

As reported in the above sections 1 to 4, maximum photocatalytic degradation rates in the hybrid systems can be achieved with the optimal combinations via different permutations of the operation variables. All the optimal values were located within the experimental span and varied around the center points to a limited extent. Subsequently, to validate the predicted maximum PAHs degradation experiments with four optimum combinations of the three factors were carried out. The experimental results have been compared with the predicted maximum value of PAHs degradation by the developed model. According to **Table 5-21** the final response predicted by CCD models are very close to the results obtained from the experiment, demonstrating that the developed CCD models could adequately represent the hybrid oxidation systems and effectively predict the possible maximum points with reasonable combinations of each parameter in the two proposed hybrid systems.

Table 5-21 CCD Model Predictions Vs. Experimental Results

	CCD Model Predicted (%)	Experimental Average (n=3) (%)
NAP Degradation under UV/TiO$_2$/O$_3$ (O$_3$=31.2ml/min; pH=8.53; UVC)	96.8901	96.4532
Highest FLO Degradation under UV/TiO$_2$/O$_3$ (O$_3$=30.78ml/min; pH=8.73; UVC)	99.0111	97.8465
Highest NAP Degradation under UV/TiO$_2$/H$_2$O$_2$ (H$_2$O$_2$=30g/l; pH=10; UVC)	96.9244	97.0357
Highest FLO Degradation under UV/TiO$_2$/H$_2$O$_2$ (H$_2$O$_2$=30g/l; pH=10; UVC)	98.7591	99.1909

5.3.5 Degradation Mechanism

When O_3 is combined with UV irradiation, several processes take place. The first step is mass transfer of O_3:

$$O_3(g) \rightarrow O_3(aq) \qquad \text{(5-46)}$$
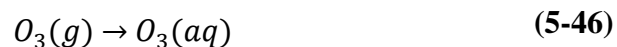
O_3 can react directly with the targeting PAHs, through a slow and selective reaction:

$$O_3 + PAH \rightarrow Products \qquad \text{(5-47)}$$

Irradiation of O_3 in water will lead to quantitative formation of H_2O_2 (Cisneros et al., 2002):

$$O_3 + H_2O \xrightarrow{\phi_{O_3}, h\nu} H_2O_2 + O_2 \qquad \text{(5-48)}$$
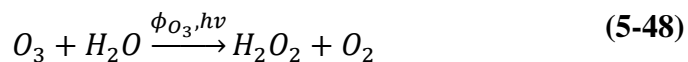
Photolysis of H_2O_2 by UV irradiation can yields two hydroxyl radicals per each molecule of H_2O_2; the reagent also reacts with O_3:

$$O_3 + H_2O_2 \rightarrow HO_2 \cdot + OH \cdot + O_2 \qquad \text{(5-49)}$$

$$O_3 + OH \cdot \rightarrow HO_2 \cdot + O_2 \qquad \text{(5-50)}$$

$$2HO_2 \cdot \rightarrow H_2O_2 + O_2 \qquad \text{(5-51)}$$

$$HO_2 \cdot + OH \cdot \rightarrow H_2O + O_2 \qquad\qquad \textbf{(5-52)}$$
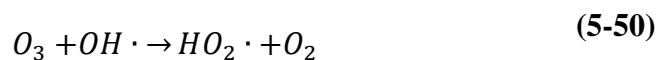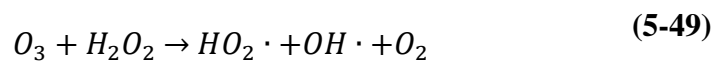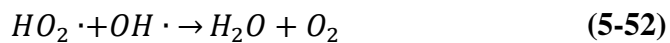
Since O_3 was reported to have a higher absorption coefficient than H_2O_2 (Litter and Quici, 2010), this combined AOP can be used to treat PW with high UV absorption background, which is significant to the treatment of OPW with complicated matrix.

In the presence of oxygen and organic compounds, multiple pathways are operative in the UV/H_2O_2 system, firstly the generation of hydroxyl radicals:

$$H_2O_2 \overset{hv}{\rightarrow} 2OH \cdot \qquad\qquad \textbf{(5-53)}$$

It has been observed from the experimental results that the oxidizing power of H_2O_2 was sensibly improved with UVC irradiation, which could be explained by the high-energy requirement (i.e., $\lambda < 280$ nm according to Litter, 2005) for the O-O union cleavage.

It was also found that in alkaline media (i.e., pH = 10), the photochemical process was more efficient. The reason could be that the concentration of the conjugate anion of H_2O_2 increases with pH, and this species has a higher absorption coefficient than H_2O_2 (Litter and Quici, 2010), favoring light absorption and increasing $OH \cdot$ production:

$$H_2O_2 \xrightarrow{pK=11.8} HO_2^- + H^+ \qquad \textbf{(5-54)}$$
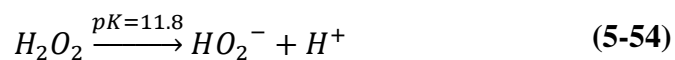
At high H_2O_2 concentrations, competitive reactions occur in accordance with the following scheme (Litter, 2009):

$$OH \cdot + H_2O_2 \rightarrow HO_2 \cdot + H_2O \qquad \textbf{(5-55)}$$

$$HO_2 \cdot + H_2O_2 \rightarrow OH \cdot + H_2O + O_2 \qquad \textbf{(5-56)}$$
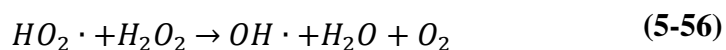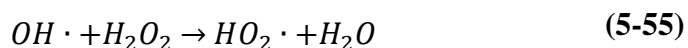
5.4 Summary

In this chapter, batches of lab-scale bench-top experiments have been conducted to evaluate the efficiency of UV-enhanced treatment in the degradation of PAHs. The key technology is to develop in situ photolysis enhanced oxidation approaches to remove PAHs from OPW. The major activities are based on the development of photolysis enhanced oxidation systems by integrating the effects from ozonation and hydrogen peroxide.

OPW samples have been transferred into chambers of the developed UV reactors for process optimization. CCD has been applied in testing the hybrid systems for developing system models and optimization. The key testing parameters during the experiments include UV wavelength, temperature, pH value, radical inhibitors, and oxidant (O_3/H_2O_2)

254

concentration. After treatment, the PW sample have been collected and pretreated and analyzed based on the developed analytical methods. The half-life was suggesting that photolysis-enhanced oxidation was a significantly fast reaction for removal of the targeting PAHs from OPW under certain conditions. Nevertheless, process dynamics and mechanisms have also been discussed based on the experimental results. By identifying and quantifying the variables controlling the photolysis enhanced oxidation process and establishing the optimum treatment conditions, this research would lead to a novel OPW treatment system for use on offshore platforms where space, changing flow rates, maintenance, and cost are major concerns.

Finally, a note should be added here that while the studies show that the method works for FLO and NAP, once other contaminants are introduced and turbidity associated with the oil the efficiency and time to treat will certainly change. For example, this study would have been interesting to see the impact on other dissolved compounds that are toxic such as phenols. When analyzing interactions, the dispersed oil will have a significant effect on the efficiency and their performance of the system. This needs to be looked at independently in the next step of research.

255

Chapter 6 Conclusions and Future Work

With the accelerating economic development and population growth, petroleum production is shifting from "shallow" wells to offshore, deep-water operations, from which a huge volume of offshore produced water (OPW) is generated, placing the marine environment under ever-growing pressure and have the potential to radically alter already fragile ecosystems. From the perspective of both industry and government, the proper testing and treatment of OPW has been recognized as one of the major environmental and operational issues particularly under ongoing regulatory and economic pressure to reduce emissions of wastes, especially within a harsh environmental context and taken into account in the strategic planning of the marine sustainability.

For a long time, only non-polar oil in water (OIW) was regulated by government, while little attention was given to dissolved organics such as dissolved PAHs in OPW, which contribute most to its toxicity. Owing to the more stringent environmental regulations imposed in recent years as well as the increasing awareness of the impacts of dissolved PAHs in OPW, a thorough treatment of these waste streams should be carried out prior to discharge. According to the literature, the most widely used treatment techniques focus on removing dispersed oil to meet the regulated oil and grease concentration, which are ineffective in removing dissolved fractions of PAHs. There are a couple of currently developed treatment options, which can further reduce and/or remove PAHs from the OPW, however, are more or less constrained by limited space, shock-loading conditions,

256

and/or requirements of low maintenance and high cost efficiency. And the harsh and changing offshore environment (e.g., cold and high motion) make the application of the current approaches even more challenging.

Therefore, driven by environmental concerns about the long-term impacts on the ambient marine ecosystems from the OPW discharge and future more stringent wastewater treatment guidelines, the objective of this research was to address the knowledge/technical gaps in current OPW management, targeting the toxic and persistent contaminants that of the key environmental concern in OPW, PAHs, to develop compact, efficient, and environmental friendly technologies for onsite treating PAHs in OPW, particularly in the Arctic and Atlantic regions to assure the protection of ocean environment and sustainable utilization of our marine resources.

6.1 Summary

Firstly, two pre-treatment methods were developed to extract PAHs from the sample OPW by refining and optimizing traditional or commercial solid phase extraction (SPE) and liquid phase micro extraction (LPME). The polished SPE system was established through screening of conditioning/elution solvents and their appropriate volumes and the suitable pH value. In the 6ml/500mg C_{18} SPE cartridge, sequentially conditioned with 6 mL DCM, 6 mL methanol and 6 mL distilled water, loaded by sample water with unadjusted pH, and eluted twice with 1 mL DCM, provided the best results. The refined LPME system was built by optimizing parameters affecting the extraction efficiency,

257

including solvent selection, organic solvent volume, shaking rate and time, content of salts, and centrifuge speed. The optimum conditions for LPME of PAHs from water was reached by using 250 μl dichloromethane (DCM) as the extraction solvent; 15 min shaking at 25 ^{0}C with no addition of NaCl, and setting centrifugation speed at 1,000 rpm.

Secondly, combined gas chromatography and mass spectrometry (GC-MS) has been significantly improved for PAHs detection in OWP. The developed methods have been applied to analyze the artificial and real OPW samples. Refined multiple ramp oven program (i.e., at 60 ℃, 4 ℃/min to 300 ℃) demonstrated better separation of the targeting PAHs in the DB-5MS UI fused silica capillary column; Increased ion-source temperature (i.e., 350 ℃) was applied with the use of ultra-inert filament, which was proved to provide a shorter run time and ppt level method detection limit (MDL). The method linearities (R^2s) for all 16 PAHs were above 0.99 at concentration range between 10-1000 ng/ml. The recoveries of the method were 84-101% (except ACY in SPE-GC-MS analysis); the method detection limits were as low as 2 to 8 ng/l (except NAP). The relative standard deviations (RSDs) were 4.2~10.6%. The developed method was also validated in real water sample and showed good capability in determination of 16 PAHs in OPW.

Thirdly, photochemical oxidation reactors have been designed and fabricated and batches of lab-scale bench-top experiments have been conducted to evaluate the efficiency of UV-enhanced treatment in the degradation of PAHs. Naphthalene (NAP) and Fluorene (FLO)

258

were used as model PAHs in this research. They represent the two- and three-ring PAHs commonly found in OPW and were identified as the main contributors to the ecological risk of PAHs in OPW discharge due to their elevated concentration levels in OPW and bioavailability to the water-column organisms, especially the sensitive marine species. The key technology developed was the photolysis enhanced oxidation approaches to remove PAHs from OPW. The major activities are firstly based on the development of an optimized UV photolysis system; and then move into the development of photolysis enhanced oxidation system by integrating the effects from ozonation (O_3) and hydrogen peroxide (H_2O_2).

Phased One-Factor-A-Time (OFAT) experimental design has been adapted for better understanding the direct photolysis and photocatalysis process. The results indicated a relatively higher treatment efficiency of UVC for both PAHs, followed by UVB, and then UVA. A clear trend was identified that the performance of UVC irradiation increased at higher pH values. The results also indicated a much more significant impact of pH on the photolysis of FLO than that of NAP. Taking into consideration the influence of oxygen and t-BuOH on the removal rates of the targeting PAHs, the superoxide pathway of the NAP and FLO decomposition was proposed in the direct photolysis system. Limited ability from Degussa P-25 TiO_2 was observed due to the suspended form.

Hybrid oxidation systems by integrating photolysis and ozonation and/or hydrogen peroxide (H_2O_2) were developed next. Experimental tests were initially conducted to

259

evaluate the synergism between UV photolysis and ozonation or H_2O_2 and the possibility of enhanced treatment efficiency. The test demonstrated that the participation of O_3, at appropriate dose setting, was able to accelerate the PAHs degradation under the photo catalysis system. The result also indicated that NAP was more sensitive to the dose change of O_3 than FLO. The participation of H_2O_2, at appropriate dose setting, was also able to speed the PAHs degradation under the photo catalysis system. A clear trend can be identified that the FLO removal rates increased by increasing dose of H_2O_2, while the NAP removal rates were detected to be inversely proportional to the concentration of H_2O_2. Influence of temperature and radical scavenger has been further explored either for the purpose of offshore application or for the better understanding of the reaction mechanism in the hybrid systems. An interesting finding was observed that the degradation rates of the target PAHs significantly decreased by increasing temperature from 23 to 50 ^{0}C, however, the reaction rates progressively "recovered" back with the elevation of temperature from 50 to 90 ^{0}C, which is close to most real OPW temperature bringing practical implication by using AOP process. It was also found that the retarding effects of BuOH were more significant in the hybrid systems, which reaffirm the role of hydroxyl radicals.

Central Composite Design (CCD) has been applied in testing the hybrid systems for developing system models and optimization. The key testing parameters during the experiments include UV wavelength, irradiation duration, temperature, pH value, photo-catalysts, radical inhibitors, and oxidants ($O_2/O_3/H_2O_2$) concentration. Nevertheless,

process dynamics and mechanisms have also been briefly discussed based on the experimental results.

6.2 Research Contributions

The current research is innovative in its development, integration and optimization of the cutting edge advanced oxidation technologies for the treatment of municipal drinking water and industrial wastewater to combine the use of newly developed instrumental analysis methodologies and degradation mechanism/dynamic data to evaluate the effectiveness of enhanced photolysis as a treatment option for OOG OPW effluents. Firstly, the current study has developed simple, low-cost, time efficient, highly selective and sensitive methods based on SPE, LPME and GC-MS for offshore real-time PAHs testing in OPW. The developed methods were demonstrated to be robust, viable, simple, rapid, easy to use, cost efficient and environmental friendly for the real-time PAHs testing in OPW. Secondly, this research has developed efficient and eco-friendly technologies for on-site OPW treatment that can be incorporated into most existing systems.

Since the properties of OPW are significantly different from most wastewater, insight observation and optimization of this treatment technique through the proposed study become necessary before on-site implementation. The resulting technology has been proved to be an effective and viable alternative to existing treatment regimes, and has strong potential to extend to municipal and industrial wastewater which present immediate favorable marketing for its application for supplementing or substituting some

261

existing treatment methods.

The research is not only technically sound but also shows great potential in bringing significant environmental, economic and social benefits to industry, government and academia by providing not only cost-effective but also environmentally benign methods for treating OPW generated from OOG production, including: 1) filling knowledge and technical gaps and facilitating in-depth understanding of the adverse impact and advanced treatment of OPW; 2) creating a unique opportunity for an effective, economical and environmentally-friendly treatment of OPW, improving environmental performance, and enhancing abilities in managing petroleum wastes in the course of OOG production; 3) strengthening adaptation capacity to more stringent environmental policies and regulations as well as impacts of environmental changes in a sustainable way.

A list of publications as a result of this thesis research is summarized below:

1. **Ping, J.,** Chen, B., Husain, T., and Lee, K. (2010) Produced water treatment. Presented at the National Multidisciplinary Aldrich Conference 2010. March 27-28, 2010, St. John's, NL.

2. **Ping, J.,** Chen, B., Zheng, J.S., Liu, B., and Zhang, B.Y. (2011) A preliminary study on the ultraviolet irradiation effect on degradation of polycyclic aromatic hydrocarbons in offshore produced water. Proceedings of the 10th Specialized Conference on Small Water and Wastewater Treatment Systems of International Water Association (IWA). April 18-

22, Venice, Italy.

3. **Ping, J.,** Zheng, J.S., Liu, B., Lee, K., Husain, T., Zhang, B.Y., and Chen, B. (2011) Gas chromatography-mass spectrometry (GC-MS) analysis of PAHs in offshore produced water. Presented at the 64th CWRA National Conference. June 28-30, St. John's, NL.

4. Liu, B., **Ping, J.,** Zheng, J.S., Zhang, B.Y., and Chen, B. (2011) A review of mechanisms and the photoproducts of PAHs photo-oxidations. Presented at the 64th CWRA National Conference. June 28-30, St. John's, NL.

5. Liu B., **Ping J.**, Zheng J.S., Zhang B.Y., Lee K., Chen B. and Cai Q.H. (2012) Two analytical methods for real-time monitoring of polycyclic aromatic hydrocarbons in oil contaminated seawater. Proceedings of the 35yh Arctic and Marine Oilspill Program (AMOP) Technical Seminar on Environmental Contamination and Response, June 5-7, Vancouver, BC.

6. Zheng, J.S., Liu, B., **Ping, J.**, Zhang, B. Y., and Chen, B. (2012) Two analytical methods for real-time monitoring of PAHs in oil contaminated seawater. Proceedings of the 35th Arctic and Marine Oilspill Program (AMOP) Technical Seminar on Environmental Contamination and Response, June 5-7, Vancouver, BC.

7. Ping, J., Li Z.Y., Chen, B., Zheng J.S., Liu B., and Zhang, B.Y. (2013) Direct photolysis on polycyclic aromatic hydrocarbons (PAHs) in offshore produced water. Poster Presentation at the 48th Central Canadian Symposium on Water Quality Research. March 6-8, Hamilton, ON.

8. Li, Z.Y., **Ping J.**, and Chen B. (2013) Direct photolysis and advanced oxidation for polycyclic aromatic hydrocarbons removal from offshore produced water. 2013 Water

Pollution and Treatment Conference (WPT). Oct. 22-24, 2013, Sanya, China.

9. Zheng, J.S., **Ping, J**., Li, Z.Y., Chen, B., and Zhang, B.Y. (2013) Advanced oxidation of polycyclic aromatic hydrocarbons (PAHs) in offshore produced water. Poster Presentation at the 2013 Arctic Oil & Gas North America Conference. April 10-11, St. John's, NL.

10. Li, Z.Y., Chen, B. and **Ping, J.** (2014) Study of ultraviolet(UV) photolysis of polycyclic aromatic hydrocarbons in produced water. Chinese Journal of Environmental Engineering, 8(6): 2267-2270. DOI: 1673-910806-2267-04

11. Zheng, J.S., Chen, B., Zhang, B.Y., Liu, B, **Ping, J.** (2014) Photodegradation of polycyclic aromatic hydrocarbons in offshore produced water by ultraviolet irradiation. 3rd Water Research Conference. January 11-14, 2015. Shenzhen, China.

12. Zheng, J.S., Liu, B., **Ping, J**., Chen, B., Wu, H.J., and Zhang, B.Y. (2015) Vortex- and Shaker-assisted liquid–liquid Microextraction (VSA-LLME) coupled with gas chromatography and mass spectrometry (GC-MS) for analysis of 16 polycyclic aromatic hydrocarbons (PAHs) in offshore produced water. Water. Air, & Soil Pollution, 226: 318.

6.3 Recommendation for Future Research

1. Pretreatment

Vortex can produce dispersive solvent cloud to increase the interfacial surface while the shaking can keep the solvent dispersed in the tube to reduce the gradient distance. Integrating vortex has high potential to improve the performance of LLME treatment.

264

2. Catalyst

Limited ability from Degussa P-25 TiO_2 was detected due to the suspended form. And in real case application, the separation of catalysts after treatment is difficult and costly. Thus, the immobilization of catalyst could be an alter approach that avoids any post-treatment.

3. Matrix Effects Integration

The photolysis enhanced oxidation technologies were developed based on the artificial OPW only accounting for its salinity feature. In addition, due to the low initial concentration of both PAHs, the effects of competition were assumed to be minimum. Incorporating the complicated OPW matrix is much desired for further research. Further work can be focused on developing the kinetic model based on the photolysis and light competition kinetic to justify and predict the effect of sample matrix on photolysis of low concentration organic pollutant.

4. Intermediates Identification and Toxicity Assessment

Photo–oxidation of hydrocarbons has sometimes been documented to possibly increase toxicity. Further research is in high demand to investigate the treatment efficiency and the associated risk or toxicity effects of photolysis enhanced oxidation in combination or on their own on OPW. In that case, the possible research focus could be on the identification and quantification of intermediates created in the treatment process and toxicity assessment.

265

5. Technology Scaling up and Field Application

The approach adopted in this research can also be used in investigating other PAH/organic compounds in OPW. In addition, the removal efficiencies for PAHs could be impacted by many other factors in the hybrid treatment systems. The developed approach can be expanded to test more process factors regarding their contribution to the proposed systems. Many of these works are being conducted at the NRPOP Lab, who is developing pilot model to test these technologies using real OPW and working with industry partners to do field tests.

Bibliography

Al-Muntasheri, G.A., Sierra, L., Garzon, F.O., Lynn, J.D., Izquierdo, G.A., 2010.Water shut-off with polymer gels in a high temperature horizontal gas well: a success story. SPE Improv. Oil Recover. Symp.

Amini, S., Mowla, D., Golkar, M., Esmaeilzadeh, F., 2012. Mathematical modelling of a

Ayers, R. C. and Ayers, M. (2001) Offshore produced water waste management. Technical report prepared under the guidance of a special Task Force of the Environment sub-committee of the Canadian Association of Petroleum Producers (CAPP) East Coast Committee.

Ayers, R. C. and Parker, M. (2001). Offshore produced water waste management. CAPP technical report.

Azetsu-Scott, K., Yeats, P., Wohlgeschaffen, G., Dalziel, J., Niven, S., and Lee, K. (2007) Precipitation of heavy metals in produced water: Influence on contaminant transport and toxicity. Marine Environmental Research, 63(2), 146-167.

Bader, M.S.H., 2007. Seawater versus produced water in oil-fields water injection operations. Desalination 208, 159–168.

Bares, A., Ramoy, A., Battigelli, D., Au, K. K., and Hagan, D. (2006) Enhanced UV disinfection by Ozone/Peroxide - a Study in Tampa, Florida. WEFTEC Oct. 21.

Belavendram, D. (2011). An Engineer's Approach to Design of Experiments. Retrieved 2014/8/14, from Improvement and Innovation.com: http://www.improvementandinnovation.com/features/articles/engineers-approach- design-

experiments

Beltran, F. J., Ovejero, G., and Rivas, J. (1995c) Oxidation of polynuclear aromatic hydrocarbons in water. 3. UV radiation combined with hydrogen peroxide. Industrial and Engineering Chemistry Research, 35, 883-890.

Beltran, F. J., Ovejero, G., Garcia-Araya, J. F., and Rivas, J. (1995) Oxidation of polynuclear aromatic hydrocarbons in Water. 2. UV radiation and ozonation in the presence of UV radiation. Industrial and Engineering Chemistry Research, 34, 1607-1615.

Brandsma, M. G., and Smith, J. P. (1996) Dispersion modeling perspectives on the environmental fate of produced water discharges. In: M. Reed and S. Johnsen (Eds.) Produced Water 2. Environmental Issues and Mitigation Technologies. Environmental Science Research. 52: 215-224.

Braun, A. M., Maurette, M. T., and Oliveros, E. (1991) Photochemical Technology. Wiley, Chichester.

Brock, S., Delves, J., Chard, S., Dominguez, M., and Rust, L. J. D. (2003) Fil-Tore® media filter, presented at the 13th Produced Water Seminar, Houston, TX, Jan. 15-17.

Buller, A.T., Johnsen, S., Frost, K. (2003) Offshore produced water management—knowledge, tools and procedures for assessing environmental risk and selecting remedial measures. Memoir 3. Statoil Research and Technology Offshore.

Canadian Association of Petroleum Producers (CAPP). Produced Water Waste Management. Technical Report, August 2001. Report No. 2001–0030.

Canadian Council of Ministers of the Environment. (1999) Canadian sediment quality guidelines for the protection of aquatic life: Polycyclic aromatic hydrocarbons (PAHs). In: Canadian environmental quality guidelines, 1999, Canadian Council of Ministers of the

Environment, Winnipeg.

Cangelosi, A. A., Mays, N. L., Balcer, M. D., Reavie, E. D., Reid, D. M., Sturtevant, R., and Gao, X. (2007) The response of zooplankton and phytoplankton from the North American Great Lakes to filtration. Harmful Algae, 6(4), 547-566. doi:10.1016/j.hal.2006.11.005.

Casas, V., Llompart, M., Garcá-Jares, C., Cela, R., and Dagnac, T. (2006). Multivariate optimization of the factors influencing the solid-phase microextraction of pyrethroid pesticides in water. Journal of chromatography. A, 1124 (1-2), 148– 56. doi:10.1016/j.chroma.2006.06.034

Casini, S., Marsili, L., Fossi, M. C., Mori, G., Bucalossi, D., Porcelloni, S., Caliani, I., Stefanini, G., Ferraro, M., and Catenaja, C. A. (2006) Use of biomarkers to investigate toxicological effects of produced water treated with conventional and innovative methods. Marine Environmental Research, 62 (SUPPL. 1).

Cater, S. R., Stefan, M. J., Bolton, J. R., and Safarzadeh-Amiri, A. (2000) UV/H_2O_2 treatment of methyl t-butyl ether in contaminated waters. Journal of Environmental Science and Technology, 34, 659.

Caudle, D.D. (2000) Treating produced water – back to basics, presented at the 10th Produced Water Seminar, Houston, TX, Jan. 19-21.

Charalabaki, M., Psillakis, E., Mantzavinos, D., and Kalogerakis, N. (2005) Analysis of polycyclic aromatic hydrocarbons in wastewater treatment plant effluents using hollow fibre liquid-phase microextraction. Chemosphere. 60: 690-698.

Chen, L., Zhang, G., Ge, J., Jiang, P., Liu, Y., Ran, Y., 2014. Colloids and surfaces a : physicochemical and engineering aspects property evaluation of a new selective water

shutoff agent for horizontal well. Colloids Surf. A Physicochem. Eng. Asp. 446, 33–45.

Choi, W., and Hoffman, M. R. (1997) Novel photocatalytic mechanisms for $CHCl_3$, $CHBr_3$ and $CClCO_2^-$ degradation and the fate of photogenerated trihalomethyl radicals on TiO_2. Environmental Science and Technology, 37, 89.

Cisneros, L. R., Espinoza, G. A., Litter, M. I. (2002) Photodegradation of an azodye from the textile industry. Chemosphere, 248, 393-399.

Clark, C., Veil, J., 2009. Produced water volumes and management practices in the United States. Argonne National Laboratory Report.

Cline, J. T. (2000) Survey of gas flotation technologies for treatment of oil & grease," presented at the 10th Produced Water Seminar, Houston, TX, Jan. 19-21.

Collins, A.G. (1975) Geochemistry of Oilfield Waters. New York: Elsevier Scientific Publishers.

Colorado School of Mines (2009) Technical Assessment of produced water treatment technologies. An Integrated Framework for Treatment and Management of Produced Water. RPSEA Project 07122-12, Colorado, 2009, 8–128.

Correa, A. X. R., Tiepo, E. N., Somensi, C. A., Sperb, R. M., and Radetski, C. M. (2010) Use of Ozone-Photocatalytic Oxidation (O_3/UV/TiO_2) and Biological Remediation for Treatment of Produced water from Petroleum Refineries. Journal of Environmental Engineering, 136 (1), 40-45.

Cranford, S. W., Ortiz, C., and Buehler, M. J. (2010) Mechanomutable properties of a PAA/PAH polyelectrolyte complex: rate dependence and ionization effects on tunable adhesion strength. Soft Matter, 6, 4175 - 4188.

Crozier, P. W., Plomley, J. B., and Matchuk, L. (2001) Trace level analysis of polycyclic

aromatic hydrocarbons in surface waters by solid phase extraction (SPE) and gas chromatography-ion trap mass spectrometry (GC-ITMS). The Analyst. 126, 1974-1979.

Curran, K. J., Wells, P. G., and Potter, A. J. (2006) Proposing a coordinated environmental effects monitoring (EEM) program structure for the offshore petroleum industry, Nova Scotia, Canada. Marine Policy, 30(4), 400-411.

Daniel, A. J., Langhus, B. G., Patel, C. (2005) Technical Summary of Oil & Gas Produced Water Treatment Technologies. NETL.

Delgado, B., Pino, V., Ayala, J. H., González, V., & Afonso, A. M. (2004). Nonionic surfactant mixtures: a new cloud-point extraction approach for the determination of PAHs in seawater using HPLC with fluorimetric detection. Analytica Chimica Acta, 518 (1-2), 165– 172. doi:10.1016/j.aca.2004.05.005

Dieckmann, M. S., and Gray, K. A. (1996) A Comparison of the Degradation of 4-Nitrophenol via Direct and Sensitized Photocatalysis in TiO_2 Slurries. Water Resources, 30, 1169-1183.

Dijkstra, M. F. J., Buwalda, H., De Jong, A. W. F., Michorius, A., Winkelman, J. G. M., and Beenackers, A. A. C. M. (2001) Experimental comparison of three reactor designs for photocatalytic water purification. Chem. Eng. Sci. 56: 547.

Directive 2000/60/EC of the European Parliament and of the Council of 23 October 2000, establishing a framework for Community action in the field of water policy.

DOE NETL. Produced Water Management Technology Descriptions. Retrieved from: http://www.netl.doe.gov/technologies/pwmis/techdesc/physep/index.html

D'Oliveira, J. C., A1-Sayyed, G., and Pichat, P. (1990) Photodegradation of 2- and 3-Chlorophenol in TiO_2 aqueous suspensions. Environmental Science and Technology, 24,

990-996.

Dong, L., Xiaojun, Z., Hai'an, Z., 2011. Experimental study on inlet structure of the rod pump with down-hole oil–water hydrocyclone. Procedia Eng. 18, 369–374.

Donthuan, J., Yunchalard, S., & Srijaranai, S. (2014). Ultrasound-assisted dispersive liquid-liquid microextraction combined with high performance liquid chromatography for sensitive determination of five biogenic amines in fermented fish samples. Analytical Methods, 6 (4), 1128. doi:10.1039/c3ay41572d

Dórea, H. S., Bispo, J. R. L., Aragão, K. a. S., Cunha, B. B., Navickiene, S., Alves, J. P. H., et al. (2007). Analysis of BTEX, PAHs and metals in the oilfield produced water in the State of Sergipe, Brazil. Microchemical Journal, 85 (2), 234–238. doi:10.1016/j.microc.2006.06.002

Dutta, T. K., and Harayama, S. (2000) Fate of crude oil by the combination of photooxidation and biodegradation. Environmental Science and Technology, 34(8), 1500-1505.

Eisert, R. and Pawliszyn, J. (1997) New trends in solid-phase microextraction. Critical Reviews in Analytical Chemistry, 27, 103–135.

Ekins, P., Vanner, R., and Firebrace, J. (2005) Management of produced water on offshore oil installations: A comparative assessment using flow analysis. Final report prepared for the Policy Studies Institute.

Ekins, P., Vanner, R., and Firebrace, J. (2005) Management of Produced Water On Offshore Oil Installations: A Comparative Assessment using Flow Analysis, 2005. Final report prepared for the Policy Studies Institute.

Estrada, A. L., Li, Y. Y., Wang, A. (2012) Biodegradability enhancement of wastewater

containing cefalexin by means of the electro-Fenton oxidation process. J Hazard Mater, 227-228: 41-8.

Fakhru'l-Razi, A., Pendashteh, A., and Abdullah, L.C. (2009) Review of technologies for oil and gas produced water treatment. Journal of Hazardous Materials, 170, 530-51.

Faucher, M., and Sellman, E. (1998) Produced water deoiling using disc stack centrifuges, presented at the API Produced Water Management Technical Forum and Exhibition, Lafayette, LA, Nov. 17-18.

Favret, U. B., and Doucet, K. A. (1999) Total system design for the treatment of produced water & open drains on offshore production facilities, presented at the 9th Produced Water Seminar, Houston, TX, Jan. 21-22.

Fingas, M. (2011) Introduction of Oil Chemistry and Properties, Oil Spill Science and Technology, Gulf Professional Publishing, Burlington, USA, pp. 51-59.

Fontana, A. R., Wuilloud, R. G., Mart ńez, L. D., and Altamirano J. C. (2009) Simple Approach Based on Ultrasound- Assisted Emulsification-Microextraction for Determination of Polibrominated Flame Retardants in Water Samples by Gas Chromatography–Mass Spectrometry. Chromatogr. A, 1216, 147–153.

Fox, M. A., Chen, C. C., and Younathan, J. N. N. (1984) Oxidative cleavage of substituted naphthalene induced by irradiated semiconductor powders. J. Org. Chem. 49: 1969-1974.

Frankiewicz, T. (2001) Understanding the fundamentals of water treatment, the dirty dozen − 12 common causes of poor water quality, presented at the 11th Produced Water Seminar, Houston, TX, Jan. 17-19.

Fraser (2007) Priority organic pollutants in fresh and wastewaters of Konya-Turkey.

Fresen. Environ. Bull. 13: 118–123.

Fraser, G. S., Russell, J., and Zharen, W. M. V. (2006) Produced water from offshore oil and gas installations on the grand banks, Newfoundland and Labrador: are the potential effects to seabirds sufficiently known? Marine Ornithology, 34, 147–156.

French, A.P., and Taylor, E.F. (1978). An Introduction to Quantum Physics. Van Nostrand Reinhold, London, ISBN 0-442-30770-5.

Frost, T. K., Johnsen, S., and Utvik, T. I. R. (1998) Produced Water Discharges to the North Sea, Fate and Effects in theWater Column. OLF (Oljeindustriens Landsforening) December, 1998. http://www.olf.no/static/en/rapporter/producedwater/.

Fung, P. C., Poon, C. S., Chu, C. W., and Tsui, S. M. (2000b) Degradation kinetics of reactive red by UV/H_2O_2/US process under continuous mode operation. Proceedings of the IWA conference-Managing waterqwaste in the New Millennium: Challenges for developing areas, Midrand/Johannesburg, South Africa, pp. 3C-1.

Garland, E. (2005) Environmental regulatory framework in Europe: an update. SPE 93796. Paper presented at the 2005 SPE/EPA/DOE Exploration and Production Environmental Conference, Galveston, TX 7-9 March, 2005. Society of Petroleum Engineers, Richardson, TX. 10pp.

Garrett, R. M., Pickering, I. J., Haith, C. E., and Prince, R. C. (1998) Photooxidation of crude oils. Environmental Science and Technology, 32(23), 3719-3723.

Gilmour, C. R. (2012) Water Treatment Using Advanced Oxidation Processes: Application Perspectives. Masters Thesis. University of Western Ontario.

Glaze, W. H., and Kang, J. W. (1989a) Advanced oxidation processes. Description of a kinetic model for the oxidation of hazardous materials in aqueous media with ozone and

hydrogen peroxide in a semibatch reactor. Industrial & Engineering Chemistry Research, 28, 1573-1580.

Gogate, P. R., and Pandit, A. B. (2004) A review of imperative technologies for wastewater treatment I: oxidation technologies at ambient conditions. Advances in Environmental Research. 8, 501-551.

Gomes, J., Cocke, D., Das, K., Guttula, M., Tran, D., Beckman, J. (2009) Treatment of Produced Water By Electrocoagulation, Proceedings of TMS Annual Meeting, pp. 459-466, San Francisco, CA, February 15-19, 2009.

Gomez, M. J., Herrera, S., Sole, D., Garcia-Calvo, E., and Fernandez-Alba, A. R. (2011) Automatic searching and evaluation of priority and emerging contaminants in wastewater and river water by stir bar sorptive extraction followed by comprehensive two-dimensional gas chromatography-time-of-flight mass spectrometry. Analytical Chemistry, 83, 2638-2647.

Greenwood, P. (2003) Produced water management from an offshore operator's perspective, presented at the Produced Water Workshop, Aberdeen, Scotland, March 26-27.

Grini P. G., Hjelsvold M, Johnsen S. Choosing produced water treatment technologies based on environmental impact reduction. In: HSE Conference, Kuala Lumpur, Malaysia, 2002. 20–22 March, SPE paper 74002.

Grini, P. G., Clausen, C., and Torvik, H. (2003) Field Trials with Extraction Based Produced Water Purification Technologies, presented at the 1st NEL Produced Water Workshop, Aberdeen, Scotland, March 26–27.

Guieysse, B., Viklund, G., Toes, A. C., and Mattiasson, B. (2004) Combined UV-

biological degradation of PAHs. Chemosphere, 55, 1493-1499.

Hamme, J. D. V., Singh, A., and Ward, O. P. (2003) Recent advances in petroleum microbiology. Microbiology and Molecular Biology Reviews, 67(4), 503-549.

Han 2012

Haritash, A. K. and Kaushik, C. P. (2009). Biodegradation aspects of polycyclic aromatic hydrocarbons (PAHs): a review. Journal of Hazardous Materials, 169, 1-15.

Harman, C., Brooks, S., Sundt, R. C., Meier, S., and Grung, M. (2011) Field comparison of passive sampling and biological approaches for measuring exposure to PAH and alkylphenols from offshore produced water discharges. Marine Pollution Bulletin, 63 (5– 12), 141–148.

Hayes, D. A. T. (2004) Overview of Emerging Produced Water Treatment Technologies. 11th Annual International Petroleum Conference, Albuquerque, NM.

Hoigne, J. (1998) Chemistry of aqueous ozone and transformation of pollutants by ozonation and advanced oxidation processes. In the Handbook of Environmental Chemistry, ed. J. Hrubec. Springer-Verlag, Berlin, Heidelberg.

Hou, L., & Lee, H. K. (2004). Determination of pesticides in soil by liquid-phase microextraction and gas chromatography–mass spectrometry. Journal of Chromatography A, 1038 (1-2), 37– 42. doi:10.1016/j.chroma.2004.03.01Hou, L., and Lee, K. (2002) Application of Static and Dynamic Liquid-phase microextraction in the determination of polycyclic aromatic hydrocarbons. Journal of Chromatography A, 976, 377-385.

Hubschmann, H. J. (2000) Handbook of GC/MS , John Wiley & Sons, Ltd, Chichester, UK.

Hussein, F. H. (2011). Photochemical treatments of textile industries wastewater,

advances in treating textile effluent, Prof. Peter Hauser (Ed.), ISBN: 978-953-307-704-8, InTech, Available from: http://www.intechopen.com/books/advances-in-treating-textile-effluent/photochemical-treatments-of-textile- industries-wastewater

hydrocyclone for the down-hole oil–water separation (DOWS). Chem. Eng. Res. Des. 90, 2186–2195.

Igunnu, E. T., and Chen, G. Z. (2012). Produced water treatment technologies. International Journal of Low-Carbon Technologies, 9 (3), 157–177. doi:10.1093/ijlct/cts049

International Association of Oil and Gas Producers (OGP) (2004) Environmental Performance in the E&P Industry. 2003 Data. Report No. 359. OGP, London, UK. 32pp.

International Energy Agency (2008) Toxicology and risk assessment: a comprehensive introduction. NJ, USA: John Wiley & Sons, Hoboken.

IPCS (1998) Selected non-heterocyclic polycyclic aromatic hydrocarbons. Geneva, World Health Organization, International Programme on Chemical Safety, 883 pp. (Environmental Health Criteria 202).

Jain Irrigation Systems Ltd. Sand separator—Jain hydro cyclone filter, 2010. http://www.jains.com/irrigation/filtration%20equipments/jain%20hydrocyclone%20filter.htm.

Jelmert, A. (1999) Testing the effectiveness of an integrated hydrocyclone/UV treatment system for ballast water. Havforskninginstituttet, ordered and founded by OptiMarin Marketing A/S.

Jing, L., Chen, B., Zhang, B. Y., and Peng, H. X. (2012). A review of ballast water management practices and challenges in harsh and arctic environments. Environmental

Reviews, 20, 83-108.

Jing, L., Chen, B., Zhang, B. Y., Zheng, J. S., and Liu, B. (2014) Naphthalene degradation in seawater by UV irradiation: The effects of fluence rate, salinity, temperature and initial concentration. Marine Pollution Bulletin, 81, 149-156.

John Walsh (2012) Retrieved from: http://eo2.commpartners.com/users/spe/downloads/121129_Presentation_Slides.pdf

Johnsen, S. T. K., Frost, M., Hjelsvold, T. R., and Utvik, T. I. R. (2000) The environmental impact factor – a proposed tool for produced water impact reduction, management and regulation. SPE 611/78, Presented at the SPE HSE conference, Stavanger 2000.

Johnsen, S., Utvik, T. I. R, Garland, E., de Vals, B., and Campbell, J. (2004) Environmental fate and effects of contaminants in produced water. SPE 86708. Paper presented at the Seventh SPE International Conference on Health, Safety, and Environment in Oil and Gas Exploration and Production. Society of Petroleum Engineers, Richardson, TX. 9 pp.

Kayali-Sayadi, M. N., Rubio-Barroso, S., Cuesta-Jimenez, M. P., and Polo-Diez, L. M. (1998) Rapid determination of polycyclic aromatic hydrocarbons in tea infusion samples by high-performance liquid chromatography and fluorimetric detection based on solid-phase extraction. Analyst, 123, 2145.

Kemmochi, Y., Tsutsumia, K., Arikawaa, A., and Nakazawab, H. (2001) Centrifugal concentrator for the substitution of nitrogen blow-down micro-concentration in dioxin/polychlorinated biphenyl sample preparation. Journal of Chromatography A, 943 (2), 295-297.

King, A. J., Readman, J. W., and Zhou J. L. (2004) Determination of polycyclic aromatic hydrocarbons in water by solid-phase microextraction–gas chromatography–mass spectrometry. Anal. Chim. Acta, 523, 259–67.

Kishimoto, N., and Nakamura, E. (2011) Effects of Ozone-gas bubble size and pH on Ozone/UV treatment. Ozone: Science & Engineering: The Journal of the International Ozone Association. 33(5), 396-402.

Knudsen, B.L., Hjelsvold, M., Frost, T.K., Svarstad, M.B E., Grini, P.G., Willumsen, C.F., and Torvik, H. (2004) Meeting the Zero Discharge Challenge of ProducedWater. Presented in Calgary Canada 29–31 March, 2004. SPE paper 86671.

Krzemińska1, D., Neczaj, E., Borowski, G. (2015) advanced oxidation processes for food industrial wastewater decontamination. Journal of Ecological Engineering, 16(2), 61–71. DOI: 10.12911/22998993/1858

Ledakowicz, S., Miller, J. S., and Olejnik, D. (1999) Oxidation of PAHs in water solutions by ultraviolet radiation combined with hydrogen peroxide. International Journal of Photoenergy, 1, 1-6.

Lee R., Seright R., Hightower M., Sattler A., Cather M., McPherson B., Wrotenbery L., Martin D., and Whitworth M.: "Strategies for Produced Water Handling in New Mexico," paper presented at the 2002 Ground Water Protection Council.

Lee, J., Chun, S.W., Kang, H.J., Talke, F.E., 2011. Photo oxidative degradation of perfluoropolyether lubricant for data storage. Macromol. Res. 19 (6), 582–588.

Legrini, O., Oliveros, E., and Braun, A. M. (1993) Photochemical processes for water treatment. Chemical Reviews, 93, 671-698.

Levine, J., Barnes, F.S., 2010. Energy variability and produced water: two challenges,

one synergistic management approach using pumped hydroelectric energy storage. J. Energy Eng. ASCE 136 (1), 6–10.

Li Z.Y., Ping J., and Chen B. (2013) Direct Photolysis and Advanced Oxidation for Polycyclic Aromatic Hydrocarbons Removal from Offshore Produced Water. 2013 Water Pollution and Treatment Conference (WPT). Oct. 22-24, 2013, Sanya, China.

Li, K., Li, H. F., Liu, L., Hashi, Y. K., Maeda, T., and Lin, J. M. (2007) Solid-phase extraction with C_{30} bonded silica for analysis of polycycic aromatic hydrocarbons in airborne particulate matters.

Li, Z. Y. (2014) Factor analysis and condition optimization for Phtocatalytic oxidation of Polycyclic Aromatic Hydrocarbons in Oilfied Produced Water. Master thesis. North China Electric Power University.

Li, Z. Y., Chen, B. and Ping, J. (2014) Study of ultraviolet(UV) photolysis of polycyclic aromatic hydrocarbons in produced water. Chinese Journal of Environmental Engineering, 8(6): 2267-2270. DOI: 1673-910806-2267-04

Li, Z. Y., Chen, B., and Ping, J. (2014) Study of ultraviolet (UV) photolysis of polycyclic aromatic hydrocarbons in produced water. Chinese Journal of Environmental Engineering, 8(6), 2267-2270. DOI: 1673-9108(2014)06-2267-04

Lin, C., and Lin, K. S. (2007) Photocatalytic oxidation of toxic organohalides with TiO_2/UV: The effects of humic substances and organic mixtures. Chemosphere, 66(10), 1872-1877.

Litter, M. I. (2009) Treatment of chromium, mercury, lead, uranium and arsenic in water by heterogeneous photocatalysis. In: De Lasa H, Serrano B, Eds. Advances in chemical engineering, photocatalytic technologies. Elsevier: Academic Press, 36, 37-67.

Liu, B., Ping, J., Zheng, J. S., Zhang, B. Y., and Chen B. (2011) The mechanisms and the photoproducts of polycyclic aromatic hydrocarbons (PAHs) photo-oxidations - A review. Presented at the 64th CWRA National Conference. June 28-30, St. John's, NL.

Lodha, S., Jain, A., Punjabi, P. B. (2011) A novel route for waste water treatment: Photocatalytic degradation of rhodamine B. Arabian Journal of Chemistry. 4 (4), 383–387. DOI:10.1016/j.arabjc.2010.07.008

Low, G., McEvoy, S. R., and Matthews, R. W. (1991) Formation of nitrate and ammonium ions in titanium dioxide mediated photocatalytic degradation of organic compounds containing nitrogen atoms. Environmental Science and Technology, 25, 460-467.

Luquedecastro, M., and Priegocapote, F. (2007). Ultrasound-assisted preparation of liquid samples. Talanta, 72 (2), 321– 334. doi:10.1016/j.talanta.2006.11.013

Ma, H. and Chen, B. (2011) Treatment of produced water before discharge: challenges and opportunities. Proceedings of the 9th Research Symposium of NECPU, Beijing, China.

Mackay, D., Shiu, W. Y., Ma, K. C., and Lee, S. H. (2006) Hand Book of Physical - Chemical Properties and Environmental Fate for Organic Chemicals, Second Edition. Boca Raton, FL: CRC Press, Taylor & Francis Group, LLC. Amyx

Maersk OIL, 2011. Environmental Status Report 2011–The Danish North Sea.

Marce′, R. M., and Borrull, F. (2000) Solid-phase extraction of polycyclic aromatic compounds. Journal of Chromatography A, 885, 273-290.

Meijer, D. T., and Kuijvenhoven, C. A. T. (2002) Field-proven removal of dissolved hydrocarbons from offshore produced water by the macro porous polymer-extraction technology, presented at the 12th Produced Water Seminar, Houston, TX, Jan. 16-18.

Meijer, D. T., and Madin, C. (2010) Removal of dissolved and dispersed hydrocarbons from oil and gas produced water with mppe technology to reduce toxicity and allow water reuse. Appea Journal, 1-11.

Meijer, D.T., Kuijvenhoven, C. A. T., Karup, H. (2004) Results from the latest MPPE field trials at NAM and total installations. In: NEL Produced Water Workshop, Aberdeen, UK, April 21–22, 2004.

Michor, G., Carron, J., Shelley, B., and Cancilla, D. (1996) Analysis of 23 polynuclear aromatic hydrocarbons from natural water at the sub-ng/l level using solid-phase disk extraction and mass-selective detection. Journal of Chromatography A, 732 (1), 85-99.

Miller, J. S., and Olejnik, D. (2001) Photolysis of polycyclic aromatic hydrocarbons in water. Water Research, 35(1), 233-243.

Murov, S. L., Carmichael, I., and Hug, G. L. (1993) Handbook of photochemistry, 2nd ed. Dekker.

Nadal, M., Wargent, J. J., Jones, K. C., Paul, N. D., Schuhmacher, M., and Domingo, J.L. (2006) Influence of UV-B radiation and temperature on photodegradation of PAHs: preliminary results. The Journal of Atmospheric Chemistry, 55, 241–252.

National Energy Technology Laboratory, Produced Water Management Technology Descriptions Fact Sheet. Retrieved from: http://www.netl.doe.gov/technologies/pwmis/tech-desc

Nature Technology Solution (2013) Introduction to produced water treatment. Published by Blake Charles Diniz Marques. Retrieved from: http://www.scribd.com/doc/119188791/Introduction-to-produced-water-treatment#scribd

Nedwed, T. J., Smith, J. P., and Brandsma, M. G. (2004) Verification of the OOC mud

and produced water discharge model using lab-scale plume behavior experiments. Environmental Modelling & Software, 19, 655-670.

Neff, J. M. (2002) Bioaccumulation in Marine Organisms. Effects of Contaminants from Oil Well Produced Water. Elsevier Science Publishers, Amsterdam. 452pp.

Neff, J. M. (2005) Composition, environmental fates, and biological effect of water based drilling muds and cuttings discharged to the marine environment: A synthesis and annotated bibliography. Report prepared for the Petroleum Environment Research Forum (PERF). Available from American Petroleum Institute, Washington, DC. 73 pp.

Neff, J. M., Johnsen, S., Frost, T., Utvik, T. R., and Durell, G. (2006) Oil well produced water discharged to the North Sea. Part II: Comparison of deployed mussels (Mytilus edulis) and the DREAM Model to predict ecological risk. Marine Environmental Research, 62, 224-246.

Neff, J., Lee, K., and Deblois, E. M. (2010) Produced Water: Overview of composition, fates, and effects. DOI: 10.1007/978-1-4614-0046-2_1.

NETL (The National Energy Technology Laboratory). Produced Water Management Information System. http://www.netl.doe.gov /technologies/pwmis/index.html (accessed July, 2014).

Nicolaisen, B., and Lien L. (2003) Treating oil and gas produced water using membrane filtration technology, presented at the Produced Water Workshop, Aberdeen, Scotland, March 26-27.

O'Hara, P. D., and Morandin, L.A. (2010) Effects of sheens associated with offshore oil and gas development on the feather microstructure of pelagic seabirds. Marine Pollution Bulletin, 60 (5), 672–678.

Office of the Auditor General of Canada (OAG) (2012) Report of the Commissioner of the Environment and Sustainable Development. CHAPTER 1: Atlantic Offshore Oil and Gas Activities. Retrieved from: http://www.oag-bvg.gc.ca/internet/docs/parl_cesd_201212_01_e.pdf

Offshore Magazine (2006) C-Tour technique on course to manage two–thirds of Norway's produced water. April 1, 2006.

OGP (2002) Aromatics in produced water: occurrence, fate and effects, and treatment

OSPAR Commission (2002) Background Document concerning Techniques for the Management of Produced Water from Offshore Installations.

OSPAR Commission (2008) Discharges, spills and emissions from offshore oil and gas installations in 2008.

Owens, N., and Lee, D. W. (2008) The Use of Micro-Bubble Flotation Technology in Secondary & Tertiary Produced Water Treatment - A Technical Comparison With Other Separation Technologies. Presented at the Produced Water Workshop - Aberdeen, Scotland - May 2007.

Ozcan, S., Tor, A., and Aydin, M. E. (2009) Determination of selected polychlorinated biphenyls in water samples by ultrasound-assisted emulsification-microextraction and gas chromatography-mass-selective detection. Analytica Chimica Acta, 647, 182–188.

Ozcan, S., Tor, A., and Aydin, M. E. (2010) Determination of polycyclic aromatic hydrocarbons in waters by ultrasound-assisted emulsification-microextraction and gas chromatography-mass spectrometry. Analytica Chimica Acta, 665, 193-199.

Pelizzetti, E., Minero, C., Piccinini, P., and Vincenti, M. (1993) Phototransformations of nitrogen containing organic compounds over irradiated semiconductor metal oxides.

Nitrobenzene and Atrazine over TiO2 and ZnO. Coordination Chemistry Reviews, 125,183-194.

Ping, J., Chen, B., Zheng, J. S., Liu, B., and Zhang, B. Y. (2011) A preliminary study on the ultraviolet irradiation effect on degradation of polycyclic aromatic hydrocarbons in offshore produced water. Proceedings of the 10th Specialized Conference on Small Water and Wastewater Treatment Systems of International Water Association (IWA). April 18-22, Venice, Italy.

Ping, J., Li, Z. Y., Chen, B., Zheng, J. S., Liu, B., and Zhang, B. Y. (2013) Direct Photolysis on Polycyclic Aromatic Hydrocarbons (PAHs) in Offshore Produced Water. Poster Presentation at the 48th Central Canadian Symposium on Water Quality Research. March 6-8, Hamilton, ON.

Pino, V., Ayala, J. H., Afonso, A. M., and González, V. (2002). Determination of polycyclic aromatic hydrocarbons in seawater by highperformance liquid chromatography with fluorescence detection following micelle-mediated preconcentration. Journal of chromatography. A, 949 (1-2), 291-299. http://www.ncbi.nlm.nih.gov/pubmed/11999746

Plebon, M. J., Saad, M. A., Chen, X. J., and Fraser, S. (2006) De-oiling of produced water from offshore oil platforms using a recent commercialized technology which combines adsorption, coalescence and gravity separation. Proceedings of the Sixteenth International Offshore and Polar Engineering Conference, 1: 503-507.

Pollestad A. The Troll oil case—practical approach towards zero discharge. In: Tekna Produced Water Conference, 18–19 January 2005, Tekna, 2005.

Popp, P., Bauer, C., & Wennrich, L. (2001). Application of stir bar sorptive extraction in combination with column liquid chromatography for the determination of polycyclic

aromatic hydrocarbons in water samples. Analytica Chimica Acta , 436 (1), 1-9. doi:10.1016/S0003-2670(01)00895-9

Pramauro, E., Prevot, A. B., Augugliaro, V., and Palmisano, L. (1995) Photocatalytic treatment of laboratory wastes containing aromatic amines. Analyst, 120, 237-242.

Pramauro, E., Prevot, A. B., Vincenti, M., Gamberini, R. (1998) Photocatalytic degradation of Naphthalene in aqueous TiO_2 dispersions: effect of nonionic surfactants. Chemosphere, 36 (7), 1523-1542.

Prince, R. C., Garrett, R. M., Bare, R. E., Grossman, M. J., Townsend, T., Suflita, J. M., Lee, K., Owens, E. H., Sergy, G. A., and Braddock, J. F. (2003) The roles of photooxidation and biodegradation in long-term weathering of crude and heavy fuel oils. Spill Science and Technology Bulletin, 8(2), 145-156.

Psillakis, E., and Kalogerakis, N. (2001) Application of solvent microextraction to the analysis of nitroaromatic explosives in water samples. Journal of Chromatography A, 907, 211-219.

Psillakis, E., and Kalogerakis, N. (2003) Developments in liquid-phase microextraction. Trends in Analytical Chemistry, 22, 565-574.

Psillakis, E., Mantzavinos, D., & Kalogerakis, N. (2004). Monitoring the sonochemical degradation of phthalate esters in water using solid-phase microextraction. Chemosphere , 54 (7), 849-857. doi:10.1016/j.chemosphere.2003.09.039

Pyle, S. M., Betowski, L. D., Marcus, A. B., Winnik, W., and Brittain, R. D. (1997) Analysis of polycyclic aromatic hydrocarbons by ion trap tandam mass spectrometry. Journal of the American Society for Mass Spectrometry, 8, 183.

Qu, R. (2006) Applied photochemical remediation technology for degradation of

hydrocarbon compounds in petroleum produced water. Master thesis. University of Regina.

Regueiro, J., Llompart, M., Psillakis, E., Garcia-Monteagudo, J. C., and Garcia-Jares, C. (2009) Ultrasound-assisted emulsification-microextraction of phenolic preservatives in water. Talanta, 79, 1387–1397.

Rein Munter (2001) Advanced oxidation processes – current status and prospects. Proceedings of the Estonian Academy of Sciences, Chemistry, 50 (2), 59–80.

Reuters. (2007) Canada Hibernia oil output declines as field ages. Press release, Oct. 22, 2007. Reuters.

Robinson, K. (2003) Produced Water Management – An Integrated Approach, presented at the Produced Water Workshop, Aberdeen, Scotland, March 26-27.

Saad, M., Plebon, M.J., and Fraser, S. (2006) Fundamental Approach to Produced Water Treatment: Validation of An Innovative Technology. Presented at the 16th Produced Water Seminar, Houston, TX, January 2006.

Salter, E., and Ford, J. (2000) Environmental pollution challenges and associated planning and management issues facing offshore oil and gas field development in the UK. Journal of Environmental Planning and Management, 43(2), 253-276.

Sanchez-Prado, L., Barro, R., Garcia-Jares, C., Llompart, M., Lores, M., Petrakis, C., et al. (2008). Sonochemical degradation of triclosan in water and wastewater. Ultrasonics Sonochemistry, 15 (5), 689– 694. doi:10.1016/j.ultsonch.2008.01.007

Sarafraz-Yazdi, A., & Amiri, A. (2010). Liquid-phase microextraction. TrAC - Trends in Analytical Chemistry. doi:10.1016/j.trac.2009.10.003

Saraji, M., & Boroujeni, M. K. (2014). Recent developments in dispersive liquid-liquid

microextraction. Analytical and bioanalytical chemistry, Vol. 406. doi:10.1007/s00216-013-7467-z

Satir, T. (2008) Ship's ballast water and marine pollution. NATO Science for Peace and Security Series C: Environmental Security, 4, 453–463. doi:10.1007/978-1-4020-6575-0_30.

Schmelling, D. C., Gray, K. A., and Kamat, P. V. (1996) Role of Reduction in the Photocatalytic Degradation of TNT. Journal of Environmental Science and Technology, 30, 2547-2555.

Sehensted, K., Corfitzen, H., Holcman, J., Fischer, C. H., and Hart, E. J. (1991) The primary reaction in the decomposition of ozone in acidic aqueous solutions. Environmental Science and Technology, 25, 1589-1596.

Singh, S. N. (Ed.) (2012) Microbial Degradation of Xenobiotics. DOI: 10.1007/978-3-642-23789-8

Sinker, A. (2007) Produced Water Treatment Using Hydrocyclones: Theory and Practical Applications. 14th Annual International Petroleum Environmental Conference, Houston TX,

Smith, J. P., Brandsma, M. G., and Nedwed, T. J. (2004) Field verification of the Offshore Operators Committee (OOC) mud and produced water discharge model. Environmental Modelling & Software, 19, 739-749.

Song, X., Li, J., Liao, C., & Chen, L. (2011). Ultrasound-Assisted Dispersive Liquid-Liquid Microextraction Combined with Low Solvent Consumption for Determination of Polycyclic Aromatic Hydrocarbons in Seawater by GC– MS. Chromatographia, 74 (1-2), 89– 98. doi:10.1007/s10337-011-2048-9

Staehelin, J., and Hoigne ́, J. (1985) Decomposition of ozone in water in the presence of organic solutes acting as promotors and inhibitors of radical chain reactions. Environ. Science & Technology, 19, 1206-1213.

Steenken, S., Warren, C. J., and Gilbert, B. C. (1990) Generation of radical cations from naphthalene and some derivatives, both by photoionization and reaction with SO_4^-: formation and reactions studied by laser flash photolysis. Journal of the Chemical Society, Perkin Transactions, 2, 335-342.

Stege, P.W., Sombra, L. L., Messina, G. A., Martinez, L. D., and Silva, M. F. (2009) Environmental monitoring of phenolic pollutants in water by cloud point extraction prior to micellar electrokinetic chromatography. Analytical and Bioanalytical Chemistry, 394(2), 567-573.

Stephenson, M. T. In Components of produced water: a compilation of results from several industry studies., Proceedings of the First International Conference on Health, Safty and Environment, The Hague, Netherlands, 1991; Richardson, T. X., Ed. Society of Petroleum Engineers, Inc.: The Hague, Netherlands, 1991.

Stepnowski, P., Siedlecka, E. M., Behrend, P., and Jastorff, B. (2002) Enhanced photo degradation of contaminants in petroleum refinery wastewater. Water Research, 36(9), 2167-2172.

Stevens, J., Stone, P., and Flanagan, M. (2010) Trace analysis of potable water by on-line SPE LCMS/MS Employing Thermal Gradient Focusing and Dual Ion Funnel Technologies, ASMS 2010, TP 529, Retrieved January, 2010 from www.chem.agilent.com/Library/posters/Public/Online-SPE LCMSMS_ASMS_2010_Rev1_M%20Flanagan.pdf

Sugihara, M.N. (2010) UV-TIO$_2$ Photocatalytic degradation of the X-RAY contrast agent diatrizoate: Kinetics and mechanisms in oxic and anoxic solutions. Master thesis. University of Illinois at Urbana-Champaign.

Supelco (2010) Application manual - Extract Polynuclear Aromatic Hydrocarbons from Water, Using Solid Phase Extraction Disks.

Tanaka, K., Padermpole, K., and Hisanaga, T. (2000) Photocatalytic degradation of commercial azo dyes. Water Resources, 34(1), 327.

Tankeviciute, A., Kazlauskas, R., and Vickackaite, V. (2001) Headspace extraction of alcohols into a single drop. Analyst, 126, 1674 -1677.

Tarek, S. J., Montaser, Y. G., Ibrahim E. E. S., Eglal R. S., Rabab, A. N. (2011) A comparative study among different photochemical oxidation processes to enhance the biodegradability of paper mill wastewater. J. Hazard. Mater., 185, 353–358.

Tchobanoglous, G., Burton, F. L., and Stensel, H. D. (2003) Wastewater engineering: treatment and reuse (4th edition). McGraw-Hill, Boston, MA. 545PP.

Templeton, M. R., Hofmann, R., Andrews, R. C., and Whitby, G. E. (2006) Biodosimetry Testing of a Simplified Computational Model for the UV Disinfection of Wastewater. Journal of Environmental Engineering and Science, 5(1), 29-36.

Theurich, J., Lindner, M., and Bahnemann, D. W. (1996) Photocatalytic degradation of 4-s Study. Langmuir, 12, 6368-6376.

Thomas, K. V., Balaam, J., Hurst, M. R., and Thain, J. E. (2004) Identification of in vitro estrogen and androgen receptor agonists in North Sea offshore produced water discharges. Environmental Toxicology and Chemistry, 23(5), 1156-1163.

Titato, G. M., & Lanças, F. M. (2006). Optimization and validation of HPLC-UV-DAD

and HPLC-APCI-MS methodologies for the determination of selected PAHs in water samples. Journal of chromatographic science, 44 , 35– 40.

Titato, G. M., and Lancas, F. M. (2005) Comparison between different extraction (LLE and SPE) and determination (HPLC and capillary–LC) techniques in the analysis of selected PAHs in water samples. Journal of Liquid Chromatography & Related Technologies, 28, 3045.

Tor, A., Cengeloglu, Y., Aydin, M.E., Ersoz, M., Wichmann, H., and Bahadir, M. (2003) A Survey of Polychlorinated Biphenyls (PCBs) and Polycyclic Aromatic Hydrocarbons (PAHs) in Waste Water Samples from Sewage System in Konya-TURKEY. Fresen Environ Bull, 12 (7), 732-735.

Torvik, H., Bergersen, L., and Paulsen, C. (2005) One year of operational experience with CTour at Statfjord C. Presented at the 3rd NEL Produced Water Workshop, Aberdeen, Scotland, April 20–21, 2005. Hill Company, New York.

Trillas, M., Peral, J., and Donenech, X. (1996) Photo-oxidation of phenoxyacetic acid by TiO_2 illuminated catalyst. Applied Catalysis B: Environmental, 3, 45.

Tsapakis, M., Dakanali, E., Stephanou, E.G., Karakassis, I. (2010) PAHs and n-alkanes in Mediterranean coastal marine sediments: aquaculture as a significant point source. Journal of Environmental Monitoring, 12, 958-963.

Tuhkanen, T. (1994) Oxidation of organic compounds in water and waste water with the combination of hydrogen peroxide and UV radiation. Ph.D. thesis, University of Kuopio, Finland.

Tulloch, S. J. (2003) Development & Field Use of the Mare's Tail® Pre-Coalescer, presented at the Produced Water Workshop, Aberdeen, Scotland, March 26-27.

Turchi, C. S., and Ollis, D. F. (1989) Mixed reactant photocatalysis: intermediates and mutual rate inhibition. Journal of Catalysis, 119, 483-496.

Tyrie, C. C. (2000) Produced Water Management, presented at the 10th Produced Water Seminar, Houston, TX, Jan. 19-21.

Veil, C. C. (2009). Produced Water Volumes and Management Practices in the United States . Argonne National Laboratory Report.

Veil, J. A., Kimmell, T. A., and Rechner, A. C. (2005) Characteristics of produced water discharged to the Gulf of Mexico Hypoxic Zone. Report to the U.S. Dept. of Energy Technology Laboratory from Argonne National Laboratory, Washington, DC.

Veil, J. A., Puder, M. G., Elcock, D., and Redweik, R. J. (2004) A white paper describing produced water from production of crude oil, natural gas, and coal bed methane. Report to the U.S. Dept. of Energy, National Energy Technology Laboratory. Argonne National Laboratory, Washington, DC. 79pp.

Vinas, L., Franco, M. A., Soriano, J. A., Gonzalez, J. J., Ortiz, L., Bayona, J. M., and Albaiges, J. (2009) Accumulation trends of petroleum hydrocarbons in commercial shellfish from the Galician Coast (NW Spain) affected by the Prestige Oil Spill. Chemosphere, 75(4), 534-541.

Vohra, M. S., and Davies, A. P. (2000) TiO_2 assisted photocatalysis of lead-EDTA. Water Research, 34(3), 952.

Watson, R. (1996) A review of water disinfection technology to determine suitable equipment for use at sea for the disinfection of sea water. Sea fish report. No. SR497.

Werres, F., Balsaa, P., and Schmidt, T. C. (2009) Total concentration analysis of polycyclic aromatic hydrocarbons in aqueous samples with high-suspended particulate

matter content. Journal of Chromatography A, 1216, 2235-2240.

Wolska, L., Rawa-Adkonis, M., and Namiesnik, J. (2005) Determining PAHs and PCBs in aqueous samples: Finding and evaluating sources of error. Analytical and Bioanalytical Chemistry, 382, 1389-1397.

Wu, H. J., Lye, L. and Chen, B. (2012). A DOE aided sensitivity analysis and parameterization for hydrological modeling. Canadian Journal of Civil Engineering, 39, 460-472.

Wu, Y., Xia, L., Chen, R., and Hu, B. (2008). Headspace single drop microextraction combined with HPLC for the determination of trace polycyclic aromatic hydrocarbons in environmental samples. Talanta, 74 (4), 470– 7. doi:10.1016/j.talanta.2007.05.057

Xu, L., Basheer, C., and Lee, H. K. (2007) Developments in single-drop microextraction. Journal of Chromatography A, 1152, 184-192.

Xu, P., and Drewes, J. E. (2006) Viability of nanofiltration and ultra-low pressure reverse osmosis membranes for multi-beneficial use of methane produced water. Sep Purif Technol, 52, 67-76.

Yiantzi, E., Psillakis, E., Tyrovola, K., & Kalogerakis, N. (2010). Vortex-assisted liquid – liquid microextraction of octylphenol , nonylphenol and. Talanta , 80 (5), 2057-2062. doi:10.1016/j.talanta.2009.11.005

Younker, J., Lee, S. Y., Gagnon, G., and Walsh, M. E. (2011) Atlantic Canada Offshore R&D: Treatment of oilfield produced water by chemical coagulation and electrocoagulation. Offshore Technology Conference, 2-5 May, Houston, Texas, USA.

Zhao, R. S., Cheng, C. G., Yuan, J.P., Jiang, T., Li, L., and Xu, X. B. (2006) Application of liquid-phase microextraction and gas chromatography-mass spectrometry for the

determination of chloroform in drinking water. Analytical Sciences. 22, 563-566.

Zhao, R. S., Lao, W. J., and Xu, X. B. (2004) Headspace liquid-phase microextraction of trihalo-methane in drinking water by gas chromatography determination. Talanta, 62 (4), 751-756.

Zheng, J. S., Chen, B., Thanyamanta, W., Hawboldt, K., Zhang, B. Y., Liu, B. (2016) Offshore produced water management: A review of current practice and challenges in harsh/Arctic environments. Marine Pollution Bulletin. pii:S0025-326X(16)30004-2. doi: 10.1016/j.marpolbul.

Zheng, J. S., Chen, B., Zhang, B. Y., Liu, B, Ping, J. (2014) Photodegradation of polycyclic aromatic hydrocarbons in offshore produced water by ultraviolet irradiation. 3rd Water Research Conference. January 11-14, 2015. Shenzhen, China.

Zheng, J. S., Liu, B., Ping, J., Chen, B., and Zhang, B. Y. (2012) Two analytical methods for real-time monitoring of PAHs in oil contaminated seawater. Proceedings of the 35th AMOP Technical Seminar on Environmental Contamination and Response, Environment Canada, Ottawa, ON, pp. 448-459. (June 5-7, Vancouver, BC.)

Zheng, J. S., Liu, B., Ping, J., Chen, B., and Zhang, B. Y. (2013) Advanced Oxidation of Polycyclic Aromatic Hydrocarbons (PAHs) in Offshore Produced Water. Poster Presentation at the 2013 Arctic Oil & Gas North America Conference. April 10-11, St. John's, NL.

Zheng, J. S., Ping, J., Li, Z. Y., Chen, B., and Zhang, B. Y. (2013) Advanced Oxidation of Polycyclic Aromatic Hydrocarbons (PAHs) in Offshore Produced Water. Poster Presentation at the 2013 Arctic Oil & Gas North America Conference. April 10-11, St. John's, NL.